Diss. ETH No. 19832

# Structure-Property Relationship Studies on Various Phosphoramidates as Potential Flame Retardants for Cellulose

A dissertation submitted to

**ETH ZURICH**

for the degree of

**Doctor of Sciences**

presented by

**Viktoriya Salimova**

M.Sc. in Chemistry, North Kazakhstan State University

born on August 5, 1984

citizen of Petropavlovsk, Kazakhstan

accepted on the recommendation of

Prof. Dr. Hansjörg Grützmacher, examiner

Prof. Dr. Paul Pregosin, co-examiner

Dr. Joëlle Grützmacher, co-examiner

Prof. Dr. Manfred Heuberger, co-examiner

Dr. Sabyasachi Gaan, co-examiner

2013

Моему мужу и моим родителям посвящаю

# Acknowledgements

Alex, Tong, Rafael, Theo, Judith, Georgina, Dominikus, Vito, Monika, Florian, Matthias, Amos) for teaching me to work with vacuum lines, for helping with measuring and interpreting NMR data, encouraging discussions during group seminars and cheering time spent together. A very special "thank you" I would like to address to Katrin for many exciting discussions about structure and properties of textile fabrics and for being my harbor in times of thunderstorms.

Another huge thank you is addressed to my EMPA lab mate Erich for numerous open-hearted discussions, hours of laughter and sarcastic jokes. Your confidence in that I could write the Thesis using LaTeX has turned to me in a great discovery, and I am eternally grateful for that. Thank you, Sébastien and Barbara, for highly interesting three months spent exploring plasma coatings, for your support, optimism and kindness. These precious memories will stay with me forever.

Additionally I would like to thank the supervisor of my master's degree Dr. Kazbek Bolatbayev and my chemistry professor Marianna Lezhneva for your commitment, concern and faith in me. A very special thanks I would like to address to my friend Olga: without your support and unwavering belief in me I would not have completed this long dissertation journey. Thanks also to my friends Alex, Yury, Jelena, Kirill, Rustem and Tanya.

My gratitude is also extended to Patrik Ryser for your generosity and patience.

Last but not least, I would like to give thanks to my parents, my sister and my relatives in Kazakhstan. You have been a great support for me through my entire life abroad. In this context I would like to express my deep gratitude to my husband Roland. I hardly can find words to describe my appreciation for your constant support, for giving me confidence and motivation in any situation to move on. Thank you!

# Abstract

Cellulose is the most abundant polymer found on Earth. About $33\,\%$ of all plant matter is made up of cellulose. Nowadays it is hard to think of life without cellulose being the main component of paper, natural textiles and wood. With the rapid improvement of living standards, the consumption of these materials has increased swiftly, therefore demanding more strict and rigid safety requirements. This has put forward the challenge to the scientific community to develop methods for mitigating the risks which arise from burning cellulosic materials, in particular textiles.

What can render cellulose flame retardant (FR)? A vast amount of chemical compounds exist that can provide cellulose with excellent FR properties, be it halogen-, antimony-, boron- or phosphorus-containing molecules. All these compounds have their advantages and disadvantages. The class of FRs we will be focusing on in the present work are organophosphorus compounds being widely used for cellulose and cellulosic materials. The chemically active site in these compounds is phosphorus. Phosphorus is able to phosphorylate cellulose upon thermal treatment, thus preventing its full degradation and liberation of heat. Addition of nitrogen can facilitate this process and hence, improve the FR behaviour of cellulosic materials to a great extent (phosphorus-nitrogen synergism). Nitrogen can be introduced as an additive using urea derivatives, melamine formaldehyde or guanidine or it can be incorporated in the FR molecules like in various phosphoric amides.
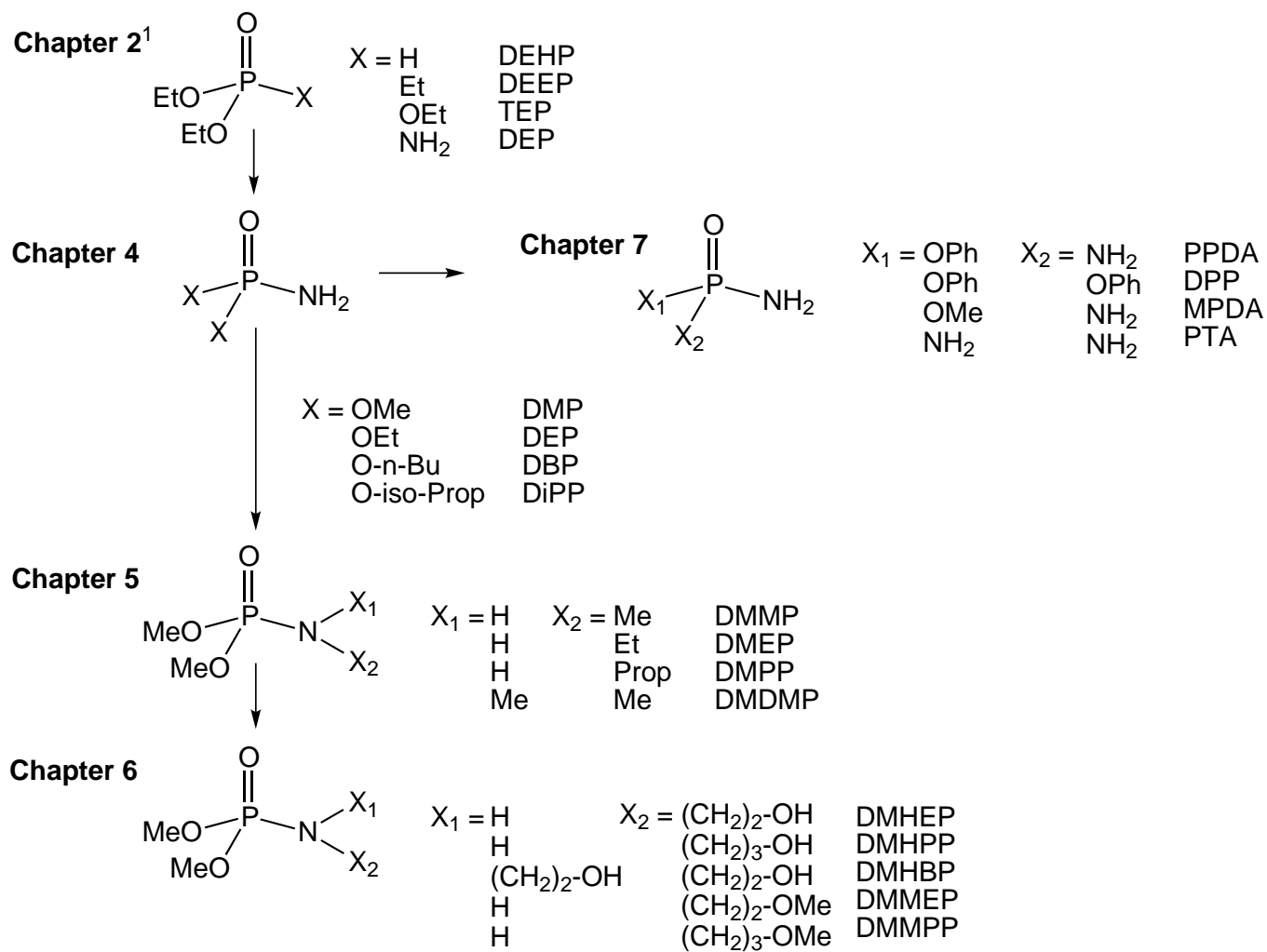
A great variety of papers have been published in the literature, dealing with the investigations on potential flame retardants for cellulose, where nitrogen is present in the molecule together with phosphorus. After discovery of 3-(dimethylphosphono)-N-methylolpropion-amide in 1940s, better known under its commercial name Pyrovatex©, organophosphorus

compounds with nitrogen in their structure have attracted particular attention. Therefore, a great number of publications deal with the research directed on search of best flame retardant agent without affecting the physical properties of textiles like stiffness, mechanical strength and air permeability. However, there exists no systematic study to this day where the effect of nitrogen (being incorporated in the molecule) on the flammability of cellulose would be shown. It is still not clear, whether the phosphorus-nitrogen synergism or structural effects play the major flame-retarding role in phosphorus- and nitrogen-containing compounds. In several studies it was observed that the bonding of phosphorus to different elements affects the overall FR properties of compounds. In other studies, it was found that the presence of some functional groups like hydroxyls influences the performance of compound as FR for cellulose. However, none of these studies came up with a systematic investigation on the FR properties of materials in relation to their structure.

The main goal of the present study is to explore the structure-property relationship in P-N-containing compounds and to correlate structural changes with the changes in flame retardant behaviour. The studies have been carried out on twenty different organophosphorus compounds. As a core structure, the structure of phosphoric acid has been taken and the hydroxyl groups were substituted either with alkyl- or aryl ester groups, alkylamino, hydroxyalkylamino and/or aminogroups.

The molecules investigated in this study were selected such that structural differences between them were minor. This allowed us to attribute changes in the FR properties to the specific structural variations. In the present study, the structural changes were correlated to FR properties and following effects were qualitatively analyzed:

- bonding of phosphorus to hydrogen, carbon, oxygen and nitrogen,

- impact of alkyl chain length attached to phosphorus atom,

- influence of the nature of aminogroup - primary, secondary or tertiary,

- effect of hydroxyl group,

- effect of substituting the hydroxyl group to methoxy group,

- impact of the number of aminogroups.

**Chapter 2**[1]

$$\text{EtO}-\underset{\underset{\text{EtO}}{|}}{\overset{\overset{O}{\|}}{P}}-X$$

| X = H | DEHP |
|---|---|
| Et | DEEP |
| OEt | TEP |
| NH$_2$ | DEP |

**Chapter 4**

$$X-\underset{\underset{X}{|}}{\overset{\overset{O}{\|}}{P}}-NH_2$$

**Chapter 7**

$$X_1-\underset{\underset{X_2}{|}}{\overset{\overset{O}{\|}}{P}}-NH_2$$

| X$_1$ = OPh | X$_2$ = NH$_2$ | PPDA |
|---|---|---|
| OPh | OPh | DPP |
| OMe | NH$_2$ | MPDA |
| NH$_2$ | NH$_2$ | PTA |

| X = OMe | DMP |
|---|---|
| OEt | DEP |
| O-n-Bu | DBP |
| O-iso-Prop | DiPP |

**Chapter 5**

$$\text{MeO}-\underset{\underset{\text{MeO}}{|}}{\overset{\overset{O}{\|}}{P}}-N\overset{X_1}{\underset{X_2}{}}$$

| X$_1$ = H | X$_2$ = Me | DMMP |
|---|---|---|
| H | Et | DMEP |
| H | Prop | DMPP |
| Me | Me | DMDMP |

**Chapter 6**

$$\text{MeO}-\underset{\underset{\text{MeO}}{|}}{\overset{\overset{O}{\|}}{P}}-N\overset{X_1}{\underset{X_2}{}}$$

| X$_1$ = H | X$_2$ = (CH$_2$)$_2$-OH | DMHEP |
|---|---|---|
| H | (CH$_2$)$_3$-OH | DMHPP |
| (CH$_2$)$_2$-OH | (CH$_2$)$_2$-OH | DMHBP |
| H | (CH$_2$)$_2$-OMe | DMMEP |
| H | (CH$_2$)$_3$-OMe | DMMPP |

[1]Chapters 1 and 3 are devoted to introduction and synthesis of phosphoramidates

FR properties and thermal behaviour of cellulose treated with above mentioned compounds were investigated using various analytical and thermal techniques. The morphology of charred cellulose was analyzed using SEM. Elemental analysis was implemented to get further insights into the composition of the chars. Further, degradation of organophosphorus compounds was studied using NMR, and attempts to explain the decomposition mechanism have been performed.

The FR behaviour of treated cellulose was correlated to the structural arrangement of the functional groups which allowed to establish several interesting structure-property relationships. The FR properties were found to be a function of not only the carbon content in the phosphoramidate molecule, but also the chemical nature of carbon (alkyl vs. aryl phosphoramidates). Moreover, presence of reactive functional groups such as amino- or/and hydroxygroups was found to be advantageous as the interaction of these groups with cellulose prior to combustion was determined. As a result of such interaction improved FR properties were established. Increased nitrogen content in the phosphoramidate molecule was shown to have a positive impact on the FR properties of treated cellulose. Investigations performed in the present Thesis revealed the multi-dimensional character of the relationship between structure of phosphoramidates and their FR action.

# Zusammenfassung

Zellulose ist das am weitesten verbreitete Polymer auf der Erde. Über 33 % des gesamten Pflanzenmaterials (Biomasse) besteht aus Zellulose. Heutzutage lässt sich ein Leben ohne Zellulose kaum mehr vorstellen, ist sie doch Hauptbestandteil von Papier, natürlichen Textilien und Holz. Der Verbrauch dieser Materialien hat sich mit der rapiden Verbesserung des Lebensstandards sehr schnell erhöht, was strengere Sicherheitsanforderungen mit sich brachte. Die Wissenschaftler sind daher gefordert, Methoden zur Verringerung der Risiken zu entwickeln, welche aus der Verbrennung von Zellulose-Materialien und insbesondere Textilien entstehen können.

Wie kann Flammstabilität (FS) bei Zellulose erzielt werden? Es gibt eine Vielzahl chemischer Verbindungen, die zu hervorragenden Flammschutz-Eigenschaften führen, wie beispielsweise Halogen-, Antimon-, Bor- oder phosphorhaltige Moleküle. Alle diese Verbindungen haben ihre Vor- und Nachteile. In der vorliegenden Arbeit haben wir uns auf phosphororganische Verbindungen konzentriert, da diese Klasse von Flammschutzmitteln am häufigsten für Zellulose und zellulosehaltige Materialien verwendet wird. Das chemisch-aktive Zentrum in diesen Verbindungen ist Phosphor. Phosphor ist in der Lage, Zellulose bei der thermischen Behandlung zu phosphorylieren und somit seine vollständige Zersetzung und damit Freisetzung von Wärme zu verhindern. Zugabe von Stickstoff unterstützt diesen Vorgang und verbessert somit das Flammschutz-Verhalten von zellulosehaltigen Materialien wesentlich (Phosphor-Stickstoff Synergismus). Stickstoff kann als Additiv unter Verwendung von Harnstoff-Derivaten, Melamin-Formaldehyd- oder Guanidin eingeführt werden, oder es kann in die FS-Moleküle analog wie in verschiedene Phosphorsäuren-Amide integriert werden.

In der Literatur wurde eine grosse Vielfalt von Studien veröffentlicht, die sich mit der Un-

tersuchung von potentiellen Flammschutzmitteln für Zellulose, wo Stickstoff im Molekül zusammen mit Phosphor präsent ist, beschäftigen. Nach Entdeckung von 3-(Dimethyl-phosphono)-N-methylolpropionamid in den 1940-er Jahren, besser bekannt unter dem Handelsnamen Pyrovatex[r], haben phosphororganische Verbindungen mit Stickstoff in ihrer Struktur besondere Aufmerksamkeit erhalten. Es beschäftigen sich viele Publikationen mit der Forschung nach den besten Flammschutz-Agenten, welche die physikalischen Eigenschaften von Textilien wie Steifheit, Festigkeit und Luftdurchlässigkeit nicht treuflussen. Allerdings existiert bis heute keine systematische Untersuchung, in welcher die Wirkung von Stickstoff (eingebaut in das FS-Molekül) auf der Entflammbarkeit von Zellulose angezeigt wird. Es ist immer noch unklar, ob der Phosphor-Stickstoff-Synergismus oder strukturelle Effekte eine wichtige Rolle in Phosphor- und Stickstoffhaltigen Verbindungen spielen. In mehreren Studien wurde beobachtet, dass die Bindung von Phosphor zu verschiedenen Elementen die gesamten Flammschutz-Eigenschaften der Verbindung beeinflusst. In anderen Studien wurde festgestellt, dass die Präsenz bestimmter funktioneller Gruppen wie Hydroxyl sich auf die flammhemmende Leistung der Verbindung für Zellulose auswirkt. Allerdings wurden in keiner dieser Studien die Flammschutz-Eigenschaften von Werkstoffen im Hinblick auf ihre Struktur systematisch untersucht.

Das Hauptziel der vorliegenden Studie liegt deshalb darin, die Struktur-Eigenschaften-Beziehungen in P-N-haltigen Verbindungen zu erforschen und strukturelle Veränderungen in Relation zu den Veränderungen im flammhemmenden Verhalten zu setzen. Die Untersuchung wurde an zwanzig verschiedenen phosphororganischen Verbindungen durchgeführt. Als Kernstruktur wurde die Struktur der Phosphorsäure genommen und die Hydroxylgruppen wurden entweder mit Alkyl- oder Aryl Estergruppen, Alkylamino, Hydroxyalkylamino- und/oder Aminogruppen ersetzt.

Die in dieser Studie untersuchten Moleküle wurden zudem so gewählt, dass strukturelle Unterschiede zwischen ihnen gering waren. Dies erlaubte uns, Änderungen in den flammhemmenden Eigenschaften den vorgenommenen strukturellen Veränderungen zuzuschreiben. In der vorliegenden Studie wurden die strukturellen Veränderungen mit den Flammschutz-Eigenschaften korreliert, wobei folgende Auswirkungen qualitativ analysiert wurden:

- Chemische Bindung von Phosphor zu Wasserstoff, Kohlenstoff, Sauerstoff und Stickstoff,

- Auswirkungen der Alkylkettenlänge,

- Einfluss der Art der Aminogruppe - primäre, sekundäre oder tertiäre,

- Wirkung von Hydroxyl-Gruppen,

- Wirkung des Substituierens der Hydroxylgruppe an Methoxygruppe,

- Auswirkungen der Anzahl der Aminogruppen.

FS-Eigenschaften und das thermische Verhalten von Zellulose, welche mit oben genannten Verbindungen behandelt wurde, wurde mit verschiedenen analytischen und thermischen Techniken untersucht. Die Morphologie der verkohlten Zellulose wurde mittels Rasterelektronmikroskopie analysiert. In dieser Analyse-Phase wurde zusätzlich die Elementenanalyse eingesetzt, um weitere Einblicke in die Zusammensetzung der Asche zu erhalten. Weiter wurde der Abbau der phosphororganischen Verbindungen mittels Kernmagnetischen Resonanzspektroskopie (NMR) untersucht. Als Resultat wurden mögliche Erklärungen für die Zersetzungs-Mechanismen diskutiert.

Das flammhemmende Verhalten der behandelten Zellulose wurde mit der strukturellen Anordnung der funktionellen Gruppen korelliert, was einige interessante Struktur-Eigenschaft-Beziehungen zu etablieren erlaubte. Es wurde gefunden, dass die Flammschutz-Eigenschaften eine Funktion nicht nur vom Kohlenstoffgehalt im Phosphoramidat-Molekül, sondern auch von der chemischen Natur des Kohlenstoffs (Alkyl und Aryl Phosphoramidaten) sind. Ausserdem hat sich die Präsenz der reaktiven funktionellen Gruppen wie Amino- oder/und Hydroxygruppen als vorteilhaft erwiesen, da die Wechselwirkung dieser Gruppen mit Zellulose vor der Dekomposition nachgewiesen wurde. Als Ergebnis solcher Wechselwirkungen wurden verbesserte Eigenschaften der Phosphoramidaten etabliert. Ein hoher Stickstoffgehalt in den Phosphoramidat-Molekülen hatte eine positive Auswirkung auf die Flammschutz-Eigenschaften behandelter Zellulose. Untersuchungen, die in der vorliegenden Dissertation durchgeführt wurden, zeigten den multidimensionalen Charakter der Beziehung zwischen Struktur der Phosphoramidate und ihres flammhemmenden Verhaltens.

# Abbreviations

| | |
|---|---|
| ATR | Attenuated Total Reflectance |
| bp | boiling point |
| Cell | cellulose |
| DAP | dialkyl- and diarylphosphoramidates |
| DCM | dichloromethane |
| DEE | diethyl ether |
| EDX | energy dispersive X-ray |
| e.g. | for example (latin *exempli gratia*) |
| ESI | electrospray ionization |
| EtOH | ethanol |
| FR | flame retardant |
| FT-IR | Fourier Transform Infrared Spectroscopy |
| GC | Gas Chromatography |
| h | hour |
| ICP-OES | Inductively Coupled Plasma – Optical Emission Spectroscopy |

| | |
|---|---|
| i.e. | in other words (latin *id est*) |
| LC | Liquid Chromatography |
| LOI | Limiting Oxygen Index |
| MCC | Microscale Combustion Calorimetry |
| min | minute |
| mp | melting point |
| MS | Mass Spectrometry |
| MW | molecular weight |
| NMR | Nuclear Magnetic Resonance |
| SEM | Scanning Electron Microscopy |
| t | time |
| TEA | triethylamine |
| TGA | Thermogravimetric Analysis |
| THF | tetrahydrofuran |
| THPOH | tetrakis-(hydroxymethyl)-phosphonium hydroxide |

# Symbols

| | |
|---|---|
| $\beta$ | heating rate |
| $\mu$ | char yield |
| $h_c^0$ | total heat of combustion |
| $Q(t)$ | heat release rate |
| $N_s$ | nitrogen content in the compound |
| $P_n$ | target phosphorus content |
| $P_p$ | phosphorus content measured before combustion |
| $P_r$ | phosphorus content measured after combustion |
| $P_s$ | phosphorus content in the compound |
| $P_t$ | calculated phosphorus content |
| $T$ | temperature |
| $W$ | weight uptake |
| $\phi$ | relative humidity |

# Glossary
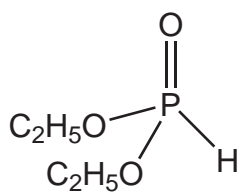
**DEHP**

diethyl hydrogen phosphite
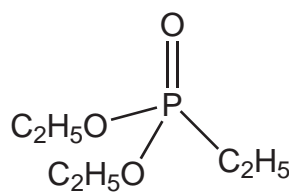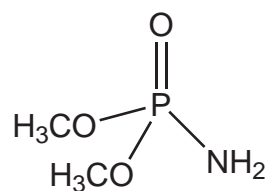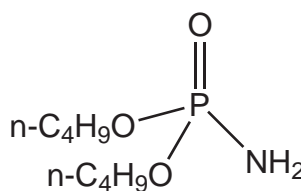
**DEEP**

diethyl-(ethyl) phosphonate
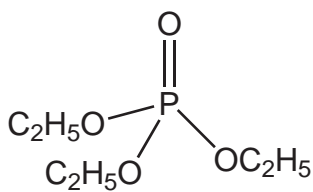
**TEP**
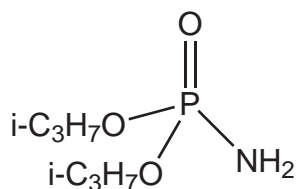
triethylphosphate
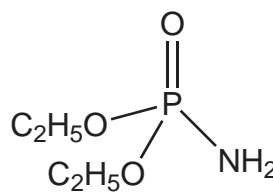
**DEP**

diethyl phosphoramidate
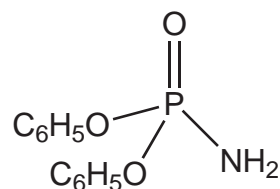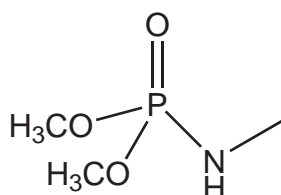
**DMP**

dimethyl phosphoramidate
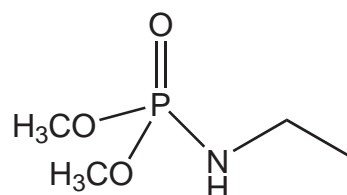
**DBP**

di-n-butyl phosphoramidate
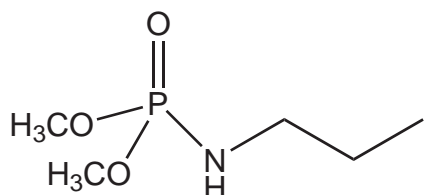
**DiPP**

di-isopropyl phosphoramidate

**DPP**

diphenyl phosphoramidate

**DMMP**

dimethyl-(N-methyl) phosphoramidate

**DMEP**

dimethyl-(N-ethyl) phosphorodiamide

**DMPP**

dimethyl-(N-propyl) phosphoramidate
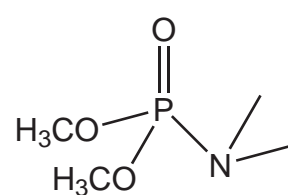
**DMDMP**

dimethyl-(N-dimethyl) phosphoramidate
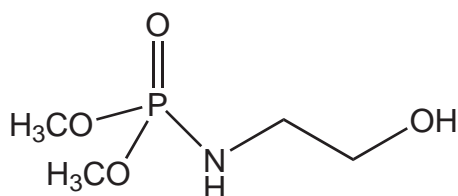
**DMHEP**

dimethyl-(N-2-hydroxyethyl)-

phosphoramidate

**DMHPP**

dimethyl-(N-2-hydroxypropyl)-

phosphoramidate
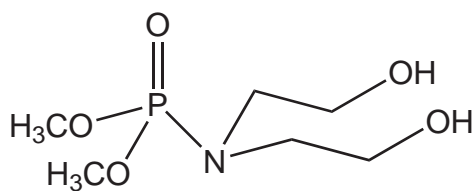
**DMBHEP**

dimethyl-bis(N-2-hydroxyethyl)-

phosphoramidate
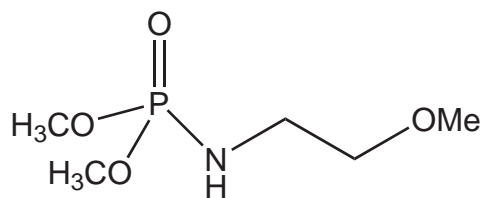
**DMMEP**

dimethyl-(N-2-methoxyethyl)-
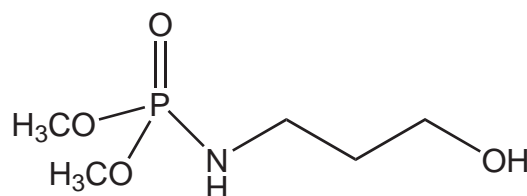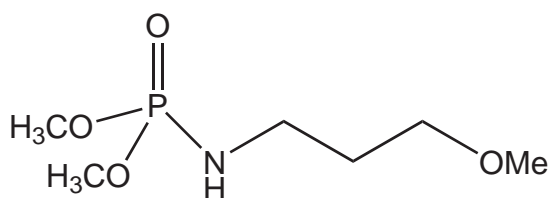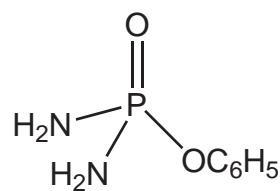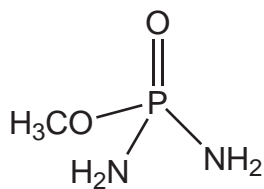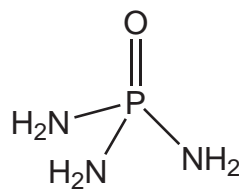
phosphoramidate

**DMMPP**

dimethyl-(N-2-methoxypropyl)-

phosphoramidate

**PPDA**

phenyl phosphorodiamide

**MPDA**

methylphosphorodiamide

**PTA**

phosphoric triamide

# Contents

# Chapter 1

# Introduction

The main disadvantageous property of most organic polymeric materials that restrains their industrial application is their high flammability. According to the fire statistics, the number of fires increased as a consequence of the more widespread consumption of polymeric materials. The European population (ca. 700 millions inhabitants) experiences approx. 2.5 million reported fires annually, resulting in 20'000 to 25'000 fire fatalities and 250'000 to 500'000 fire injuries every year (Centre of Fire Statistics of the International Association of Fire and Rescue Competency CTIF, 2006).

Fig. 1.1 reflects the statistical data on the number of annual fatalities per million for various European countries. About 80% of all fires globally take place in dwellings (Centre of Fire Statistics of CTIF, 2006). While about 20% of those fires are caused by textiles being the material first ignited, over 50 % of all fatalities are caused by these fires [1]. Burning textiles, especially those based on the natural cellulosic fibres as cotton and linen expose serious hazards in such fires, because of their ease ignition and rapid fire propagation.

The hazards related to textile fires were recognized already in early civilizations, and the search for FRs for fabrics goes back over 300 years. The first patent for a textile flameproofing process was applied in 1735 by Jonathan Wyld [2] for a mixture containing "allom, borax or vitreol" to flameproof "paper, linen, canvass and similar substances". Task-oriented research in the area of flame retardant cotton dates back to the early 19$^{th}$ century. Gay Lussac (1820) discovered the ability of ammonium salts of phosphoric acid to flame retard linen fabric. Perkin (1913) conducted research on flameproofing of flan-
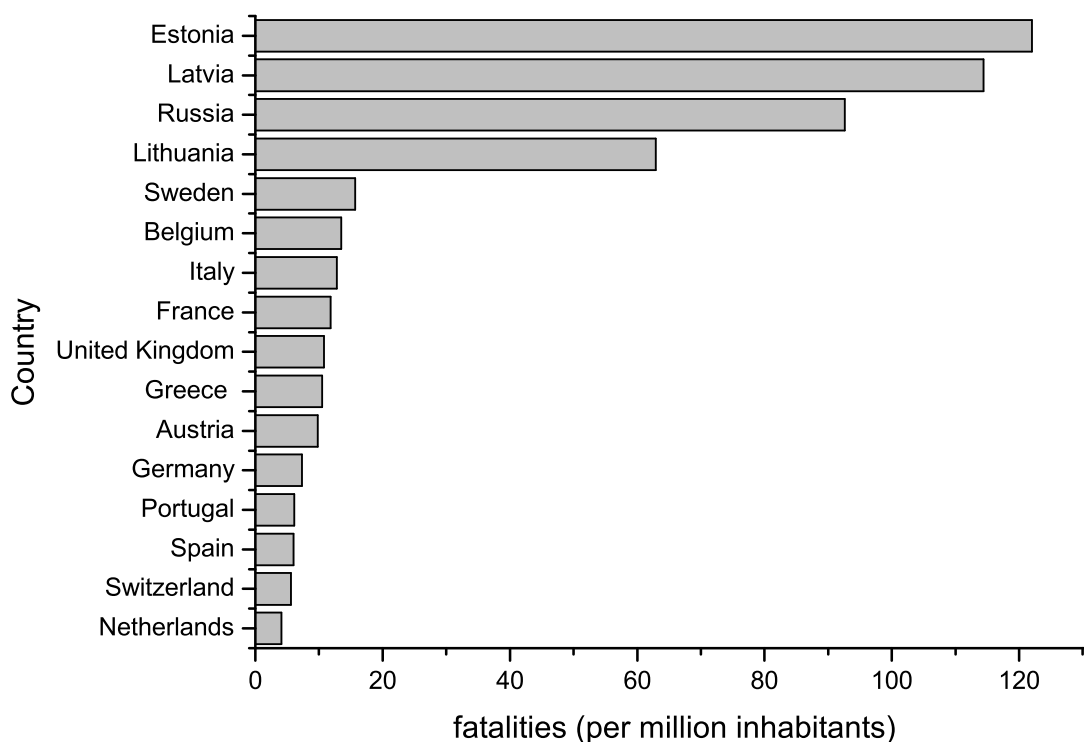
Figure 1.1 Annual fire fatalities in Europe per million inhabitants (Netherlands Institute for
         Safety, 2010)

nelette and defined the requirements for flameproofing processes [3]. A detailed overview
of historical developments since that time until 1960's can be found in the book by Lyons
[4]. Investigations of the later period are reviewed by Lomakin [5].

The requirements for FR materials are steadily changing and expanding. Whereas in the
1950's flame retardancy was considered important only for apparel and building materials,
nowadays various products of electronic, automotive, aircraft and aerospace industries
require new FR treatments to meet stringent governmental regulations. Obtaining FR
cotton fabrics is still a great challenge for the scientific community, as FR cotton fabrics
need to withstand more than 50 hot alkaline launderings in soft and hard water. It is also
important for treated cotton fabric to retain most of its tensile, tear and burst strength,
as well as resistance to abrasion. Further requirements are not to lose its soft hand, air
permeability, appearance and dyeability. No medical problems must arise after treating
cotton flame retardant. Additionally, the industrial requirement such as low cost is also
to be fulfilled, as it is essential in manufacturing of FR textiles.

## 1.1 Flame retardants for cellulose

Cellulosic fabrics can be rendered flame retardant by a number of compounds. These include halogens and antimony combinations (combinations based on antimony oxide $Sb_4O_6$ and chlorine bearing compounds), boron compounds (e.g., borax $H_3BO_3$ alone and in combination with ammonium phosphates), sulfur compounds (e.g., urea sulfamates), salts of different metals (e.g., zinc , calcium, magnesium, aluminum chlorides) and phosphorus compounds (inorganic salts like ammonium phosphate [6, 7, 8, 9], phosphine oxides [10], polyphosphates [11, 7, 12, 8], phosphates [13, 14], phosphorylamides [4], phosphorimides [15, 16, 17, 18, 19, 20, 21] etc.).

All FR cottons are usually produced by after-treating fabrics chemically as a textile finishing process [1]. Two kinds of impregnations can be easily recognized: physically adsorbed species present at the surface which can easily be washed away (e.g. ammonium phosphates, polyphosphate and bromide; borate-boric acid mixtures), and chemically bonded species, which impart a degree of permanency to the treated fabrics (e.g. alkylphosphonamide derivatives, tetrakis-hydroxymethyl phosphonium salt condensates) [22].



tris(aziridinyl) phosphine oxide (APO)

tetrakis hydroxymethyl
phosphonium chloride (THPC)

3-dimethylphosphono-
N-(methylol)propionamide
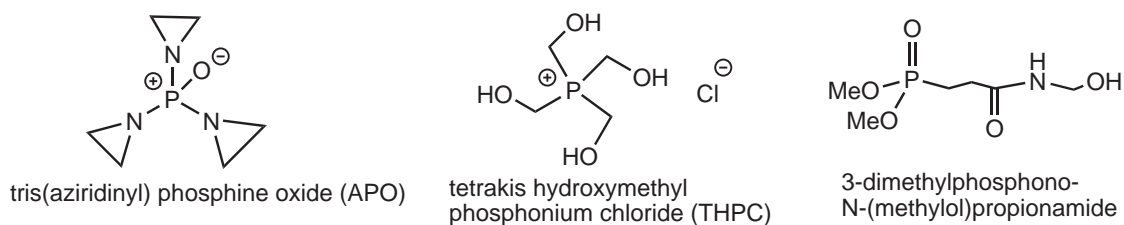
Figure 1.2 Commercial flame retardants for cellulosic materials

Particular attention was attracted to FR that can be chemically bonded to cellulose. Fig. 1.2 presents the most successful commercial FRs for cellulose. The FR formulations on the basis of tris(aziridinyl)-phosphine oxide (APO) were developed by the U.S. Department of Agriculture and by Dow Chemical Co (USA) in 1950's. APO was used in combinations with urea, ethylenediamine, carboxylic acids etc. Cotton fabrics treated with it showed excellent durability to laundering [23]. However, the production was discontinued later in 1970's mainly because of the toxicity of APO and high production costs.

A little later FR formulations based on tetrakis-(hydroxymethyl)-phosphonium chloride

(THPC) were introduced. THPC was combined with melamine, urea, sodium hydroxide etc. and applied to cotton to render it flame retardant. The main difficulty with THPC was the release of HCl during curing step, so the chlorine was exchanged for hydroxide and tetrakis hydroxymethyl phosphonium hydroxide (THPOH) was obtained. A commercially available FR system based on THPOH is Proban[©] developed by Rhodia (UK).

Another commercial product is Pyrovatex[©], developed by Ciba-Geigy (Switzerland). The basis of Pyrovatex[©] is 3-(dimethylphosphono)-N-methylolpropionamide. Treatment of cotton with Pyrovatex[©] gave outstanding results in durability to multiple launderings. The main disadvantage, however, is the release of formaldehyde during curing procedure, which is associated with health risks during processing and end use. FR formulations based on Pyrovatex[©] are still widely used with novel additives, aimed at the reduction of formaldehyde release. However, the quest for a truly formaldehyde-free durable and effective FR for cellulosic materials in particular remains a challenge. Pyrovatex[©] is successful not only because it is capable of reacting with cellulose.

Pyrovatex[©] shows excellent FR properties also due to the nitrogen incorporated in the molecule. The interaction of phosphorus and nitrogen is believed to produce a more effective catalyst for the dehydration of cellulose, which in turn leads to a decrease of combustible volatiles, increase in char formation and to greater phosphorus retention in char. The importance of nitrogen has been emphasized by many researchers in the phenomenon called phosphorus-nitrogen synergism [24, 25, 26, 14]. One speaks of synergism, if the combined action of phosphorus and nitrogen is several times higher than the action of either of the elements alone. Little *et al.* have studied the FR properties of cellulose treated with phosphoric acid and urea and has observed, that a lower loading of both acid and urea was sufficient to reach the same FR effect as if the compounds were used separately [27]. Jones *et al.* have shown the importance of nitrogen by investigating the FR properties of phosphates [28]. They found that increasing the nitrogen content improved the FR properties. Further studies confirmed this finding [29]. Therefore, the search for molecules with good FR properties should be directed towards the class of organophosphorus compounds having both nitrogen and reactive sites in their structure. In order to find a way to develop FRs, it is essential to understand how currently available FR function and to explore the reactions taking place during combustion.

## 1.2 Mode of action of phosphorus flame retardants on cotton

The flammability of any material is determined by its ability to ignite and spread the flame during the combustion process. In the flaming combustion of an organic polymer, the first stage can be regarded as pyrolysis of the polymer in the condensed phase to give volatile combustible products (Fig. 1.3). These products then mix with the surrounding air or other gaseous oxidants and the resulting mixture burns in the gas phase, giving rise to final combustion products and liberating heat, at least some of which is transferred back to the polymer to continue the cycle [30].

The primary role of FR is to interrupt this mechanism. According to Horrocks [15], this can be accomplished in several ways:

- enhancement of decomposition temperature;
  this mode of action is not exploited by conventional FRs as it is usual for materials with inherent heat-resistant properties (e.g, Kevlar fabric, aramides);

- dilution of flame or decreasing formation of flammable volatiles;
  typical for halogen-containing FRs that release hydrogen halide and thus quench the free radicals;

- increasing formation of char.
  This mode of action is characteristic for most phosphorus- and nitrogen-containing FRs in cellulose and wool.

This classification is usually simplified to the terms 'condensed' and 'gas or vapor' phase modes of action. Both terms are composite: if the formation of flammable gases is decreased during the combustion, one says the FR acts in a gas phase. If the increase in char is observed, the FR is acting in a condensed phase. FR acting in condensed phase are believed to be the most-effective, as they promote char formation by converting organic material to char and hence reduce volatile (e.g. fuel) formation [30]. In addition, char can function as a thermal barrier between the condensed and the gas phases which prevents
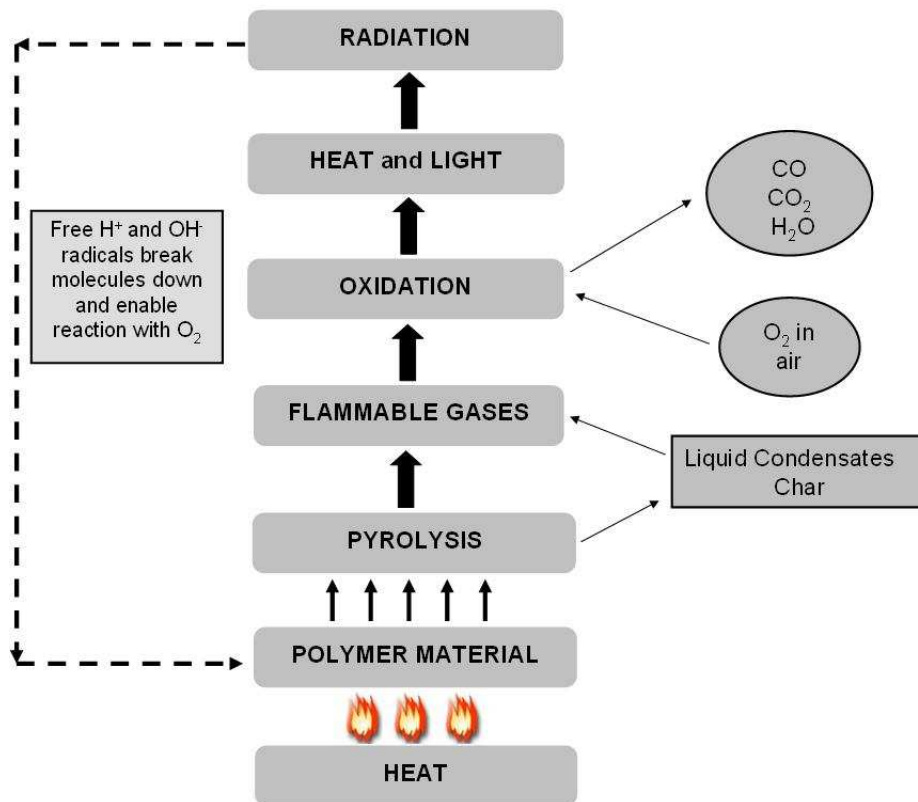
Figure 1.3 Combustion as a feedback mechanism (adopted from [1])

heat transfer back to the pyrolyzing polymer and inhibits the generation of gaseous fuel. FRs which act in this way usually catalyze the formation of char on the polymer surface [31]. In order to understand the char formation during the combustion of treated cellulose, it is important to know, which stage of cellulose combustion can be interfered by FR to produce char instead of combusitble volatiles.

## 1.3   Cellulose and its decomposition

In cellulose, the most abundant polymer (about $30\,\%$ of all live matter), two structures are distinguished: primary and secondary. The primary structure of cellulose consists of $\beta$-1,4-linked glucopyranose units in alternating orientation in a linear chain (Fig. 1.4). In its native form such as cotton, the degree of polymerization of cellulose is believed to vary from 800 to 10'000 units.
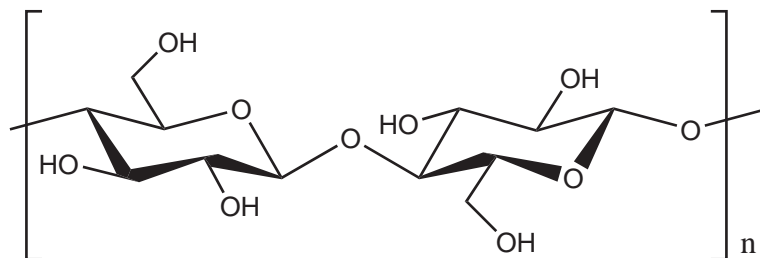
Figure 1.4 Chemical structure of cellulose

The secondary structure of native cellulose is thought to comprise crystalline (highly ordered) and amorphous (disordered) regions. The ratio of crystalline to amorphous structures is around 70:30. Crystalline cellulose is stabilized by extensive hydrogen bonding between parallel chains, involving the hydroxy groups and the hemiacetal (ring) oxygen Fig. 1.5. These groups in the glucopyranose units of the crystalline regions are therefore relatively unreactive compared to those in the amorphous regions.
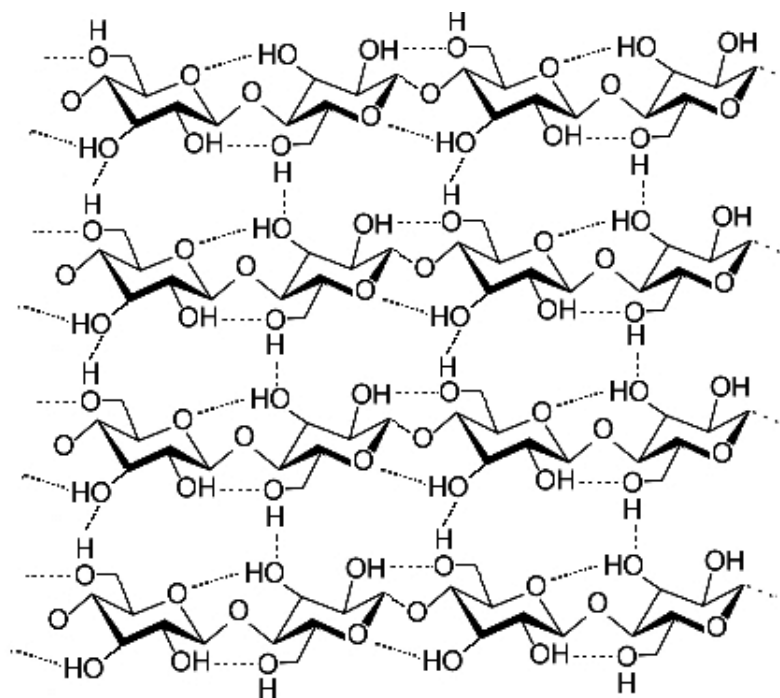


Figure 1.5 Hydrogen bonding in cellulose

Numerous studies which have been conducted on the thermal degradation of cellulose have been motivated by the search for flame retardant textiles [32, 33, 34, 35, 36, 37, 38, 39].

It was shown, that the thermal decomposition of cellulose proceeds through several stages (Fig. 1.6). The first stage occurs at low temperatures (25 – 150°C) and is characterized by the desorption of physically absorbed water (Fig. 1.6). During the second stage at 150 – 240°C, dehydration of cellulose along the chain of glucose units occurs to form the fragments containing carboxyl groups. At the temperature interval 240 – 400°C parallel reactions of depolymerization (intramolecular transglycosylation with breaking of the glycosidic linkage) and dehydration are taking place (third stage). Levoglucosan (1,6-anhydro-$\beta$-D-glycopyranose) is formed [6, 40, 41] at this step, which gives rise to flammable tars. Between 240 – 280°C the reaction is mainly intermolecular dehydration. At the temperatures 280 – 400°C dehydration is combined with decarboxylation and decarbonylation.

The major part of thermal degradation occurs above 280°C, resulting from thermal scission of C–C and C–O bonds. Bond-breaking may occur either within the ring or at the glycosidic linkage between the individual monomer units [35]. At this stage, a complete breakdown of the molecular structure of dehydrocellulose occurs with the formation of volatile organic species, including carbon dioxide, carbon monoxide, water and a carbonaceous char [43]. As a last step, aromatization of carbonaceous intermediates occurs at temperatures of 400 – 700°C.

The formation of levoglucosan and thus the reduction of combustible volatiles can be minimized or eliminated by introduction of FRs. FR are state-of-the-art additives, which are able to catalyze dehydration reaction in the direction of CO and $CO_2$ formation [44]. Phosphorus compounds presumably act by reducing the pyrolysis temperature of cellulose, thus favouring the dehydration pathway of decomposition. However, the chemical mechanism for the reduction of combustible volatile products involves not only the ability of the FR to inhibit the formation of levoglucosan and to catalyze dehydration of the cellulose, but also its potential to enhance the condensation of char to form cross-linked and thermally stable cyclic aromatic structures [45, 33, 34].

The most accepted theory nowadays is that the phosphorus compounds are acid precursors and that the acids perform key functions [46]. These acids are non-volatile at the temperature of burning cellulosic fibres (420°C) and can act as dehydration catalysts. The phosphorus acid is believed to participate by actually phosphorylating the cellulose [47]. Phosphorylation is postulated via alcoholysis of an acidic P–O–P linkage. This reaction
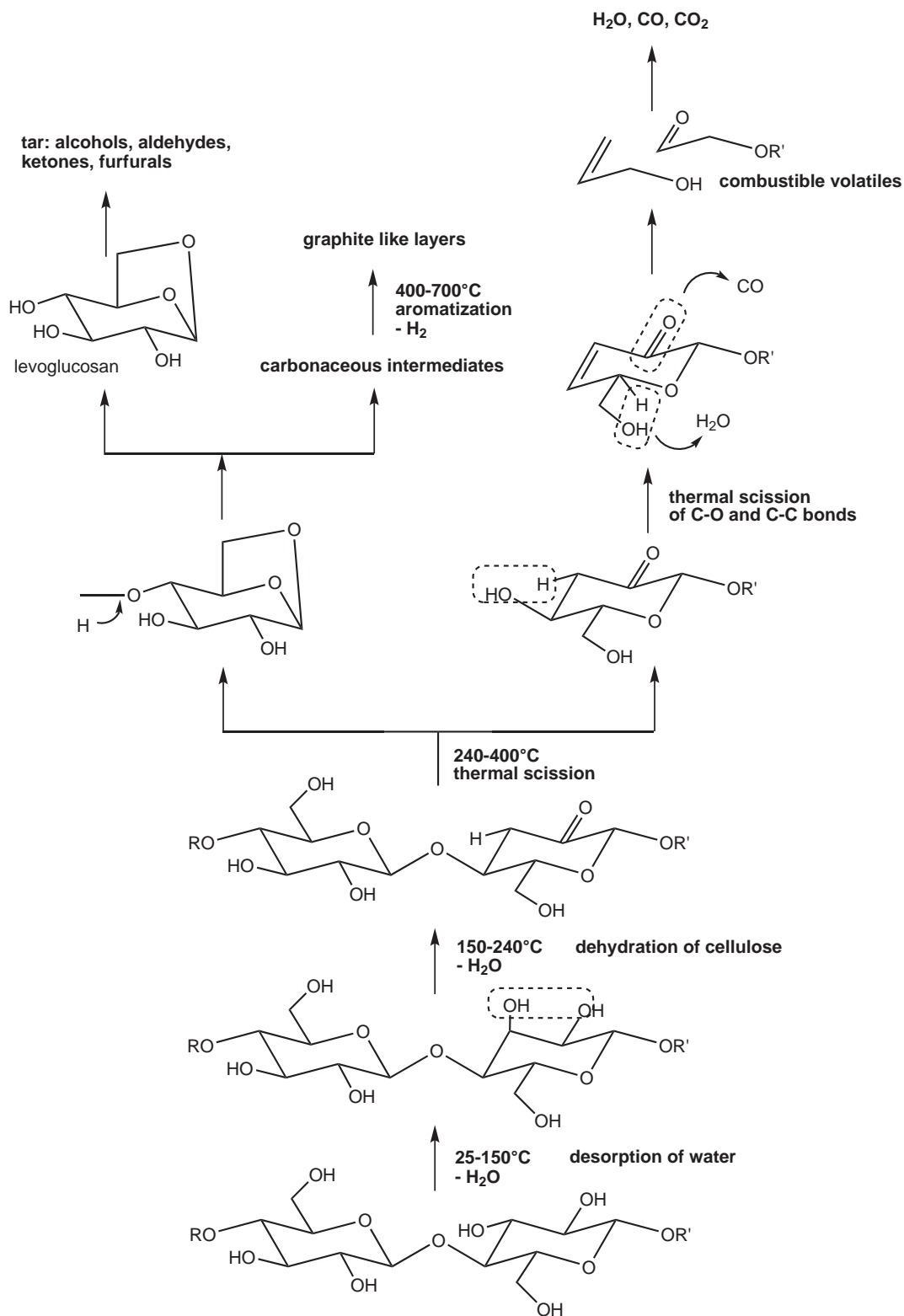
Figure 1.6 Scheme of the pyrolytic degradation of cellulose (adopted from [42])

is known to proceed rapidly at low temperatures [48].

The hydroxyls at C-2 and C-3 positions in cellulose are normally participants via hydrogen bonding in linkages with neighboring cellulose molecules [46], so that it is believed the reaction to happen at the C-6 atoms of the glucosydic units. While considerable research has been undertaken into char formation of flame retarded cellulose, the actual mechanisms of both unretarded and retarded cellulose charring are not well understood yet [49].

In an experimental study of the combustion of a polymer material it is especially important to investigate all the stages in which phase and chemical transformations of the substance are taking place. The complete scheme of the combustion process could be deduced from the study of such characteristics as the thermal properties of treated materials, the morphological structure of the burning surface, the heat liberation and heat losses, the structural transformations during the thermal heating or combustion. In the next section, methods for the investigation of flame retardant behaviour of treated cellulose are introduced.

## 1.4   Methods for investigating the flame retardancy

The methods of assessing polymer combustibility can be subdivided into following types which are ignitability, flame spread and smoke tests, limiting oxygen index test (LOI), calorimetric, thermal analysis methods [5] and hyphenated techniques like TGA-FTIR for the detailed studies of the combustion products. Only methods involved in the present Thesis are described further.

### 1.4.1   Limiting oxygen index test

The limiting oxygen index (LOI) test is normally used to measure the relative flammability of material under carefully controlled conditions. It actually serves as a measure of the extinction ease of the materials. In this test, the sample is burned in a vertical downward direction in an oxygen-nitrogen atmosphere of controlled composition (Fig. 1.7). The oxygen content of the gas mixture is reduced until the atmosphere is no longer able to support

the combustion of the sample, and as a result extinction occurs. This minimum oxygen concentration is termed LOI. Highly flammable materials have low LOI values, and less flammable materials have higher LOI values.
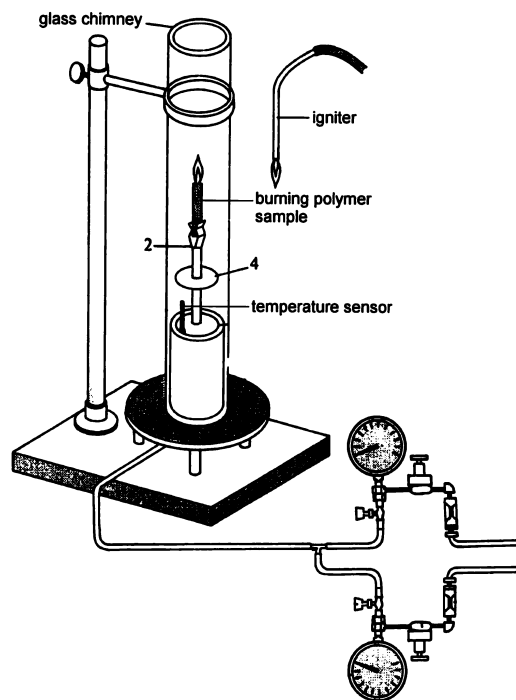


Figure 1.7 Schematic representation of the LOI testing equipment

The LOI is defined as

$$LOI = \frac{[O_2]}{[O_2] + [N_2]} \tag{1.1}$$

LOI is material specific and relatively insensitive towards changes in the sample dimensions. Samples to be tested are normally sized to 5 x 15 cm. The test is very fast, no special preparations are necessary. These advantages make the LOI test to be widely used by many researchers as primary estimation of the flame retardant properties of the material.

However, attention should be paid to temperature during the measurement, as the LOI values decrease with increasing temperature. Since the temperature in fire situation is almost always above ambient, and the burning is most likely to occur in upward direction, the true flammability hazards are usually greater than reflected by the LOI values

[31]. Nevertheless researchers have been using this test for a long time since the required equipment is inexpensive and relatively small sample size is used.

## 1.4.2   Microscale combustion calorimetry

Measuring the amount of heat which is released from a burning material and the temperature at which this heat is released provides important parameters for assessing the flammability of materials. The rate at which heat is released by a burning material is the single most important parameter determining its hazard in a fire, particularly in an enclosed space such as a building, a ship, or an aircraft cabin [50]. This heat release rate $Q(t)$ can be determined using calorimetric techniques. However, heat release rate is difficult to quantify in fire calorimeters, because the test results depend on the external heat flux, sample thickness, sample orientation, edge conditions, ventilation rate etc.

Microscale Combustion Calorimeter, developed by Lyon and Walters [51, 52, 53, 50], was used to determine flammability parameters of various samples. It became an international standard ISO 5660-1. The MCC method has been established as a standard ASTM method (ASTM 7309) for the analysis of solid materials. MCC measurements yield high repeatability with coefficients of variation for three and more replicated measurements less than $3\%$ [54]. The $Q(t)$ measured by MCC using controlled pyrolysis and complete combustion of the fuel gases depends only on the material being tested [55].

The principle of this instrument is relatively simple (Fig. 1.8). The sample (usually 1-5 mg) is placed in the pyrolyzer, where it is heated from ambient temperature to 750°C in nitrogen flowing at 80 cm$^3$min$^{-1}$ at a heating rate ($\beta$) of 1°C s$^{-1}$. Rapid pyrolysis of the polymer in flowing nitrogen generates gaseous products and solid char residue. The gaseous pyrolyzate mixture exits the pyrolyzer and is combined with excess of oxygen, and completely combusted in combustion furnace at 900°C for 10 sec. The heat released during this combustion $Q(t)$ is determined by measuring oxygen depletion and mass-flow rate of the scrubbed gases exiting the furnace. A sharp, reproducible heat release peak $Q(t)$ is obtained which is normalized to the initial sample mass. The sample is also weighed before and after the test to determine the char yield $\mu\,(\%)$.

In the present work, three parameters – the peak specific heat release rate $Q(t)$, heat of
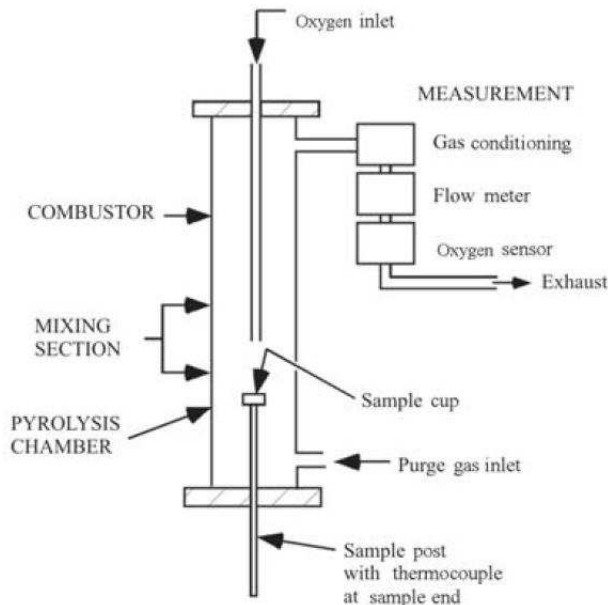
Figure 1.8 Schematic representation of the MCC instrument [55])

combustion $h_c^0$ and char yield $\mu$ at 900°C were determined using MCC. $Q(t)$ is of particular interest to fire scientists, because it is considered as a quantitative measure of its fire hazard. It is obtained by multiplying the height of the fuel pulse with the instantaneous heat of combustion of the fuel at peak mass loss rate [51]. The average heat of combustion $h_c^0$ of the fuel is proportional to the area under the oxygen consumption curve (Eq. 1.2).

$$h_c^0 = \int_0^\infty Q(t)\, dt \tag{1.2}$$

The char yields were determined by measuring the weight of the samples before and after the MCC measurement.

## 1.4.3 Thermogravimetric analysis

Thermogravimetric Analysis (TGA) is a type of testing that is performed on samples to determine changes in weight in relation to change in temperature. TGA is extensively used for evaluation of the thermal stability of various materials, and is commonly employed in research and testing to determine characteristics of materials such as degra-

dation temperatures, absorbed moisture content of materials, the level of inorganic and organic components in materials, decomposition points of explosives and solvent residues.

Fig. 1.9 shows a schematic of the equipment used for this analysis. The sample (usually 5-10 mg) is placed in an alumina pan in a furnace tube. Carrier gas like nitrogen (or any other inert gas) is passed through the system to remove pyrolysis products. The furnace tube is slowly heated at a constant rate. The percentage of weight-loss is recorded as a function of temperature (or time in isothermal TGA [45]). The experiment is conducted in an inert (nitrogen or argon) or oxidizing (air) atmosphere.
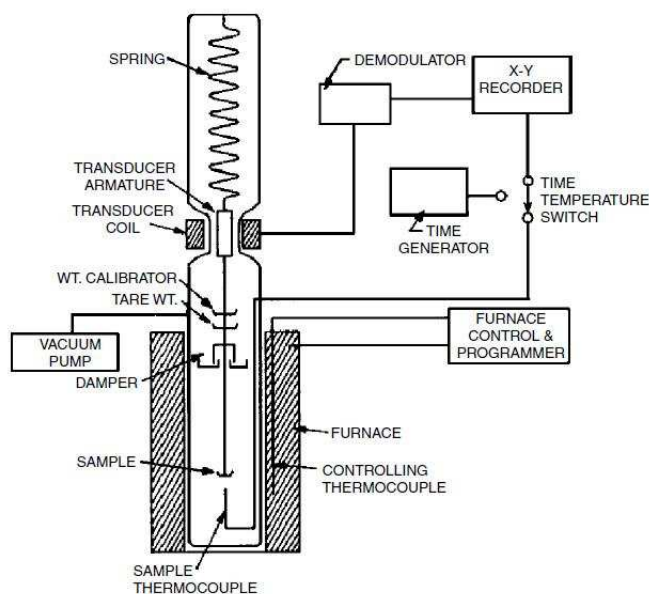
Figure 1.9 Schematic representation of a thermogravimetric analysis system [45]

Analysis is carried out by raising the temperature of the sample gradually and plotting weight (percentage) against temperature. The temperature in many testing methods routinely reaches 1000°C or greater. After the data is obtained, curve smoothing and other operations may be done in order to find the exact points of inflection.

TGA as well as LOI and MCC were extensively employed in the present studies in order to study the flame retardant behaviour of treated fabrics.

### 1.4.4  TGA-FTIR and TGA with subsequent NMR analysis

Combined techniques are very useful for the characterization of various materials. Often a combination of two instrumental methods resolves the inadequacies obtained by individual techniques. The main advantage of the coupled techniques like TGA-FTIR is the identification of gaseous products, which together with the thermal effects and mass changes allow interpreting the course of the investigated reactions. Hyphenated techniques such as TGA-FTIR, TGA-MS, Pyrolysis-GC-MS have been actively used by many researchers [56, 57, 58, 59, 60].
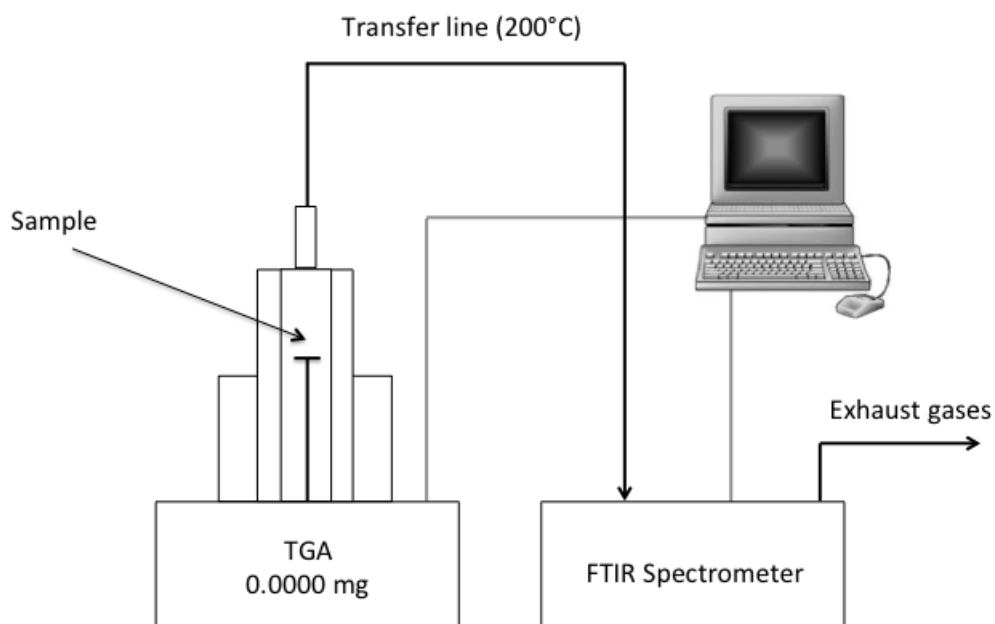


Figure 1.10 Schematic diagram of a TGA coupled with FTIR spectrometer

In the present Thesis, decomposition of treated cellulose was studied using TGA combined on-line with Fourier transform infrared spectrometer. Attempts have been made to identify gaseous products during the thermal decomposition. The coupling of these two techniques allows the gathering of more complete quantitative and qualitative information on FR

behaviour of treated cellulose during the thermal decomposition, which neither technique could provide independently.

Fig. 1.10 provides a schematic diagram of a TGA-FTIR coupled system. In order to obtain the IR spectra of the gases evolved during a thermogravimetric analysis a thermobalance is coupled by means of a heated transfer line to a heated gas cell located inside the TG-IR interface. The gaseous decomposition products are flushed with argon (or nitrogen) through the heated transfer line (200°C) into the gas cell where the IR spectra are measured. The heated cell is fitted with infrared transmitting windows, normally made from KBr, that are spring-loaded to maintain a gas seal at all operating temperatures. The temperatures of the cell and of the transfer line are controlled independently from the TG-IR interface. The gases are transferred from the TGA instrument using a heated transfer-line to avoid condensation. The qualitative analysis is routinely done by comparing recorded spectra with reference spectroscopic signals. The development of hyphenated techniques have been reviewed in detail by Materazzi *et al.* [61, 62].

Using TGA-FTIR the gases evolved during decomposition have been analyzed. To investigate the fraction of the condensed phase, that is soluble in solvents like deuterated chloroform or methanol an off-line NMR have been performed. The heating of a sample was interrupted at specific temperatures, sample was taken out of the oven and cooled down with liquid nitrogen to stop any possible oxidation processes. Further, sample was dissolved in appropriate solvent and solution was analyzed using NMR. The combined analysis of results obtained by means of these techniques allowed precise identification of decomposition products in condensed phase.

## 1.5   Objectives and Outline of the Thesis

Although empirical research has led to the development of highly effective phosphorus-containing systems, no unified theory exists at present that explains the differences in flame retardant action of various flame retardants. The generally discussed modes of action of phosphorus FRs have not been confirmed by experimental data. It is still not clear to what extent the oxidation state of phosphorus affects the efficiency of a phosphorus compound

during combustion of cellulose. Explaining different FR behaviour of organophosphorus compounds was our motivation to conduct a systematic study on a number of organophosphorus compounds, designed in such way, that it was possible to correlate their structural differences with the FR properties.

The goal of this Thesis is to identify the nature of the influence of the phosphorus chemical environment on its FR efficiency. The research was focused on phosphoramidates and phosphoric amides as most promising FRs for cellulose. In order to correlate structural changes to the variations in FR properties, twenty compounds containing various functional groups were investigated (see Glossary). Their efficiency in flame-retarding cellulose was compared in order to investigate the influence of substituents at the phosphorus atom on FR properties of treated cellulose.

The chapters are organized as follows:

In Chapter 2 a preliminary study is presented. It had as goal to show the importance of nitrogen incorporated in the structure of compound. Four simple model compounds representing the most common classes of organophosphorus compounds - phosphites, phosphonates, phosphates and phosphoramidates have been used for the study: diethyl hydrogen phosphate **DEHP**, diethyl-(ethyl) phosphonate **DEEP**, triethyl phosphate **TEP** and diethyl phosphoramidate **DEP**. The presence of nitrogen was found to be essential for good flame retardancy, therefore further research was conducted on phosphoramidates. The bonding O=P–N– was kept constant through the studies and only the substitutes at the phosphorus atom were changed (see Glossary).

Chapter 3 describes synthetic procedures to obtain phosphoramidates, and selected phosphoramidates for this study in particular. The detailed process on the preparation of FR cellulose is also described.

In Chapter 4 the FR properties of dimethyl phosphoramidate **DMP**, diethyl phosphoramidate **DEP**, di-n-butyl phosphoramidate **DBP** and di-isopropyl phosphoramidate **DiPP** have been investigated. The main goal was to find correlations between increasing the carbon content (elongation of alkyl chain) in phosphoramidates and FR properties of cellulose treated with these phosphoramidates.

In Chapter 5 the effect of the substituents at the nitrogen atom of four phosphorami-

dates with secondary and tertiary aminogroups was investigated.  For that purpose the properties of cellulose treated with dimethyl-(N-methyl)- **DMMP**, dimethyl-(N-ethyl)- **DMEP**, dimethyl-(N-propyl)- **DMPP** and dimethyl-(N, N-dimethyl) phosphoramidates **DMMDP** have been studied.

The importance of polar functional groups in the phosphoramidate structure was evaluated in Chapter 6.  Three phosphoramidates having terminating hydroxyl group - dimethyl-(N-2-hydroxyethyl)- **DMHEP**, dimethyl-(N-2-hydroxypropyl)- **DMHPP** and dimethyl-bis(N-2-hydroxyethyl)- **DMBHP** phosphoramidates together with two phosphoramidates with methoxy as terminating group - dimethyl-(N-2-methoxyethyl) **DMMEP** and dimethyl-(N-2-methoxypropyl)- **DMMPP**-phosphoramidates have been investigated.

The impact of substitution of alkoxy groups to aminogroups was studied in Chapter 7 using four compounds: phenylphosphorodiamide **PPDA**, diphenyl phosphoramidate **DPP**, methylphosphorodiamide **MPDA** and phosphoric triamide **PTA**. The effect of increasing the nitrogen content in the FR molecule was shown.

Chapter 8 was dedicated to the detailed studies of decomposition of selected phosphoramidates using combined techniques like TGA-FTIR and TGA with subsequent NMR analysis. Similarities and differences in the decomposition processes of phosphoramidates have been shown.  Based on the results, an attempt to draw a possible decomposition pathway was put forward.

Conclusions are drawn in Chapter 9. Moreover, some interesting suggestions for the continuation of the studies have been put forward in the outlook.  The detailed synthesis of phosphoramidates, their chemical characterization and measurement parameters are presented in Chapter 10.

# Chapter 2

# Initial assessment of structure-property relationship using four model compounds

The present chapter serves as initial assessment where the effect of the functional groups bound to phosphorus atom on the FR properties of treated cellulose is demonstrated. It also establishes the experimental tools exemplarily for a group of four model flame retardants that will serve as a basis for more complex structural modifications in the subsequent chapters.

O
‖
C$_2$H$_5$O — P — R
C$_2$H$_5$O

**DEHP**: R = H
**DEEP**: R = C$_2$H$_5$
**TEP**:   R = OC$_2$H$_5$
**DEP**:   R = NH$_2$

Figure 2.1 General structure of phosphorus compounds studied in Chapter 2

Four simple model compounds representing the most common classes of organophosphorus compounds were taken for the initial studies. They were selected in such way, that the differences in the chemical structure were minor, i.e. only one substituent bound to the phosphorus atom was replaced. The choice of these compounds was also justified by their commercial availability.

## 2.1  Structure-property relationship studies in literature

Organophosphorus compounds is probably the most studied class of compounds used as FRs for cellulose. Over the last 50 years numerous studies related to this topic have been published. The search for effective organophosphorus FRs has resulted in a large volume of literature, but only few studies have been concerned with developing correlations between the chemical structure of organophosphorus compounds and their FR efficiency. Some of them are disclosed further.

Arney *et al.* [63] have performed comparative studies on various classes of organophosphorus compounds. They have shown that the FR effect is reduced from phosphates over phosphonates to phosphites. This effect was not clearly explained, and was attributed to the lower volatility of phosphites, and hence, their decreased gas phase action. Cullis *et al.* [10] have observed differences in flaming behaviour of cellulosic samples, treated with tricresyl phosphate, triphenyl phosphite, triphenyl phosphine oxide and triphenyl phosphine. It was found, that with the same uptake of FR, samples treated with triphenyl phosphite and triphenyl phosphine oxide gave the lowest LOI values. The highest LOI values were observed for dimethyl(methyl)phosphonate-treated cotton.

Tsafack *et al.* [64] have found differences in FR behaviour of diethyl(acryloyloxyethyl) phosphate and diethyl(acryloyloxyethyl) phosphoramidate. The FR action of phosphoramidate was found to be better than of phosphate. Gaan *et al.* [65, 66] have studied the thermal behaviour of cellulose treated with tributyl phosphate, triallyl phosphate and triallyl phosphoramide. They have found that for the same content of phosphorus on cotton, the LOI values for all three compounds were the same. However, the triallyl phosphoramide treated samples yielded slightly higher amounts of char in TGA experiments (nitrogen atmosphere) than triallyl phosphate treated samples (35 % vs. 29 %). They suggested that the presence of nitrogen in the compound not only can lead to the formation of non-volatile species, but also can prevent the oxidation of char. However, the cause for the differences in FR behaviour in these compounds has never been explained.

Systematic investigations on the structure-property relationship in flame retardancy have

been attempted by the group of Schartel [67]. Although this study was performed for epoxy resins, it is worth to mention it here as a good example of the investigations that have only rarely been performed for cellulose. In this work the FR effect of phosphine oxide, phosphinate, phosphonate and phosphate (compounds with different oxidation state) on the thermal properties of neat epoxy resin composites were compared. It was discovered that the ability to inhibit the flame in the gas phase is the best for phosphine oxide epoxy composite, and reduces in order phosphinate, phosphonate, phosphate. The charring effect was found to be the strongest for phosphate, and decreased with decreasing oxidation state till it became of minor importance for phosphine oxide.

Further it is also important to mention numerous studies on the phosphorus-nitrogen synergism. As early as in 1947, Little [27] pointed out that a combination of urea and phosphoric acid used in a pad-and-cure process of phosphorylation produced greater flame resistance in cotton fabrics at a lower add-on than either phosphoric acid or urea used alone. He also reported that other nitrogenous compounds like guanidine and guanylurea could be used instead of urea. Pyrovatex CP$^{©}$ and tris(azirinidyl)phosphate together with some nitrogen-containing additives were studied by Willard *et al.* [68]. When phosphorus content was kept constant and nitrogen amount added was varied, the increase of LOI was found not to obey the linearity.

Reeves *et al.* have discovered that nitrogen contributes most efficiently to phosphorus-containing FRs when it is present in low concentrations relative to the phosphorus. N/P atomic ratios of about one in the fabric lead to maximum flame retardancy [69]. Hendrix *et al.* whilst investigating the FR behaviour of phenylphosphoramides and phenylphosphates have observed that phosphoramides interact with methyl-$\alpha$-D-glucopyranoside at lower temperatures and produced more char than did phenylphosphates or mixtures of phenylphosphates with nitrogenous bases [14].

The compounds used in the present chapter are widely used as FR plasticizers in various resins and engineering plastics [63, 48, 12, 70]. They have also been extensively used to synthesize polymeric molecules with good FR properties [71]. Alkyl esters of phosphoric acid as FRs for cellulose (without any modifications or the use of additives) were barely studied in the literature. However, **DEP** was mentioned in a number of publication as excellent FR agent for cellulose [72, 73, 74, 75].

## 2.2   Treatment of cotton cellulose

Cotton fabrics (180 g/m$^2$, bleached, without optical brightener) were cut into pieces of 15 cm x 15 cm. The weight of one piece was around $4 \pm 0.2$ g. The fabrics were impregnated with the solution of corresponding FR in acetone (liquor). The concentration of liquor was calculated individually for each cotton sample in order to obtain the desired phosphorus uptake on cellulose.

Knowing the phosphorus content in the compound $P_s$, the exact weight of each cotton sample and the necessary amount of phosphorus on cotton $P_n$ (Table 2.1), liquors have been prepared and applied to cotton fabrics in a petri-dish. Fabrics were left for 1–2 hours in air to remove the solvent. The weight of samples before and after impregnation was measured in order to calculate the amount of phosphorus retained on the fabrics $P_t$.

Table 2.1 Molecular mass, boiling point, phosphorus and carbon content of **DEHP**, **DEEP**, **TEP** and **DEP**

| Compound | MW [g/mol] | $P_s$ [%] | C [%] | bp [°C] | $P_t$ [%] |
|---|---|---|---|---|---|
| **DEHP** | 138.10 | 22.43 | 34.75 | 199 | 1.55 |
| **DEEP** | 166.16 | 18.64 | 43.34 | 198 | 1.43 |
| **TEP** | 182.15 | 17.00 | 39.53 | 216 | 1.45 |
| **DEP** | 153.12 | 20.23 | 31.34 | 236 | 1.42 |

The measurement of phosphorus content was performed on fresh samples using Inductively Coupled Plasma - Optical Emission Spectroscopy (ICP-OES) not later than 2 hours after the impregnation. The reason for that was the loss of **DEHP**, **DEEP** and **TEP** from cotton samples if they were exposed long enough to air. The data on phosphorus uptake, presented in Table 2.1 is to exemplarily show the deviation from the calculated (target) content. The content of phosphorus in samples, used in further measurements, is specified for each measurement separately.

## 2.3   Flammability testing

The combustion of untreated cellulose fabrics in the mixture of oxygen and nitrogen occurs in two stages: first, the flame runs quickly over the fabrics leaving a black char, and then

the afterglow (flameless combustion) consumes the char and leaves a negligible amount of ash. The LOI value of untreated cotton was measured to be 18.4 ± 0.5 %. This value differed by ± 3 % with the literature data [76, 77, 66, 78, 79]. This difference is governed by the density of the fabric and the weaving method which was employed in the production of fabrics. The LOI of treated fabrics was increased on average by 12-15 % and the afterglowing effect was observed to vanish. (Table 2.2).

Table 2.2 LOI values and char yields of fabrics treated with **DEHP**, **DEEP**, **TEP** and **DEP**

| Sample | $P_t$ [%] | LOI [%] | $\mu$ [%] |
|---|---|---|---|
| Virgin cotton | 0 | 18.4 ± 0.3 | 2.1 |
| **DEHP** | 1.55 | 22.9 ± 0.3 | 7.5 |
| **DEEP** | 1.43 | 23.6 ± 0.2 | 8.9 |
| **TEP** | 1.45 | 23.8 ± 0.3 | 9.2 |
| **DEP** | 1.42 | 24.7 ± 0.3 | 17.4 |

The LOI of cotton fabrics treated with **DEHP**, **DEEP**, **TEP** and **DEP** were observed to be similar. The chars left after combustion were collected, separated from the unburned pieces of fabric and weighed. Untreated cellulose leaves almost no char (2.1 %, Table 2.2). The char yields of treated cellulose were increased in the same order as LOIs and the highest yield was obtained for **DEP**-treated cellulose samples. It is known that compounds, which are able to yield higher char amounts upon combustion, are better flame retardants. What property can trigger the char formation? In order to find answers on this question, let us examine the chars in detail.

## 2.4 Differences in char compositions and morphology

Pieces of chars left after LOI test were sized to approx. 5 x 5 mm and subjected to EDX analysis. The calculated amount of phosphorus for unburnt fabrics was about 2 ± 0.1 wt. %. In each measurement the sum of C, O, P and N (only for **DEP**) was normalized to 100 at. % as no other elements have been detected in significant contributions. As the relative error in the atomic concentration determination by EDX method lies normally in the range of 2-10 % [80], measurements on five to six different surface areas for each sample were performed to reduce this error.

Table 2.3 shows the atomic percentage concentrations (at. %) of P and C on the surfaces of chars. For almost the same initial phosphorus content on the fabrics (prior to combustion), the highest content of phosphorus after combustion (about 17 %) was found for the char of the **DEP**–treated fabric. Also, the value of phosphorus-to-carbon ratio for **DEP** was the highest, meaning that **DEP** was able to convert the most of tars (fuel for combustion) to thermally stable char. What might be the cause for the higher P-retention? Apparently, the presence of nitrogen triggered phosphorus to remain in the char. Moreover, the morphologies of chars were observed to be different even by naked eye. Therefore, they were further analyzed using Scanning Electron Microscopy (SEM).

Table 2.3 The atomic percentage of carbon and phosphorus measured on chars after combustion of fabrics treated with **DEHP**, **DEEP**, **TEP** and **DEP**

| Sample | $P_t$ [%] | P [%] | C [%] | P/C |
|---|---|---|---|---|
| **DEHP** | 1.95 | 12.8 | 64.9 | 0.19 |
| **DEEP** | 2.13 | 10.9 | 66.7 | 0.16 |
| **TEP** | 2.13 | 12.3 | 59.0 | 0.21 |
| **DEP** | 2.12 | 17.2 | 60.0 | 0.29 |

For the morphological analysis, pieces of chars of about $1\,cm^2$ were cut with razor blades and attached to SEM sample holders with double faced adhesive carbon tape. Prior to the SEM analysis, the samples were sputtered with a layer of gold to increase the conductivity of chars. The voltage of the field gun emission was adjusted to $5.0\,kV$.

SEM images of chars showed that the fibrous structure of cellulose was retained after combustion (Fig. 2.2). The chars of **TEP**- and **DEP**-treated samples exhibited interesting morphologies. In contrast to **DEHP**- and **DEP**-treated fabrics, the surface of chars of **TEP**- and **DEP**-treated samples was covered with some fuzzy particulate matter. The coating was noticeably denser in case of diethyl phosphoramidate. It is possible that such dense coating on fibres contributed to the char yield so that the highest was found for the **DEP**-treated fabric. Apparently, the formation of such coating is associated with higher retention of phosphorus in the char for **DEP**, which in turn can be correlated with stability of FR in thermal conditions (for more details on the origin of such coatings please refer to Chapters 4 and 6). Some researchers have already addressed this question and correlated the FR properties with the boiling point of compounds [63, 46, 81]. In the next step similar correlation was attempted.

a) **DEHP**, 1.68 % P, x2500



b) **DEEP**, 1.54 % P, x2500



c) **TEP**, 1.52 % P, x2500



d) **DEP**, 1.58 % P, x2500
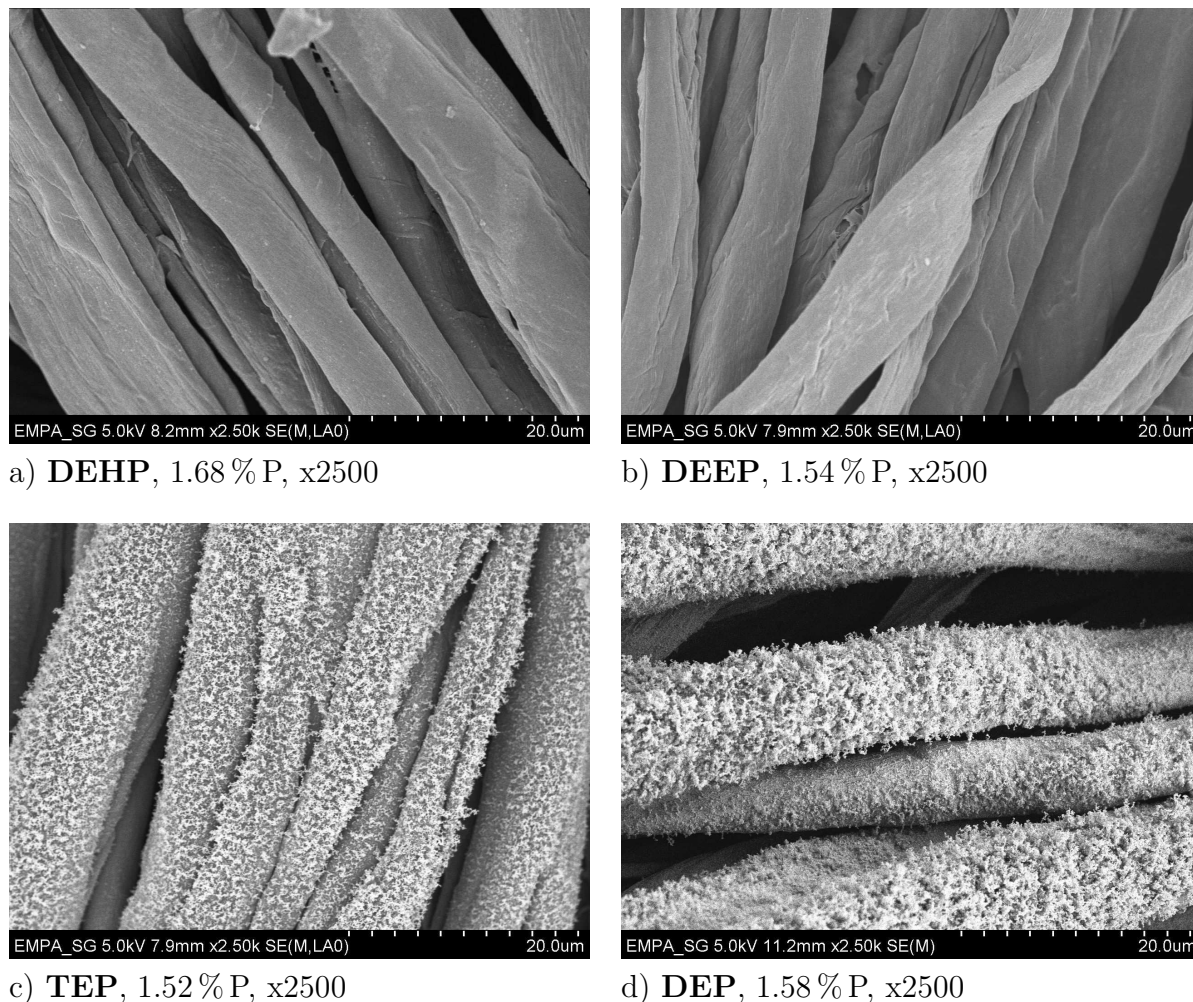
Figure 2.2 SEM micrographs of the chars of **DEHP**-, **DEEP**-, **TEP**- and **DEP**-treated fabrics obtained after LOI test

## 2.5 Boiling point as a factor influencing the flame retardancy

In [46, 81] the higher volatility of compounds was suggested as a reason for improved gas phase interactions. The interactions in the gas phase are believed to involve free radical chain termination reactions that were proposed to explain the flame retardancy of halogen-containing compounds [1] (p. 149). Within the studied compounds, **DEHP**, **DEEP** and **DEEP** have the lowest boiling points, and accordingly should have gained moderate flame retardancy. In fact, their LOI values were increased if compared to untreated cotton.

However, the increased char formation of **DEHP**, **DEEP** and **TEP** as compared to untreated cellulose indicates, that gas phase reactions do not seem to play a major role in flame inhibition, although dialkylphosphites were found to be highly reactive in free radical reactions [82] and trialkylphosphates are capable of abstracting oxygen from alkoxy radicals [83]. The FR activity of volatile compounds will mostly depend on the type and activity of phosphorus radicals formed in flame.

However, one cannot underestimate the significance of the boiling point for flame retardancy. It was indicated earlier, that **DEHP**, **DEEP** and **TEP** might be lost from the surface of cellulose if exposed to air. This was not the case for **DEP**. **DEP** is a solid compound with a melting point of 53°C. Being non-volatile it is more likely to stay on cellulose at increasing temperature, thus increasing the interaction with cellulose, although other factors (which will be addressed in further chapters) are becoming more important. The superior action of **DEP** as FR is related to the presence of nitrogen, which affects the decomposition of cellulose, leading to an increase in char formation. In the next section, the decomposition of **DEHP**, **DEEP**, **TEP** and **DEP** was studied in detail.

## 2.6    Thermal degradation of treated cellulose

Treated cellulose samples were pyrolyzed at a rate of $1°Cs^{-1}$ and the heat release response as a function of temperature was measured. Fig. 2.3 represents the $Q(t)$ dependence on the temperature for treated fabrics and for untreated cotton. The highest peaks are the main decomposition peaks of cellulose treated with phosphorus-containing compounds. For untreated cotton, the crest of the main decomposition peak was observed at 384°C. The decomposition temperature of treated cellulose was lower than that, because phosphorus-containing compounds reduce this temperature (Table 2.4).

The differences in the decomposition temperatures among treated cellulose samples are the first indication on the ability of compound to suppress the cellulose combustion. The decomposition temperature of cellulose treated with **DEP** was reduced to 298°C, which was the lowest among the four compounds. Moreover, the heat of combustion $h_c^0$ (the integral of the area under the $Q(t)$ curve) of **DEP**-treated cellulose was the lowest, meaning
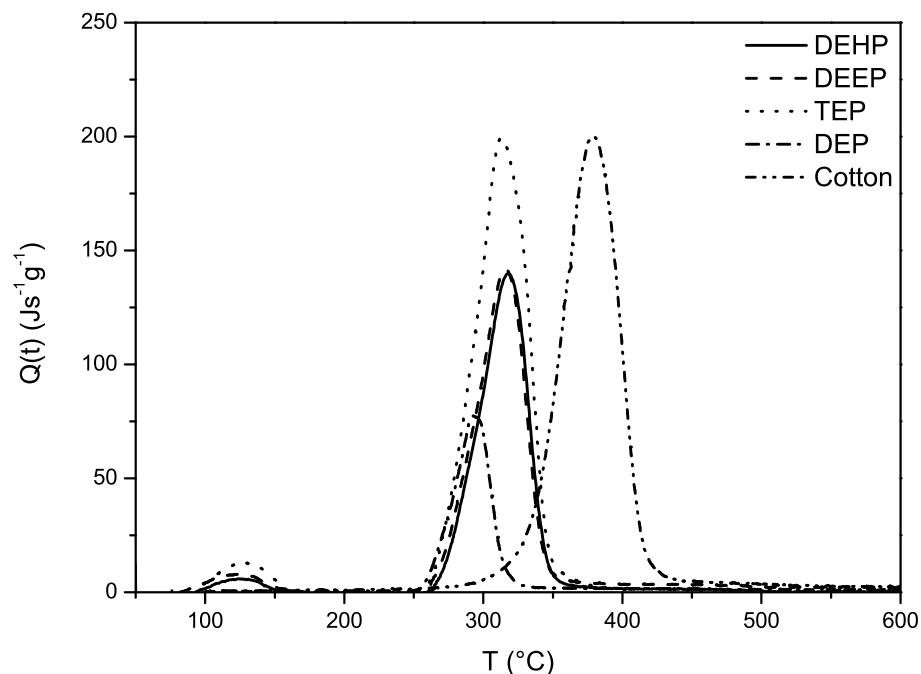
Figure 2.3 Dependence of the heat release rate on the temperature for cellulose treated with
**DEHP**, **DEEP**, **TEP** and **DEP** (ca. 2 % of phosphorus)

that **DEP** was able to reduce the heat evolved during combustion to the minimum. In
other words, the combustible fuel (carbon and hydrogen) was protected from oxidation to
a higher extent than for **DEHP**, **DEEP** and **TEP**. Most probably, nitrogen available in
the molecule has affected this behaviour. Why is nitrogen capable of doing that? It is the
question we will try to answer in the present Thesis.

Another interesting feature was observed just before the beginning of the main decom-
position: at 130°C three small peaks appeared in the **DEHP**-, **DEEP**- and **TEP**-
treated samples. The value of the heat release rate $Q_{t1}$ was increased in the order
**DEHP** < **DEEP** < **TEP** at the same $T_1$. The occurrence of these peaks might be ex-
plained as a result of desorption of FR from cellulose and combustion in the furnace. The
$Q_{t1}$ increases as the loading of chemical increases (different molecular weight) at the same
phosphorus content. For **DEP**, however, no peak at this temperature was observed. It
was now an interesting question whether this finding could be correlated with the boiling

Table 2.4 Thermal data on **DEHP**-, **DEEP**-, **TEP**- and **DEP**-treated cellulose obtained from MCC

| Sample | $P_t$ [%] | $Q_{t1}$ [Js$^{-1}$g$^{-1}$] | $T_1$ [°C] | $Q_{t2}$ [Js$^{-1}$g$^{-1}$] | $T_2$ [°C] | $h_c^0$ [kJg$^{-1}$] |
|---|---|---|---|---|---|---|
| Cotton | 0 | 0 | 0 | 196 | 384 | 10.5 |
| **DEHP** | 1.95 | 3.4 | 129 | 138 | 322 | 7.4 |
| **DEEP** | 2.13 | 7.5 | 130 | 139 | 324 | 7.6 |
| **TEP** | 2.13 | 12.7 | 129 | 197 | 320 | 13.1 |
| **DEP** | 2.12 | 0 | 0 | 125 | 298 | 5.9 |

point of FR?

The boiling points of **DEHP** and **DEEP** are around 200°C (Table 2.2), the one of **TEP** is at 216°C. The maximum heat release rate $Q_{t1}$ was found to be for **TEP**. If the occurrence of the $Q_{t1}$ peaks had been caused by the volatility of FR, the $Q_{t1}$ would have been expected to be the highest for **DEHP** and **DEEP**, because the boiling points of **DEHP** and **DEEP** are the lowest. However, this was not the case. We rather believe the origin of these peaks lies in the reduced interaction with cellulose. Hydroxyls of cellulose are most likely to interact with other molecules via formation of hydrogen bonds. **DEP** is the only compound that is capable of providing the mobile proton for the hydrogen-bond formation with hydroxyl groups of cellulose. The peak was therefore not recorded for **DEP**. This phenomenon will be studied in more detail for all phosphoramidates.

As next the total heat of combustion at the main decomposition step was evaluated. The value of total heat of combustion $h_c^0$ for untreated cellulose is 10.5 kJg$^{-1}$ (Table 2.4). FRs normally reduce this value through the production of char instead of combustible volatiles and therefore, reduce the amount of volatile species that typically contribute to the total heat of combustion. The maximum $h_c^0$ of 13.1 kJg$^{-1}$ was measured for the **TEP**–treated sample. Although the $T_2$ was reduced (indicating the interaction with cellulose took place) the $h_c^0$ of **TEP**-treated cellulose was higher than for untreated cellulose. **TEP** contributed to the total heat of combustion, increasing its value to 13.1 kJg$^{-1}$. The total heat of combustion for **DEP** was found to be the lowest.

## 2.7 Conclusions

The FR properties of **DEHP**, **DEEP**, **TEP** and **DEP** have been studied. It was demonstrated, that the FR properties strongly depend on the structure of the molecule and on the presence of functional groups.

**DEP** was shown to possess superior flame retardancy towards cellulose than compounds without nitrogen in their structure, as the LOI values and char yields were observed to be the highest and the heat of combustion the lowest. The retention of phosphorus in the char was also the highest for **DEP**. This phenomenon occurs most probably due to the presence of nitrogen.

The possible interaction of aminogroup with cellulose was suggested as one of the reasons for the improved FR activity of **DEP**. The absence of mobile protons in **DEHP**, **DEEP** and **TEP** leads to the desorption of FR compound from cellulose before the actual decomposition process could begin.

The questions raised in this preliminary study form the basis of this Thesis. It was attempted to answer these questions by conducting a through the thorough analysis of the FR properties of phosphoramidates as the most interesting and promising class of organophosphorus compounds to use as FR for cellulose.

# Chapter 3

# Synthesis of phosphoramidates and their treatment on cellulose

Different synthetic approaches to obtain phosphoramidates are described in the present chapter. The physical and chemical characterization of the FR molecules is also presented. Furthermore, a description of the preparation of FR cellulose using these compounds is provided.

## 3.1   Synthetic routes to phosphoramidates

There exist several methods to obtain phosphoramidates. One method is via the reaction of dialkylphosphochloride with ammonia (or corresponding amine in case of N-substituted phosphoramidates) (Fig. 3.1) [84, 85, 86]. Although this method is quite efficient in terms of setup, the cost of initial dialkylphosphochloride is very high, which hinders its use as adduct for large scale synthesis. Moreover, the yield of the product was found to be very low [85].

Another way to obtain phosphoramidates is to react the trialkyl phosphite with corresponding amine in the presence of carbon tetrachloride (Fig. 3.2) [87]. The disadvantage of this method involves the high content (20 %) of impurities such as trialkylphosphate, alkylphosphorodiamide and sometimes also phosphoric acid triamide.
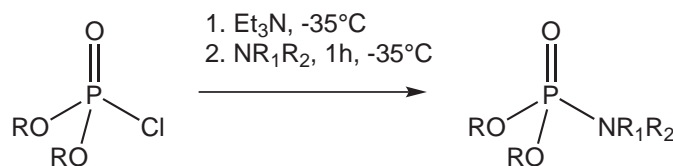
Figure 3.1 Synthesis of phosphoramidates through the use of dialkyl phosphochlorides [84]
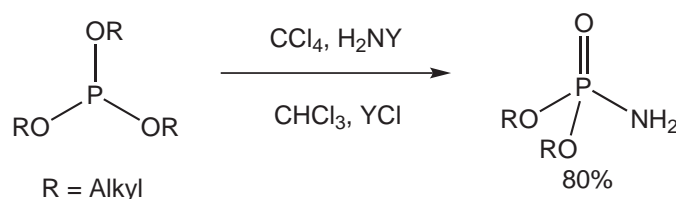


Figure 3.2 Synthesis of phosphoramidates according to Steinbach, Herrmann und Riesel [87]

One further approach involves reaction of a trialkylphosphite with an alkaliazide in the presence of trialkylammoniumhalogenides [88]. In order to obtain products with a good yield, longer reaction times and increased temperatures (especially for aryl-substituted phosphites) were necessary.

The analysis of different synthetic procedures and practical attempts to find the optimal approach have convinced us to use the Todd-Atherton reaction as the easiest in handling and cost-saving method. It was suggested by Atherton and Todd in 1945. They discovered this reaction upon trying to purify dibenzyl phosphite in carbon tetrachloride with an aqueous solution of ammonia [89].

The reaction proceeds in two stages (Fig. 3.3): in the first stage carbon tetrachloride reacts with the phosphite in the presence of base (e.g. triethylamine) to give trichloromethylphosphonate. In the second step, trichloromethylphosphonate reacts with a molecule of amine to yield chloroform and an aminophosphonate. The exact mechanism of Todd-Atherton reaction was thoroughly studied and is described in details in the literature [90, 91, 92, 93, 94].
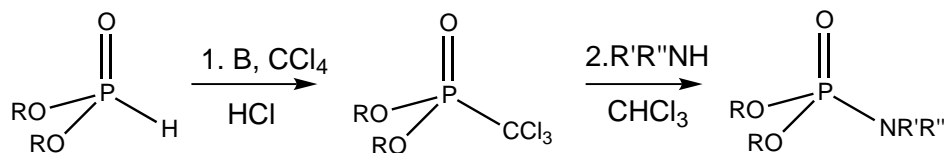
where B = base; R = benzyl or alkyl; R' and R" = hydrogen or organic radicals

Figure 3.3 Synthesis of phosphoramidates after Todd-Atherton approach

## 3.2   Synthesis of dialkyl phosphoramidates

The vast majority of phosphoramidates used in the present Thesis were synthesized using the Todd-Atherton reaction. The basic procedure to synthesize unsubstituted phosphoramidates was the following: dialkyl hydrogen phosphite and carbon tetrarchloride were mixed in equimolar quantities in dried dichloromethane, DCM (or tetrahydrofuran, THF). The reaction mixture was cooled to $-5°C$ using an ice-salt bath. Ammonia was purged through the solution during approximately 2 hours. After the reaction was complete (the completion of reaction was controlled by $^{31}P$ NMR), ammonium chloride was filtered off and washed with DCM (THF) to collect the rest of the product. The solvent was then evaporated and the resulting product was collected.

The procedure to obtain substituted phosphoramidates was slightly different. To a solution of the corresponding amine and triethylamine in (mostly) THF, dialkyl hydrogen phosphite was added dropwise during 1-2 hours. The reaction mixture was cooled analogously to the previous procedure to $-5°C$ using ice-salt bath. At the end of the reaction, the solution was filtered off to separate the product from triethylamine hydrochloride. THF was removed under vacuum. The product was washed with diethyl ether (triethylamine hydrochloride is less soluble in diethyl ether) in order to purify it from the remainder of triethylamine hydrochloride.

## 3.3 Synthesis of methyl phosphorodiamide and phosphoric triamide

One procedure to synthesize methyl phosphorodiamide was put forward by Kasparek *et al.* [95]. They have described the method of obtaining alkyl diamidophosphates through transesterification of aryl diamidophosphates according to the Fig. 3.4. This method was described by the authors as being preferable to the aminolysis of esters of dihalogenphosphoric acids due to the lower cost of initial reagents and easier handling of the materials. However, we were unsuccessful in obtaining phosphoramidates using this reaction. Even modifying the conditions like increasing temperature did not bring a successful result.
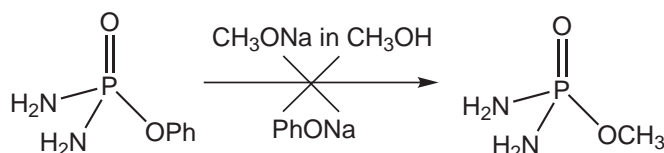


Figure 3.4 Transesterification of aryl diamidophosphates after Kasparek *et al.* [95]

Therefore, methyl phosphorodiamide was obtained using a different procedure: methyl dichlorophosphate was reacted with ammonia according to Fig. 3.5. This procedure was initially described by Klement *et al.* in [96] and was used in the present work to synthesize phosphoric triamide along with methyl phosphorodiamide.
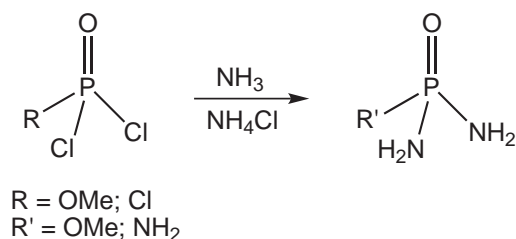


Figure 3.5 Synthesis of phosphoramides after Klement *et al.* [96]

The procedure to synthesize methylphosphorodiamide **MPDA** and phosphoric triamide **PTA** was as follows: gaseous ammonia was bubbled through dry chloroform at -10°C. The solution of methyl phosphoric dichloride (**MPDA**) or phosphorus oxychloride (**PTA**) in chloroform was added dropwise to ammonia dissolved in chloroform during 1.5 hours and intensively stirred at -10°C. After the full addition the reaction mixture was stirred

additionally for 2 hours. Chloroform was removed from the system and the rest dried in vacuum. The product was then dissolved in fresh chloroform and reacted with diethylamine to obtain diethylammonium chloride. The reaction mixture was refluxed during 4 hours. As diethylammonium chloride is soluble in chloroform, it was easy to separate it from the product via filtration. Finally, the product was dried in vacuum. Using this procedure, it was possible to obtain methylphosphoric diamide and phosphoric triamide in good yields (over 90 %).

## 3.4   Characterization of the compounds

The phosphoramidates and phosphoramides prepared were characterized using $^{31}$P, $^1$H and $^{13}$C Nuclear Magnetic Resonance (NMR), Fourier Transform Infrared Spectroscopic and Liquid Chromatography – Mass Spectrometric techniques. Some physical properties such as melting and/or boiling points, colour and $^{31}$P shift are collected in Table 4.1.

Table 3.1 Physical properties of synthesized compounds

| FR | MW [g/mol] | $P_s$ [%] | $N_s$ [%] | mp [°C] | bp [°C] | State, colour | Yield [%] | $^{31}$P [ppm] |
|---|---|---|---|---|---|---|---|---|
| **DMP** | 127.08 | 24.37 | 11.02 | 44 | 224 | crystals, white | 98.7 | 12.0 |
| **DEP** | 153.12 | 20.23 | 9.15 | 52 | 236 | crystals, colourless | n/a | 12.3 |
| **DBP** | 209.22 | 14.80 | 6.69 | 150 | 378 | oil, yellowish | 87.4 | 9.5 |
| **DiPP** | 181.17 | 17.10 | 7.73 | 67 | 234 | crystals, yellowish | 92.7 | 7.6 |
| **DPP** | 249.20 | 12.43 | 5.62 | 112 | - | crystals, white | n/a | 3.2 |
| **DMMP** | 139.09 | 22.27 | 10.07 | - | 204 | oil, yellowish | 88.1 | 12.9 |
| **DMEP** | 153.17 | 20.23 | 9.15 | - | 217 | oil, yellowish | 87.7 | 12.0 |
| **DMPP** | 167.14 | 18.53 | 8.38 | - | 216 | oil, yellowish | 89.8 | 12.0 |
| **DMDMP** | 153.17 | 20.23 | 9.15 | - | 182 | oil, yellowish | 87.6 | 13.6 |
| **DMHEP** | 169.12 | 18.32 | 8.28 | - | 221 | oil, colourless | 95.0 | 12.5 |
| **DMHPP** | 183.14 | 16.91 | 7.65 | - | 220 | oil, colourless | 89.6 | 13.2 |
| **DMBHP** | 213.17 | 14.53 | 6.57 | - | 218 | oil, yellowish | 95.6 | 13.7 |
| **DMMEP** | 183.14 | 16.91 | 7.65 | - | 215 | oil, yellowish | 82.2 | 11.8 |
| **DMMPP** | 197.17 | 15.71 | 7.10 | - | 212 | oil, yellowish | 95.6 | 11.9 |
| **PPDA** | 172.12 | 17.99 | 16.27 | 183 | - | powder, dark violet | n/a | 9.4 |
| **MPDA** | 110.05 | 28.14 | 25.45 | 128 | - | powder, white | 92.6 | 17.4 |
| **PTA** | 95.04 | 32.59 | 44.21 | 135 | - | powder, white | 92.3 | 18.8 |

Most phosphoramidates are oily-like substances, yellowish to colourless. **DMP**, **DEP**, **DiPP** and **DPP** exist as colourless or yellowish crystals. The boiling points of phosphoramidates were found in the range 200 to 380°C, depending on the molecular weight. The yield of almost all reactions was higher than 85 %. The detailed data on the characterization of compounds by NMR and GC-MS can be found in Chapter 10.

## 3.5 Preparation of flame retardant cellulose

The treatment of cotton fabrics was performed analogously to the procedure described in Chapter 2. However, before and after the impregnation, cellulose samples were conditioned in a standard atmosphere (25°C, 760 Torr, $\phi = 65$ %). Thus it was possible to control the moisture uptake (it is known that cellulose absorbs up to 8 % of moisture when exposed to standard conditions) and calculate the FR uptake of fabrics more precisely.
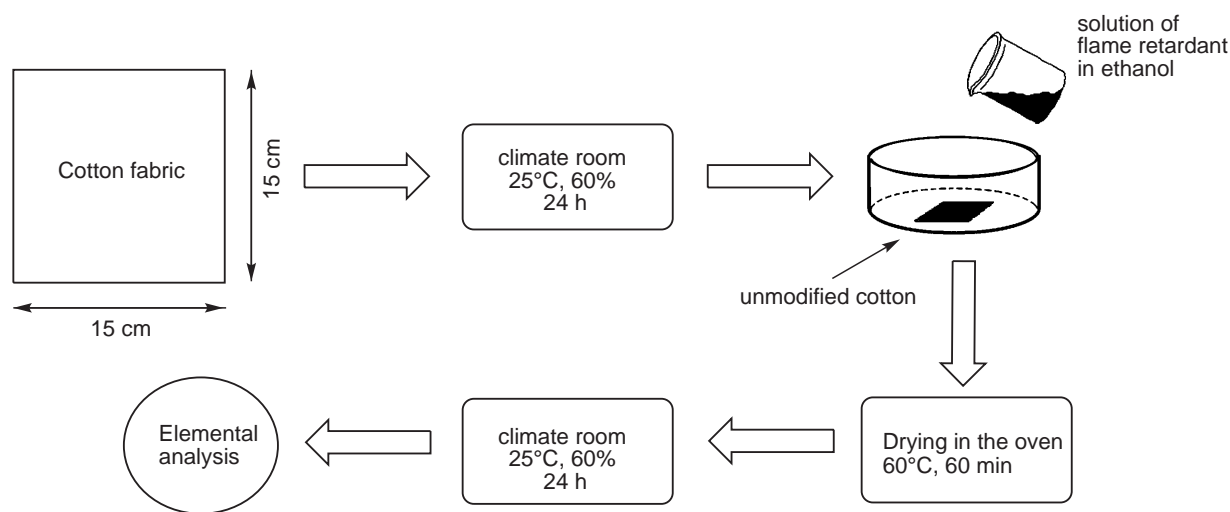


Figure 3.6 Schematic presentation of the cotton cellulose treatment

Samples of cotton were placed in the standard atmosphere and left there for conditioning for at least 24 hours. In order to conduct comparative studies, it was important to obtain similar phosphorus uptakes on cotton fabrics. The needed concentrations of phosphoramidates in ethanol were calculated in order to obtain the target amount of phosphorus on the fabrics $P_n$ (1 and 2 %).

The calculation was performed based on the molecular weights of the compounds, the phosphorus content $P_s$ (Table 4.1), weight of the textile and the amount of solvent (normally 10 ml of ethanol per sample was used). The required phosphoramidate was dissolved in ethanol (in methanol for **PPDA**, **MPDA** and **PTA**), and the cotton samples were impregnated with these solutions (Fig. 3.6). Fabrics were then exposed to air to remove the residual ethanol, and afterwards placed on a frame and dried in a convection oven at 60°C for 1 hour. As next step, fabrics were placed again into the climate room and conditioned for at least 24 hours. The weight of the samples before and after conditioning was recorded. The uptake of the phosphorus on the fabrics was measured using ICP-OES.

## 3.6   Conclusions

Several synthetic methods to obtain phosphoramidates were described. The most effective method in terms of workup and cost was found to be the Todd-Atherton reaction. Using this reaction, all phosphoramidates except for **MPDA** and **PTA** were synthesized for the subsequent investigations.

In an attempt to obtain methylphosphorodiamide from phenyl diamidophosphate, the method suggested by Kasparek was found to be inappropriate. Therefore, methylphosphorodiamide as well as phosphoric triamide were synthesized by reacting methylphosphoric dichloride (**PPDA**) and phosphorus oxychloride (**PTA**) with ammonia.

Synthesized phosphoramidates were characterised using NMR, FTIR and LC-MS techniques and applied to cellulose in order to obtain 1 and 2 % of phosphorus on cellulose to enable further comparative studies.

# Chapter 4

# Dialkyl phosphoramidates. The impact of the alkyl chain length

The FR properties of four dialkyl phosphoramidates (Fig. 4.1): dimethyl phosphoramidate **DMP**, diethyl phosphoramidate **DEP**, di-n-butyl phosphoramidate **DBP** and di-isopropyl phosphoramidate **DiPP** were studied in chapter 4. The differences in the FR properties of cellulose treated with these phosphoramidates were demonstrated. Several hypotheses for their different behaviour were put forward.

**DMP**: R = OMe
**DEP**: R = OEt
**DiPP**: R = O-isoPr
**DBP**: R = O-nBu
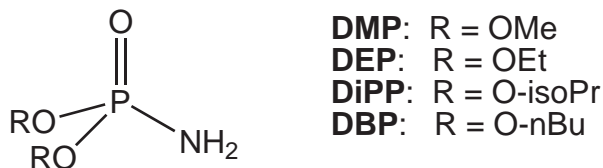
Figure 4.1 General structure of phosphorus compounds studied in Chapter 4

Dimethyl– **DMP**, diethyl– **DEP** and di-n-butyl– **DBP** phosphoramidates were selected to investigate whether the chain length of the alkoxy group affects the flammability of treated cotton cellulose. Using di-isopropyl phosphoramidate **DiPP** it was intended to determine whether the branched alkoxy chain has any significant influence on the flammability of cellulose in comparison to linear alkyl chain.

## 4.1  Physical properties of DMP, DEP, DiPP and DBP and their use as FRs

Let us start with a brief review of physical properties, which will be helpful for the discussion in the upcoming sections. **DMP** is a white crystalline highly hygroscopic compound (Table 4.1) with a melting point of 44°C. **DEP** is a crystalline compound with transparent, highly hygroscopic crystals. It melts at 52°C and boils at 236°C similarly to **DMP**. **DBP** was obtained as a yellowish oily substance. It is slightly soluble in water and boils at 270°C. **DiPP** is a crystalline compound with slightly yellow water-soluble crystals. All four compounds are soluble in polar solvents such as water or alcohols.

Some of these phosphoramidates have already been used to impart flame retardant properties to cellulose. **DEP** and **DMP** have been first mentioned as potential flame retardants for cotton by Glade *et al.* [97]. The authors have found that cotton gained excellent flame retardant properties, when phosphoramidates were impregnated on the fabrics via a pad-dry process in the mixture with several melamine derivatives. However, flame resistant properties were reported to decrease, when cotton was treated solely with phosphoramidates. Unfortunately, there was no data reported on the differences in the efficiency of those phosphoramidates to retard the flammability of cellulose.

Later Gonzales *et al.* [73, 74] have used **DEP** as a flame retardant for cotton in combination with THPOH and trimethylolmelamine to obtain fabrics with increased phosphorus content. The durability of various combinations to laundering was tested as well as the influence of catalyst, concentration of FR and THPOH and cross-linking agents. However, no insight on **DEP** as flame retardant alone was given.

Table 4.1 Physical properties of **DMP**, **DEP**, **DiPP** and **DBP**

| Compound | MW [g/mol] | $P_s$ [%] | $N_s$ [%] | $C_s$ [%] | bp [°C] |
|----------|-----------|-----------|-----------|-----------|---------|
| **DMP**  | 127.08    | 24.37     | 11.02     | 19.21     | 224     |
| **DEP**  | 153.12    | 20.23     | 9.15      | 31.38     | 236     |
| **DBP**  | 209.22    | 14.80     | 6.69      | 45.93     | 270     |
| **DiPP** | 181.17    | 17.10     | 7.73      | 39.78     | 234     |

Burke *et al.* [75] have used **DEP**, **DMP** and **DBP** to synthesize N-hydroxymethyl-

derivatives for the application as durable phosphorus-containing flame retardants for cellulose. They observed that the LOI values decreased in the order dimethyl-(N-hydroxymethyl) phosphoramidate > diethyl-(N-hydroxymethyl) phosphoramidate > di-n-propyl-(N-hydroxymethyl) phosphoramidate. This phenomenon did not receive any closer attention and was not explained in the publication.

Along with the use of these phosphoramidates for cellulose, their application to other natural and synthetic polymers has also been described. Blatz and Del [98] have used **DiPP** and its modifications to impart thermostability properties to several copolymers of acrylic, methacrylic, fumaric and maleic acids. However, no literature was found where **DiPP** would have been used as FR for cellulose.

## 4.2 Treatment of cellulose with DMP, DEP, DiPP and DBP

The FR cotton was obtained utilizing the same procedure as described in Chapter 3. In order to be able to compare the properties of treated fabrics, it was aimed to obtain similar phosphorus uptakes on the fabric samples. The concentration of liquor was calculated such that the dry pickup of phosphoramidate would contain 1 and 2% of phosphorus (Table 4.2).

Table 4.2 Weight uptakes and phosphorus content of the treated fabrics

| FR | $P_n$ [%] | $W_p$ [%] | $P_t$ [%] | $P_p$ [%] |
|---|---|---|---|---|
| **DMP** | 1 | 3.45 | 0.95 | 1.01 |
|  | 2 | 7.46 | 1.34 | 1.53 |
| **DEP** | 1 | 4.89 | 0.98 | 1.01 |
|  | 2 | 5.84 | 1.42 | 1.53 |
| **DBP** | 1 | 7.56 | 1.12 | 1.24 |
|  | 2 | 14.58 | 2.01 | 2.17 |
| **DiPP** | 1 | 3.35 | 0.74 | 0.67 |
|  | 2 | 6.55 | 1.70 | 1.64 |

The expected P-uptakes were different from the measured ones. In most of the cases,

the measured amount of phosphorus was higher than the calculated value. Presumably this results from the change in the ability of cellulose to absorb moisture from air after treatment, because weight uptake has been calculated as the difference between the weight of untreated conditioned and treated conditioned cotton. The further comparative analysis was performed on the samples with similar phosphorus uptakes.

## 4.3   The influence of carbon and hydrogen content as fuel for combustion

In the preliminary studies (Chapter 2) the effect of carbon and hydrogen content in the FR molecule on the flammability of cellulose has been already addressed. However, the exact comparison of the FR properties of studied molecules was rather difficult, as they belong to four different classes and hence, their chemistry is totally different from each other. We believe that with four dialkyl phosphoramidates it was more appropriate to make such comparison.

Firstly, the content of carbon and hydrogen in all four compounds in relation to phosphorus was analyzed. For that measured phosphorus content $P_p$ [%] was multiplied with the C/P and H/P elemental ratio in order to calculate the carbon and hydrogen amount that were introduced to cotton fabrics from the phosphoramidate molecule (Table 4.3).

Table 4.3 Weight uptakes and phosphorus content of the treated fabrics

| FR | $P_p$ [%] | C [%] | H [%] | $\sum$ (C + H) |
|---|---|---|---|---|
| DMP | 1.01 | 0.79 | 0.27 | 1.06 |
|     | 1.53 | 1.20 | 0.40 | 1.60 |
| DEP | 1.01 | 1.55 | 0.40 | 1.95 |
|     | 1.53 | 2.35 | 0.60 | 2.95 |
| DBP | 1.24 | 3.85 | 0.81 | 4.66 |
|     | 2.17 | 6.73 | 1.41 | 8.14 |
| DiPP | 0.67 | 1.56 | 0.35 | 1.91 |
|      | 1.64 | 3.81 | 0.85 | 4.66 |

Treated cotton fabrics were further subjected to the measurement of LOIs. For each sam-

ple, measurement was performed at least 3 times, and the average value including relative error was plotted in Fig. 4.2. To ease the differentiation among four phosphoramidates the trend line was fitted and plotted on the scatter chart. The highest values were obtained for **DMP** and the lowest for **DBP** (Fig. 4.2): the higher was the amount of carbon and hydrogen, the lower was the LOI (Table 4.3). However, no decisive trend could be established, as at different phosphorus content, different flammability behaviour was observed.
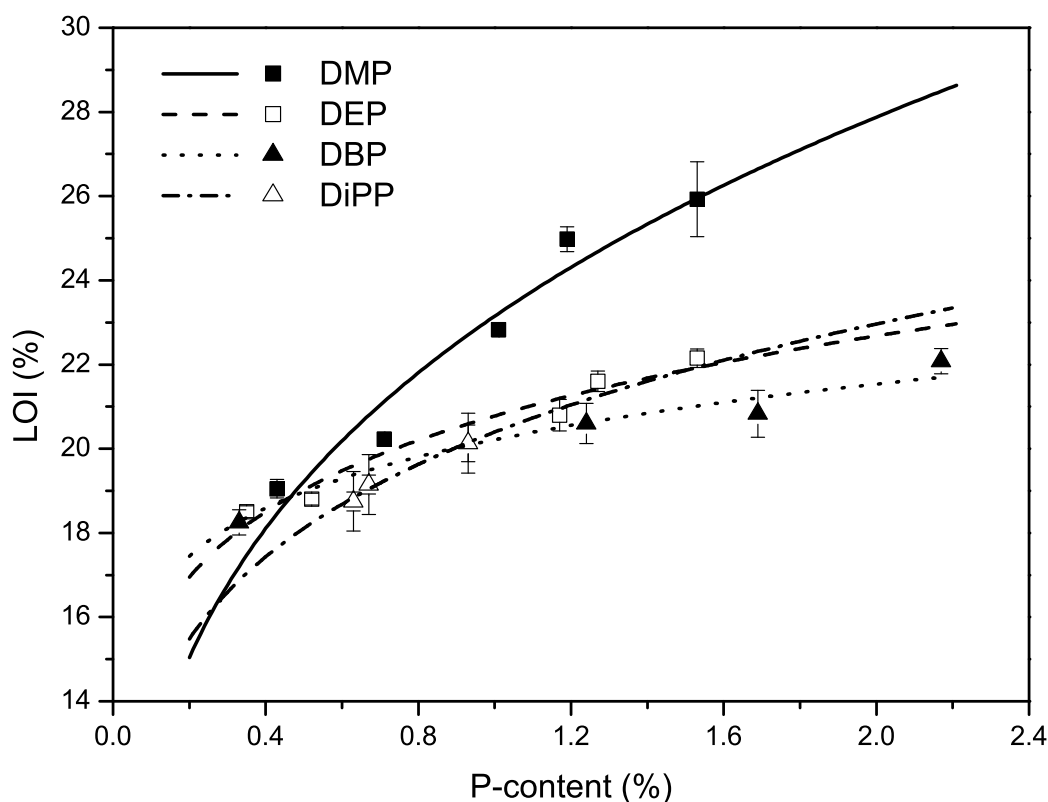


Figure 4.2 LOI vs. phosphorus content for fabrics treated with phosphoramidates **DMP**, **DEP**, **DBP** and **DiPP**

At low phosphorus content (below 0.5%), **DiPP**– and **DMP**–treated samples show lowest LOI values, whereas with increasing of the P-content this trend has changed. Starting from 1% P, **DBP**–treated samples have the lowest LOI and **DMP** – the highest. The slopes are steeper at low concentrations of phosphorus and gradually flatten out at higher concentrations. This phenomenon has already been observed by some scientists [68]. It

was explained as the saturation effect: for every FR molecule a critical phosphorus loading exist, further increase of which will not lead to the increase in LOI. In other words, the dependence of LOI on the content of phosphorus is parabolic. The same effect was observed for dialkyl phosphoramidates. At the P-content of more than 2%, further increase in phosphorus did not produce additional increase in LOI.
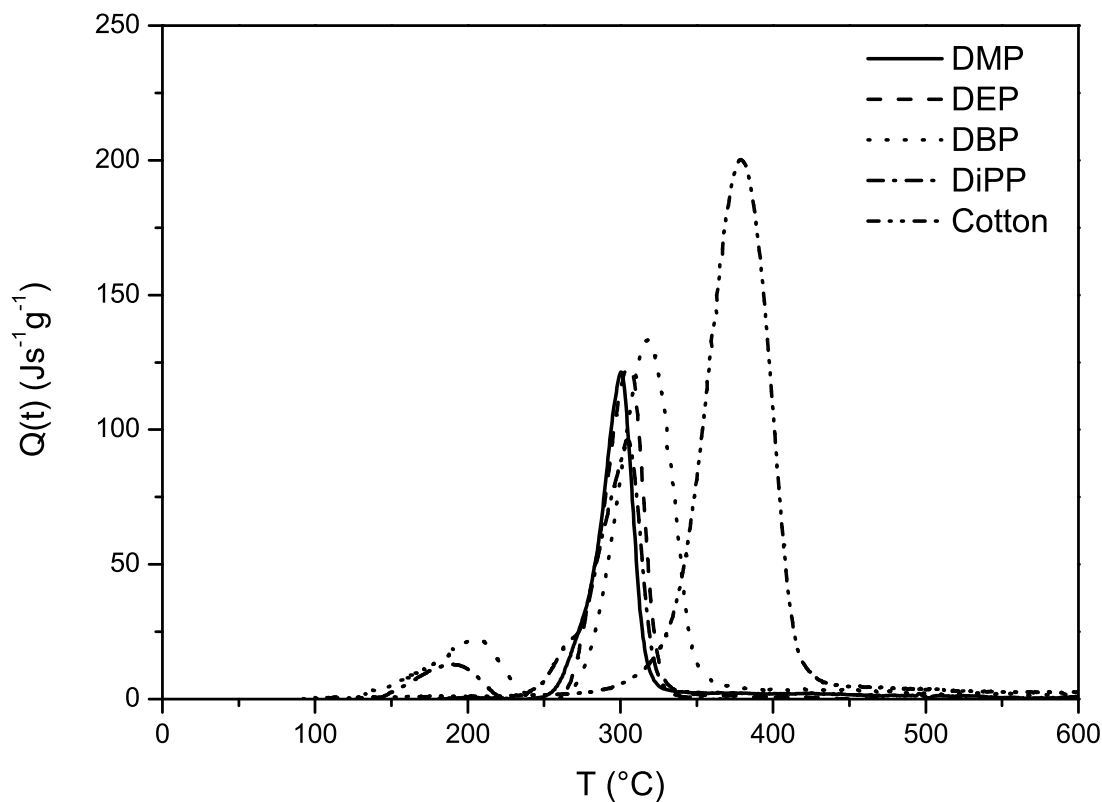


Figure 4.3 Specific heat release rates of fabrics treated with **DMP**, **DEP**, **DiPP** and **DBP** (approx. $1.0\%$ of phosphorus content)

Continuing, an analysis of the same set of compounds using data from microscale combustion calorimetry was performed. Fig. 4.3 shows the dependence of heat release of cotton treated with phosphoramidates (approximately $1\%$ of phosphorus on the fabrics) and of virgin cotton on temperature. When the total heat of combustion $h_{ct}^0$ was compared, the lowest values were found for **DMP**. The $h_{ct}^0$ as well as $T_2$ decreased in the following or-

der: **DBP** < **DiPP** < **DEP** < **DMP**. For **DBP** the total heat release rate was found to be almost twice as high as for **DMP**. Do we deal again with the increasing carbon content and as a result higher flammability? Or does the elongation of the alkyl chain influences the ability of phosphoramidate to reduce the heat release during combustion? The results correlate well with the second hypothesis. The char yields show the same trend as heat release rates and heat of combustion with the lowest being obtained for **DBP**–treated cellulose. Therefore, elongation of the alkyl chain clearly deteriorates the FR properties of treated cellulose.

Table 4.4 Combustion data of cotton fabrics treated with phosphoramidates

|  | P [%] | $Q_{t1}$ [Js$^{-1}$g$^{-1}$] | $T_1$ [°C] | $Q_{t2}$ [Js$^{-1}$g$^{-1}$] | $T_2$ [°C] | $h_{c1}^0$ [kJg$^{-1}$] | $h_{c2}^0$ [kJg$^{-1}$] | $h_{ct}^0$ [kJg$^{-1}$] | $\mu$ [%] |
|---|---|---|---|---|---|---|---|---|---|
| Cotton | 0 | - | - | 192.7 | 384.3 | - | 9.7 | 9.7 | 3.7 |
| **DMP** | 1.01 | - | - | 119.5 | 301.7 | - | 3.5 | 3.5 | 28.2 |
|  | 1.54 | - | - | 115.7 | 299.3 | - | 3.3 | 3.3 | 30.9 |
|  | 2.00 | 7.2 | 194.1 | 110.7 | 297.4 | 0.3 | 2.8 | 3.1 | 35.1 |
| **DEP** | 1.17 | - | - | 120.2 | 302.5 | - | 4.1 | 4.1 | 23.0 |
|  | 1.53 | 1.8 | 165.2 | 119.5 | 299.4 | 0.6 | 4.1 | 4.7 | 22.6 |
|  | 2.12 | 20.8 | 168.1 | 118.9 | 299.2 | 1.4 | 3.5 | 4.9 | 26.5 |
| **DBP** | 1.24 | 18.1 | 207.0 | 132.3 | 319.5 | 1.2 | 6.0 | 7.2 | 15.4 |
|  | 1.69 | 20.0 | 197.7 | 116.5 | 317.8 | 1.8 | 4.4 | 6.2 | 17.9 |
|  | 2.13 | 45.2 | 224.5 | 111.8 | 315.4 | 2.5 | 4.7 | 7.2 | 19.7 |
| **DiPP** | 0.93 | 11.9 | 197.4 | 111.7 | 305.4 | 0.6 | 3.5 | 4.1 | 22.6 |
|  | 1.64 | 14.3 | 190.4 | 96.1 | 303.0 | 0.7 | 3.6 | 4.3 | 25.8 |

## 4.4 Interaction of dialkyl phosphoramidates with cellulose at lower temperatures

As readily observed in Fig. 4.3, two smaller peaks that belong to **DBP** and **DiPP**–treated cellulose samples (at approximately 1% of applied phosphorus) appear at about 200°C. From Table 4.4 it is seen that at higher phosphorus loadings, such peaks appear for **DMP** and **DEP** as well. As already addressed in Chapter 2, these peaks arise due to desorption of phosphoramidate from cotton cellulose and subsequent combustion in the furnace such

that the heat, evolved during this combustion, contributes to the total heat of combustion $h_{ct}^0$ ($h_{ct}^0$ is found as the sum of $h_{c1}^0$ and $h_{c2}^0$).

In order to ensure that desorption might be the reason for appearance of this small peak, the MCC measurements were performed for the pure phosphoramidates. To avoid boiling and rapid volatilization of the liquid oil-like phosphoramidates (**DMP**, **DiPP** and **DBP**), the samples were mixed together with alumina powder, and then subjected to the analysis.
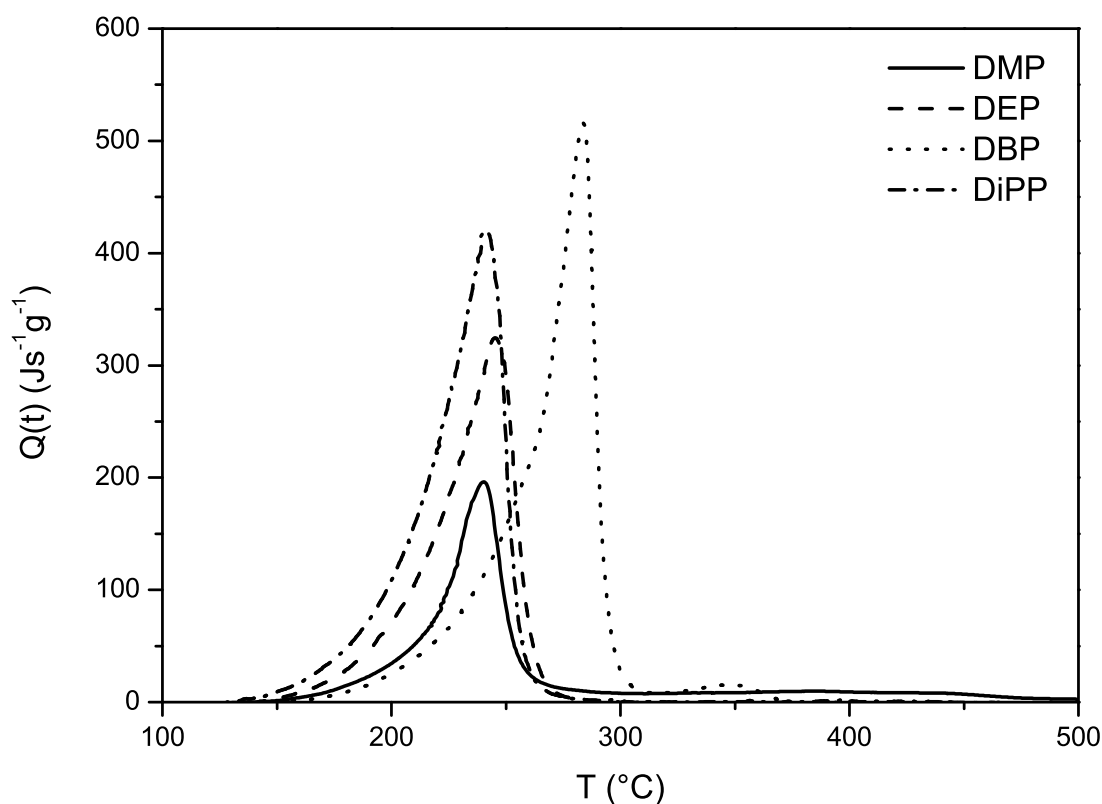


Figure 4.4 Specific heat release rates of **DMP**, **DEP**, **DiPP** and **DBP**

Fig. 4.4 reflects the dependence of the heat release of pure phosphoramidates on the temperature. In the absence of cellulose the heat starts to evolve at around 140-160°C. If compared to the data from Fig. 4.3, the results seem to be consistent. This allows one to conclude that the peaks at 140-160°C arise due to the desorption of phosphoramidate from the vicinity of cellulose. Why these peaks have not been observed for **DMP** at the

phosphorus content of e.g., 1%? Probably because of the difference in the phosphoramidate uptake. For the same P-content of 1%, the phosphoramidate uptake of **DBP** on the cellulose fabric was more than 2 times higher than for **DMP** (Table 4.2). According to Table 4.5 1 g of **DBP** releases the heat which is three times higher than the heat evolved from 1 g of **DMP**. What might cause this behaviour?

Table 4.5 Combustion data of pure phosphoramidates

| FR | $Q_t$ [Js$^{-1}$g$^{-1}$] | $T$ [°C] | $h_c^0$ [kJg$^{-1}$] | $\mu$ [%] |
|---|---|---|---|---|
| **DMP** | 238.4 | 238.7 | 7.2 | 11.6 |
| **DEP** | 312.0 | 255.1 | 14.7 | 5.0 |
| **DBP** | 417.3 | 282.4 | 20.7 | 7.4 |
| **DiPP** | 426.1 | 241.3 | 18.5 | 9.1 |

Two factors can cause it: stronger interaction of **DMP** with cellulose as opposed to **DEP**, **DBP** and **DiPP** and the size or the bulkiness of the phosphoramidate molecule. The first hypothesis will be addressed in detail in Chapter 5, where the effect of primary, secondary and tertiary aminogroups will be investigated. Second hypothesis is discussed in the next section.

## 4.5 Influence of molecular size on the flame retardant properties

In the previous section the saturation effect (LOI measurements) and heat release at low temperatures (MCC measurements) were described. Based on this experimental data, we have attempted to explain these effects.

Fig. 4.5 illustrates the schematic representation of the interaction of phosphoramidate molecules with cellulose. In the upper part space-filling (van der Waals) models of **DMP**, **DEP**, **DiPP** and **DBP** are presented. As the surface of the models represents the van der Waals radius of the molecule, using this type of modeling helps visualizing the space occupied by each atom and the overall molecular size.

In the lower part the desorption process is shown. "S" stays for cellulose surface. The "ac-
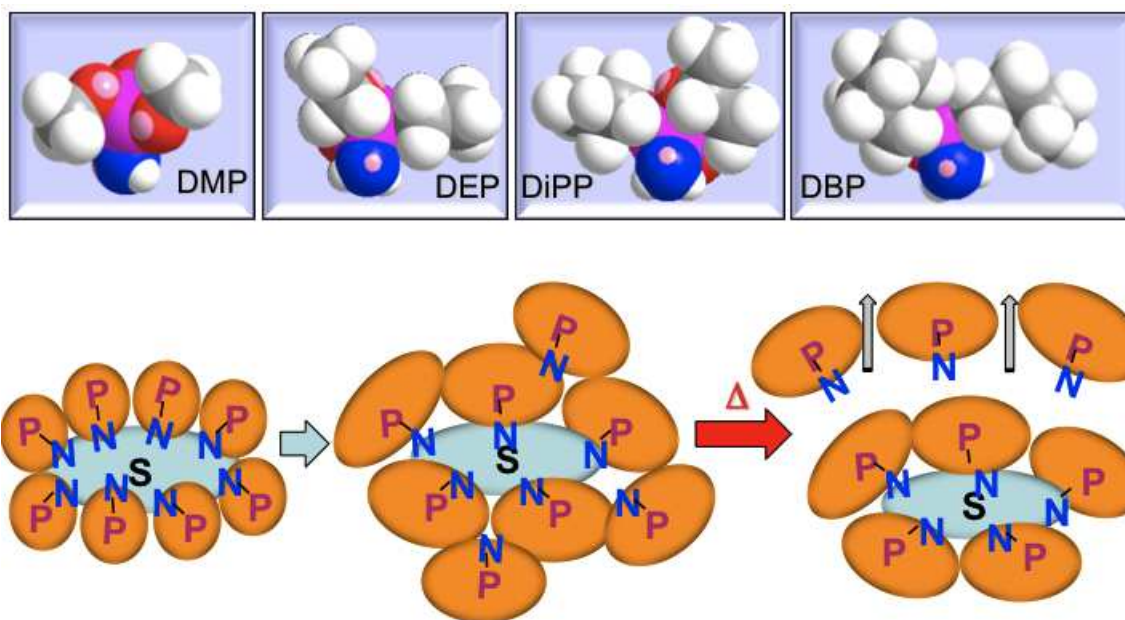
Figure 4.5 Schematic illustration of the interaction of phosphoramidate molecules with cellulose showing the steric hindrance effects, "S" - cellulose surface

tive" part of phosphoramidate molecule that is able to interact with cellulose is aminogroup. If the size of phosphoramidate molecule is rather small, more molecules will be able to interact with cellulose than if the molecule is big (at the same phosphorus content). This will lead to the desorption of unreacted phosphoramidate molecules from the surface of cellulose during the burning, so that these molecules will not contribute to the reduction of cellulose flammability.

The calorimetric data supports this hypothesis. The heat release at around 120°C $Q_{t1}$ was detected neither for **DMP** at 1 and 1.5 % of phosphorus loading, nor for **DEP** at 1 % of phosphorus loading. Indeed, at lower uptakes the entire phosphoramidate is able to interact with cellulose at this temperature to phosphorylate it later at 300-320°C. For bigger molecules like **DBP** even 1.24 % of P-uptake causes saturation effect, and as result, unbound molecules are desorbed and combusted with release of heat.

## 4.6 Differences in char composition and morphology

During calorimetric analysis of the pure phosphoramidates, an interesting trend was observed for the $Q_t$ values. $Q_t$ increased in the order **DMP** < **DEP** < **DiPP** < **DBP** together with the increase of carbon content in compounds. Here, the direct correlation of the carbon content of the phosphoramidate and the evolved amount of heat was established. Moreover, at first sight the peaks exhibit the shape, which is characteristic for volatilization: rather slow increase in heat release in the beginning, rapid increase after 200-220°C and abrupt end at about 260°C for **DMP**, **DEP** and **DiPP** and at 300°C for **DBP**. However, from Table 4.5 one can learn that phosphoramidates were not simply volatilized. The char yields above zero indicated that some kind of decomposition took place that lead to the formation of thermally stable residue. The amount of this residue was different for all four phosphoramidates. Could it be that different kinds of reactions are taking place during the combustion of treated cellulose? Whether the intermediate reaction were similar or not the detailed analysis of the residues can provide answers. In the next step the investigation of the chars composition and morphology was performed. For the sake of consistency morphological analysis and analysis of elemental composition have been performed on the same char samples left after LOI test. At first step the data on the char yield amounts is disclosed.

Fig. 4.6 shows the char yields of treated cotton as function of phosphorus content. The trendline was best fitted in the scatter plot (calculation of R-squared coefficient was performed to obtain the best fit). The char yields generally increase with the amount of applied phosphorus (or phosphoramidate). Among the studied phosphoramidates, char yields were increased in order **DBP** < **DiPP** < **DEP** < **DMP**. Similar correlation was established for char yields obtained after MCC studies (Table 4.4). The higher char yields of **DMP**–treated cellulose again indicate superior FR properties of **DMP**, which have been already discussed in previous sections.

The amount of phosphorus retained on the fabrics before and after combustion as well as of carbon, hydrogen and nitrogen were measured using LECO CHN analysis. Knowing the percentage of the weight uptake before burning, the char yield after burning and the elemental composition before and after burning, it was possible to calculate the gram-
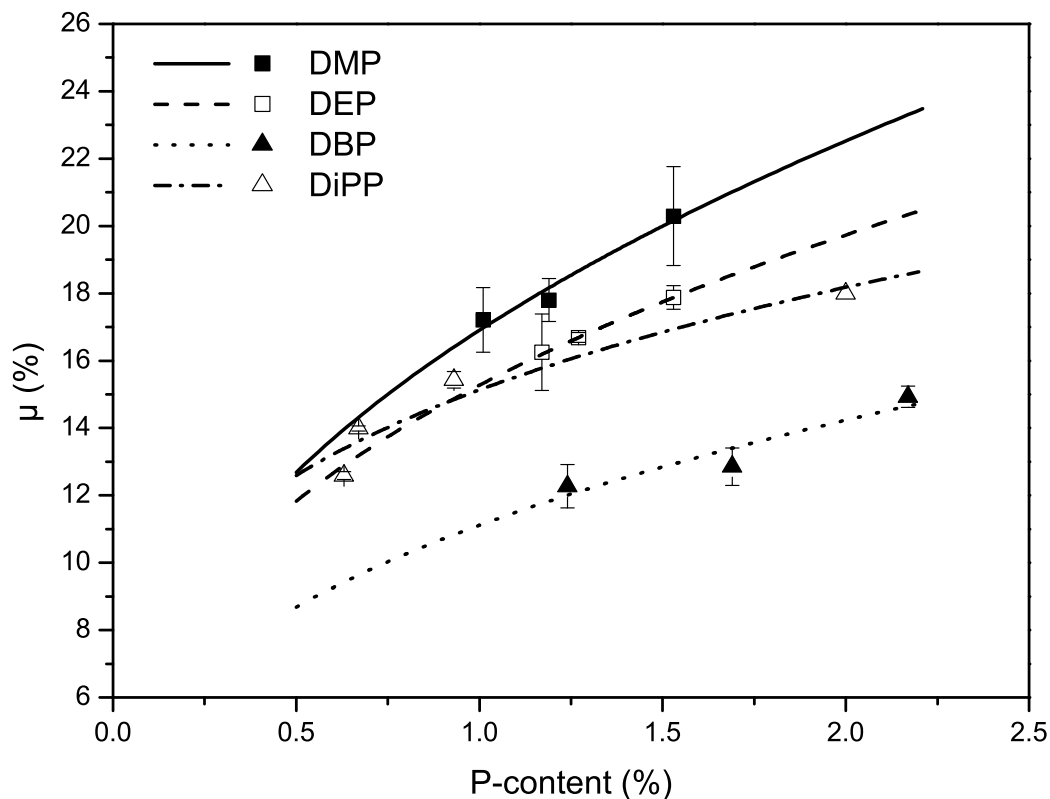
Figure 4.6 The char yields vs. phosphorus content for fabrics treated with **DMP**, **DEP**, **DBP** and **DiPP** (ca. 1.5 % phosphorus content)

atoms of each element (carbon, hydrogen, nitrogen and phosphorus). Using these data the empirical formulae of char and losses during the combustion were derived (Table 4.6).

The species lost to the environment during combustion as well as the composition of remaining char were identical for all four phosphoramidates. Moreover, when multiplying the indices of C, H and O in formulae of loss by two, one obtains $C_6H_{14}O_7$ which corresponds to one mol of glucose $C_6H_{12}O_6$ and one mol of water $H_2O$. Hence, during combustion mostly cellulose and water are lost in the form of CO, $CO_2$ and $H_2O$. The amounts of phosphorus and nitrogen lost during combustion in comparison to other elements were negligible (around 1 %).

Table 4.6 Empirical formulae of chars and losses during combustion of **DMP**–, **DEP**– **DBP**– and **DiPP**–treated cellulose

| Compound | $P_p$ [%] | Formula of loss | Formula of char |
|---|---|---|---|
| **DMP** | 1.54 | $C_{3.00}H_{7.05}N_{0.04}P_{0.03}O_{3.46}$ | $C_{5.90}H_{2.17}N_{0.10}P_{0.15}O_{1.29}$ |
| **DEP** | 1.63 | $C_{3.22}H_{6.92}N_{0.05}P_{0.04}O_{3.27}$ | $C_{5.78}H_{2.39}N_{0.09}P_{0.15}O_{1.41}$ |
| **DBP** | 1.69 | $C_{3.27}H_{7.50}N_{0.06}P_{0.04}O_{3.18}$ | $C_{6.45}H_{2.23}N_{0.10}P_{0.19}O_{1.56}$ |
| **DiPP** | 1.64 | $C_{3.12}H_{7.15}N_{0.05}P_{0.04}O_{3.30}$ | $C_{6.28}H_{2.21}N_{0.08}P_{0.11}O_{1.13}$ |

A relatively large amount of phosphorus and nitrogen is retained in the char. The formulae for the chars were very similar for all four phosphoramidates. This finding is in accordance with literature. Kulshreshtha *et al.* have investigated chars using Attenuated Total Reflectance (ATR)-FTIR technique and have observed that the spectral characteristics of different chars were similar despite the use of structurally different flame retardants [99]. This indicates the reactions that took place during combustion were similar. These reactions obviously lead to the formation of the phosphorus- and nitrogen-containing residue with the same chemical structure. However, the question of different FR properties still remains. In order to obtain further insights into the differences in char formation, treated fabrics as well as char residues remained after LOI test were subjected to the Scanning Electron Microscopy analysis.

Fig. 4.7 shows the surface of treated fabrics (P-content around 1.5 %) at the magnification of x2000. When viewed in SEM, a cellulose fibre is seen as having a twisted convoluted ribbon-like structure with a furrowed surface. It is rather difficult to distinguish between untreated and treated cellulose, even though some chemical treatments of cellulose are accompanied with degradation and sometimes by tearing of the fabric. In our case, no high-temperature were used to treat cellulose, and the phosphoramidates themselves do not lead to the damage of cellulose. There was little sign of the phosphoramidate coating on the fibres. Moreover, the dry uptake $W$ on the fabrics was quite low (3.5–7.5 %), and no particular differences were observed on the surface of the cellulose.

Figures 4.8 and 4.9 show the micrographs of chars left after LOI test. At higher magnification some kind of fuzzy coating was observed, as noted previously. The density of this coating appeared to be different for studied phosphoramidates. For the chars of **DMP**-treated samples the amount of such deposits was the lowest (Fig. 4.8 *b*). From
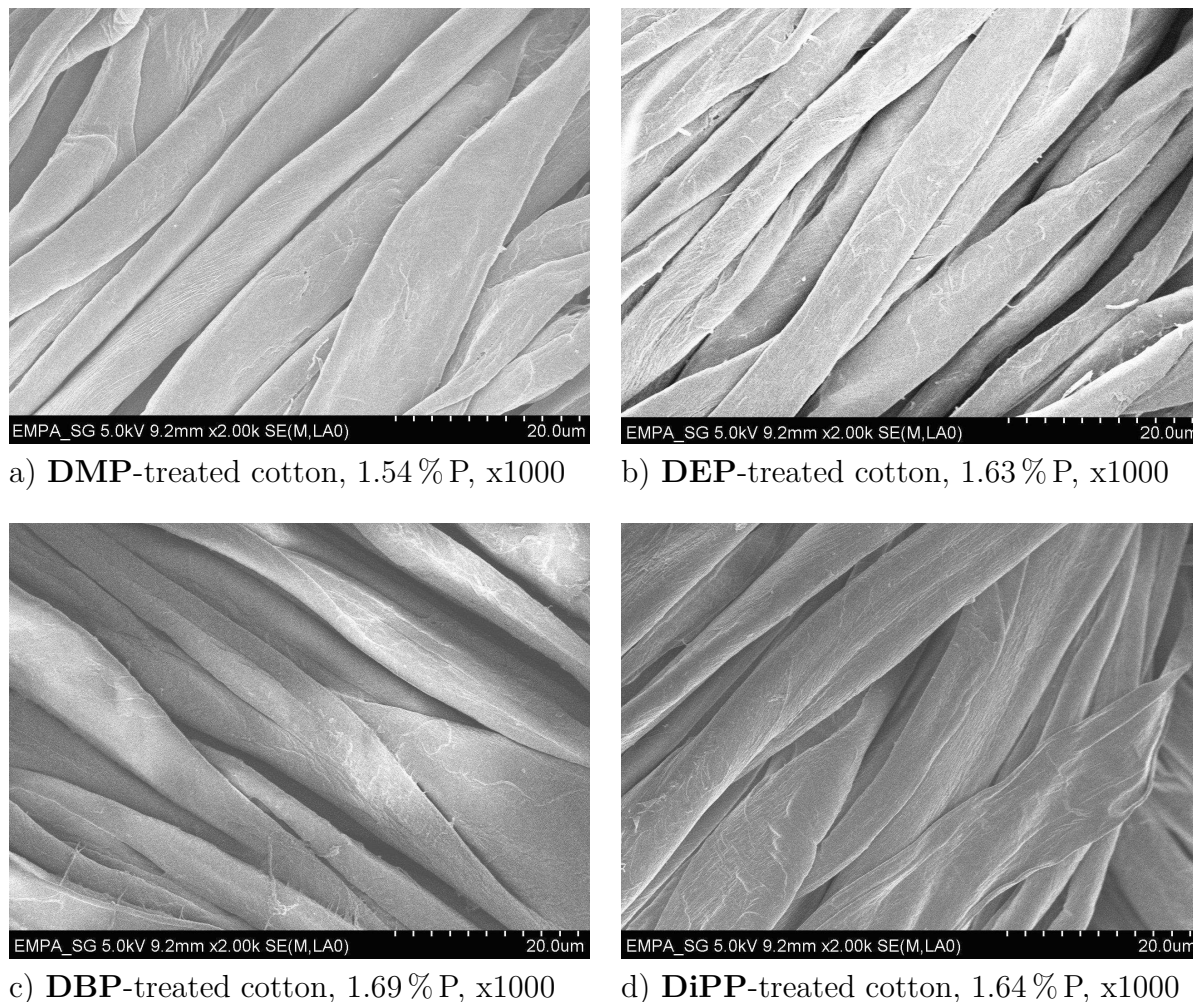
a) **DMP**-treated cotton, 1.54 % P, x1000        b) **DEP**-treated cotton, 1.63 % P, x1000

c) **DBP**-treated cotton, 1.69 % P, x1000        d) **DiPP**-treated cotton, 1.64 % P, x1000

Figure 4.7 SEM micrographs of **DMP**–, **DEP**–, **DBP**– and **DiPP**–treated fabrics

micrographs 4.8 *b* and 4.9 *b* it was also observed that the layer of the deposited material is not uniform, i.e. more deposits were detected on the surface layers of char than on the deeper lyeing fibres. Similar phenomenon has been already observed by Pandya *et al.* in [100] in early 80's. They have attributed this observation to the difference in the direction of flame propagation during the LOI test. We have tried to verify if this finding is true for our materials.

Fig. 4.10 reveals the morphology of charred surface obtained from combusting **DMP**– treated cotton cellulose at the oxygen level of 30 %. The sample on the left was ignited from bottom, whereas sample on the right was ignited from top (ignition from top is typical procedure for the LOI determination). When the fabric was ignited from the bottom no

a) **DMP**, 1.54 % P, x100



b) **DMP**, 1.54 % P, x1000



c) **DEP**, 1.63 % P, x100
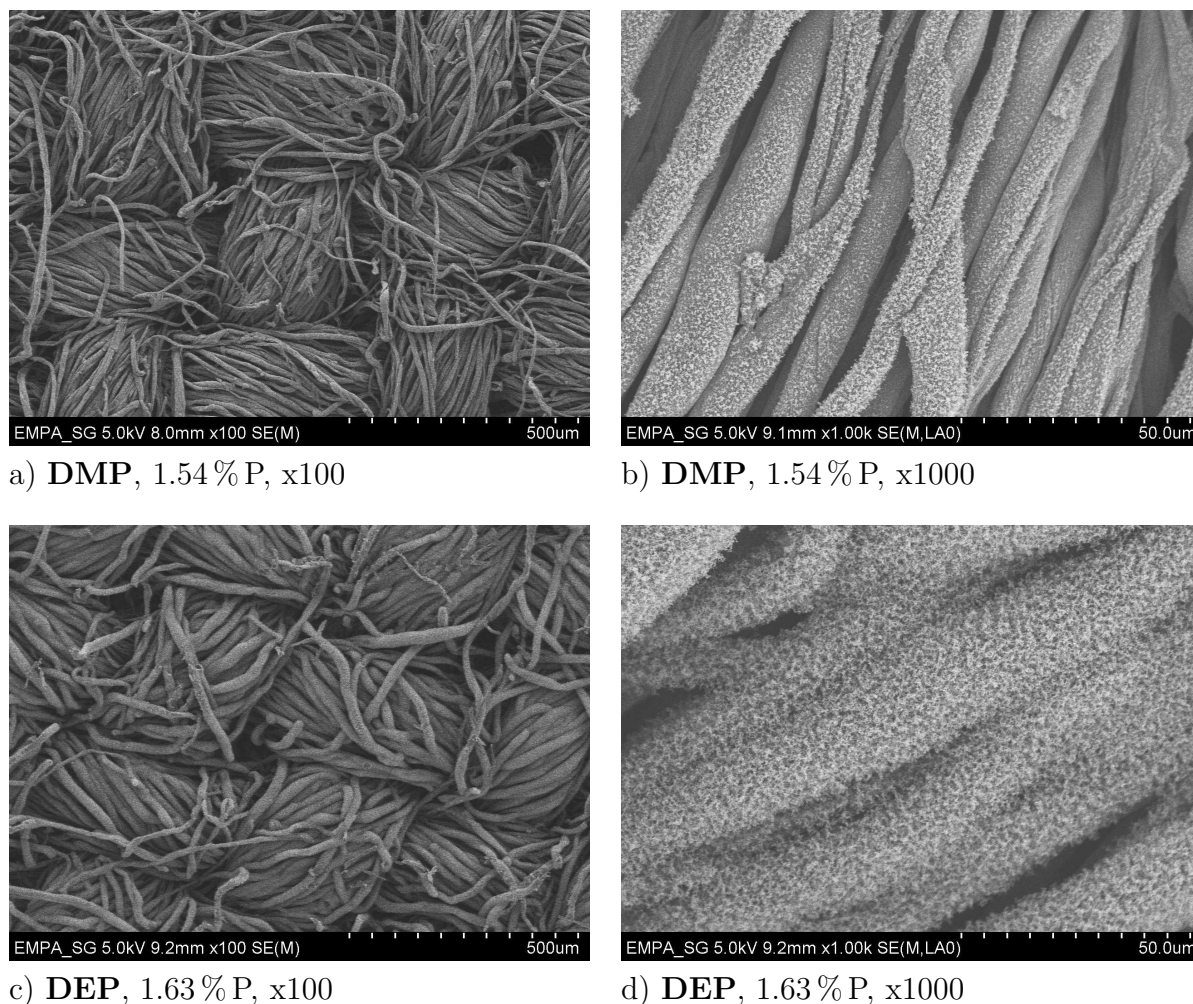


d) **DEP**, 1.63 % P, x1000

Figure 4.8 SEM micrographs of the chars of **DMP**- and **DEP**-treated fabrics obtained after combustion at oxygen index 30 %

formation of particulate matter took place. This phenomenon can be explained simply by redeposition of unburned ash particles on the surface of burned fabric (char) when the sample was ignited from the top. The particles are normally carried by the gas flow which is set bottom-up and easily redeposit leading to such surface morphologies. On the other hand, if the ignition is performed from the bottom the ash particles are easily blown away before the cellulose is ignited.

One other important factor here which influences the morphology is the time of combustion. The oxygen index was intentionally set above the LOI level in order to accelerate the top-bottom combustion process. However, the speed of top-bottom combustion was
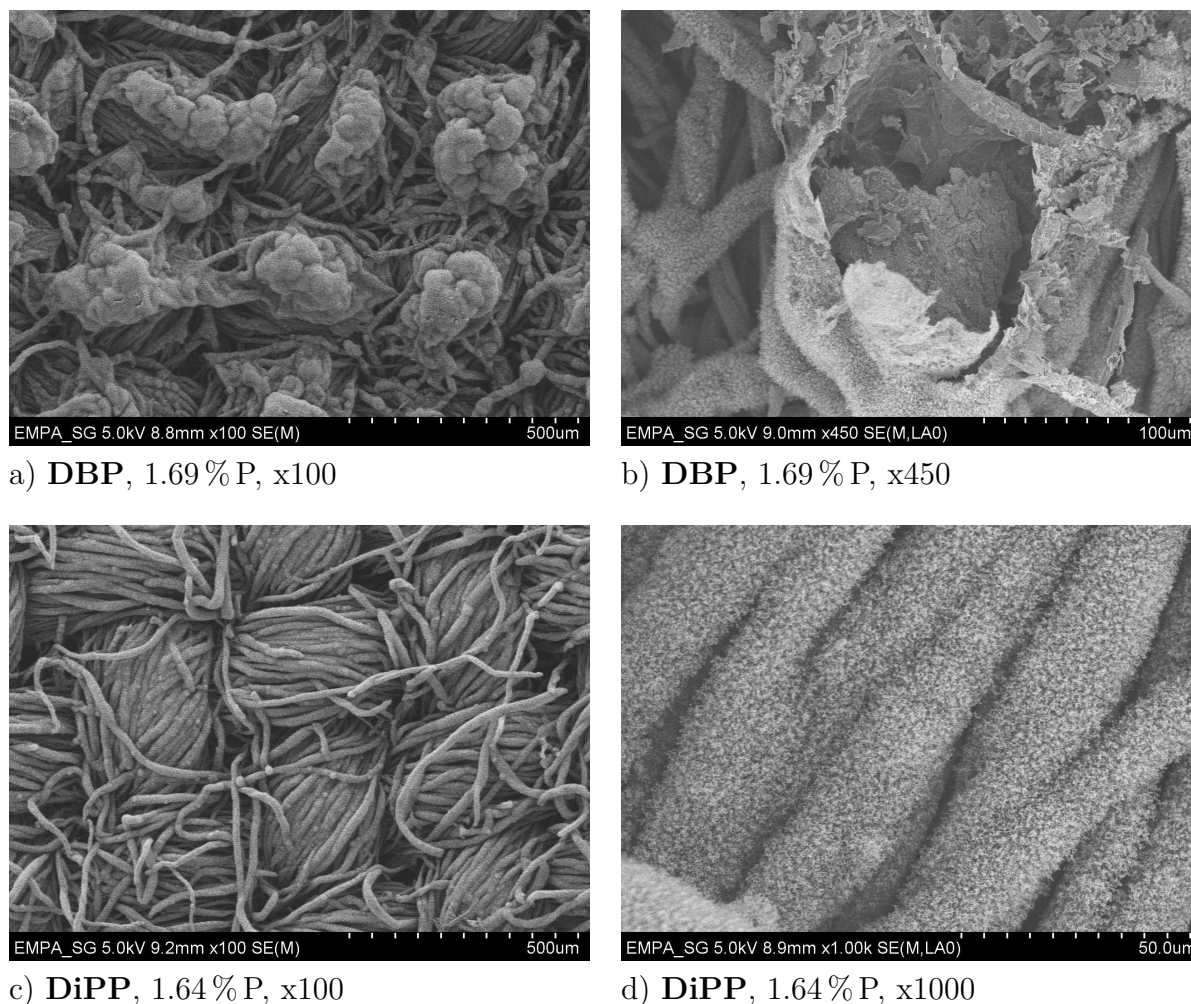
a) **DBP**, 1.69 % P, x100



b) **DBP**, 1.69 % P, x450



c) **DiPP**, 1.64 % P, x100



d) **DiPP**, 1.64 % P, x1000

Figure 4.9 SEM micrographs of the chars of **DBP**– and **DiPP**– treated fabrics obtained after combustion at oxygen index 30 %

10 times lower than the speed of bottom-top combustion, which was certainly driven by the direction of the gas flow. The flame spread in the case of bottom-top combustion was much faster which lead to the presented results. Hence, the formation of such coatings was triggered solely by the direction of the flame.

Another interesting observation was made when looking at the char surfaces. The char surface of **DBP**–treated cellulose in contrast to the other chars displayed numerous shapeless protrusions, which had an appearance of localized surface blisters (Fig. 4.9 a). These blisters seemed to appear strictly on the yarn. Their size was around 150–200 $\mu$m and when the crust was broken one could observe that they were hollow from inside (Fig. 4.9
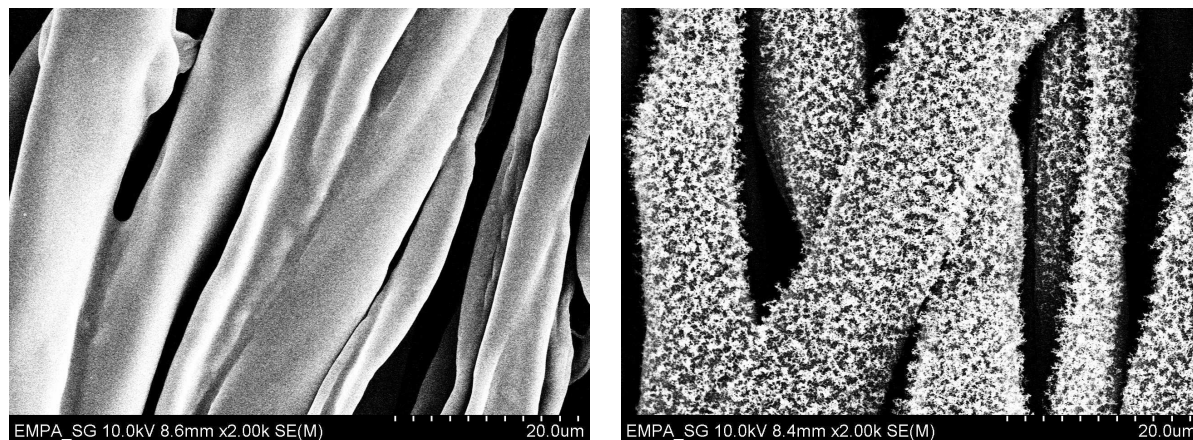
Figure 4.10 SEM micrographs of the chars of **DMP**–treated cotton cellulose (1 % P), left: burned from bottom; right: burned from top at oxygen index 30 %

b). This blistering phenomenon has already been described by some researchers as the result of the following process: the gases formed by combustion (water vapour, CO, $CO_2$ etc.) upon escaping the vicinity of the fabric surface are entrapped by the distensible polymeric coating formed from carbon, oxygen, phosphorus and nitrogen at high temperatures [101, 100]. As such blisters were observed only for chars of **DBP**–treated fabrics, one can argue that either the properties of the polymeric coating formed for **DBP**–treated fabrics were different (more thermally stable) or greater amount of gases was formed during combustion.

From the elemental analysis we have already learned that the char composition was the same. Possibly, the blistering took place due to the formation of higher amounts of gases. This finding could be correlated with data obtained in calorimetric studies where **DBP** was found to be more combustible owing to the higher carbon content in the molecule. However, as elemental analysis was performed after the combustion process, it is not known, at what temperature these blisters were formed. The fact that no similar blistering effect was observed for **DMP**, **DEP** or **DiPP** might be caused by a formation of a polymer with different properties during combustion. The discussion on blistering will be continued in Chapter 6 where also some additional information on that topic will be presented.

## 4.7   Conclusions

The FR properties of four compounds: dimethyl–, diethyl–, di-n-butyl– and di-isopropyl phosphoramidates have been investigated. Their FR behaviour was shown to significantly differ from each other. Several reasons for this different FR behaviour have been suggested.

Firstly, the proposed hypothesis of the effect of boiling point was rejected, as the boiling point was proved to have no influence on the flammability of treated cellulose. Dimethyl phosphoramidate having the lowest boiling point exhibited excellent FR properties.

Secondly, with the increase of the number of carbon atoms in the N-alkyl chain, the FR properties of the treated cellulose decreased (LOI values). Such a direct correlation, however, is not possible for structurally different molecules such as alkyl and aryl phosphoramidates. Therefore, the effect of P/C ratio should only be considered in the scope of structurally similar phosphoramidates.

The most important finding was the ability of phosphoramidate to interact with cellulose prior to combustion. The aminogroup increases the affinity of phosphoramidate for the surface of cellulose and shortens the distance between the phosphorus and hydroxyl group of the cellulose, available for phosphorylation. The smaller size of **DMP** allows more phosphorus in close contact with the surface and consequently, higher rate of phosphorylation.

In order to demonstrate the importance of the presence of an acidic hydrogen (from primary aminogroups) in the structure of phosphoramidate, four phosphoramidates having secondary and tertiary aminogroups were studied in the next step. The influence of the substituents at the nitrogen atom is demonstrated in the next chapter as well.

# Chapter 5

# Dimethyl alkyl phosphoramidates. Influence of the substituents at the nitrogen atom

The present chapter deals with the investigations on four phosphoramidates with different number of substituents at the nitrogen atom (Fig. 5.1). Since low carbon content is essential for good FR properties, the studies were continued on dimethyl phosphoramidates. The importance of the presence of a primary aminogroup was demonstrated using two phosphoramidates with secondary and tertiary aminogroups: dimethyl-(methyl)-(**DMMP**) and dimethyl-(dimethyl) phosphoramidate (**DMDMP**).

**DMMP**: $R_1$ = H, $R_2$ = Me
**DMEP**: $R_1$ = H, $R_2$ = Et
**DMPP**: $R_1$ = H, $R_2$ = nPr
**DMDMP**: $R_1 = R_2$ = Me

Figure 5.1 General structure of phosphorus compounds studied in Chapter 5

The FR properties of these phosphoramidates were compared with the FR properties of **DMP**. Further, the FR properties of dimethyl N-ethyl phosphoramidate **DMEP** and dimethyl N-propyl phosphoramidate **DMPP** were studied to support the low carbon content hypothesis. The investigation of the FR properties of **DMPP** was essential at this

step to enable comparison with other phosphoramidates in Chapter 6.

## 5.1   Use of dimethyl-(alkyl) phosphoramidates as flame retardants for cellulose

The use of **DMMP**, **DMEP**, **DMPP** as FRs for cellulosic materials has never been mentioned in the literature. There is not much information on their synthesis and uses in general. **DMMP** was mentioned as catalyst in the reaction of benzoyl chloride with m-chloroaniline [102]. In [103] the antiallergic properties of **DMMP** were studied by Tomilets *et al.* **DMMP** is mentioned in [104, 105] in a study of phosphoric amides. In [106, 107] it was used as educt to obtain phosphorus-containing allophanates. Van Nooy *et al.* [108] have studied herbicidal properties of **DMMP**.

**DMEP** and **DMPP** were mentioned even more rarely in the literature. Nikonorov *et al.* have used them to condensate with chloral and to study chemical properties of obtained compounds [84]. Khazanchi et al. [85] have tested these phosphoramidates for phytotoxic activity and have found, that phosphoramidates with aromatic substituents at nitrogen atom have the best phytotoxic activity amongst others. Starting from early 90's **DMMP**, **DMEP**, **DMPP** as well as **DMDMP** are to find in the literature mainly because of the studies on degradation of tabun - main component in chemical weapons [109, 110, 111, 112]. The studies of the FR properties of these molecules have never been published before, a fact which certainly rendered it more interesting to perform a thorough investigation on their FR behaviour.

## 5.2   Physical properties of DMMP, DMEP, DMPP and DMDMP and treatment cellulose

The phosphoramidates **DMMP**, **DMEP**, **DMPP** and **DMDMP** have very similar physical properties. They are all liquid-like oils with yellowish color. Their boiling points are presented in Table 7.1.

Table 5.1 Physical properties of **DMMP**, **DMEP**, **DMPP** and **DMDMP**

| Compound | MW [g/mol] | $P_s$ [%] | $N_s$ [%] | $C_s$ [%] | bp [°C] |
|---|---|---|---|---|---|
| **DMMP** | 139.09 | 22.27 | 10.07 | 25.90 | 204 |
| **DMEP** | 153.17 | 20.23 | 9.15 | 31.36 | 216 |
| **DMPP** | 167.14 | 18.53 | 8.38 | 35.93 | 217 |
| **DMDMP** | 153.17 | 20.23 | 9.15 | 31.36 | 182 |

The treatment of cotton cellulose with synthesized compounds was performed analogously to the procedure described in Chapter 3. The uptake of phosphoramidates on cellulose, calculated and measured phosphorus content are presented in Table 5.2.

Table 5.2 Weight uptakes and phosphorus content of the treated fabrics

| FR | $P_n$ [%] | Weight uptake [%] | $P_t$ [%] | $P_p$ [%] |
|---|---|---|---|---|
| **DMMP** | 1 | 4.1 | 0.87 | 1.16 |
| | 2 | 9.2 | 1.88 | 2.06 |
| **DMEP** | 1 | 5.2 | 1.01 | 1.18 |
| | 2 | 9.3 | 1.98 | 2.11 |
| **DMPP** | 1 | 5.0 | 0.88 | 1.06 |
| | 2 | 9.0 | 1.86 | 1.97 |
| **DMDMP** | 1 | 2.6 | 0.45 | 0.68 |
| | 2 | 3.3 | 0.52 | 0.79 |

It was practically impossible to obtain desirable phosphorus content for the fabrics treated with **DMDMP**. The reason for that is the reduced affinity of **DMDMP** towards cellulose owing to the absence of functional groups that promote hydrogen-bond interaction with hydroxyls of cellulose. Increasing the initial liquor concentration did not result in improving the retention of **DMDMP** on cellulose. The flammability data will be further compared with regard to this finding.

# 5.3 Assessment of flammability

Analogously to section 4.3, the flammability of treated cellulose was assessed in the beginning of the investigations. For that, LOI values for samples with phosphorus content

from 1 to 2.2 % were determined and plotted against the P-content (Fig. 5.3), and trend line was fitted into the scatter plot (Chapter 4). The data for **DMDMP** was obtained only for a phosphorus content not higher than 0.8 %.

**DMMP** exhibited the same trend in LOI as **DMP**. The values obtained, however, were about 2 % lower than for **DMP**. LOI data of **DMDMP** is rather difficult to assess, because the data is available only for low phosphorus content. In the next step the flammability of **DMMP**–, **DMEP**– and **DMPP**–treated cellulose samples was evaluated (Fig. 5.3). Among all the tested compounds the highest LOI values were obtained for **DMP**-treated fabrics. Introduction of methyl (**DMMP**) and ethyl (**DMEP**) groups at the nitrogen atom lead to a slight decrease of LOI, but the trend was exactly the same.

For some reason, the LOI trend line of **DMPP** had a slope that was completely different from that for **DMP**, **DMEP** and **DMPP**. At a phosphorus content below 1.5 %, the LOI of **DMPP**-treated cellulose was even higher than for **DMMP** and **DMEP**. However, at higher concentrations, the curve flattened out and the difference in LOI between **DMP** and **DMPP** comprised almost 5 %. It is hard to give any reasonable explanation for the occurrence of this phenomenon, as one would definitely expect the FR properties of **DMPP** to be similar to those for **DMEP** and **DMMP**.

As next step it was interesting to compare the LOI values of **DEP**, **DMEP** and **DMDMP** as their elemental composition is exactly the same, but their molecular structures and thus chemical nature are entirely different. Fig. 5.4 shows measured LOI values plotted versus phosphorus content, measured using elemental analysis.

The highest LOI values were recorded clearly for **DMEP**. At 1 % of phosphorus, the LOI of **DMEP**-treated cellulose was about 2 % higher than LOI of **DEP**- and **DMDMP**-treated samples. At higher phosphorus content, this difference has increased to approx. 4 % of phosphorus. This very interesting observation gives indications on structural features in molecule that play key role in providing good flame retardancy. Firstly, having primary aminogroups is essential, as their absence leads to the remarkable reduction of FR properties (**DMEP** vs. **DMDMP**). Secondly, having methoxy groups at the phosphorus atom is advantageous. This finding is also supported by the finding in Chapter 4, where the best FR properties were found for **DMP**.
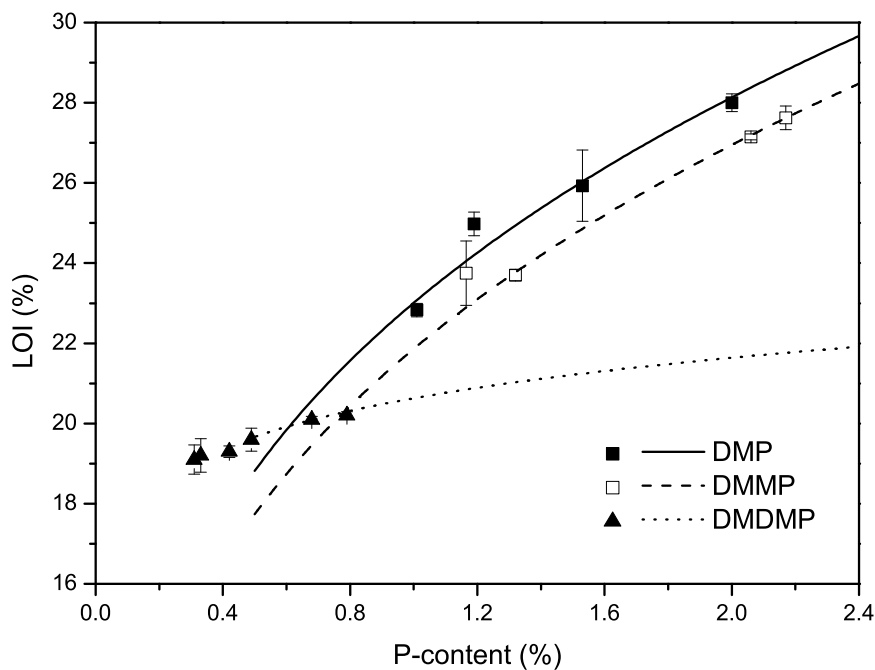
Figure 5.2 LOI vs. phosphorus content for fabrics treated with **DMP**, **DMMP** and **DMDMP**
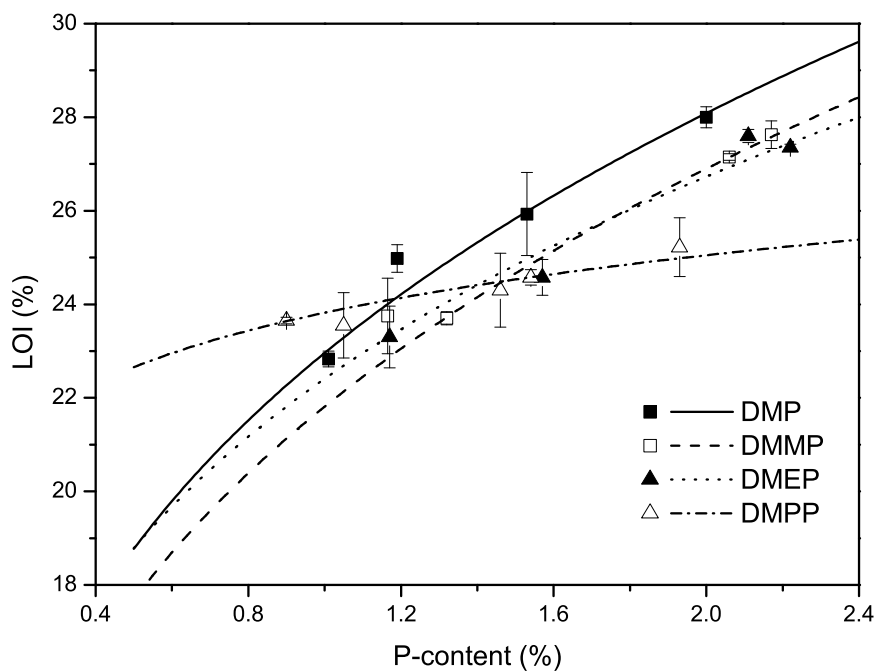


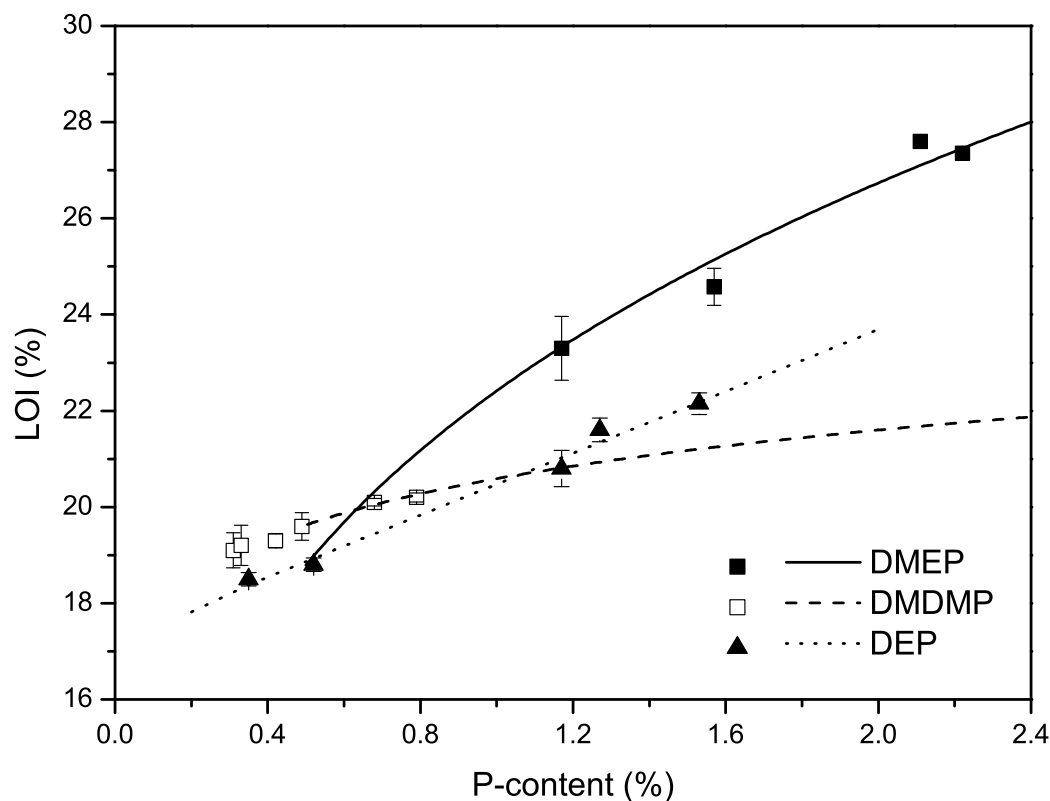Figure 5.3 LOI vs. phosphorus content for fabrics treated with **DMP**, **DMMP**, **DMEP** and **DMPP**

Figure 5.4 LOI vs. phosphorus content for fabrics treated with **DMEP**, **DMDMP** and **DEP**

## 5.4 Thermal properties of dimethyl-(alkyl) phospho- ramidates

Fig. 5.5 presents the heat release rates of fabrics treated with **DMP** and N-dialkyl phosphoramidates with approximately 1 % of phosphorus content. The main decomposition peak occurs at about 300°C for all four compounds. The shape of this peak looks very similar for all of the phosphoramidates. Therefore, the decomposition process was believed to be very similar. The values of heat release rate $Q_t$, temperature of the maximum heat release rate $T$ and total heat of combustion $h_c^0$ are collected in Table 5.3.

With the increase of the phosphorus content on cotton, the values of $Q_{t2}$ decrease and $h_c^0$

increase. This effect is obvious as with increased amount of FR on cotton, its flammability is reduced. The $T_2$ and char yields were rather similar to each other. However, when this data was compared with the data for **DMP**–treated samples (Table 4.4), significant differences were observed. $Q_{t2}$ and $h_c^0$ of **DMP** were found to be lower, and $\mu$ was by 20 % (relatively) higher than for the N-substituted phosphoramidates.
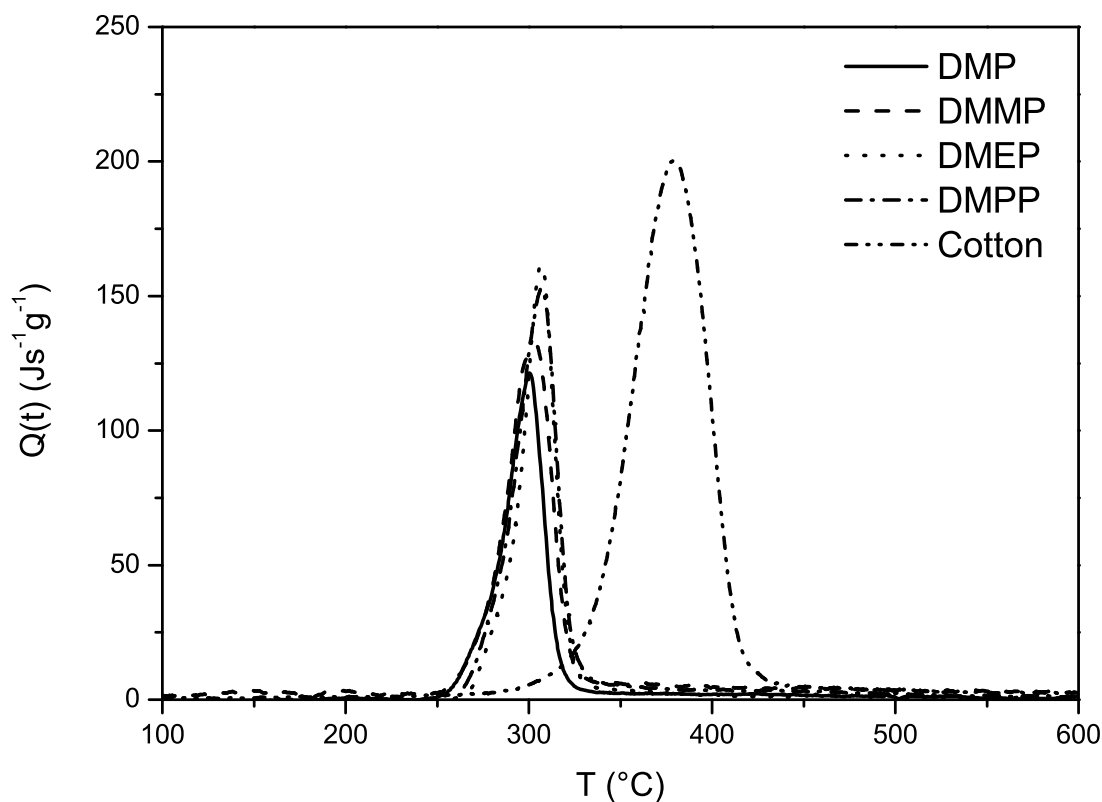


Figure 5.5 Specific heat release rates of fabrics treated with **DMMP**-, **DMEP**- and **DMPP** (approx. 1.0 % of phosphorus content)

Values found for **DEP**-treated cellulose, however, were comparable with values of N-substituted phosphoramidates. Like for **DMP**, no saturation of the surface for **DMMP** and **DMEP** occurs before 2 % of phosphorus. At higher phosphorus content, the increased size of the molecule (**DMPP**) disturbs the interaction of aminogroups with cellulose. The total heat of combustion, which should decrease with the increased amount of phosphorus,

in fact decreases due to the contribution of the excess of phosphoramidate, which is not with close contact with the surface.

Table 5.3 Combustion data of cotton fabrics treated with **DMMP**-, **DMEP**- and **DMPP**

| FR | $P_p$ [%] | $Q_{t1}$ [$Js^{-1}g^{-1}$] | $T_1$ [°C] | $Q_{t2}$ [$Js^{-1}g^{-1}$] | $T_2$ [°C] | $h_c^0$ [$kJg^{-1}$] | $\mu$ [%] |
|---|---|---|---|---|---|---|---|
| Cotton | 0 | - | - | 192.7 | 384.3 | 9.7 | 3.7 |
| **DMMP** | 1.16 | - | - | 128.2 | 305.8 | 4.5 | 25.6 |
|  | 1.32 | - | - | 129.6 | 305.4 | 4.1 | 27.7 |
|  | 2.06 | 5.1 | 174.5 | 126.2 | 303.8 | 4.0 | 29.9 |
| **DMEP** | 1.16 | - | - | 160.6 | 312.9 | 4.3 | 26.3 |
|  | 1.56 | - | - | 155.9 | 307.1 | 4.0 | 28.8 |
|  | 2.11 | 8.2 | 182.4 | 149.4 | 304.2 | 4.8 | 32.7 |
| **DMPP** | 1.05 | - | - | 149.3 | 308.9 | 4.5 | 26.1 |
|  | 1.53 | 5.3 | 184.0 | 146.4 | 308.3 | 4.7 | 27.6 |
|  | 1.97 | 8.5 | 188.9 | 150.3 | 305.7 | 4.8 | 28.6 |

## 5.5   Conclusions

The introduction of carbon at nitrogen site in **DMMP**-, **DMEP**- and **DMPP** was shown to influence the FR properties of treated cellulose. If compared among each other no significant differences were detected for **DMMP**-, **DMEP**- and **DMPP**. When the FR properties were compared to N-unsubstituted phosphoramidates like **DMP** and **DEP** slight difference in FR action was detected. In fact, substitution of one hydrogen atom for a methyl group in **DMMP** had almost no effect if compared to **DEP**. Moreover, the presence of an alkyl group on nitrogen increases the acidity of the remaining hydrogen by an inductive effect, hence improving its ability to form hydrogen bonds with hydroxyl groups of cellulose.

Deterioration of FR properties of cellulose treated with **DMDMP** occurred due to the low affinity of **DMDMP** to cellulose as a result of hydrogen to methyl substitution. The aminogroup in phosphoramidates plays a role of an "anchor", which, if not available, will make the adhesion of FR on cellulose impossible. Without close interaction of phosphoramidates to cellulose, no phosphorylation can occur, hence the FR properties are reduced.

In order to obtain the FR with better properties, it makes sense to improve such adhesion. This can be realized by introducing more polar functional groups into the phosphoramidate molecule, e.g. hydroxyl group. In the next chapter, FR properties of hydroxyl-containing phosphoramidates were investigated.

# Chapter 6

# Dimethyl hydroxy– and methoxyalkyl phosphoramidates. The effect of hydroxyl group

The FR behaviour of three hydroxyl-containing phosphoramidates was investigated to support the hypothesis suggested in Chapter 5. Dimethyl-(2-hydroxyethyl)phosphoramidate **DMHEP** was prepared in order to investigate the effect of hydroxyls on the FR properties of treated cellulose by comparing its action with **DMP** and **DMPP**.
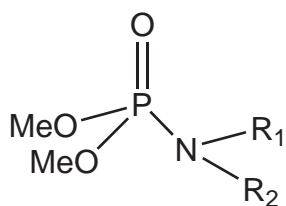


**DMHEP**: $R_1 = H$; $R_2 = (CH_2)_2$-OH
**DMHPP**: $R_1 = H$; $R_2 = (CH_2)_3$-OH
**DMBHEP**: $R_1 = R_2 = (CH_2)_2$-OH
**DMMEP**: $R_1 = H$; $R_2 = (CH_2)_2$-OMe
**DMMPP:** $R_1 = H$; $R_2 = (CH_2)_3$-OMe

Figure 6.1 General structure of phosphorus compounds studied in Chapter 6

In order to examine whether some structural changes in the molecule will affect the FR properties, dimethyl-(2-hydroxypropyl) phosphoramidate **DMHPP** was synthesized. Two functional hydroxyl groups were introduced in dimethyl-bis-(2-hydroxyethyl) phosphoramidate **DMBHEP** in an intention to increase the interaction with cellulose. In order to demonstrate the key action of hydroxyls, they were substituted for methoxy groups in dimethyl-(2-methoxyethyl)- **DMMEP** and dimethyl-(2-methoxypropyl) phosphorami-

dates **DMMPP** and their FR action was investigated.

# 6.1 Literature review and physical properties of hydroxy- and methoxyalkyl phosphoramidates

Hydroxy- and methoxyalkyl phosphoramidates are well-known in the literature. Although the synthetic part is not throughly described, there exist several publications where hydroxy- and methoxyalkyl phosphoramidates were used in various applications, some of which will be described in the following.

Verkhunov *et al.* have synthesized polyurethane elastomers from dimethyl phosphite and mono- and diethanolamine [113]. They reported excellent thermo-oxidative properties of these polymers. Diethyl analogue of **DMHEP** is described in a number of publications where its FR properties have also been reported [114, 115]. Gaan *et al.* have found outstanding FR properties for diethyl-(2-hydroxyethyl) phosphoramidate treated cellulose [116]. Moreover, they observed that if the hydroxyl group was substituted by a methoxy group the FR properties were drastically reduced. However, no explanation of this phenomenon was given. **DMHEP** was also used in the synthesis of glycol phospholipids [117]. Although no publications exist that deal with the investigations of the FR properties of **DMHEP** and **DMHPP**, **DMBHEP** was mentioned as FR agent for polyurethane foams in 1965 [113]. Some studies on preparation of **DMBHEP** are also available in the literature [118, 86].

Table 6.1 Physical properties of **DMHEP**, **DMHBP**, **DMBHEP**, **DMMEP** and **DMMPP**

| Compound | MW [g/mol] | $P_s$ [%] | $N_s$ [%] | $C_s$ [%] | bp [°C] |
|----------|-----------|-----------|-----------|-----------|---------|
| **DMHEP** | 169.12 | 18.32 | 8.28 | 28.41 | 221 |
| **DMHPP** | 183.14 | 16.91 | 7.65 | 32.79 | 220 |
| **DMBHEP** | 213.17 | 14.53 | 6.57 | 33.81 | 218 |
| **DMMEP** | 183.14 | 16.91 | 7.65 | 32.79 | 215 |
| **DMMPP** | 197.17 | 15.71 | 7.10 | 36.55 | 212 |

It is an interesting fact that a detailed description of the preparation process for **DMHEP** and **DMHPP** is not provided in the literature. Greenhalgh *et al.* have obtained dimethyl-

(N-2-hydroxyethyl) phosphoramidate as a side product when performing the reaction of tetraethylpyrophosphate with ethanolamine in [119]. This by-product was successfully isolated with a yield of 65 %. In [120], Ryu and Cates have used these compounds as "inhibitors of biotransformations" in malignant tumors. They claimed to have performed the synthesis using the phosphite method (also known as the Todd-Atherton reaction) and the phosphortrichloridate methods.

Phosphoramidates investigated in this chapter were synthesized using the Todd-Atherton reaction (for a detailed description of this synthesis please refer to the Experimental part). All compounds were colourless to slightly yellow oily odorless substances. Their boiling points were found to be very similar (Table 6.1). Hydroxyl-containing phosphoramidates were applied to cellulose right after the purification upon synthesis. The reason for this was their high hygroscopicity and as result instability of molecule [116, 121].

## 6.2   Influence of hydroxyl groups

To demonstrate how the introduction of hydroxyl can influence the flammability of treated cellulose, the LOI values of **DMHEP** were compared with the data for **DMP** and **DMPP** (Fig. 6.2). At phosphorus contents below 1.2 %, the LOI of **DMHEP** was found to be the highest. However, at higher phosphorus contents the behaviour changed so that the highest values were recorded for **DMP**. Compared to **DMPP**, the increase of LOI was significant. This effect can partly be attributed to the presence of the hydroxyl moiety, but the underlying mechanisms yet need to be investigated in more detail. We believe that two possible explanations for this phenomenon exist.

Firstly, the higher LOI values for **DMP** might be the result of its more intense interaction with cellulose, which in turn is governed by the size of the molecule (see Chapter 4). Secondly, the interaction of **DMHEP** with cellulose was influenced by the presence of hydroxyl. An excellent presentation of this effect can be seen in Fig. 6.3 where char yields of several samples left after LOI tests were measured and plotted versus their respective phosphorus content. The highest yields were obtained for **DMHEP**-treated cellulose. The difference to the yields for **DMPP** was about 5 %. As it was already mentioned in
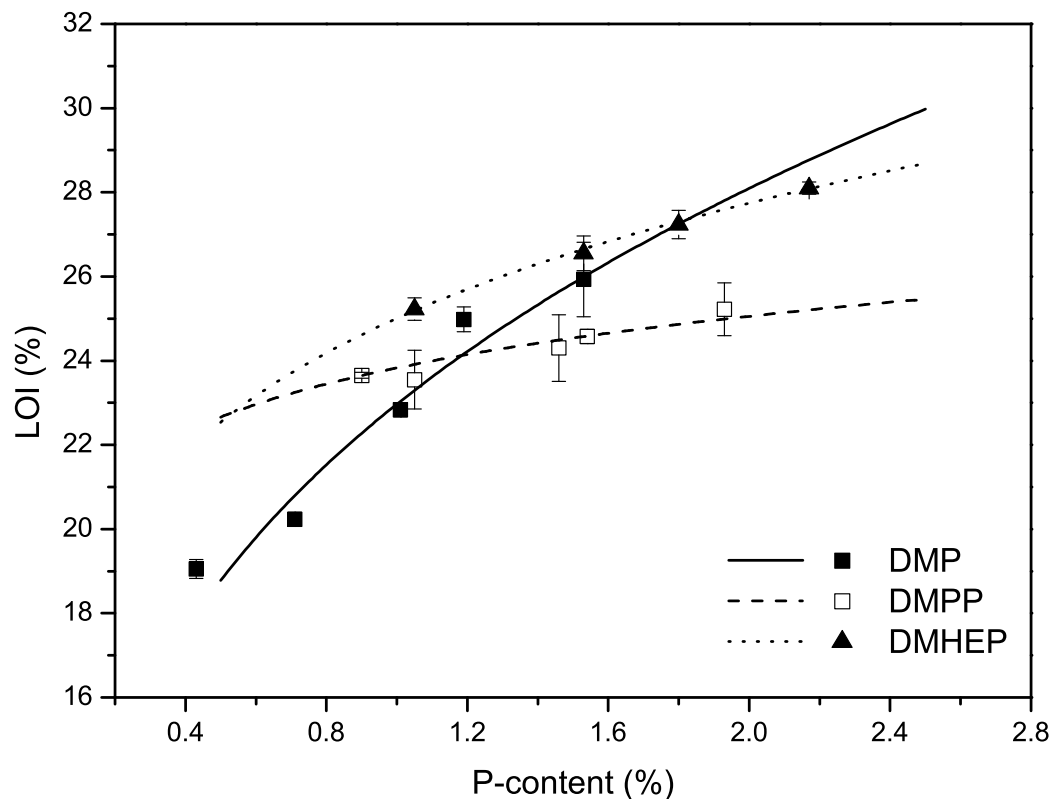
Figure 6.2 LOI vs. phosphorus content for fabrics treated with **DMP**, **DMPP** and **DMHEP**

the introduction chapter the amount of char left after combustion is the first indication on the mechanism of action of a certain compound. The higher is the char yield, the more pronounced is the condensed phase action mechanism. Hence, hydroxyls are able to trigger the char forming reactions in cellulose.

In order to determine the changes in the char composition, elemental analysis of chars was performed after combustion of **DMHEP**-treated cellulose samples (analogously to the analysis described in the chapter 4). This analysis did not reveal any differences in the elemental composition. The empirical formula of char was computed $C_{5.54}H_{2.89}N_{0.11}P_{0.15}O_{1.52}$ and the formula of loss was $C_{2.900}H_{7.29}N_{0.03}P_{0.02}O_{3.48}$. Furthermore, no differences to the data for unsubstituted phosphoramidates were detected. Therefore, we wanted to understand the origin of the different FR action.
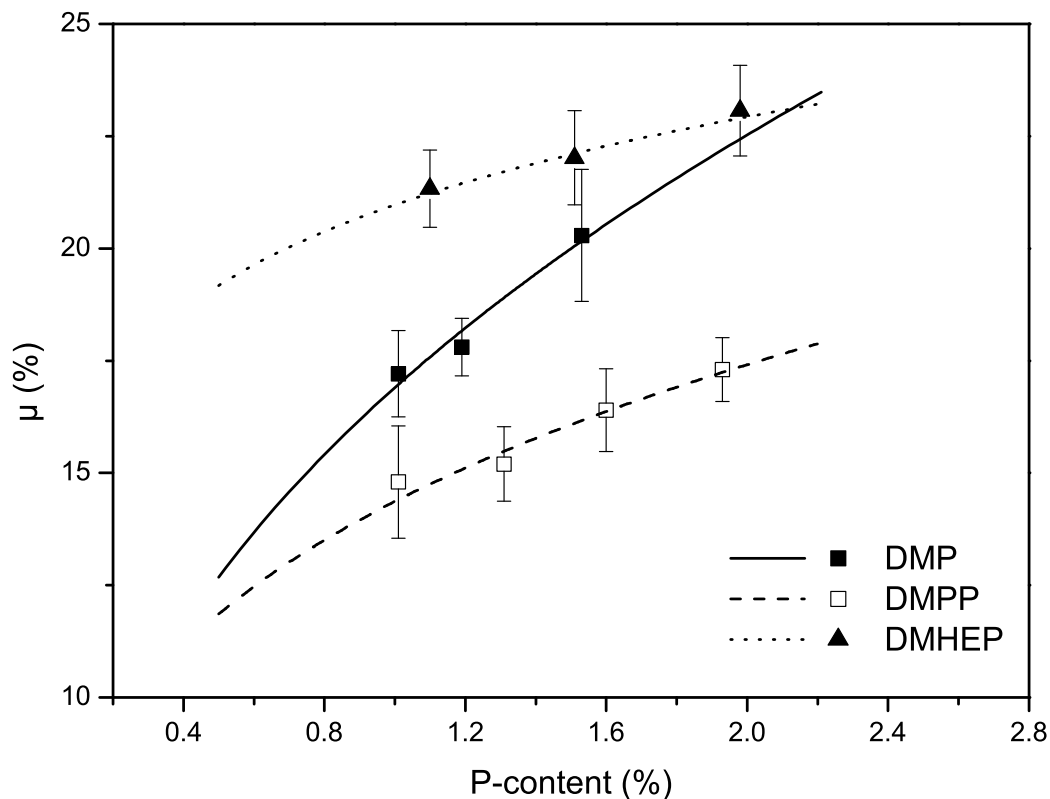
Figure 6.3 Char yield vs. P-content for fabrics treated with **DMP**, **DMPP** and **DMHEP**

In the beginning of the investigation it was expected that hydroxyls might improve the interaction of phosphoramidate with cellulose prior to combustion. This phenomenon as well as the decomposition itself was studied using combustion calorimetry. Fig. 6.4 demonstrates the heat release rates as function of temperature for cellulose samples treated with **DMP**, **DMPP** and **DMHEP**. The phosphorus uptake measured for all samples was around 1 %.

The shape of the main decomposition peak was similar for all compounds. Prior to the main decomposition step, no heat release was detected which could be accounted for the desorption of phosphoramidate from cellulose. However, at higher uptakes of phosphoramidates the heat releases were recorded (Table 6.2).
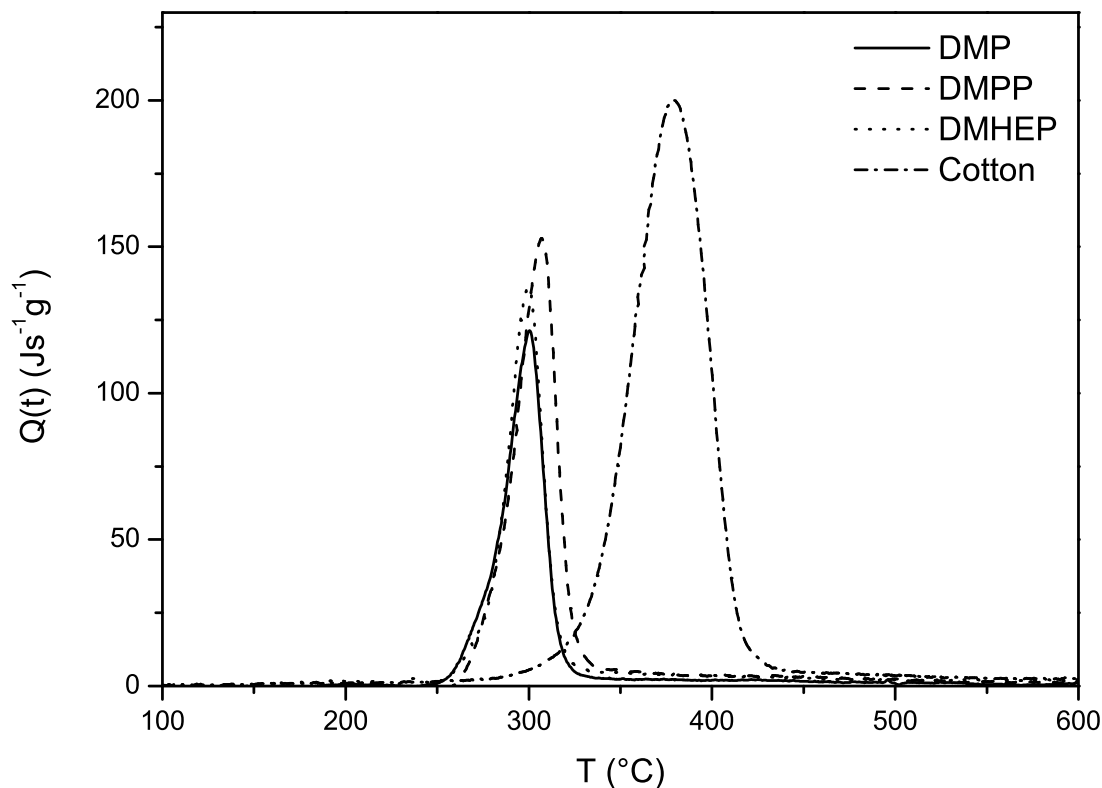
Figure 6.4 Specific heat release rates of fabrics treated with **DMP**, **DMPP** and **DMHEP** (P-content approx. 1 %)

Interestingly, the loss due to desorption was observed for **DMHEP**. Even at low phosphorus content, a part of the substance was desorbed and oxidized producing the heat. At first sight our working assumption of **DMHEP** interacting with cellulose owing to the presence of hydroxyls might not seem justified. on the other hand, the observation needs to be considered that at the same phosphorus content, the actual uptake of the phosphoramidate is not the same due to the different phosphorus content in the molecule. With phosphorus contents of around 2 %, the actual weight uptakes on cellulose fabric were 7.46 % for **DMP** and 10.01 % for **DMHEP** (Table 4.2). The heat release rates recorded at around 195°C could impossibly originate from this tiny difference in weight uptakes. Apparently, it occurs as a result of the reduced interaction of **DMHEP** with cellulose due

Table 6.2 Combustion data of cotton fabrics treated with **DMP**, **DMPP** and **DMHEP**

| | P [%] | $Q_{t1}$ [Js$^{-1}$g$^{-1}$] | $T_1$ [°C] | $Q_{t2}$ [Js$^{-1}$g$^{-1}$] | $T_2$ [°C] | $h^0_{ct}$ [kJg$^{-1}$] | $\mu$ [%] |
|---|---|---|---|---|---|---|---|
| Cotton | 0 | - | - | 192.7 | 384.3 | 9.7 | 3.7 |
| **DMP** | 1.01 | - | - | 119.5 | 301.7 | 3.5 | 28.2 |
| | 1.54 | - | - | 115.7 | 299.3 | 3.3 | 30.9 |
| | 2.00 | 7.2 | 194.1 | 110.7 | 297.4 | 3.1 | 35.1 |
| **DMPP** | 1.05 | - | - | 149.3 | 308.9 | 4.5 | 26.1 |
| | 1.53 | 5.3 | 184.0 | 146.4 | 308.3 | 4.7 | 27.6 |
| | 1.97 | 8.5 | 188.9 | 150.3 | 305.7 | 4.8 | 28.6 |
| **DMHEP** | 1.06 | 2.4 | 195.2 | 134.7 | 300.9 | 3.4 | 30.8 |
| | 1.56 | 4.1 | 193.5 | 118.3 | 290.5 | 2.9 | 35.6 |
| | 1.91 | 7.8 | 193.1 | 84.1 | 284.2 | 3.1 | 38.2 |

to increase of molecular size.

When comparing the values of $h^0_{ct}$ (total heat of combustion) the highest were obtained for **DMPP** with the values for **DMP** and **DMHEP** being quite similar. Hence, substitution of hydrogen to propyl has caused FR properties to deteriorate. Introduction of hydroxyl improved the FR properties in comparison to **DMPP**, but in relation to **DMP** no particular improvement could be detected. Would the FR properties improve, if there were two hydroxyl groups available in the molecule? This question is addressed in the following section.

## 6.3   Primary aminogroup as key functionality for flame retardancy

The FR properties of dimethyl-bis(2-hydroxyethyl) phosphoramidate **DMBHEP** were compared to the FR properties of **DMP**, **DMHEP** and **DMDMP**. Although it has been already shown in the previous chapter that a primary aminogroup is essential for obtaining good FR properties, it was necessary to determine whether introduction of hydroxyls could compensate the absence of protons in the aminogroup (similar to **DMPP** and **DMHEP**).
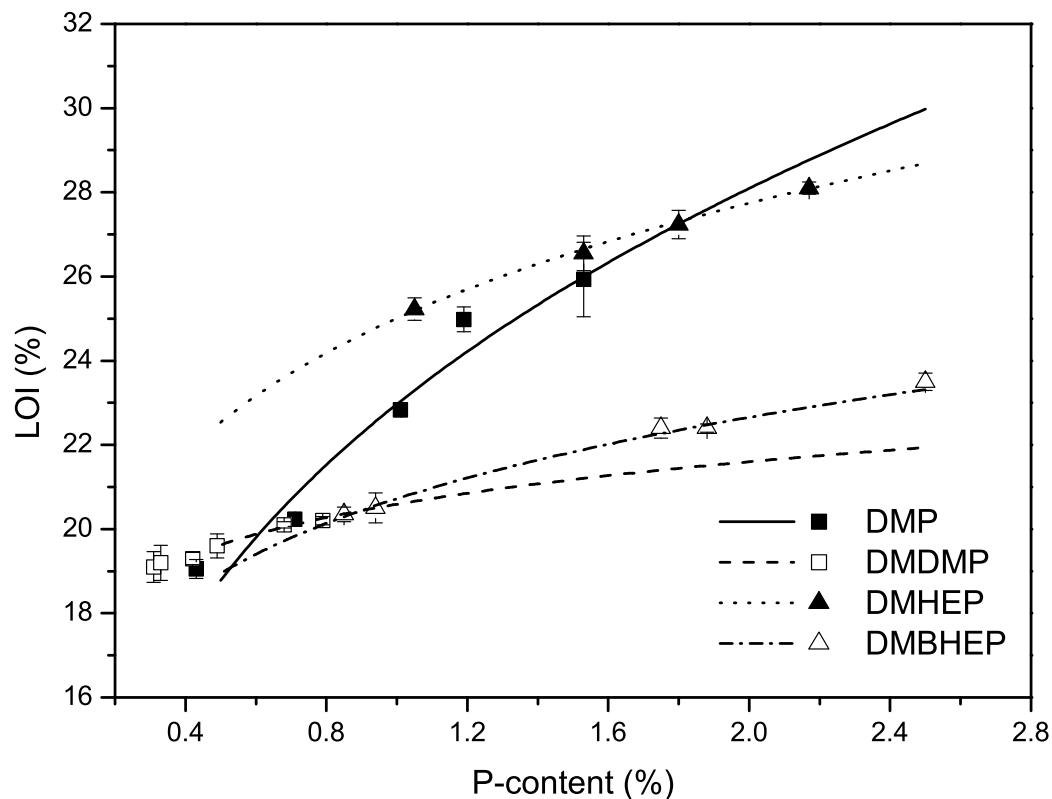
Figure 6.5 LOI vs. phosphorus content for fabrics treated with **DMP**, **DMDMP**, **DMHEP** and **DMBHEP**

Fig. 6.5 represents the dependence of LOI on the phosphorus content for fabrics treated with phosphoramidates **DMP**, **DMDMP**, **DMHEP** and **DMBHEP**. The trend line computed for **DMBHEP** lies in the same range as the trend line of **DMDMP**, indicating their similar flammability behaviour. At 2 % of phosphorus uptake, the LOI of **DMDMP** and **DMBHEP** drops by almost 6 % when compared to **DMP** and **DMHEP** and amounts just 21 %. This data clearly shows the negative influence of hydrogen substitution on the FR properties of phosphoramidate.

In the previous chapter it was mentioned that obtaining the desired uptake of **DMDMP** on cellulose was aggravated by the absence of acidic hydrogen. In case of **DMBHEP**, necessary uptakes were reached without any particular difficulties. Two hydroxyls obvi-

ously improved the retention of chemical on the cellulose, but the key factor influencing the FR properties of the molecule needs to be attributed to the aminogroup. In other words, the hydroxyl group improves the grafting, but the NH group places the P in the closest position for the phosphorylation.

## 6.4   The influence of N-alkyl chain

In [116] Gaan *et al.* suggested that FR properties of **DMHEP** can be triggered by specific rearrangement process that takes place during thermal treatment. They believed that the terminal hydroxyl of phosphoramidate can attack the phosphorus atom to form a cyclic intermediate. The stability of this intermediate was claimed to be crucial for the decomposition process. In case of **DMHEP**, it was suggested that a 5-member cycle is formed further improving stability. In order to study this phenomenon further, the FR properties of **DMBHEP** were compared to the properties of other hydroxyl-containing phosphoramidates.

Examination of Fig. 6.6, which presents the results of the LOI test for hydroxyl-containing phosphoramidates **DMHEP**, **DMHPP** and **DMBHEP**, reveals a clear trend at $1\%$ of phosphorus: **DMHEP** > **DMHPP** > **DMBHEP**. At higher phosphorus uptakes, curves for **DMHEP** and **DMHPP** almost coincide. At the same time the slope of **DMBHEP** trend line is much less steep than slopes of **DMHEP** and **DMHPP** so that the difference of LOI at phosphorus content of $2.4\%$ for **DMBHEP** increases to $5\%$ and amounts $23\%$.

It was also interesting to note the difference in LOI values for **DMHEP** and **DMHPP**. The change in the number of N-carbon atoms from two (**DMHEP**) to three (**DMHPP**) resulted in a significant decrease in LOI at low phosphorus concentrations. Most probably, the fragment P–NH–$(CH_2)_n$–OH of the phosphoramidate is involved in the reactions taking place during combustion of treated cellulose as it was readily mentioned in [116]. The elongation of the chain just by one $CH_2$ unit lead to the remarkable decrease of the FR properties.

In order to get further insights on the FR behaviour of the studied compounds, they were investigated using MCC. The thermal behaviour of all three phosphoramidates was very
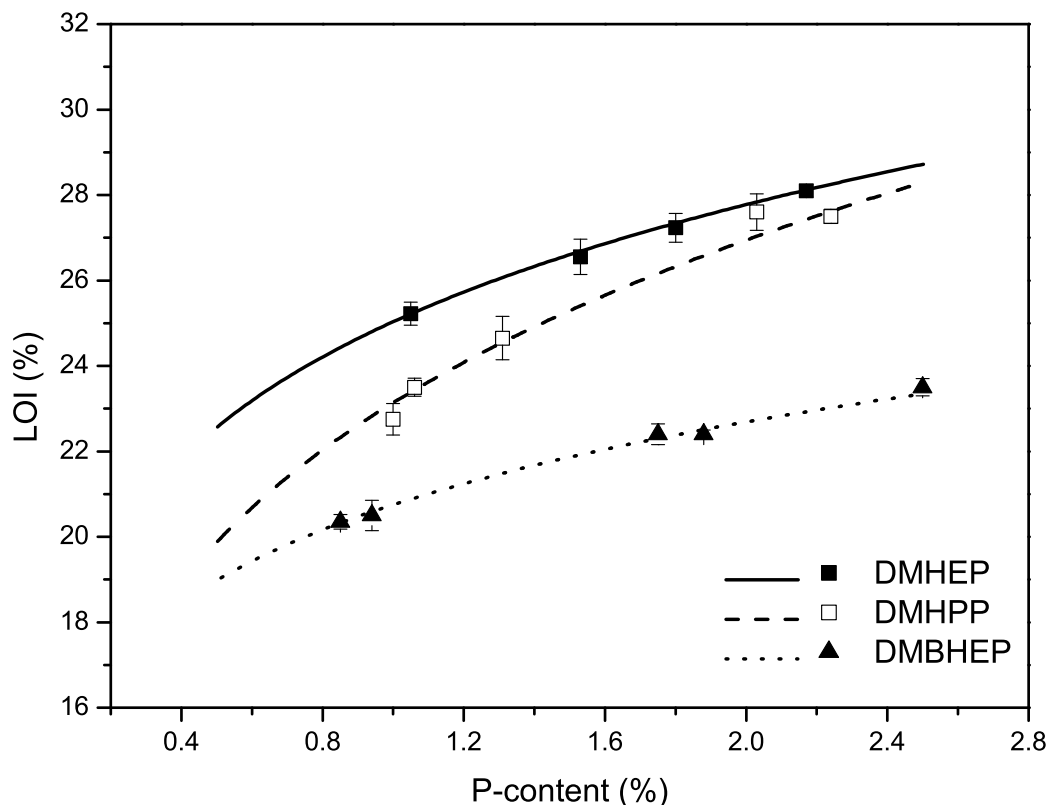
Figure 6.6 LOI vs. phosphorus content for fabrics treated with **DMHEP**, **DMHPP** and **DMBHEP**

similar. The peak corresponding to the main decomposition phase appeared at the same temperature for all three compounds, thus indicating similar processes taking place at this stage (Fig. 6.7). The relevant differences, however, were found in the values of combustion heat $h_{ct}^0$ (Table 6.3).

The lowest heat of combustion was measured for **DMHEP**, followed by **DMHPP** and **DMBHEP**. Interesting was also the fact that values of total heat of combustion for **DMHEP** and **DMHPP** varied only by 5-7 % at different phosphorus contents whereas for **DMBHEP** such differences were found to be as high as 25 %. Normally, heat of combustion ($h_2^0$) decreases when the phosphorus uptake (or phosphoramidate uptake) on cellulose is increased. However, such a small decrease as in the case of **DMHEP** and
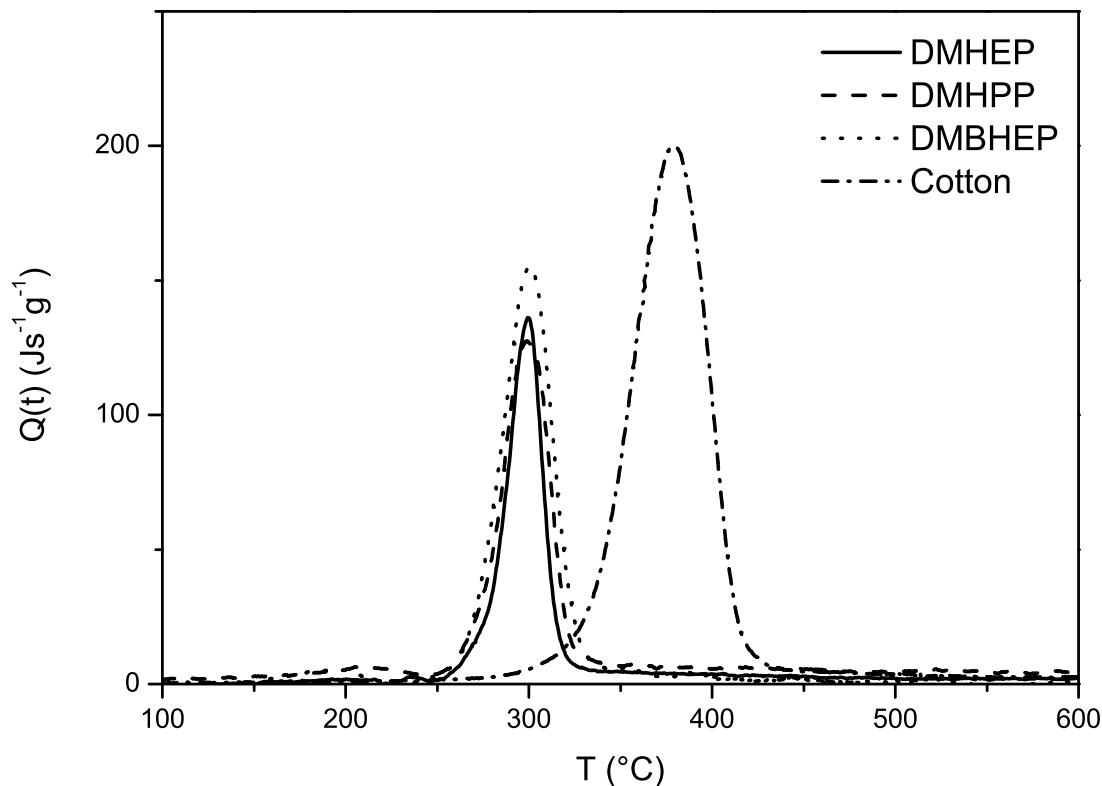
Figure 6.7 Specific heat release rates of fabrics treated with **DMHEP**, **DMHPP** and **DMB-HEP** (approx. 1 % of phosphorus)

**DMHPP** has never been observed before. This data is very well confirmed by the LOI results: the increase in LOI was rather slow (small slopes of the fitted trendlines).

This phenomenon might occur as a result of an either more effective interaction of hydroxyls and aminogroups with cellulose (as compared to **DMBHEP**), other reactions taking place during combustion (reactions where aminogroup is involved) or bulkiness of the phosphoramidate molecule. The interaction with cellulose prior to combustion can be assessed using the heat release values $Q_{t1}$. With almost the same weight uptake of phosphoramidate (Table 4.2), the loss of phosphoramidate prior to combustion was almost doubled from **DMHEP** to **DMHPP**. This finding was further supported by data from TGA (Fig. 6.8), where the loss of phosphoramidate between 100 and 200°C for **DMHPP**

Table 6.3 Combustion data of cotton fabrics treated with **DMHEP**, **DMHPP** and **DMBHEP**

| FR | $P_p$ [%] | $Q_{t1}$ $[Js^{-1}g^{-1}]$ | $T_1$ [°C] | $Q_{t2}$ $[Js^{-1}g^{-1}]$ | $T_2$ [°C] | $h_{ct}^0$ $[kJg^{-1}]$ | $\mu$ [%] |
|---|---|---|---|---|---|---|---|
| Cotton | 0 | - | - | 192.7 | 384.3 | 9.7 | 3.7 |
| **DMHEP** | 1.06 | 2.4 | 195.2 | 134.7 | 300.9 | 3.4 | 30.8 |
|  | 1.56 | 4.1 | 193.5 | 118.3 | 290.5 | 2.9 | 35.6 |
|  | 1.91 | 7.8 | 193.1 | 84.1 | 284.2 | 3.1 | 38.2 |
| **DMHPP** | 1.01 | 6.5 | 209.1 | 127.1 | 299.5 | 4.4 | 27.7 |
|  | 1.54 | 8.2 | 208.9 | 119.4 | 291.3 | 4.2 | 31.2 |
|  | 1.86 | 10.2 | 210.0 | 113.9 | 291.6 | 3.9 | 36.9 |
| **DMBHEP** | 0.94 | 6.6 | 193.1 | 155.2 | 301.3 | 5.7 | 25.2 |
|  | 1.49 | 7.1 | 193.8 | 124.7 | 295.3 | 4.3 | 26.1 |
|  | 1.80 | 8.8 | 194.6 | 97.0 | 289.8 | 3.9 | 28.8 |

was clearly higher than for **DMHEP**.

On the other hand, **DMBHEP** exhibited better interaction properties with cellulose at low temperatures than **DMHEP** and **DMHPP** (Fig. 6.8). However, the decomposition temperature of **DMBHEP**-treated cellulose was about 30°C higher, than for **DMHEP**- and **DMHPP**-treated cellulose. Obviously, introduction of another hydroxyl in **DMB-HEP** had the only effect on the pre-combustion interaction with cellulose, but in terms of increasing the FR properties the presence of NH was more important.

In order to demonstrate the effect of hydroxyls in **DMHEP** and **DMHPP**, their properties were compared with the FR properties of **DMMEP** and **DMMPP**, where hydroxyls were replaced by methoxy groups.

## 6.5   The significance of hydroxyls for flame retardancy

The substitution of hydroxyl in **DMHEP** to methoxy group in **DMMEP** caused the LOI to drop at lower concentrations of phosphorus (Fig. 6.9). At higher phosphorus contents the LOI values for both **DMMEP** and **DMMPP** were almost the same.

Extending the N-carbon chain from two to three carbon atoms resulted in the same effect
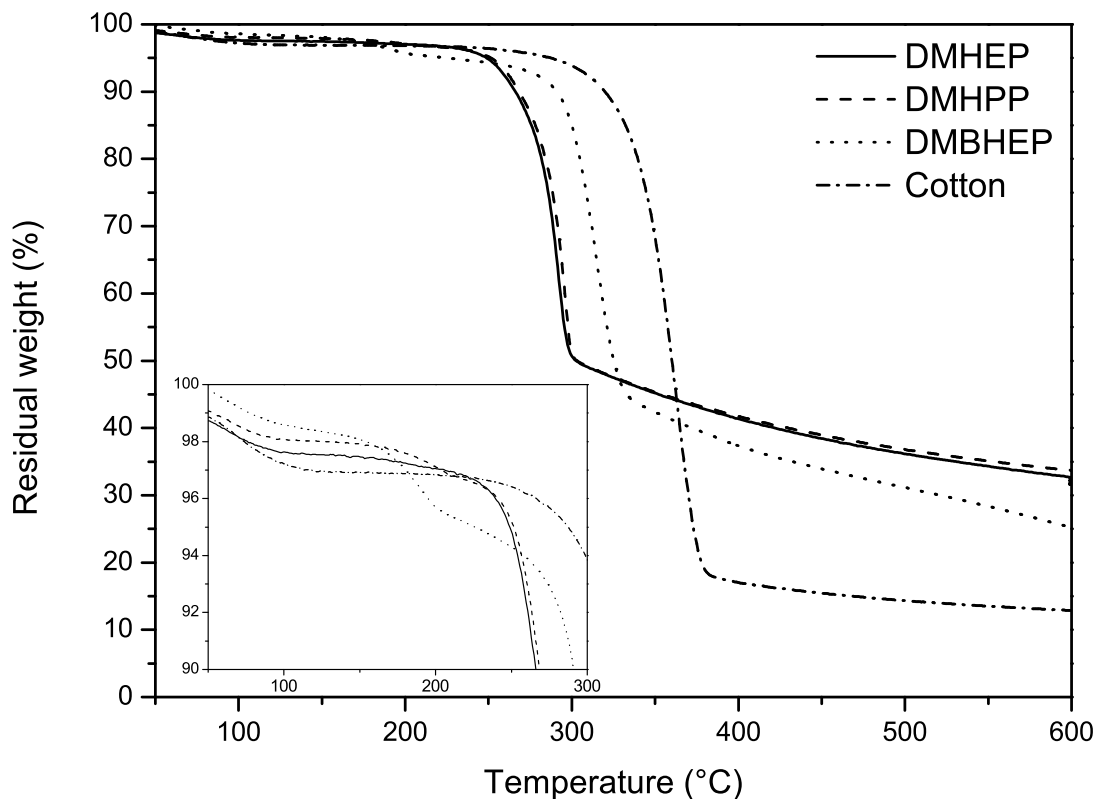
Figure 6.8 Thermogravimetric analysis of fabrics treated with **DMHEP**, **DMHPP** and **DMB-HEP** (approx. 1 % of phosphorus)

on LOI as in the case of the compounds **DMHEP** and **DMHPP**: the values decreased for **DMMPP** when compared to **DMMEP**. However, at higher phosphorus contents the slope was different as compared to **DMHEP** and **DMMEP**, i.e. the LOI values for **DMMPP** were lower. Obviously, the structural changes occurring in these molecules produced less effect on FR properties as for **DMMEP**.

When the MCC data of **DMMEP** and **DMMPP** was compared to **DMHEP** and **DMHPP**, a clear decrease in FR properties was observed. The total heat of combustion for **DMMEP** and **DMMPP** was increased by an average of 35 %. The loss of phosphoramidate at about $195 - 200$°C was increased by at least 30 %. Interestingly, the char yield was still comparable and decreased only by 5-7 %. This could indicate that the

Table 6.4 Combustion data of cotton fabrics treated with **DMMEP** and **DMMPP**

| FR | $P_p$ [%] | $Q_{t1}$ [$Js^{-1}g^{-1}$] | $T_1$ [°C] | $Q_{t2}$ [Js$^{-1}$g$^{-1}$] | $T_2$ [°C] | $h_c^0$ [kJg$^{-1}$] | $\mu$ [%] |
|---|---|---|---|---|---|---|---|
| Cotton | 0 | - | - | 192.7 | 384.3 | 9.7 | 3.7 |
| **DMMEP** | 1.14 | - | - | 138.5 | 307.5 | 4.6 | 27.6 |
| | 1.45 | 13.8 | 186.3 | 144.2 | 305.3 | 4.7 | 32.3 |
| | 2.27 | 12.2 | 194.3 | 156.5 | 305.4 | 5.1 | 32.3 |
| **DMMPP** | 0.95 | - | - | 152.5 | 307.5 | 4.7 | 24.3 |
| | 1.46 | 14.2 | 196.3 | 138.1 | 306.1 | 5.1 | 26.9 |
| | 1.93 | 15.1 | 188.2 | 121.8 | 299.6 | 4.4 | 34.8 |

amount of flammable volatiles was increased in case of **DMMEP** and **DMMPP** - but at what expense considering that the char yields were found to be the same?

Possibly, the presence of hydroxyl has indeed influenced the decomposition mechanism so that some species have been produced which were also able to react in the gas phase to reduce the amount of evolved heat. The studies of the gas phase during the thermal decomposition are documented in Chapter 8. The examination of the condensed phase were continued by morphological analysis of the chars left after LOI tests.

## 6.6 Morphological studies of cellulose treated with hydroxy- and methoxyalkyl phosphoramidates

Prior to the analysis of chars, treated fabrics were investigated using SEM technique before combustion. The micrographs of **DMHEP**– and **DMHPP**–treated fabrics are shown in Fig. 6.10. In distinction to micrographs on Fig. 4.7, the formation of thin coating was observed. These coatings looked very similar to the coatings which were obtained during plasma treatment of cellulose impregnated with diethyl(acryloyloxyethyl)phosphoramidate (Dissertation ETH No. 19827 by Katrin Prinz).

Figure 6.11 shows the micrographs of chars left after LOI test for compounds **DMHEP**, **DMHPP** and **DMBHEP**. The char surfaces of **DMHEP**– and **DMHPP**–treated cellulose exhibit surface blisters (notice that no such blisters were observed on the surface

of **DMBHEP**–char). Such blistering has been already discussed in Chapter 4, where the surface of the char left after combustion of **DBP**–treated samples showed formation of blisters. However, the phenomenon occurring here is different, as blistering was not caused by high loadings of phosphoramidate. Moreover, the blisters observed on the surface of **DMHEP** and **DMHPP** chars were 3-4 times smaller (around 50-80 $\mu$m vs. 150-200 $\mu$m in case of **DBP**) and appeared not on the yarn but on single fibers. Thus we believe they might originate from a different source.
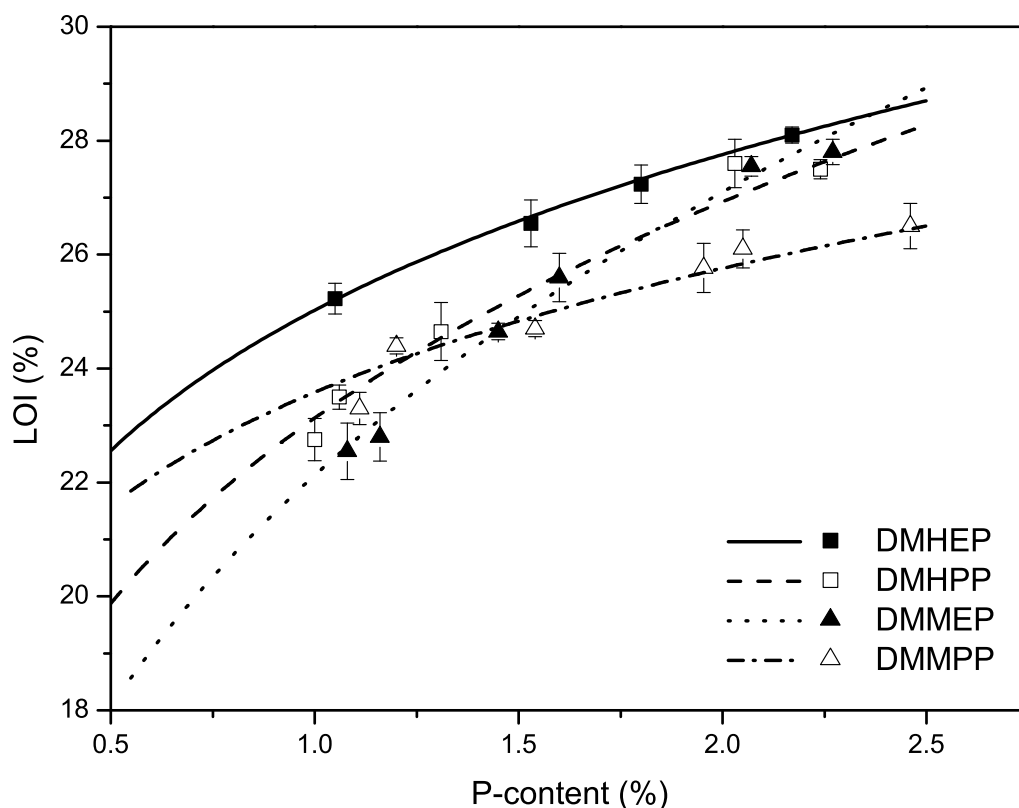


Figure 6.9 LOI vs. phosphorus content for fabrics treated with **DMHEP**, **DMHPP**, **DMMEP** and **DMMPP**

This blistering effect was studied in detail by Halua Pinto de Magalhães during his semester project in the group of Prof. Dr. Joëlle Levalois-Grützmacher. He has been studying cotton cellulose treated with diethyl-(acryloxy)ethyl phosphoramidate and diethyl-(2-
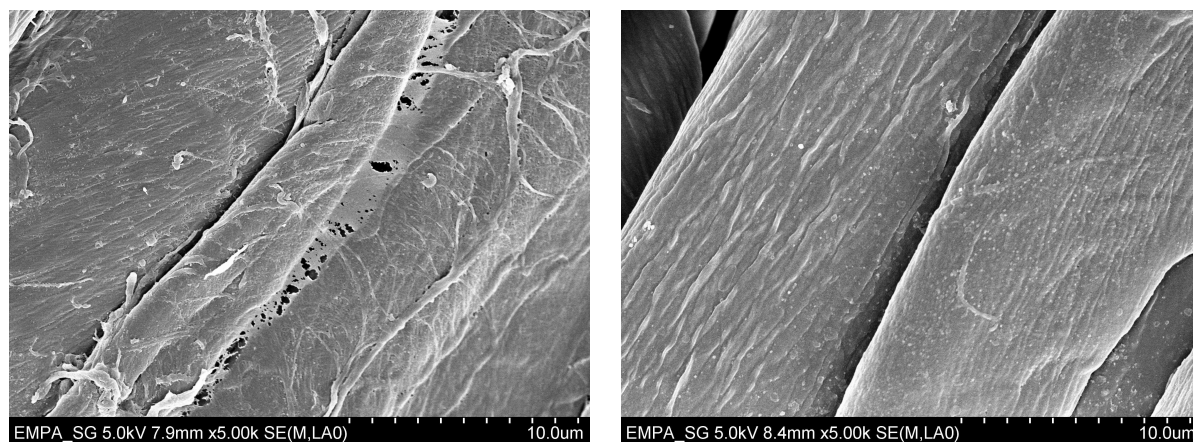
Figure 6.10 SEM micrographs of fabrics treated with **DMHEP** and **DMHPP** (content of phosphorus 1 %, x5000)

hydroxyethyl) phosphoramidate. In his experiments a similar bubble formation for both compounds was observed after the combustion in the LOI apparatus. He indicated that water evaporation might be the reason for the formation of these nodules. Subsequent drying experiments confirmed his hypothesis to be true: samples dried in the oven for at least 24 h prior to combustion did not show any bubbles in later SEM experiments. Hence, the absorbed water has created the pressure difference, under which the observed bubbles were formed.

In this respect another interesting fact deserves attention. As the formation of these nodules was not observed for fabrics treated with **DMP**, **DEP**, **DiPP** and **DPP** and the samples were put into same conditions prior to LOI and SEM measurements, we can state that the treatment of cellulose with compounds **DMHEP** and **DMHPP** improved their hydrophilicity owing to a hydroxyls of the phosphoramidate. Similar results were also obtained by Pinto de Magalhães: the FR properties of diethyl-(N-2-hydroxyethyl) phosphoramidate were found to be better than of diethyl-(acryloyl)ethyl phosphoramidate. This absorbed water probably enhanced the hydrolysis of the intermediates formed during the decomposition of the phosphoramidate to acidic species. As a result, the increased FR behaviour of hydroxyalkyl phosphoramidates was observed.

As further step, the chars left after LOI test of fabrics treated with compounds **DM-MEP** and **DMMPP** were analyzed using SEM. When the micrographs were compared
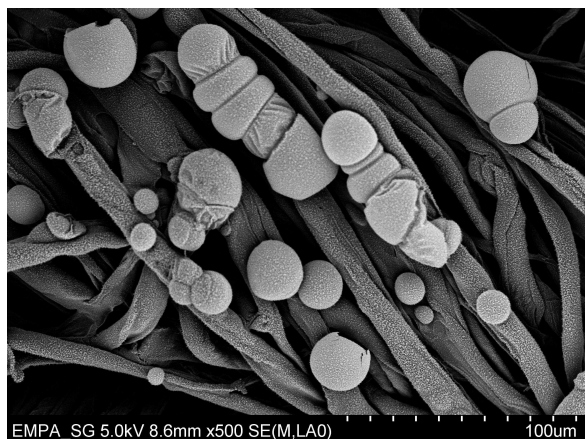
a) **DMHEP**, 1.95 % P, x500
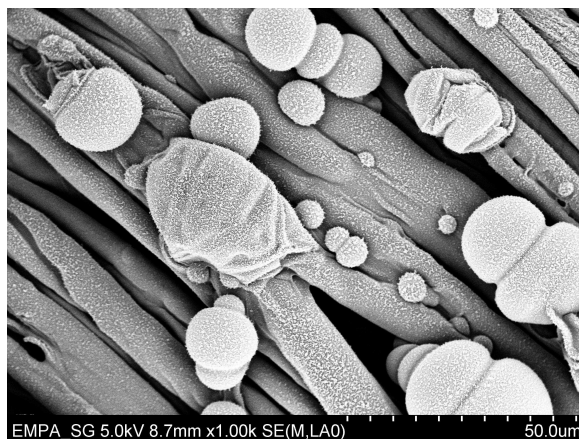


b) **DMHEP**, 1.95 % P, x1000
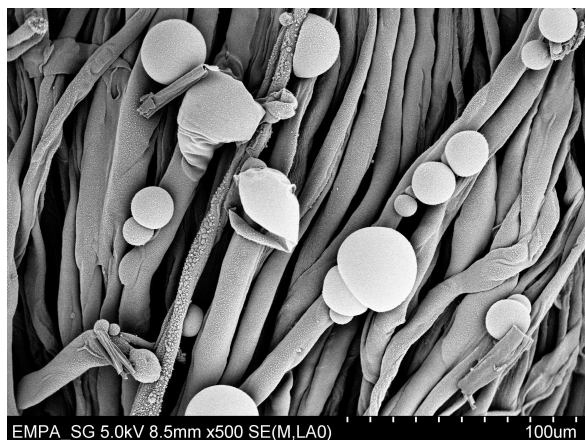


c) **DMHPP**, 1.98 % P, x500
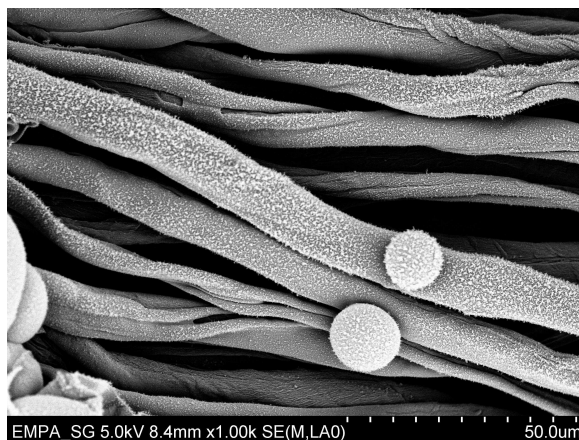


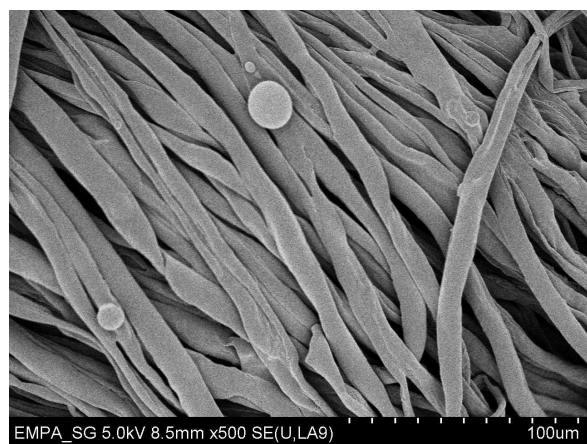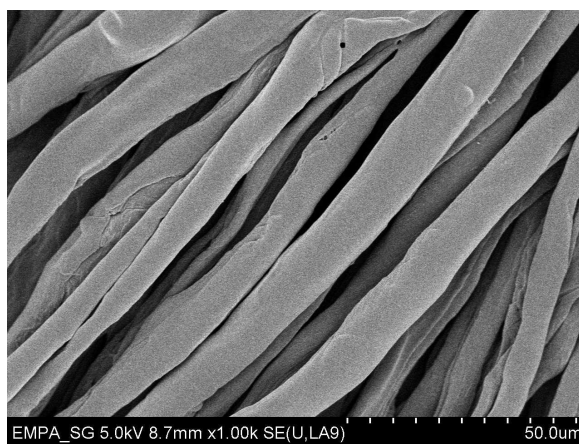d) **DMHPP**, 1.98 % P, x1000
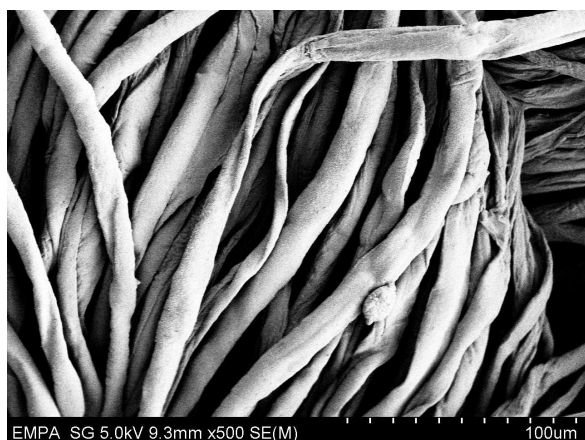


a) **DMBHEP**, 1.87 % P, x500
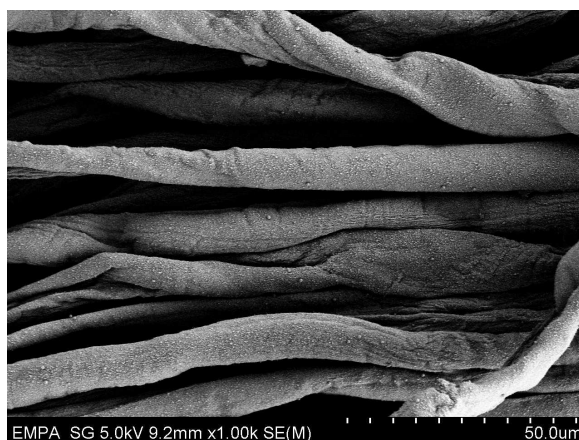


b) **DMBHEP**, 1.87 % P, x1000

Figure 6.11 SEM micrographs of the chars of fabrics treated with **DMHEP**, **DMHPP** and **DMBHEP**
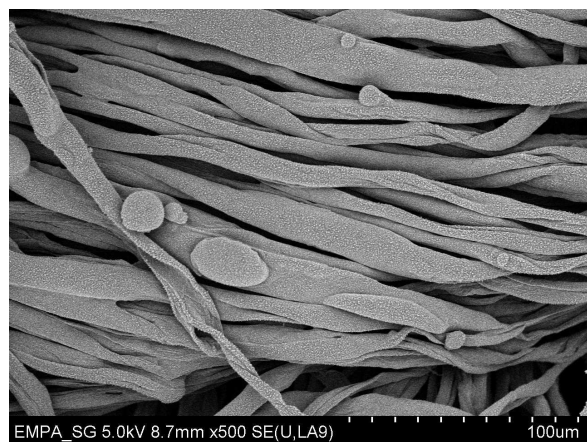
a) **DMMEP**, 2.27 % P, x500
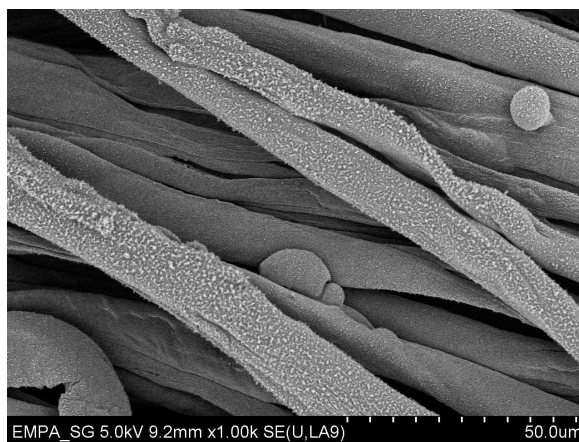
b) **DMMEP**, 2.27 % P, x1000

c) **DMMPP**, 1.93 % P, x500

d) **DMMPP**, 1.93 % P, x1000

Figure 6.12 SEM micrographs of the chars of **DMMEP**- and **DMMPP**-treated fabrics

(Fig. 6.12), no significant differences in the morphology of these char were observed. For **DMMEP**- and **DMMPP**-treated cellulose, the formation of similar nodules was observed (to a much lower extent, however). This observation might be related to a content of hydroxyl groups. In the previous section it was found that the formation of nodules occured as a result of the extensive water absorption of phosphoramidates with hydroxyl groups. The substitution of a proton for methyl group reduces the hydrophilicity of phosphoramidates. In respect to it the number of nodules per surface unity of cellulose treated with **DMMEP** and **DMMPP** was lower.

## 6.7   Conclusions

In the present chapter, the influence of hydroxyls introduced in the structure of phosphoramidate on the FR properties of treated cellulose has been shown.

Hydroxyl groups were found to positively affect FR properties. The flammability of **DMHEP**- and **DMHPP**-treated cellulose decreased and the char yields increased. Hence, the ability to promote char-forming reactions was improved. Substitution of proton in hydroxyl group for methyl in **DMMEP** or **DMMPP** caused the deterioration of FR properties, thus indicating the importance of hydroxyl group.

When the properties of hydroxyl-containing prosphoramidates were compared to the properties of **DMP**, the improvements were observed to be insignificant. As a matter of fact, the presence of a primary aminogroup was proved to be more significant in providing good FR properties. The hydroxyl groups of **DMHEP**, **DMHPP** and **DMBHPP** improved the retention of phosphoramidates on cellulose, whereas the availability of aminogroup directly influences phosphorylation. In the absence of bulky substituents at the nitrogen atom, phosphorus is in closer contact with cellulose for phosphorylation, hence increasing the FR properties. Moreover, the role of molecule size was put forward. The interaction of **DMBHEP** with cellulose was hindered by the spacial arrangement of hydroxyethyl groups, and as a result, the FR properties were reduced.

These findings let us conclude that the efficiency of phosphoramidate as FR for cellulose is sort of a compromise between the availability of acidic protons (primary aminogroups)

and their reachability. The reachability of acidic protons is in turn triggered by the size of the phosphoramidate molecule and the spatial arrangement of functional groups. Taking it all into account, the next step would be to add aminogroups to improve the interaction with cellulose and to maximally reduce the size of the molecule.

## Chapter 7

# Aryl phosphoramidates and phosphoroamides. Effects of phenyl ring and nitrogen content

The present chapter is dedicated to the investigations of FR properties of methyl phosphorodiamide **MPDA** and phosphoric triamide **PTA**. As it was found previously that aminogroups are essential for profound flame retardancy, their content was increased from one in **DMP** to two and three in **MPDA** and **PTA**, respectively, and properties of these two amides were compared to **DMP**.

**DPP**:   $R_1 = R_2 = $ OPh
**PPDA**:   $R_1 = $ OPh; $R_2 = $ NH$_2$
**MPDA**:   $R_1 = $ OMe; $R_2 = $ NH$_2$
**PTA**:   $R_1 = R_2 = $ NH$_2$
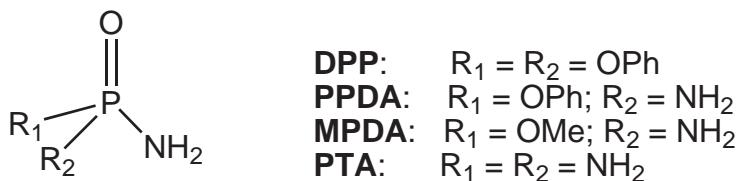
Figure 7.1 General structure of phosphorus compounds studied in Chapter 7

Prior to disclosing results for **MPDA** and **PTA**, the studies of two phenyl-containing phosphoramidates are presented. **PPDA** and **DPP** were studied originally together with n-alkyl phosphoramidates to demonstrate the effect of the phenyl ring on the FR properties of these compounds. Some very interesting results have been obtained, which deserve attention and justify the choice of **DPP** as one of the research compounds in the next

Chapter. The four compounds investigated in this chapter complete the entire study of the phosphoramidate family.

## 7.1 Literature review on aryl phosphoramidates and phosphoramides

Out of the four phosphoric amides studied in the present chapter, the use of **MPDA** and **PTA** was described in the literature.

The FR action of methylphosphorodiamide **MPDA** is reported in papers and patents dealing with FR formulations for cellulose [122, 123, 124, 125]. It has also been used in a composition of fertilizers designed to inhibit urease in soil [126, 127]. Further studies have been put forward to investigate its phytotoxic activity [85].

**PTA** was investigated as FR for cellulose [17, 18, 19, 20, 21, 128, 129, 130], wood [131, 81], polyester [132], thermoplastics [133] and as a urease inhibitor [134, 135, 136]. Its FR properties towards cellulose were shown by Morris *et al.* in [137] to be superior when compared to its N-substituted derivatives.

**DPP** and **PPDA** are not mentioned in the literature in the FR context neither for cellulose nor to any other substrates. **DPP** has found its application as inhibitor and substrate phosphamidase [138], as antihypercholesteroiemic and antiatherosclerotic agents [139], in the preparation of phosphorus-containing peptides [140] etc. Phenylphosphorodiamide **PPDA** was mostly used in fertilizers as urease inhibitors [134, 141, 135].

## 7.2 Physical properties of phosphoric amides and their treatment on cotton cellulose

**DPP** was obtained from ABCR Chemicals (Germany) as a white crystalline powder with a melting point at around 150°C and boiling point at 378°C (Table 7.1), soluble in hexane, insoluble in polar solvents. **PPDA** was obtained from Alfa Aesar (USA) as dark violet

crystals, soluble in polar solvents like water, slightly soluble in ethanol, insoluble in diethyl ether, chloroform, carbon tetrachloride. **MPDA** and **PTA** were synthesized according to the procedure described in Chapter 3. Both compounds were isolated as white powders with a characteristic odour. Their melting points are presented in Table 7.1.

Table 7.1 Physical properties of **DPP**, **PPDA**, **MPDA** and **PTA**

| Compound | MW [g/mol] | $P_s$ [%] | $N_s$ [%] | $C_s$ [%] | mp [°C] | bp [°C] |
|---|---|---|---|---|---|---|
| **DPP** | 249.20 | 12.43 | 5.62 | 57.84 | 150 | 378 |
| **PPDA** | 172.12 | 17.99 | 16.27 | 41.87 | 183 | - |
| **MPDA** | 110.05 | 28.14 | 25.45 | 10.91 | 128 | - |
| **PTA** | 95.04 | 32.59 | 44.21 | - | 135 | - |

Cotton samples were impregnated with solutions of compounds as described in chapter 3. However, some modifications were necessary as **DPP** is only slightly soluble in ethanol at ambient temperature. The solvent was heated to 60°C to ensure complete dissolution. A solution of **PPDA** was prepared in methanol at 50°C for the same reason.

The measured phosphorus content of **DPP**-treated cellulose was about 50 % lower than the calculated content. In fact, it was difficult to obtain desired phosphorus amount for **DPP**. Owing to its high molecular weight (Table 7.1) and low solubility in polar solvents (phenyl ring), application of concentrated liquor resulted in recrystallization of **DPP** on the surface of the cellulose. These crystals, we believe, were lost from cotton while handling during the elemental analysis, so that the measured phosphorus uptake was much lower than expected. For the comparative analyses samples with similar P-content were taken.

## 7.3 The effect of phenyl group on the flame retardant properties

LOI was measured for **DPP**- and **PPDA**-treated cellulose and the obtained data was compared with the data for **DMP** (Fig. 7.2). The LOI values were reduced in the order **DMP** > **PPDA** > **DPP** (**DPP**-curve was extrapolated).

In the same order the content of carbon (burnable fuel) was increased and the content of
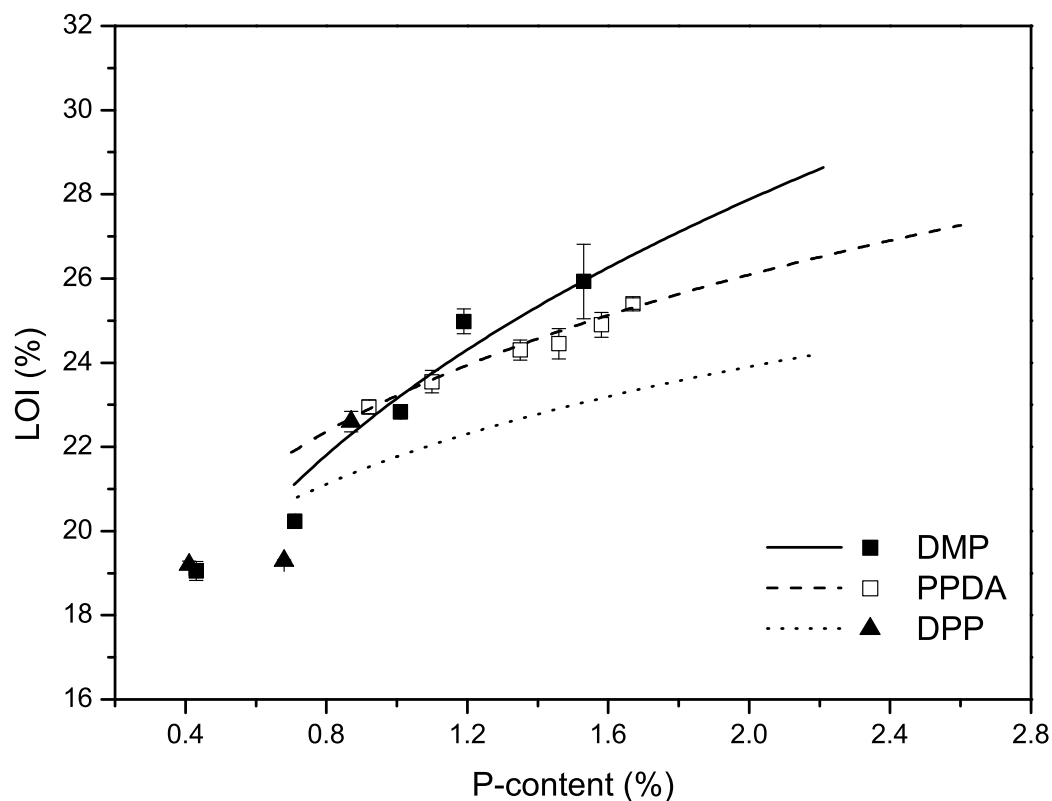
Figure 7.2 LOI vs. phosphorus content for fabrics treated with **DMP**, **PPDA** and **DPP**

phosphorus was decreased (Table 7.1). If we correlate the LOI values with carbon content as in Chapter 4 (Section 4.3), we find no linear dependence. For instance, LOI of **DBP** and **DPP** at 1.5 % phosphorus content were almost the same (22 % and 23 %, respectively), whereas the difference in carbon content was about 12 % (46 % for **DBP** and 58 % for **DPP**, Tables 4.1 and 7.1). Hence, the phenyl ring in **DPP** seemed to have less effect on fire retardancy than the long alkyl chains. Moreover, the difference in LOI values of **DMP**, **PPDA** and **DPP** comprised about 2 % (at the P-level of 1.5 %). In other words having a phenyl group is more advantageous than an ethyl group. This finding clearly indicates that carbon content cannot be directly correlated with FR properties and should be considered relevant only for compounds with similar chemical nature.

Similar conclusion can be drawn if char yields of **DMP**, **PPDA** and **DPP** are compared

(Fig. 7.3). Curves for **DMP** and **PPDA** almost coincided, and the difference to **DPP** comprised only about 1 %. The substitution of methyl groups in **DMP** to one phenyl in **PPDA** or two phenyl groups in **DPP** had almost no effect on the ability of phosphoramides to form char during combustion. Although introduction of phenyl groups increased the burnable fuel content, no changes were detected in terms of the condensed-phase mechanism of action of phosphoramides. This interesting finding will be studied in detail in the next chapter. In the following section we will further focus on the behaviour of treated fabrics in the conditions close to the real burning scenario.
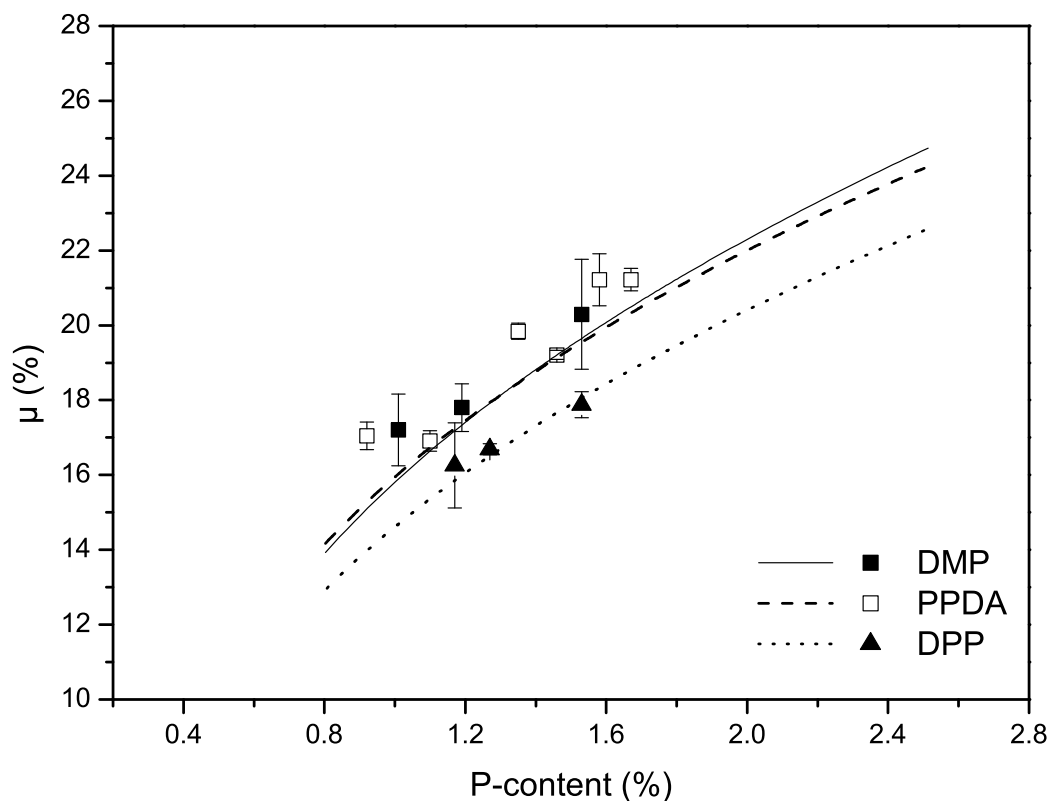


Figure 7.3 Char yields vs. phosphorus content for fabrics treated with **DMP**, **PPDA** and **DPP**

Figure 7.4 reflects the dependency of heat release rate on temperature for samples treated with **DMP**, **PPDA** and **DPP** with the measured phosphorus uptake of 1.5 %. Whereas for **DMP** only one sharp peak was observed, the curves' shapes for **PPDA** and **DPP** were

different. For all three compounds the peak at around 300°C (Table 7.2) corresponded to the process of cellulose degradation. However, in contrast to **DMP**, for **PPDA** and **DPP** the heat starts to evolve already at lower temperatures and for phenylphosphorodiamide even two convoluted peaks were observed.
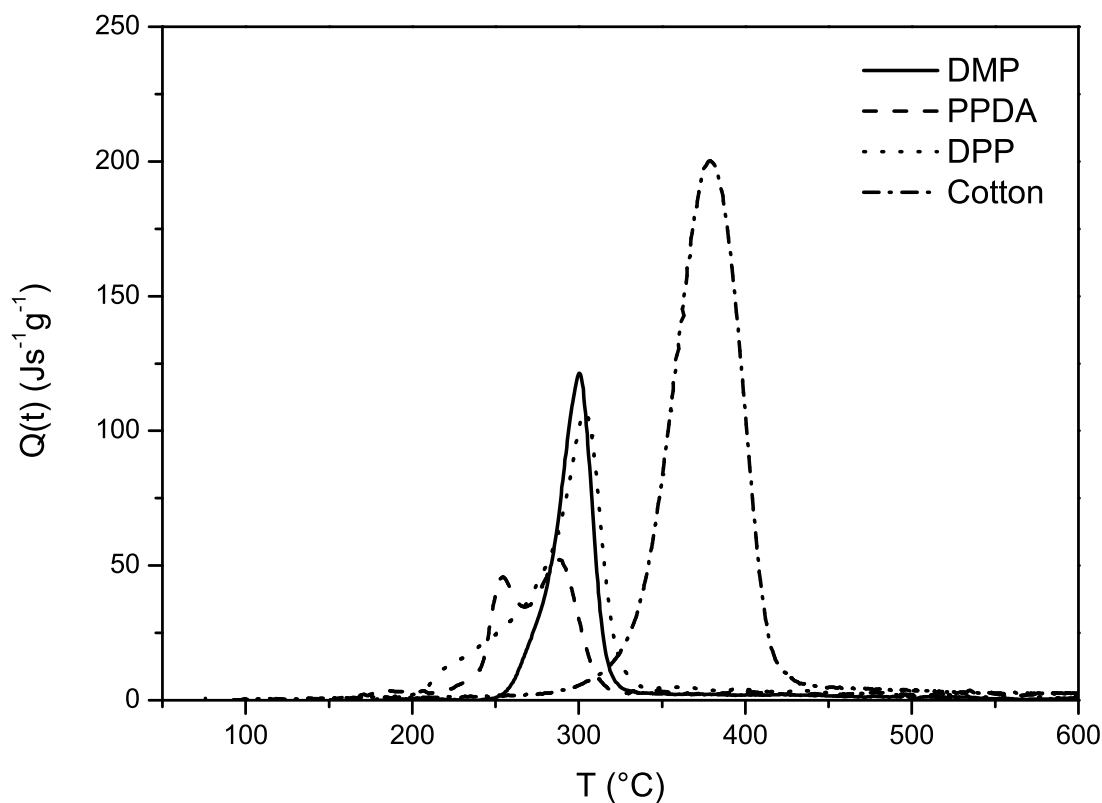


Figure 7.4 Heat release rates for fabrics treated with **DMP**, **PPDA**, **DPP**, **MPDA** and **PTA**

**PPDA** and **DPP** start to decompose at lower temperatures with the evolution of volatiles, which contribute to the total heat of combustion measured in MCC. Apparently, their interaction with cellulose is less pronounced, which lead to the desorption from the vicinity of cellulose and further combustion. To ensure the correctness of this finding, the MCC analysis of phosphoramidates alone was performed (Fig. 7.7), where the starting points of heat release were determined.

For **PPDA** the heat started to evolve readily at 100°C. We assume that this was observed

due to the evaporation of solvents, used in purification of **PPDA**. A sharp peak was seen at around 205°C.  This peak is most probably the same as the peak at 250°C on Fig. 7.4.  The difference in temperature occurred as a consequence of interaction with cellulose. The presence of polar aminogroups allowed to withstand the rise of temperature due to interaction with hydroxyls of cellulose, so that the desorption occurred later.  In other words, such NH–OH interaction assured the reaction of phosphoramidate uptake with cellulose during decomposition.
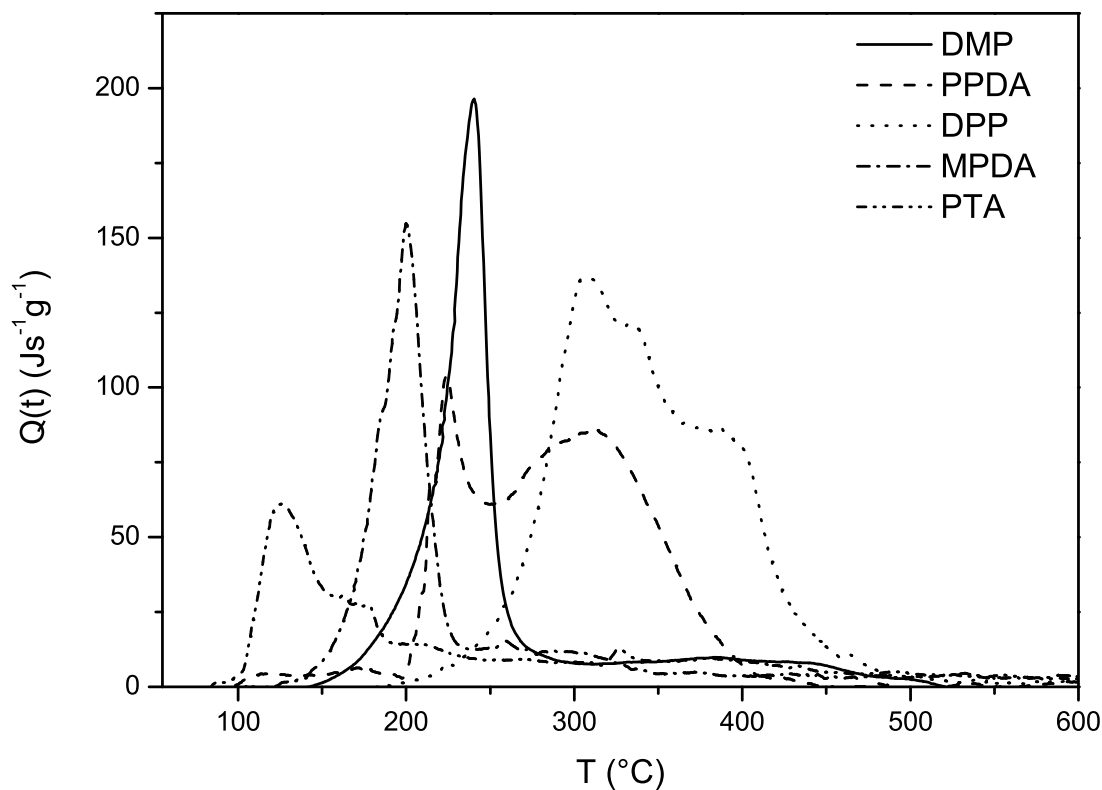


Figure 7.5 Heat release rates for pure **DMP**, **PPDA** and **DPP**

The shape of the $Q(t)$ curve for **DPP** showed completely different characteristics compared to the other phosphoramidates.  The broad distribution of $Q(t)$ in the temperature range from 200°C to 450°C and three convoluted peaks denote the different decomposition pathway of **DPP**.  Further, an interesting observation is related to the values of heat of

combustion and char yields of **DPP**, when compared to alkyl phosphoramidates (Table 4.4). The char yield of **DPP** was the highest and amounted to 22.8 %. **DPP** when undergoing thermal decomposition left more residue and less combustible volatiles after pyrolysis. It is likely that during the decomposition of **DPP**, some non-volatile or non-oxidizable species were formed leading to this result. This effect has been also described in the literature [76].

Table 7.2 Combustion data of cotton fabrics treated with phosphoramidates

|  | P [%] | $Q_t$ [Js$^{-1}$g$^{-1}$] | $T_{max}$ [°C] | $h_{ct}^0$ [kJg$^{-1}$] | $\mu$ [%] |
|---|---|---|---|---|---|
| Cotton | 0 | 192.7 | 384.3 | 9.7 | 3.7 |
| **DMP** | 1.01 | 119.5 | 301.7 | 3.5 | 28.2 |
| **PPDA** | 1.08 | 118.5 | 302.0 | 4.5 | 24.4 |
| **DPP** | 1.03 | 113.8 | 306.1 | 5.2 | 23.2 |

## 7.4 The effect of increased nitrogen content

**MPDA** and **PTA** showed an outstanding performance as FRs for cellulose. At 2 % phosphorus loading, LOI values were higher by 2 % for **MPDA** and by 4 % for **PTA** than for **DMP** (Fig. 7.6). The FR efficiency order observed was **DMP** < **MPDA** < **PTA** (the increase in LOI and char yields). Similar observation was made by Pandya *et al.* [142]. The increased nitrogen content, therefore, provided better FR properties. Same result has already been obtained in the previous section, where improved FR action of **PPDA** was determined.

If we further look at the char yields of the samples measured after their combustion, the trend here is inverse: the char yield for **MPDA** is higher than for **PTA** (Fig. 7.6). The highest amount of char for the same phosphorus uptake was measured for **MPDA**. Apparently, the remaining methoxy group is important for char-forming reactions, just as we have seen with **PPDA** and **DPP**.

Figure 7.7 reflects the dependence of heat release rate on the temperature for samples treated with **DMP**, **PPDA** and **DPP**. The shape of the peaks is quite similar. The temperature at the maximum heat release rate $T_{max}$ as well as the initial decomposition
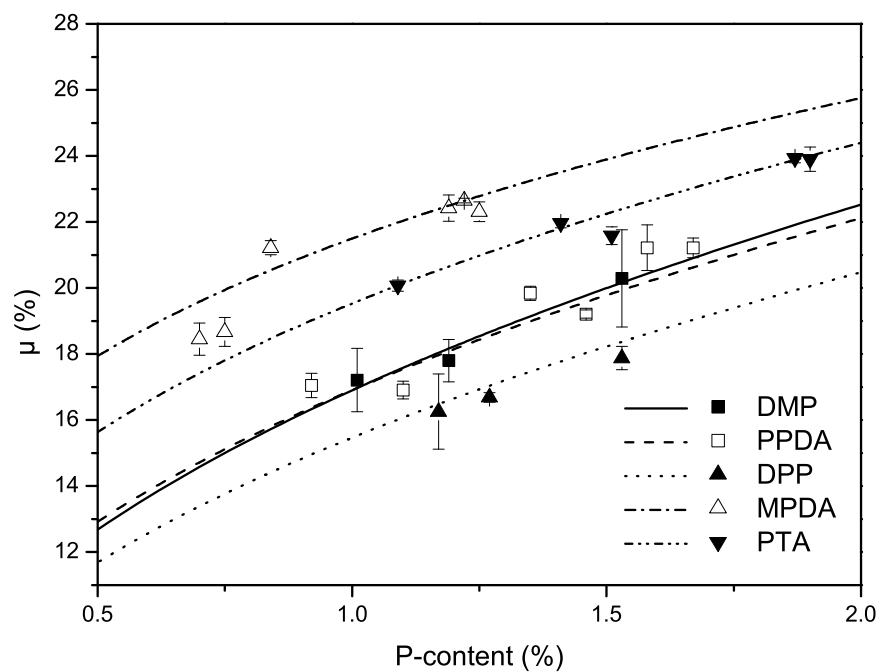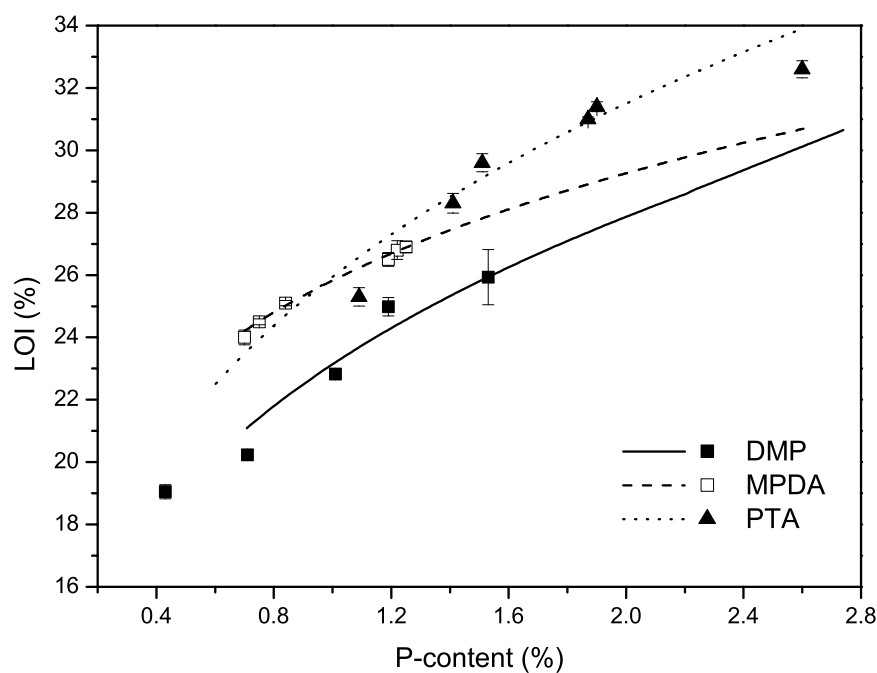
Figure 7.6 LOI (upper) and char yields (lower) vs. phosphorus content for fabrics treated with
**DMP**, **PPDA**, **DPP**, **MPDA** and **PTA**

temperatures are similar as well. This finding is an indication on similar decomposition pathways, which these compounds undergo upon combustion. The total heat of combustion $h^0_{ct}$, however, was quite different: 2.4 kJg$^{-1}$ for **MPDA** and 1.8 kJg$^{-1}$ for **PTA**. The value of 1.8 kJg$^{-1}$ was the lowest ever measured among studied phosphoramidates. When compared to untreated cotton, this value was five times lower, meaning that **PTA** was able to retard 80 % of the cellulose flammability.

Amazing is also the fact, that losses due to desorption prior to the main decomposition step were not observed for **PTA** (0-250°C). Is it because **PTA** is stable to thermal treatments? The shape of the **PTA**-heat release rate curve is totally different from **MPDA** and **DMP** (Fig. 7.5). Whereas the decomposition of **MPDA** and **PTA** seems to proceed in one stage, the decomposition of **PTA** is more complex with at least three differentiated stages.
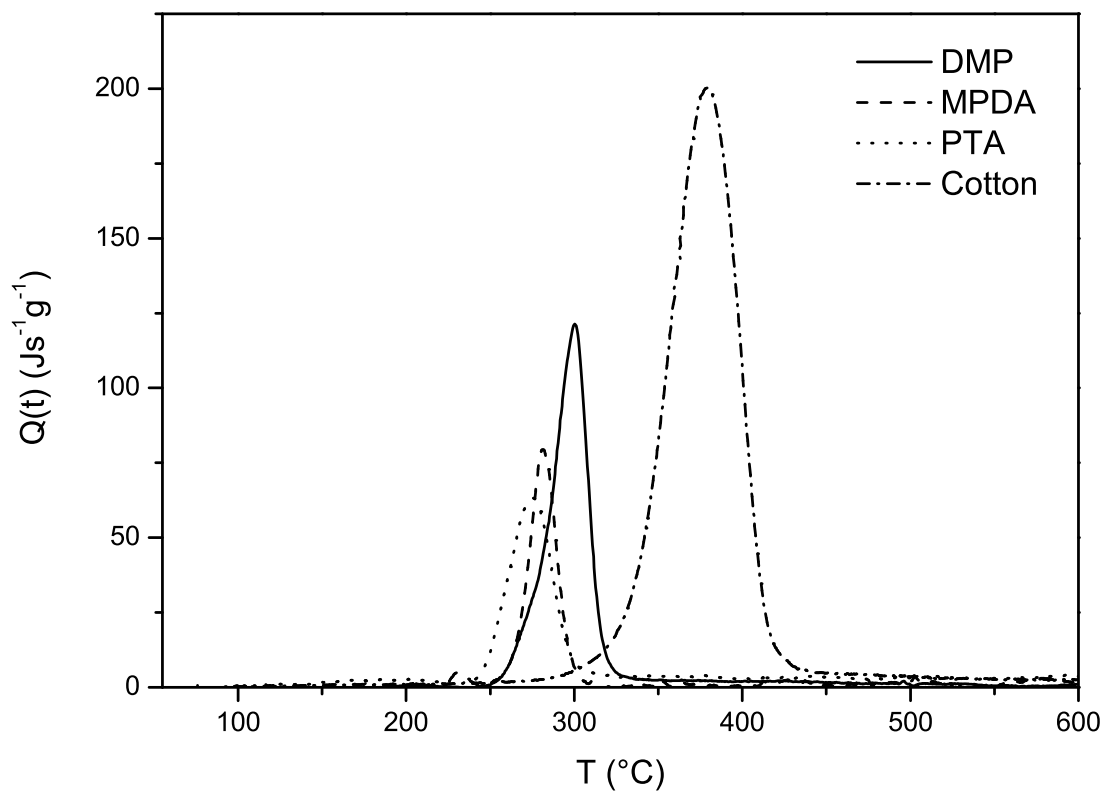


Figure 7.7 Heat release rates for cellulose treated with **DMP**, **MPDA** and **PTA**

Moreover, the temperature at the maximum heat release rate $T_{max}$ as well as the initial decomposition temperatures are quite different for all three compounds. $T_{max}$ decreases in the order **DMP** > **MPDA** > **PTA**. One explanation to this phenomenon could be the stability of phosphoramidates at high temperatures. Phosphoric triamide is probably the least stable phosphoramide as it starts to decompose readily at 100°C. It might be that the presence of aminogroups reduces the thermal stability of the compound. Similar results were already obtained by Gaan *et al.* in [65]. When properties of phosphates and phosphoramidates were compared, they have found that compounds with ester P–O–C bonds like triethyl phosphate are more stable to nucleophilic attack compared to the ones with P–N bonds, and as a result, phosphates are worse flame retardants.

## 7.5   Conclusions

The FR properties of arylphosphoramidates and phosphoramides were investigated. The FR properties of diphenyl phosphoramidate **DPP** were found to be superior when compared to **DEP** or **DBP**. Therefore, the carbon content as a a factor influencing flame retardancy should be correlated with the FR properties solely for compounds with similar chemical nature. Phenyl ring imparted superior flame retardancy for cellulose owing to the different decomposition mechanism revealed by thermal techniques.

Another important finding of this chapter concerned the influence of nitrogen content on the flammability of treated cellulose. Compounds with higher N/P ratios such as **PPDA** or **PTA** possessed excellent FR properties. The reason for this was suggested to be the low thermal stability of P–N bonding and as result, earlier decomposition of **MPDA** and **PTA** as compared to dialkyl phosphoramidates.

Moreover, it was discovered that the ester bond P–O–C is responsible for char-forming reactions, and thus, for the increase in the char yields. From chapter 4 we have learned that **DMP** is a better FR than **DEP**. Hence, methyl groups are one of the key functionalities for obtaining good FR properties.

# Chapter 8

# Decomposition of phosphoramidates: investigation of gas and condensed phases

The thermal decomposition of cellulose treated with phosphoramidates was studied in detail in the present chapter. Phosphoramidates with representative FR properties: **DMP**, **DEP**, **DMMP**, **DPP**, **DMHEP**, **MPDA** and **PTA** have been selected for this study. The chapter is divided into four sections.

In the first section the decomposition of cellulose treated with phosphoramidates was studied using thermogravimetric analysis and the results were compared. Further, decomposition products in the gas phase were investigated using an evolved gas analysis technique, i.e. thermogravimetric analysis coupled with Fourier transform infrared spectrometry (TGA-FTIR). In the third section, the composition of the condensed phase i.e. char residue at different temperatures has been studied. Based on the experimental results, attempts to draw possible reaction pathways for thermal decomposition of phosphoramidates were put forward in the fourth section.

## 8.1   Comparative decomposition studies of treated cellulose using TGA

Figures 8.1, 8.2, 8.3 and 8.4 show plots of the dependence of mass-loss on the temperature for samples treated with phosphoramidates. The thermograms indicate three to four mass-loss steps during the pyrolysis of the samples. The weight-loss for each step is indicated on each figure. This weight-loss, the decomposition temperature at the main step and the char yield at 600°C are collated in Table 8.1.

Table 8.1 Pyrolysis data of cotton cellulose treated with phosphoramidates

|  | P-con. [%] | $T_d$ [°C] | $M_1$ [%] | $M_2$ [%] | $M_3$ [%] | $M_4$ [%] | $\mu$ 600°C [%] |
|---|---|---|---|---|---|---|---|
| Cellulose | n/a | 387.1 | 5.5 | n/a | 75.9 | 4.5 | 14.2 |
| **DMP** | 1.01 | 260.2 | 5.4 | n/a | 53.3 | 12.2 | 29.1 |
| **DEP** | 1.17 | 262.8 | 6.2 | n/a | 49.0 | 16.4 | 28.4 |
| **DMMP** | 1.16 | 258.4 | 5.5 | n/a | 46.8 | 16.3 | 31.4 |
| **DMHEP** | 1.06 | 255.6 | 4.6 | n/a | 49.4 | 16.9 | 29.1 |
| **DPP** | 1.03 | 277.3 | 3.6 | 7.3 | 51.8 | 13.5 | 23.8 |
| **MPDA** | 1.13 | 253.2 | 6.3 | 8.5 | 33.9 | 16.6 | 31.9 |
| **PTA** | 1.01 | 249.7 | 7.6 | 10.7 | 32.0 | 17.4 | 32.3 |

The decomposition of cellulose treated with the selected phosphoramidates seemed to follow pathways. The first stage (up to 200°C) is characterized by the desorption of water from cellulose ($M_1$). This step is observed equally for all samples, the average of mass-loss being $5.6\pm2\,\%$. The mass-loss during the second step is phosphoramidate specific and was observed for **DPP**, **MPDA** and **PTA** ($M_2$). The third stage is characterized by a rapid and the highest weight-loss ($M_3$). This third stage is the main stage, where the actual decomposition of cellulose characterized mainly by depolymerization of the cellulose molecule is taking place. At this step, most volatiles are evolved. In the final stage from about 330°C to 600°C, the degradation of the residue is taking place ($M_4$).

In general, after treatment of cellulose with phosphoramidates the decomposition temperature $T_d$ as well as the mass loss at the main decomposition step $M_3$ were reduced and the char yields were increased (Table 8.1). The lowest decomposition temperature and the highest char yields were found for **PTA**-treated samples, however, these values were
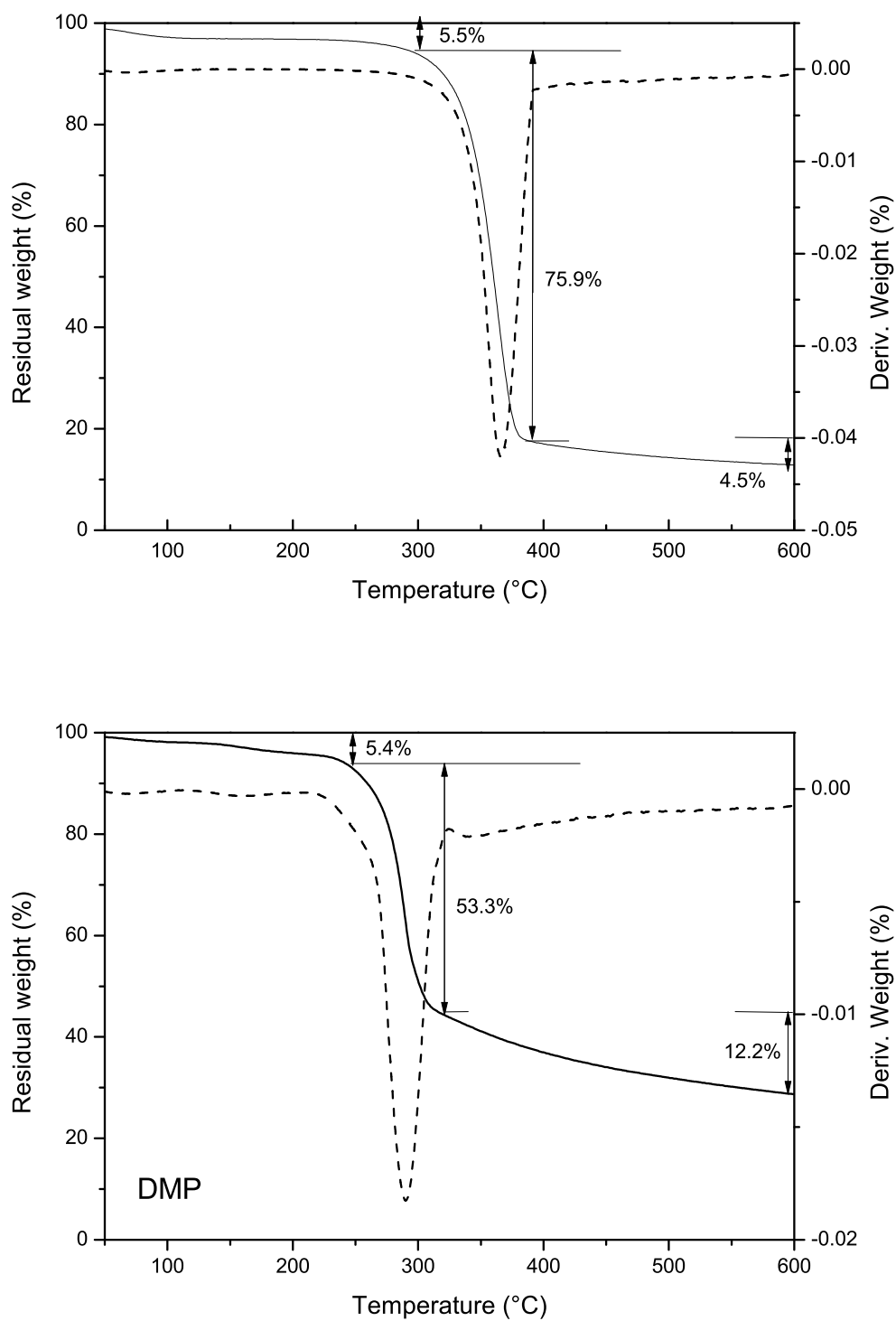
Figure 8.1 Thermogravimetric analysis of virgin cellulose and cotton treated with **DMP** (P-content 1 %)
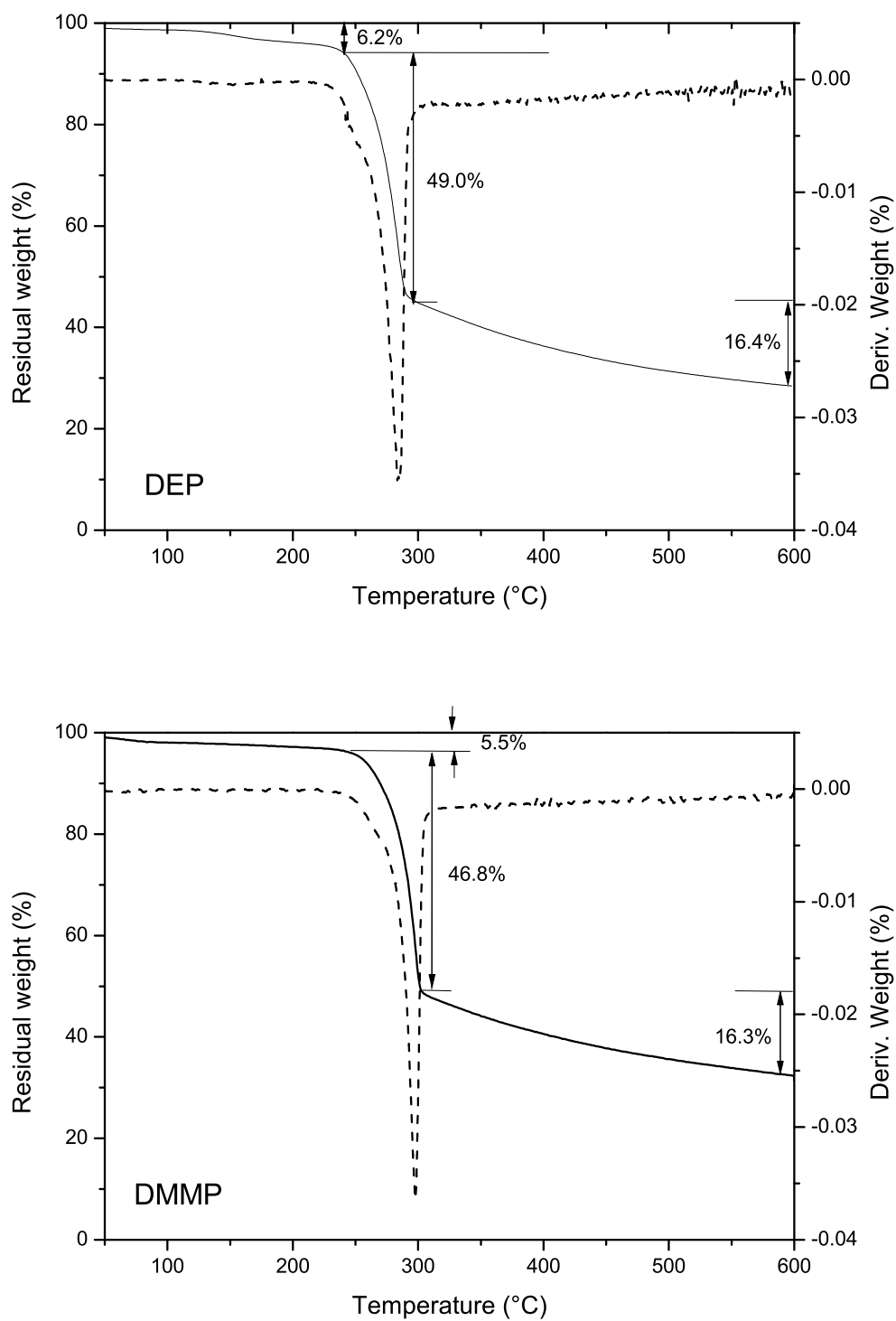
Figure 8.2 Thermogravimetric analysis of cotton treated with **DEP** and **DMMP** (P-content
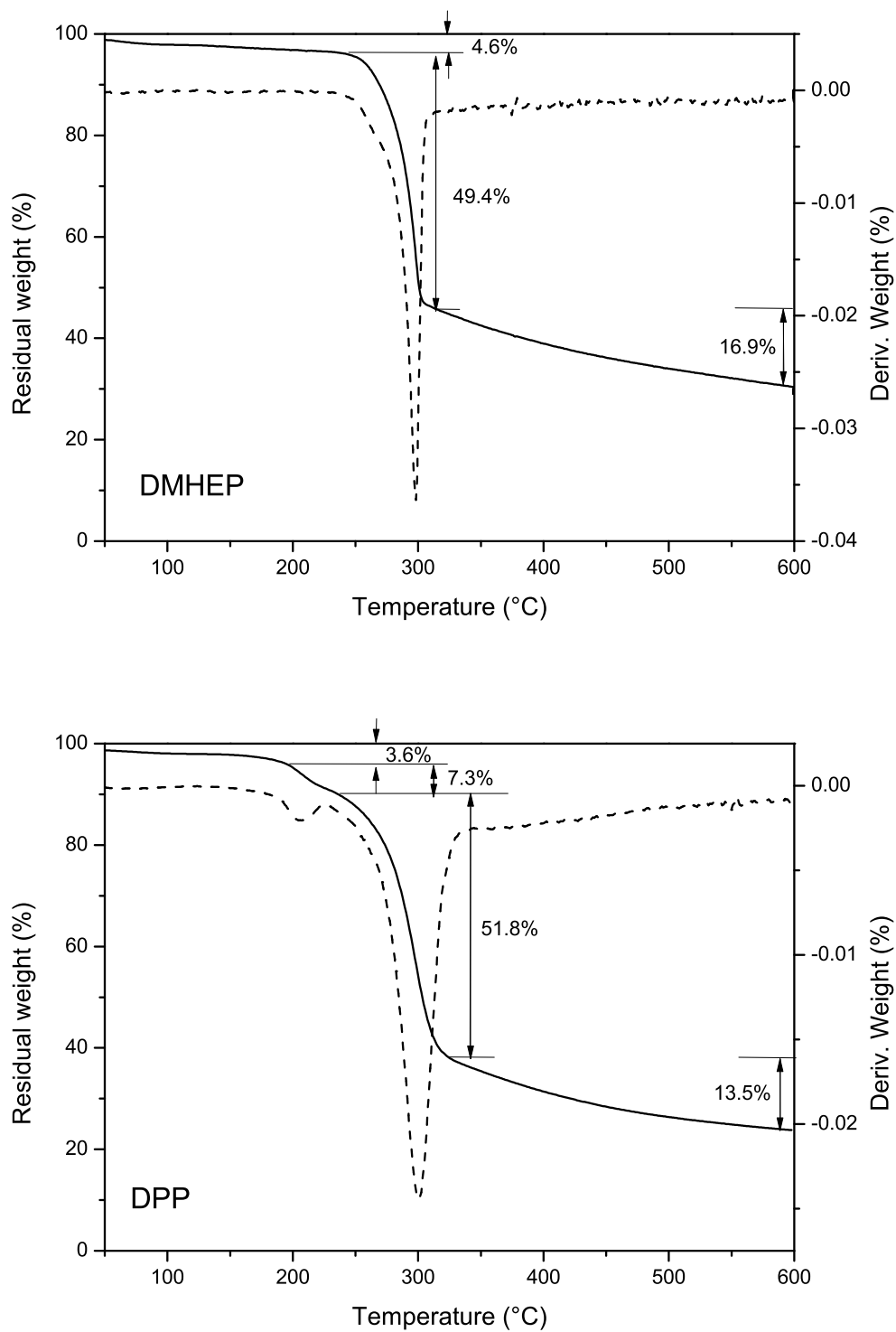         1 %)

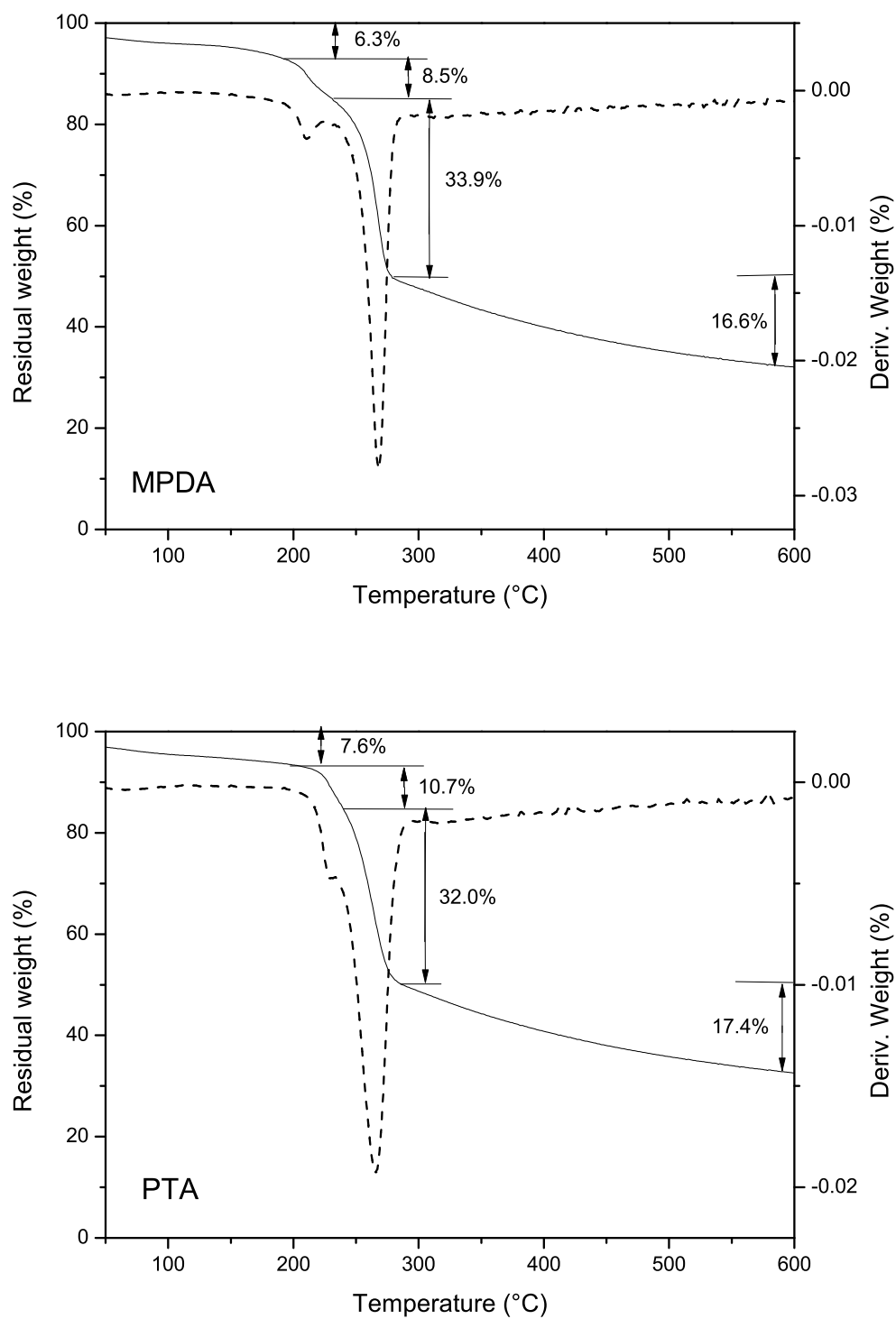Figure 8.3 Thermogravimetric analysis of cotton treated with **DMHEP** and **DPP** (P-content 1 %)

Figure 8.4 Thermogravimetric analysis of cotton treated with **MPDA** and **PTA** (P-content 1 %)

comparable with values obtained for other phosphoramidates like **DMMP** and **MPDA**. Interestingly, the decomposition of **DPP**-, **MPDA**- and **PTA**-treated cellulose proceeded through four steps in distinction to the rest of phosphoramidates. This intermediate mass-loss probably originates from the decomposition of phosphoramidate itself.
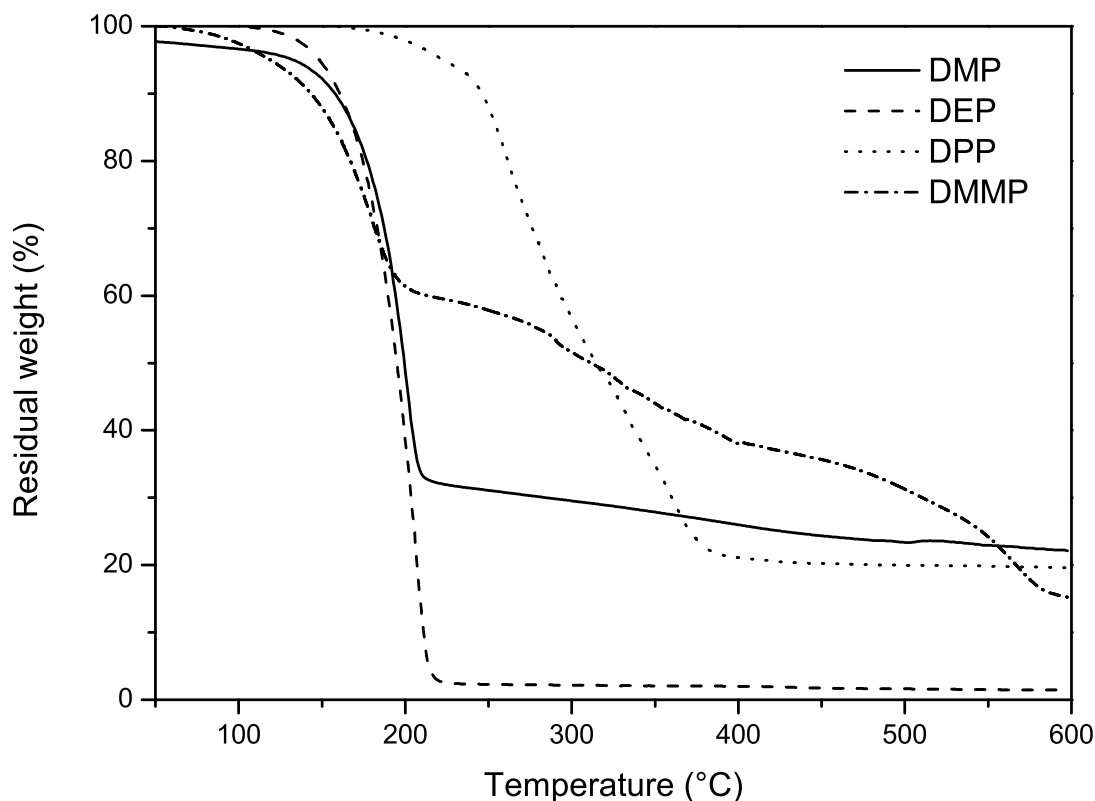


Figure 8.5 Thermogravimetric analysis of pure **DMP**, **DEP**, **DPP** and **DMMP**

Figures 8.5 and 8.6 represent the decomposition of pure phosphoramidates. The measurements were performed under the same conditions. **DMP**, **DEP** and **DMMP** start to decompose nearly at the same temperature (approx. at 150°C). By 220°C the main decomposition step is over. At this temperature the weight-loss was different for all compounds: 67.7 % for **DMP**, 97.6 % for **DEP** and 59.6 % for **DMMP** (Table 8.2). **DEP** has simply volatilized without decomposition. **DMP** and **DMMP** underwent decomposition probably via different routes, as in case of **DMMP** the products formed were stable at

high temperatures.
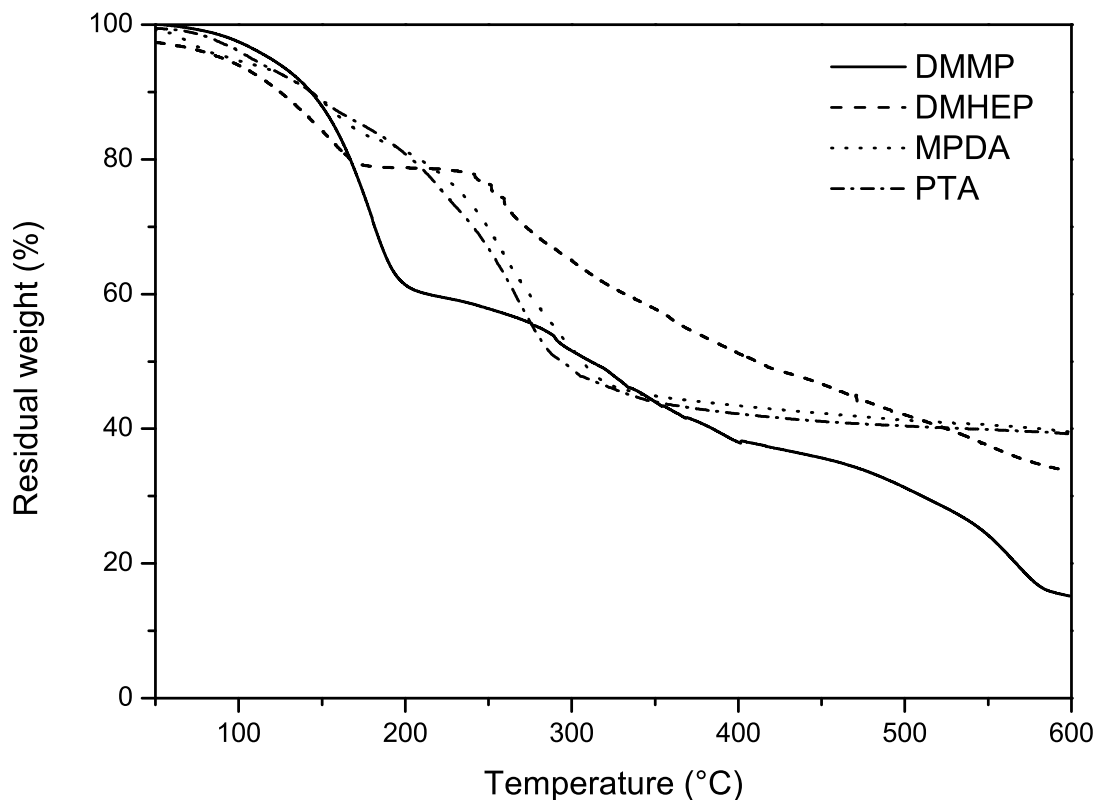


Figure 8.6 Thermogravimetric analysis of pure **DMMP**, **DMHEP**, **MPDA** and **PTA**

**DPP** is much more stable to higher temperatures. The first weight-loss (9.2 %) was recorded in the range 200°C–250°C and corresponds to the loss of 7.3 %, observed during the decomposition of **DPP**-treated cellulose (Fig. 8.3). The second weight-loss step corresponds to the actual decomposition of **DPP** and unlike for other phosphoramidates, it coincided with the main decomposition step of treated cellulose.

Decomposition of **DMHEP** resembles the decomposition of **DMMP** (Fig. 8.6). However, **DMHEP** forms even more stable decomposition products and forms more char (Table 8.2). Phosphoramides **MPDA** and **PTA** have similar decomposition mechanisms that proceed through two (evtl. three) steps. The residue is formed at approx. 300°C, which is stable up to 600°C.

Table 8.2 Pyrolysis data of pure phosphoramidates

| FR | $M_1$ [%] | $M_2$ [%] | $M_3$ [%] | $M_4$ [%] | $\mu$ 600°C [%] |
|---|---|---|---|---|---|
| **DMP** | 6.7 | n/a | 61.0 | 9.8 | 22.5 |
| **DEP** | 7.6 | n/a | 90.0 | 0.5 | 1.8 |
| **DMMP** | 8.4 | 51.2 | 21.9 | 22.6 | 15.1 |
| **DMHEP** | 5.7 | 15.5 | 45.0 | n/a | 33.8 |
| **DPP** | 9.2 | n/a | 69.6 | 0.8 | 20.4 |
| **MPDA** | 6.6 | 12.3 | 33.0 | 5.8 | 39.5 |
| **PTA** | n/a | 17.5 | 35.8 | 7.5 | 39.0 |

Clearly, the decomposition mechanisms of phosphoramidates differ from each other. In order to get further insights on the the kind of formed species, the way they may be formed, their effect on cellulose decomposition and to further understand the different FR activity of phosphoramidates, thermogravimetry with online FTIR spectrometry was employed in the next step.

## 8.2   Evolved gas analysis using TGA-FTIR

The FTIR spectra were recorded using online TGA-FTIR spectrometry. The analysis of spectra was performed at the temperatures, at which the weight-loss occurred in TG measurements of pure phosphoramidates (Figs. 8.5 and 8.6). Assignments of the absorption peaks were performed using the data from the literature or the data obtained by matching the measured spectra with library spectra (Bruker Optics, Germany; NIST Web Chemistry Library, USA).

The FTIR spectra of volatiles evolved from the heating of **DMP** in TGA are presented in Fig. 8.7. Bands characteristic for dimethyl phosphoramidate were observed (in cm$^{-1}$): N-H (3511), NH$_2$ (3417), CH$_3$ as (2960), P=O (1295, stretch), C–O (1051), P–O–C (980, aliphatic stretch) and P–O (831, stretch). The carbon dioxide band appearing at 2350 cm$^{-1}$ was attributed to the background spectrum. The library search for this spectra revealed the dimethyl phosphoramidate being the main compound with the matching index of 92 %. With the increase of the temperature in TGA, the intensity of the bands has decreased, indicating the change of the concentration of **DMP** in the gas phase.
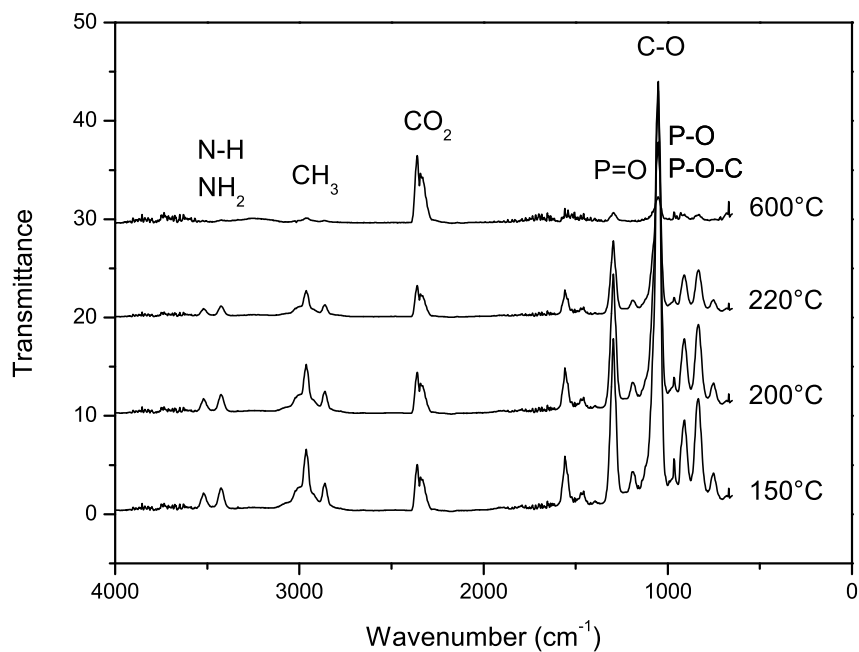
Figure 8.7 FTIR spectra of **DMP** upon heating in TGA (spectra are vertically shifted for clarity)
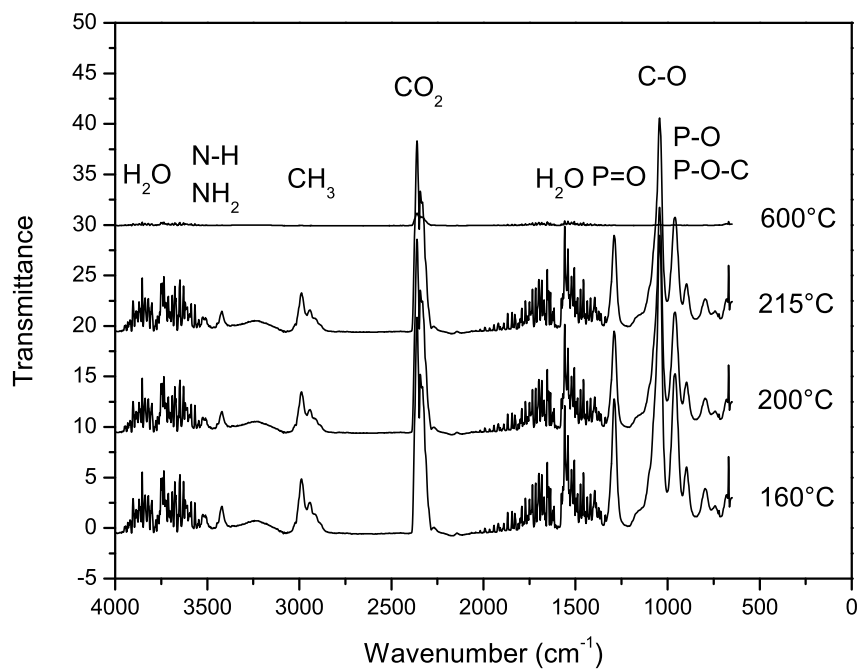


Figure 8.8 FTIR spectra of **DEP** upon heating in TGA (spectra are vertically shifted for clarity)

Similar results were obtained when TGA-FTIR analysis was performed for **DEP** (Fig. 8.8). Characteristic bands observed were (in $cm^{-1}$): N–H (3504), $NH_2$ (3419), $CH_3$ as (2985), P=O (1288), C–O (1041), P–O–C (958) and P–O (892), which matched the pattern of **DEP**. In the ranges 4000–3500 and 1800–1300 $cm^{-1}$ the signals characteristic for the presence of free hydroxyl were observed. These might have appeared due to the desorption of water (**DEP** is highly hygroscopic). As in the case with **DMP**, no other characteristic bands were detected except the ones originating from the phosphoramidate itself.
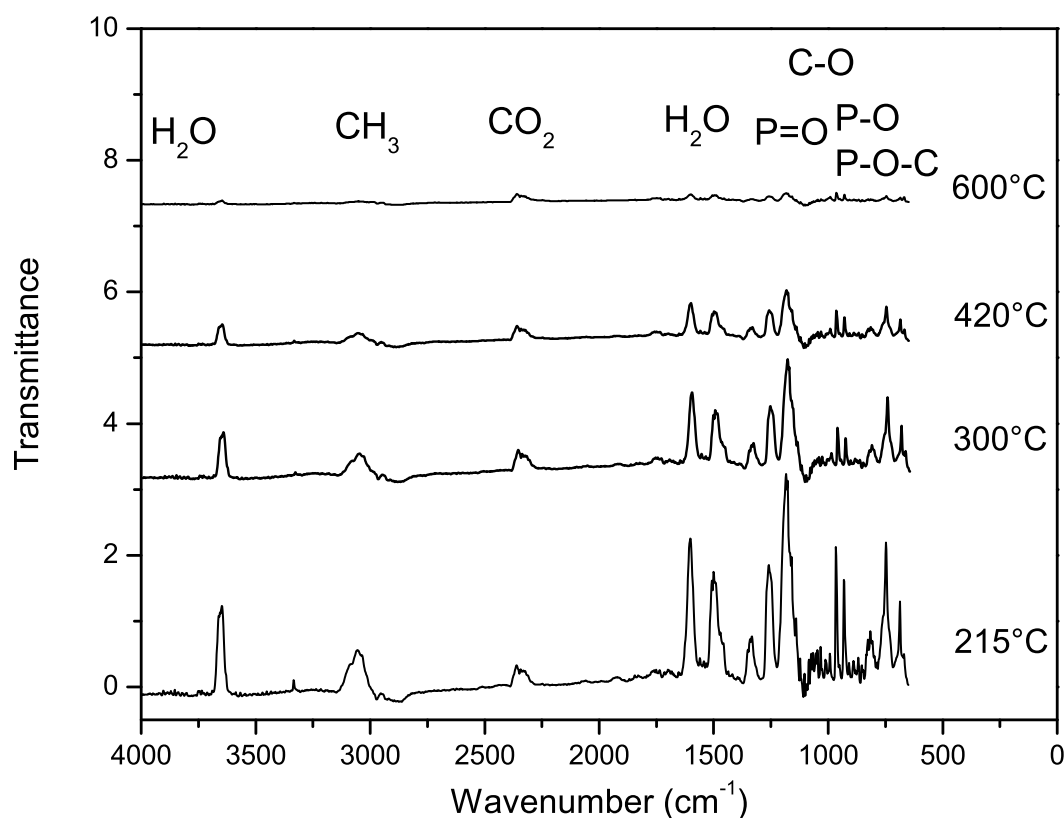


Figure 8.9 FTIR spectra of **DPP** upon heating in TGA (spectra are vertically shifted for clarity)

Further, **DPP** was analyzed using TGA-FTIR (Fig. 8.9). Matching of the FTIR spectra with the OPUS library indicated the presence of phenyl groups in the gas phase. The weight-loss at 200°C–250°C can therefore be attributed to the evolution of species, containing phenyl groups. The data was in accordance with literature: Shimasaki *et al.* have

analyzed decomposition of diphenyl phosphoramidate using TGA-MS and TG-TRAP-GC-MS methods [143] and have observed the formation of phenyl ether and phenylamine in the gas phase.

In TGA we have observed, that all phosphoramidates undergo decomposition. Detecting the species formed during this decomposition using FTIR was difficult, as a certain fraction of phosphoramidates underwent volatilization (e.g., **DMP** or **DEP**), so that finally the spectrum of phosphoramidate is obtained. It therefore was not possible to detect any bands originating from other compounds. As for **DPP** the analysis showed the formation of volatiles containing phenyl groups, but the exact assignment of spectra to the compounds was impossible. Although some phosphoramidates volatilize upon heating, the decomposition occurs in the condensed phase (TG analysis). Taking this into account, the research was continued with the investigation of the condensed phase using $^{31}$P NMR.

## 8.3   Investigation of the condensed phase using NMR

For the NMR analyses in the solid phase the samples of the phosphoramidates in alumina crucibles were taken out of the furnace at temperatures, at which either the weight-loss or the maximum weight-loss rate took place. They were cooled in liquid nitrogen, dissolved in a deuterated solvent and subjected to further analyses by means of $^{31}$P, $^{1}$H and $^{13}$C NMR (for the measurement parameters see Section *Experimental*). The results were based on the comparison with reference spectra measured under the same conditions and/or literature data. It is important to mention that the residues taken out at temperatures higher than 300°C were only slightly soluble in deuterated methanol, so that solely the soluble part was analyzed in NMR.

### 8.3.1   Decomposition of dimethyl phosphoramidate

Figure 8.10 reveals the $^{31}$P spectra of dimethyl phosphoramidate taken at four different temperatures.

Through the decomposition of **DMP** following signals were observed in $^{31}$P NMR: 14.3 ppm
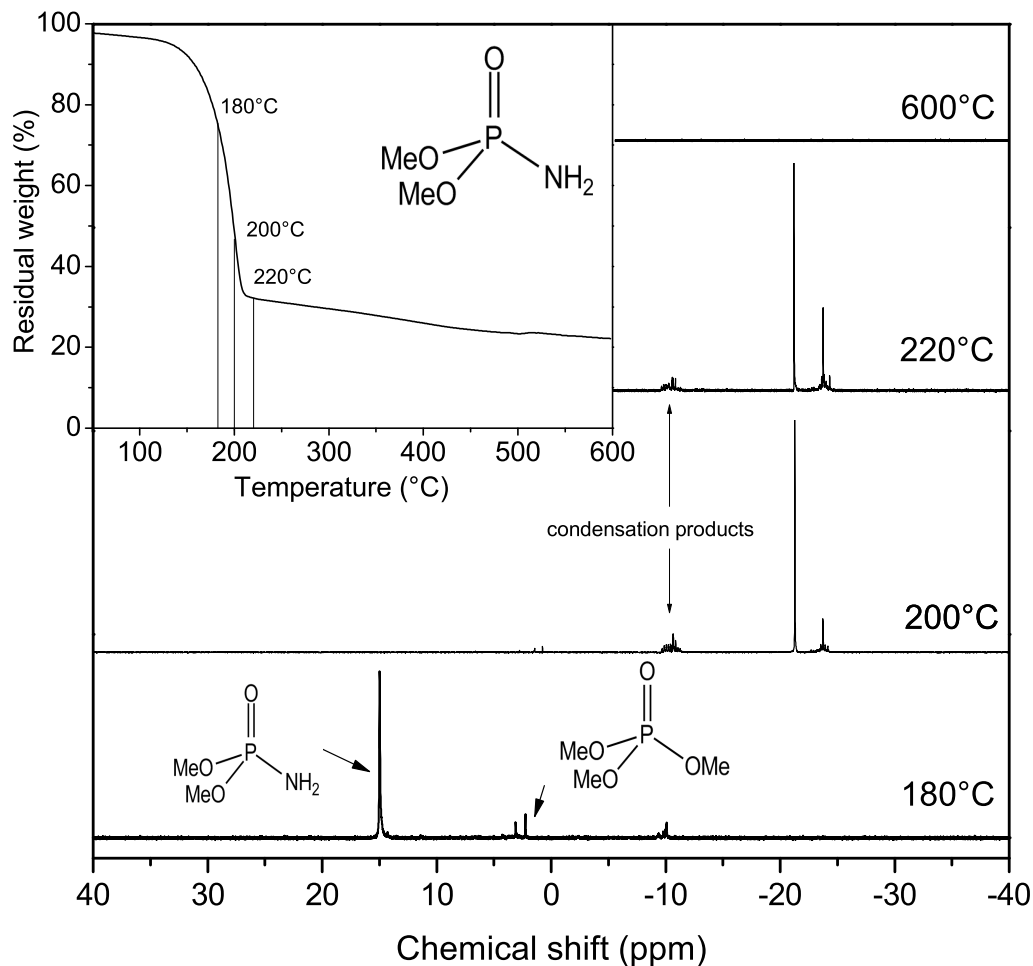
Figure 8.10 Decomposition of **DMP**: $^{31}$P NMR spectra (for clarity, spectra are shifted vertically; measured in $d_4$-CD$_3$OD)

(dimethyl phosphoramidate, lit. 15.2 ppm [144]), 2.3 ppm (trimethylphosphate, lit. 2.4 ppm [145, 146]), unassigned signals with rather low intensity relatively to **DMP** at –10.5 to –9.0 ppm and signals at –21.3 ppm and –24.5 to –23.5 ppm.

At 180°C about 10 % of **DMP** is volatilized, but 90 % remained and yielded the signal at 14.3 ppm. At this temperature, trimethylphosphate and some condensation products were also detected (derivatives of diphosphoric acid yield $^{31}$P-signals in the range –12.0 to –9.0 ppm, e.g. –9.8 ppm for dimethyl dihydrogen diphosphoric acid, [147]). The formation of pyrophosphates from phosphoramidates has also been observed by other researchers [148].

At 200°C about 70 % of weight is lost (volatilization) and in the remaining 30 % **DMP** was not observed, but its decomposition products. Apart of the possible presence of pyrophosphoric acid derivatives (–12.0 to –9.0 ppm), the high-intensity signal at –21.3 ppm and small signal at –24.5 were observed. Unfortunately, the exact assignment of these signals was rather difficult. In $^1$H and $^{13}$C NMR spectra a doublet at 3.72 ppm ($^1$H NMR), and singlet at 52.2 ppm ($^{13}$C NMR) were observed, which were assigned to methyl $CH_3O$ group. By performing a thorough literature search the possible species appearing at this range were found to be cyclic structures containing nitrogen (Table 8.3).

At 600°C about 24 % of residue was present. This residue was soluble neither in $CD_3OD$ nor in $D_2O$, therefore no signals in $^{31}$P NMR were observed. We believe that the residue is a highly cross-linked insoluble network. The formation of such structures has already been observed by Langley *et al.*. They proposed their formation as a result of the presence of P-N bonds [149].

Thereby using NMR it was possible to establish that although the **DMP** undergoes mainly volatilization (rapid weight-loss at $190 - 200°C$), some part of it decomposes with the formation of acidic species, pyrophosphates, further decomposition of which leads to the formation of stable residues. How would the decomposition look like for **DEP**?

## 8.3.2   Decomposition of diethyl phosphoramidate

The decomposition pathways of **DEP** and **DMP** are different. Decomposition of diethyl phosphoramidate does not result in the formation of residue (Fig. 8.11). Only 2.3 % remained at 600°C. Diethyl phosphoramidate its stable up to 240°C (reference signal at 12.3 ppm, lit. [144, 15]).

At 210°C two weak signals were detected at 0.53 and $-1.2$ ppm, respectively. At this temperature, more than 95 % of **DEP** was lost due to volatilization and further analysis was performed for remaining 3-5 %. The signal at $-1.2$ ppm was assigned to triethylphosphate (ref. peak $-1.1$ ppm, lit. $-1.0, -1.2$ ppm [101, 150, 151]). Several other peaks occurred at 240°C in the region of $-11.2$ to $-12.5$ ppm which were assigned as condensation products of diethyl phosphoramidate and/or diethyl phosphate.

At 280°C, **DEP** vanished giving rise to signals in the negative area of spectrum. The signal at $-0.4$ ppm belongs to phosphoric acid esters such as diethyl hydrogenphosphate ($-0.6$ ppm, $-0.9$ ppm [151, 152]) or ethyl dihydrogen phosphate. The high-intensity signal at $-11.4$ ppm originated probably from condensation products of these esters. Interestingly, one signal (1.05 ppm) was detected at 600°C, that most probably originates from oligomeric derivatives of phosphoric acid.
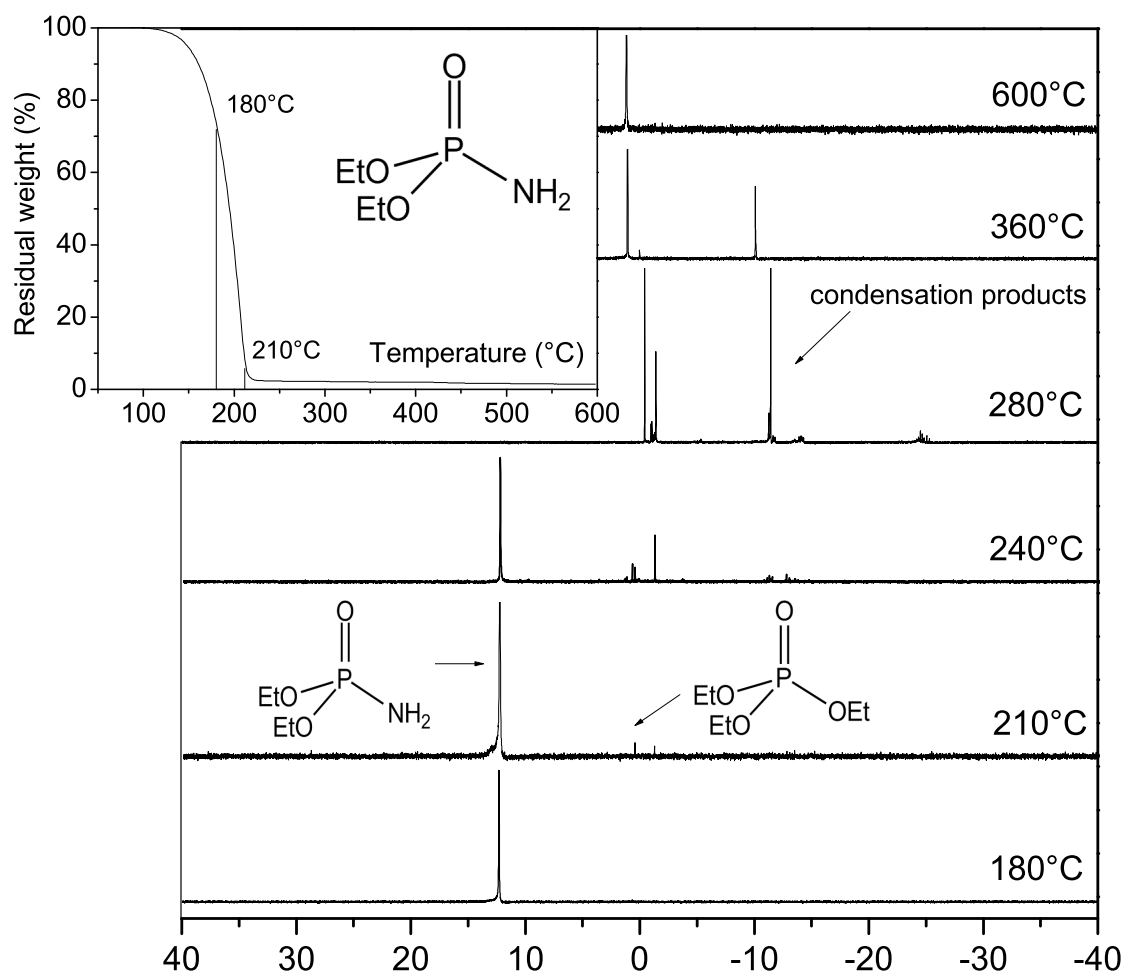


Figure 8.11 Decomposition of **DEP**: $^{31}$P NMR spectra (for clarity, spectra are shifted vertically; measured in $d_4$-CD$_3$OD)

Although about 90 % of **DEP** was volatilized before actual decomposition has started, the decomposition pattern of **DEP** had some similarities with **DMP**. Acidic species like hydrogen or dihydrogen esters were detected in both cases. These esters have probably condensed to oligomeric compounds at high temperatures (240°C-360°C). The most im-

portant finding here is that **DEP** is more thermally stable than **DMP**. **DEP** was still present at 200°C, whereas the signal of **DMP** vanished at this (or even lower) temperature. As a further step, similar analysis of **DPP** was performed.

### 8.3.3   Decomposition of diphenyl phosphoramidate

Diphenyl phosphoramidate **DPP** reveals a more complex decomposition pattern, as found in previous experiments involving cellulose (Fig. 8.6). Therefore it was interesting to correlate TGA data with results from $^{31}$P NMR.
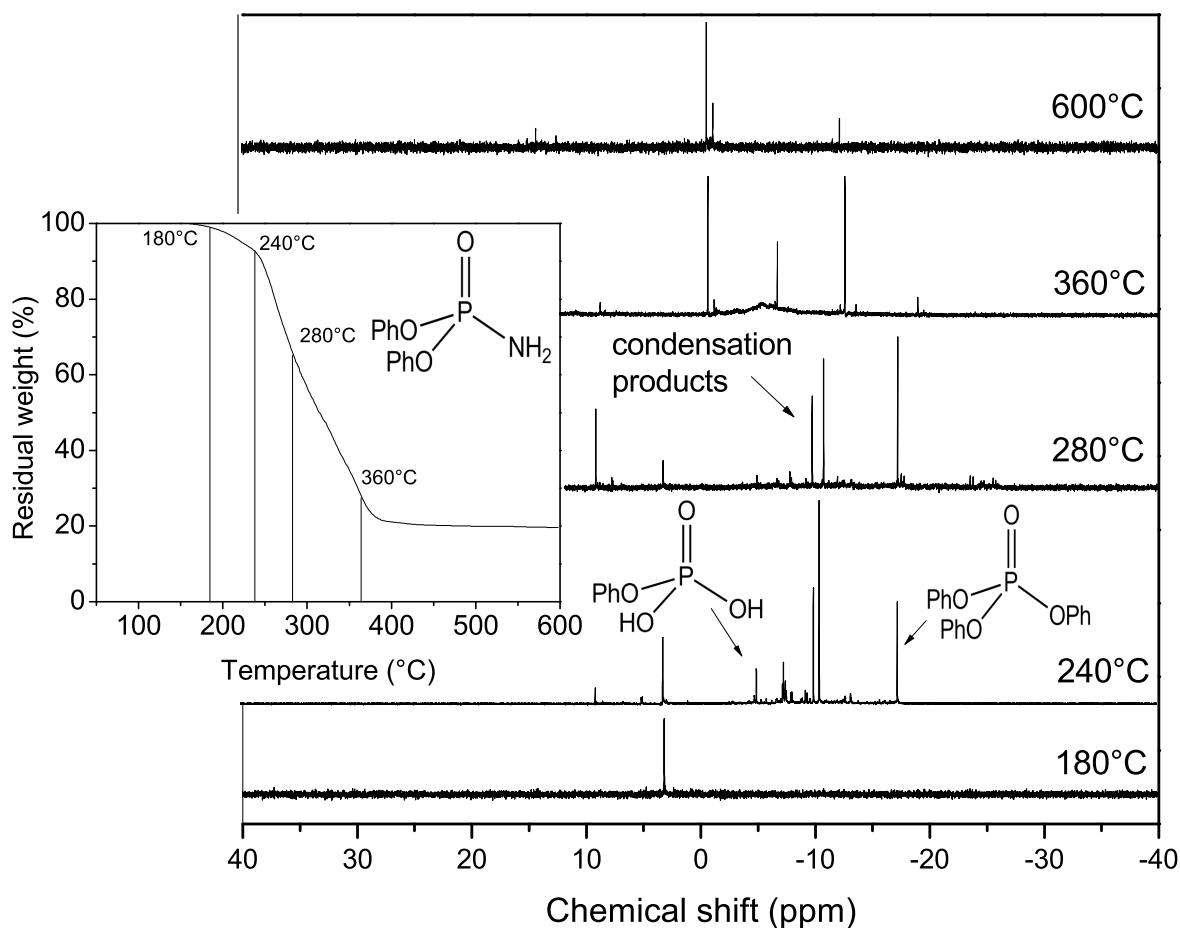


Figure 8.12 Decomposition of **DPP**: $^{31}$P NMR spectra (for clarity, spectra are shifted vertically; measured in $d_4$-CD$_3$OD)

**DPP** is stable up to 240°C. This is observed from the TGA of treated cellulose (Fig.

8.3), as well as from TGA of pure diphenyl phosphoramidate (Fig. 8.5). However, before the main decomposition starts, the weight-loss of 7.3 % was observed equally for **DPP**-treated cellulose and pure **DPP**. This weight-loss is characterized by the formation of phenyl dihydrogen phosphate (−5.05 ppm), diphenyl phosphate (−9.86 ppm), tetraphenyl iminodiphosphate (−10.85 ppm, lit. −10.7 ppm [153, 154]), triphenylphosphate (−17.32 ppm, ref. −17.3 ppm [145, 150]) and tetraphenyldiphosphate (−23.6 ppm, lit. −24.0 ppm [144, 155, 156]) (Fig. 8.12). Low intensity signal at 9.1 ppm was not assigned. Pure **DPP** yields $^{31}$P-signal at 3.2 ppm (lit. 2.3 ppm, 2.6 ppm [144, 153]).

Next $^{31}$P NMR measurement was made at 280°C during the main decomposition step (residual weight about 60 %). The decomposition pattern looked similar to the one at 240°C, except that the intensity of the **DPP**-signal decreased and the intensity of of the unassigned signal at 9.1 ppm increased. At 360°C the weight-loss comprised 26.2 %, in which diphenyl phosphoramidate as well as the majority of signals observed before have not been detected. Instead, two intense signals at –0.65 ppm and –12.6 ppm appeared which were unfortunately not assigned. The soluble part of the 23.8 %-residue at 600°C contained some acidic derivatives with $^{31}$P NMR signals at –0.60, –0.94 and –12.24 ppm.

A thorough literature search was conducted to find species giving signals in the range from –20 ppm to –10 ppm. The kind of compounds that might form and their shifts with references from the literature are put together in Table 8.3. It is possible that acidic species upon heating might condense not only to phosphoric acids and its derivatives, but also to cyclic compounds, like the ones presented in Table 8.3.

In contrast to **DMP** and **DEP**, **DPP** does not undergo volatilization, but directly starts to decompose at 200°C. At this step, the formation of diphenyl phosphate and triphenylphosphate takes place at the expense of phenol. The water required for this reaction might come either from absorbed water or from the small amounts of water present in the reaction gas (nitrogen). The acidic derivatives are then able to dehydrate cellulose to form thermally stable char. A similar mechanism was proposed by Shimasaki *et al.* [143] (signal at 9.0 ppm was not assigned as well).

If compared to **DEP**, the decomposition pattern of **DPP** appears to be very similar, as **DEP** was still present at high temperatures. However, the formation of acidic species occurred at lower temperatures for **DPP**. As a result, **DPP** was found to be a better FR

for cellulose than **DEP**. The reason for that lies in the superior leaving group ability of aryl esters of phosphoric acids relative to that of corresponding alkyl esters [63].

However, if compared to **DMP**, diphenyl phosphoramidate possesses inferior FR properties. We believe that this is due to the ability of **DMP** to degrade to acidic species at lower temperatures. In the next step, the decomposition of **DMMP**, **DMHEP**, **MPDA** and **PTA** (being exhibitory flame retardants for cellulose) was investigated in order to complete the study and draw the decomposition mechanisms.

### 8.3.4   Decomposition of dimethyl-(methyl) phosphoramidate

Decomposition of **DMMP**-treated cellulose was similar to the decomposition of **DMP**- and **DEP**-treated cellulose (Figs. 8.1 and 8.1) all exhibiting three characteristic mass-loss steps. However, the TG-curve obtained for pure **DMMP** was completely different. Therefore thermal degradation of **DMMP** was studied more in detail using $^{31}$P NMR spectrometry.

Three stages of decomposition (weight-loss) have been distinguished for **DMMP**: 0-200°C, 200-400°C and 400-600°C (Fig. 8.13). During the first stage the true degradation occurred: $^{31}$P-signal of **DMMP** (12.9 ppm) was observed up to 180°C and vanished at higher temperatures (Fig. 8.14). During this step, 40 % of weight was lost at the expense of acidic species formation, which were first detected at 130°C. The signals in the range 0 to –2 ppm and –12 to –10 ppm originated from the presence of trim ethyl phosphate, dimethyl hydrogen phosphate and their condensation products. At 180°C an intense signal at –22.7 ppm appeared. The same signal has already been observed earlier for **DMP** indicating that it might originate from the same reaction.

During the second decomposition step at 200-400°C about 25 % of weight was lost. This step was accompanied by several reactions, involving the signal at –22.7 ppm as an intermediate: it was observable up to 280°C and vanished between 280°C and 360°C, giving rise to the signal at –0.85 ppm. The intensity of this signal was observed to increase in the same temperature range.

The last decomposition step at 400-600°C might be characterized as oligomerization of

Table 8.3 Species that might arise at the decomposition of phosphoramidates

| Compound | Structural formula | $\delta$ in $^{31}$P [ppm] | | |
|---|---|---|---|---|
| | | Found | Literature | Ref. |
| dihydrogen-triphosphate ion | | - | −10.3, −22.5 | [157] |
| dihydrogen-phosphate ion | | - | 0.53 | [158] |
| pyrophosphoric acid | | - | −11.5, −10.9 | [159, 150, 160] |
| hydroxytrimethoxyphos-phonium ion | | - | 2.0 | [158] |
| tetramethoxyphos-phonium ion | | - | 2.0 | [158] |
| 1,3,5,2,4,6-trioxatriphos-phinane-2,4,6-triolate-2,4,6-trioxide | | - | −21.2, −20.8 | [153, 157] |
| 1,3,5,7,2,4,6,8-tetraoxo-tetraphosphocane-2,4,6,8-tetrolate-2,4,6-trioxide | | - | −23.13, −22.97 | [157, 161] |
| 1,3,5,2,4,6-dioxazatri-phosphinane-2,4,6-tri-olate-2,4,6-trioxide | | - | −10.4, −20.2 | [162] |

the compound detected at –0.85 ppm (broad low-intensity peak at 600°C). However, the detected signal originates only from the tiny soluble part of the residue (17.8 %).

Compared to the decomposition of **DMP** and **DEP**, the decomposition of **DMMP** was very interesting primarily because of the distinguished three steps of mass-loss. In case of **DMMP** more stable compounds have been formed at 200°C. This can be associated with the formation of some acidic species, that gave rise to the $^{31}$P NMR-signals in the range –12 to –10 ppm.
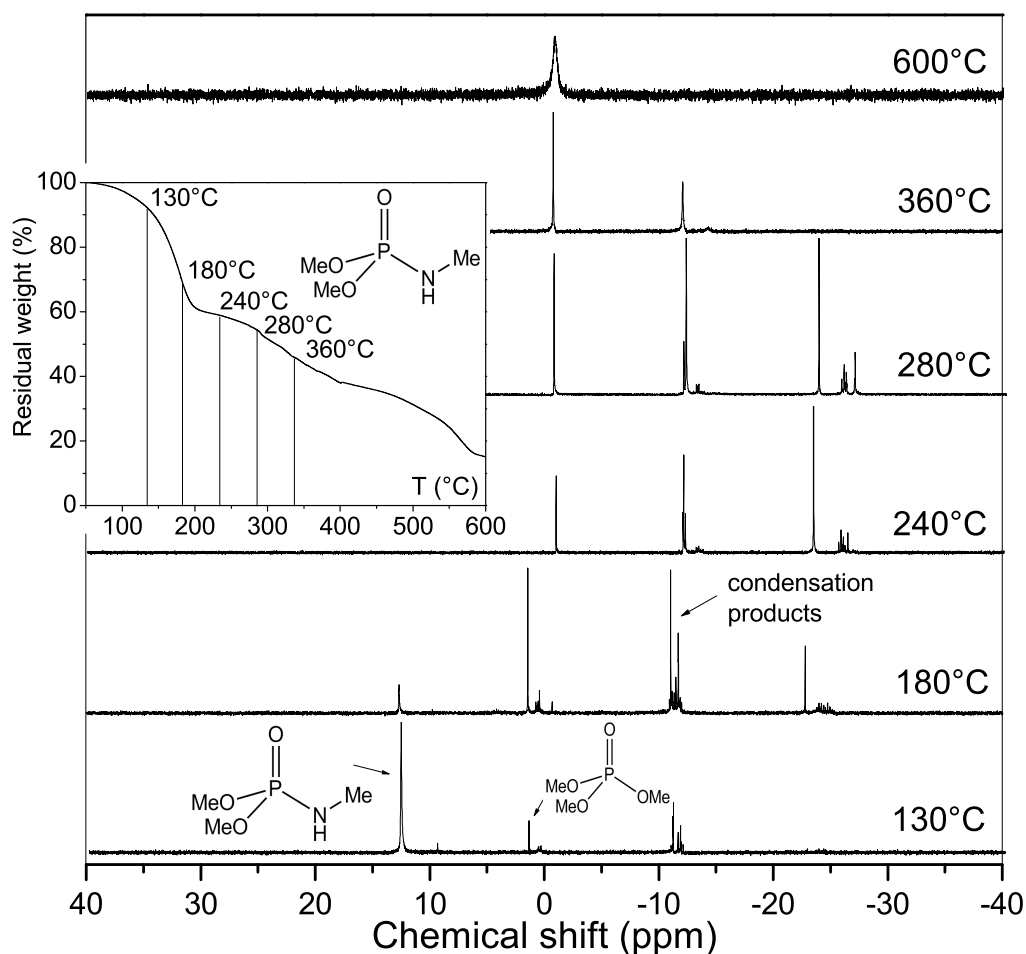


Figure 8.13 Decomposition of **DMMP**: $^{31}$P NMR spectra (for clarity, spectra are shifted vertically; measured in $d_4$-CD$_3$OD)

Although these signals were detected also for **DMP** and **DEP**, they had much lower intensity (**DMP**) and appeared at much higher temperatures (**DEP**). Apparently, the

FR properties of cellulose treated with **DMP**, **DEP** and **DMMP** were affected by the formation of these intermediate products. The FR properties of **DMMP** were reported to be better than for **DEP**, but inferior compared to **DMP**. In other words faster disintegration of these intermediates improved FR properties of **DMP**, but their absence in case of **DEP** decreased its FR properties. Obviously, the substitution of hydrogen in aminogroup to methyl is responsible for this phenomenon. How the substitution of methyl to hydroxyethyl group would affect the formation of these intermediates?
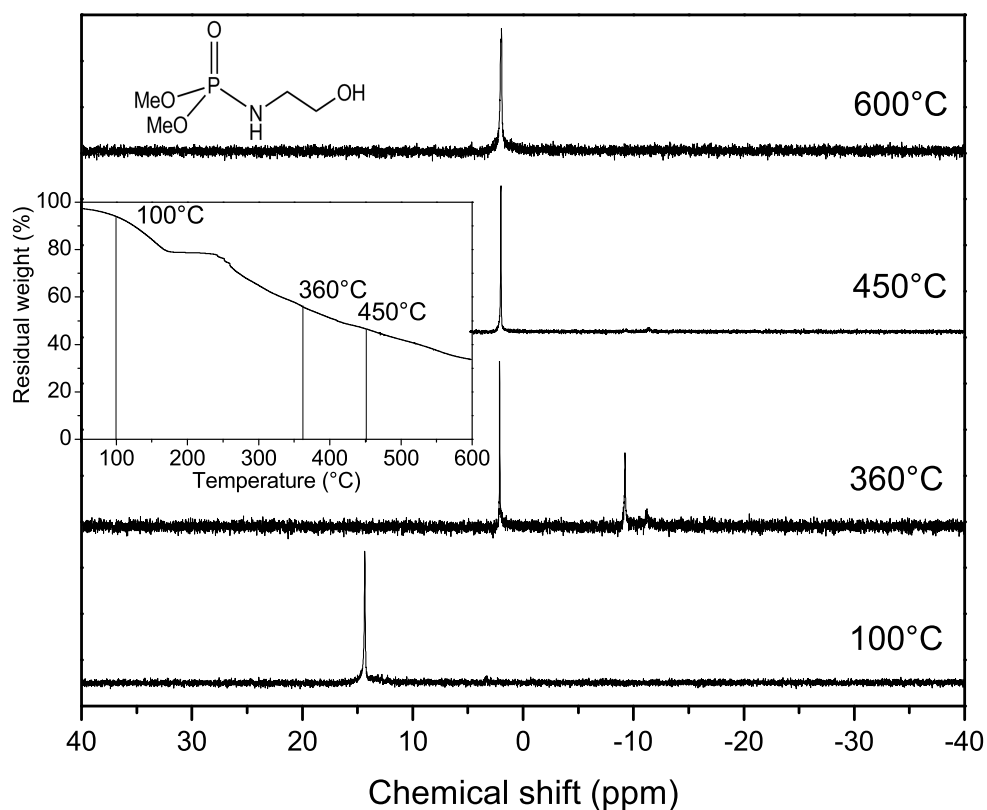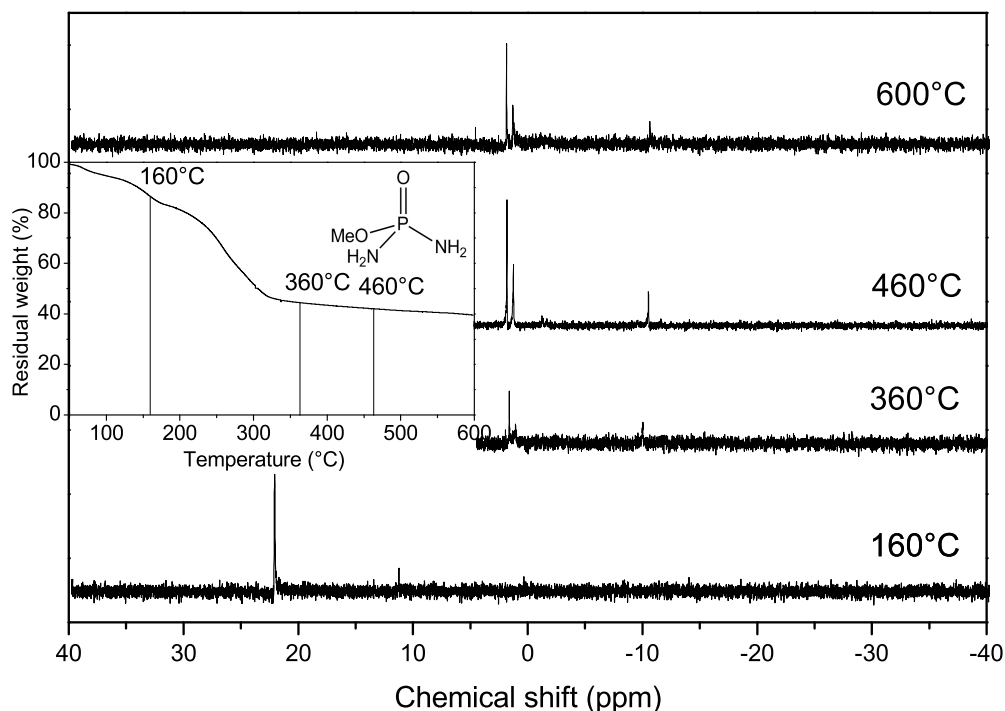


Figure 8.14 Decomposition of **DMHEP**: $^{31}$P NMR spectra (for clarity, spectra are shifted vertically; measured in $d_4$-CD$_3$OD)

### 8.3.5   Decomposition of dimethyl-(2-hydroxyethyl) phosphoramidate

Decomposition of dimethyl-(2-hydroxyethyl) phosphoramidate has been studied in detail analogously to **DMP**, **DEP**, **DPP** and **DPP**. The TGA analysis revealed the decomposition process of **DMHEP** to proceed through several steps. The first step from 0°C to 200°C was characterized by a weight-loss of 18 %. The transition between the second and the third steps could not be clearly distinguished, but we believe the decomposition proceeded through three steps similarly to the decomposition of **DMMP**.

At 100°C the only signal corresponding to **DMHEP** was observed at 13.8 ppm (Fig. 8.14). It vanished between 100°C and 260°C. Therefore, volatilization has occurred in the first step of decomposition. Further, at 260°C the signal at –20.0 ppm was observed. At 360°C it vanished giving rise to the new signals at 2.4, –9.3 and –11.2 ppm. The attention should be drawn to the intensity of these signals. In relation to the background the intensities were low, indicating low concentration of these species in the solvent, which in turn indicates low solubility of the residue at these high temperatures. Only one signal at 2.1 ppm was detected at 450°C and 600°C. The percentage of residue left at 600°C amounted to 28 %.

The decomposition pattern of **DMHEP** strongly resembles the pattern of **DEP**. Although the species yielding signals in the range –12 to –10 ppm were detected in case of **DMHEP**, their formation was observed at high temperatures similarly to **DEP**. Moreover, the signal at –11.2 ppm was observed at higher temperatures as well. At 600°C, one single peak at 1.05 ppm for **DMHEP** and at 2.1 ppm for **DEP** was observed. However, the FR properties of **DMHEP** were found to be superior as of **DEP**. We therefore conclude that in this particular case other factors interfere such as better retention of **DMHEP** on cellulose.

### 8.3.6   Decomposition of methylphosphorodiamide and phosphoric triamide

Decomposition of **MPDA** proceeds through three stages similar to **DMMP** and **DMHEP**. During the first stage up to 160°C the **MPDA** is the main component (Fig. 8.15). From 160°C to 300°C the actual decomposition occurs and the signal of **MPDA** at 11.5 ppm

vanishes.  The signal at 2.1 ppm with low intensity was observed.  One further smaller peak was seen at approx. –10 ppm indicating the formation of condensation products.  At 460°C, the intensity of both peaks at 2.1 and –10 ppm was noticeably increased.  This step is characterized by the mass-loss of 35 %.  From this temperature up to 600°C no changes were detected: the product obtained appeared to be stable at these high temperatures.

The decomposition of **PTA** proceeded through the same steps as **MPDA**.  Surprisingly, no NMR signals at each step of **PTA** decomposition were detectable.  We believe that **PTA** simply polymerized upon heating.  Klement *et al.* observed the formation of highly condensed substances insoluble in water, when they heated **PTA** to 140°C [163].  The loss of 65 % occurred most probably due to release of ammonia.

Figure 8.15 Decomposition of **MPDA**: $^{31}$P NMR spectra (for clarity, spectra are shifted vertically; measured in $d_4$-CD$_3$OD)

In chapter 7 **MPDA** and **PTA** were shown to possess superior FR properties over other studied phosphoramidates. This behaviour can be explained by the ability of **MPDA** and **PTA** to form polymers upon heating, which can further form thermal barrier and protect cellulose fibers from high temperatures.

## 8.4   Mechanism of the phosphoramidates degradation

Based on the results obtained using TGA with subsequent $^{31}$P NMR analysis we have attempted to draw the possible mechanism of action of dialkyl phosphoramidates. Fig. 8.16 reflects the mechanism of the decomposition of dialkyl/aryl/phosphoramidates. All tested phosphoramidates underwent decomposition in a similar way, through formation of structurally similar phosphoric acid esters. The main distinction was the temperature, at which phosphoramidate has started to decompose.

As the formation of condensation products was observed for all phosphoramidates, the formation of (**ii**) through (**i**) was suggested as the condensation product of two molecules of dialkyl/aryl/phosphoramidates (reaction 1). The lone pair of nitrogen could be transferred to the unoccupied orbital of phosphorus to give unstable intermediate (**i**), where P' atom is stabilized by elimination of alcohol molecule. This reaction seemed to be happening readily upon increasing the temperature.

The formation of acidic species was suggested to occur upon cleavage of condensation product (**ii**) through the reaction with alcohol. Further, alcohol can attack (**ii**) at the P'' atom because of its lower electron density forming intermediate (**iii**) (reaction 2). The rearrangement and cleavage of P–N bond would lead to the formation of monoalkyl/aryl/diphosphoramidate and trialkyl/aryl/phosphate (detected in $^{31}$P NMR for all phosphoramidates). Amides of phosphoric acid can also polymerize to form polyphosphoramide, which was found to be a more effective catalyst in dehydration reactions than phosphoric acid [15].

Moreover, compound (**iii**) might undergo dehydration, where water important for later hydrolysis is being formed (reaction 3). Trialkyl/aryl/phosphate may undergo hydrolysis (reaction 4) with the formation of dialkyl/aryl/ hydrogenphosphate, alkyl/aryl/dihydrogen

phosphate and phosphoric acid. Further, they might in turn undergo condensation to pyrophosphoric acid and its esters (peaks in $^{31}$ NMR at –10 ppm). It is known, that oligomers and polymers of phosphoric acid and its esters are even better phosphorylating agents as phosphoric acid itself [46]. These polyacids are very strong mineral acids and are capable of protonating and dehydrating other species. Char formation is believed to be greatly facilitated by the presence of such strong acids.
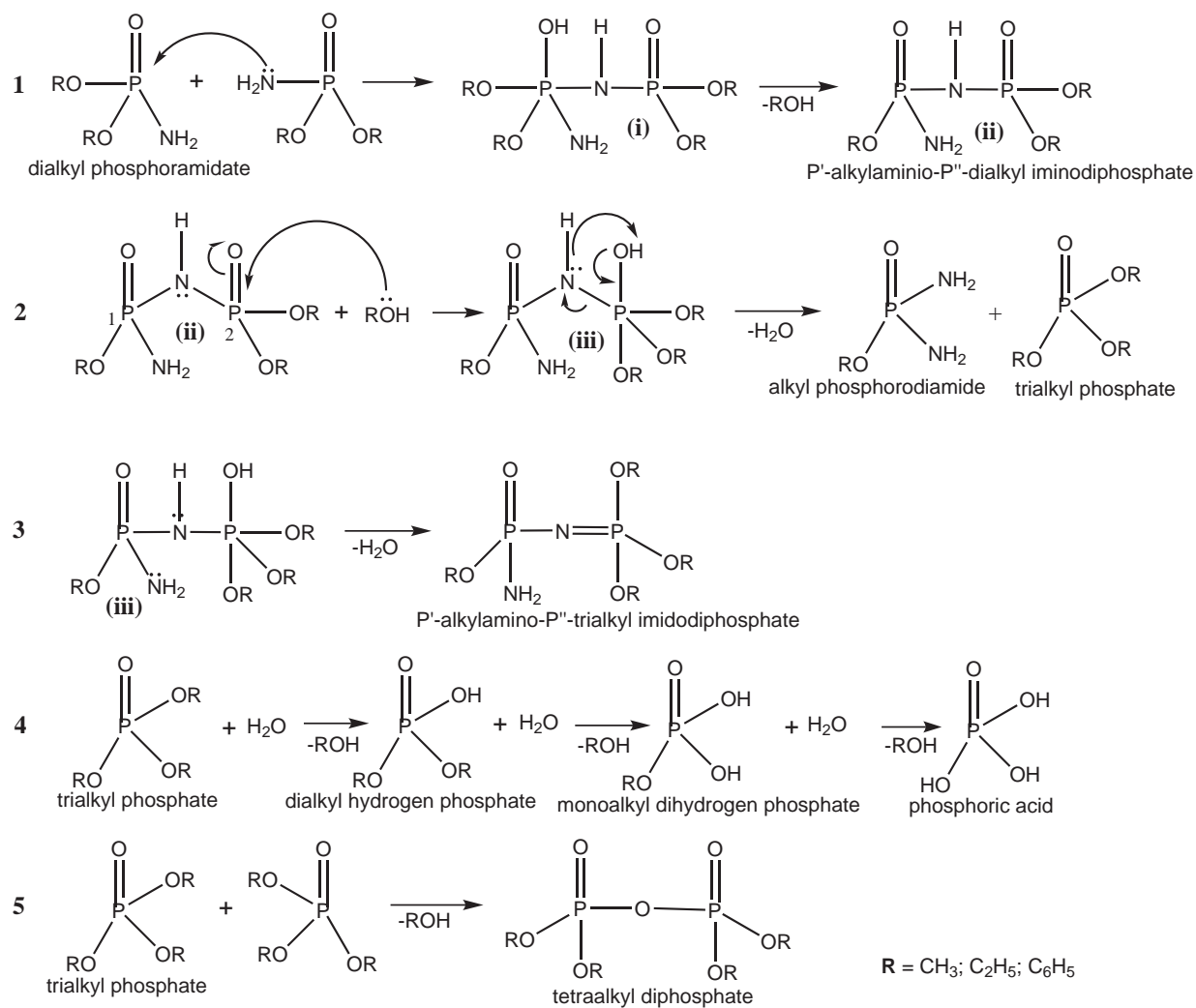
Figure 8.16 Proposed decomposition mechanism of dialkyl(aryl)phosphoramidates

## 8.5  Conclusions

Using the TG analysis with subsequent $^{31}$P NMR spectrometry it was possible to investigate the stepwise decomposition of phosphoramidates. It was determined that the decomposition pathways of phosphoramidates are quite similar to each other. At high temperatures phosphoramidates undergo condensation with the release of corresponding alcohol. The alcohol in turn reacts with condensation products to yield amides and trialkyl phosphates. Upon hydrolysis these would produce hydrogen phosphates and later phosphoric acid. Phosphoric acid and alkyl phosphates can undergo condensation reactions with the formation of polyphosphoric derivatives. These are well-known strong dehydrating agents, able to easily phosphorylate cellulose and disintegrate it.

However, some differences in the decomposition pathways of phosphoramidates and phosphoramides were detected, for example the kinetics of the decomposition was found to be different. Dimethyl phosphoramidate **DMP** decomposed to acidic species earlier than diethyl phosphoramidate **DEP** and diphenyl phosphoramidate **DPP**. The earlier desintegration of **DMP** to acidic species explains its better FR behaviour, as the acidic species catalyze the decomposition of cellulose at lower temperatures, thus decreasing the formation of flammable species and increasing char yields.

Last but not least, phosphoric amides **MPDA** and **PTA** are able to polymerize upon heating. The so-formed polymers are stable to high temperatures and are believed to act as a protective barrier between flame and cellulose fibres.

**Chapter 9**

# Conclusions and Outlook

In the present Thesis, the FR properties of cellulose, treated with twenty different phosphoramidates were investigated. The results obtained were thoroughly compared with each other in order to find the reasons for the different FR behaviour of phosphoramidates.

The most efficient FRs for cellulose were found to be **DMP**, **DMHEP** and **PTA**. Although a clear correlation of FR structure to its properties is not possible (mainly because of the large number of physical and chemical variables involved), we succeeded in establishing the basic factors that govern the FR properties of phosphoramidates:

- The ratio of carbon to phosphorus.
  Dimethyl phosphoramidate **DMP** showed excellent FR properties. The low ratio of carbon to phosphorus, or fuel-like to FR element is one of the crucial properties of successful flame retardant. However, a low C/P ratio must always be considered for molecules with similar chemical nature. Alike aryl phosphoramidates exhibited comparably good FR properties, although the C/P ratio was higher. However, these are not considered as good FRs for cellulose because of low solubility in polar solvents and low affinity to cellulose. Arylphosphoramidates are therefore excellent FRs for other polymers.

- The presence of reactive sites like primary aminogroups $NH_2$.
  The FR properties of a phosphoramidate are increased with the stronger interaction of a phosphoramidate with cellulose. In a phosphoramidate molecule, aminogroups

are an active site to interact with cellulose owing to their basic nature. Phosphoramidates with tertiary aminogroups (**DMDMP**) have no useful FR properties at all because of the absence of polar "anchors" which are important for the uptake of compound on the cellulose. Hence, successful FRs must contain polar moieties.

- Steric effects.
  Geometry and spacial arrangement of the substituents at the site of the phosphorus atom influence the ability of an aminogroup to interact with cellulose molecules. **DMP** possesses superior FR properties thanks to its smaller molecular size, which enables a higher degrees of cellulose phosphorylation. In an other example, **DMHEP** is a superior FR when compared to **DMHBP**, where hydroxyethyl groups hinder the interaction with aminogroup.

- The ability to form acidic species and stable residues upon heating.
  **DMP** undergoes decomposition with the formation of acidic species at lower temperatures. These acidic intermediates are then able to phosphorylate cellulose with the formation of char. All phosphoramidates were shown to form such species. Their formation at lower temperature improves the FR properties. Moreover, **PTA** is able to form stable polymers during heating. These polymers act as thermal barriers thus preventing combustion of cellulose fibers.

- The presence of hydroxyl groups.
  The hydroxy groups in the phosphoramidate molecules are char-promoting agents. The presence of the hydroxyls not only promotes the interaction with cellulose, but also facilitates the absorption of water, which in turn promotes the hydrolysis of the phosphoric acid derivatives and therefore increases the char formation. The substitution of a proton in the hydroxyl to methyl group was shown to have drastic consequences for the FR properties of phosphoramidate. With the reduced ability to interact with cellulose, the $P–NH–(CH_2)_n–OCH_3$ phosphoramidates loose their FR properties.

The present study is by far not exhaustive. At this stage we would like to make some propositions for further research projects:
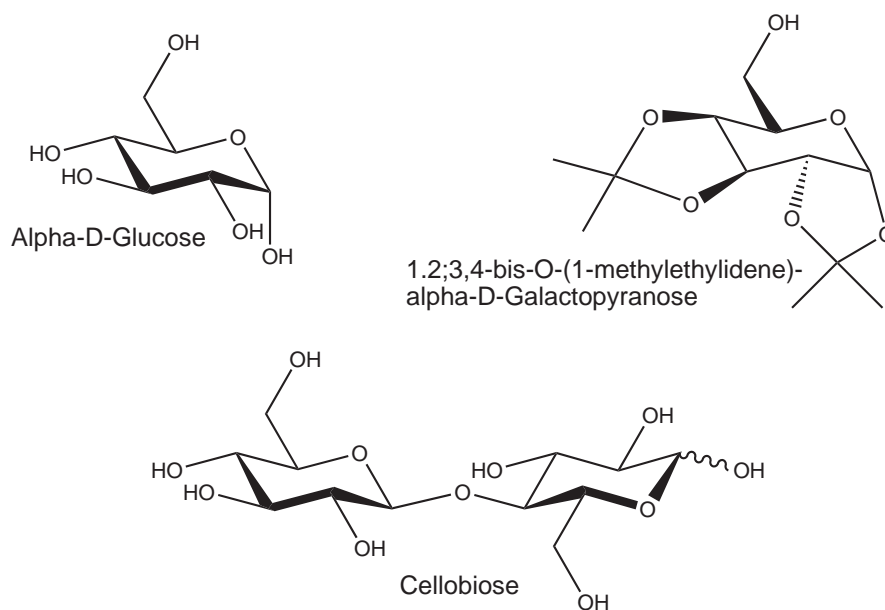
Figure 9.1 Model compounds to replace the complex molecule of cellulose in the study of the decomposition in the presence of phosphoramidates
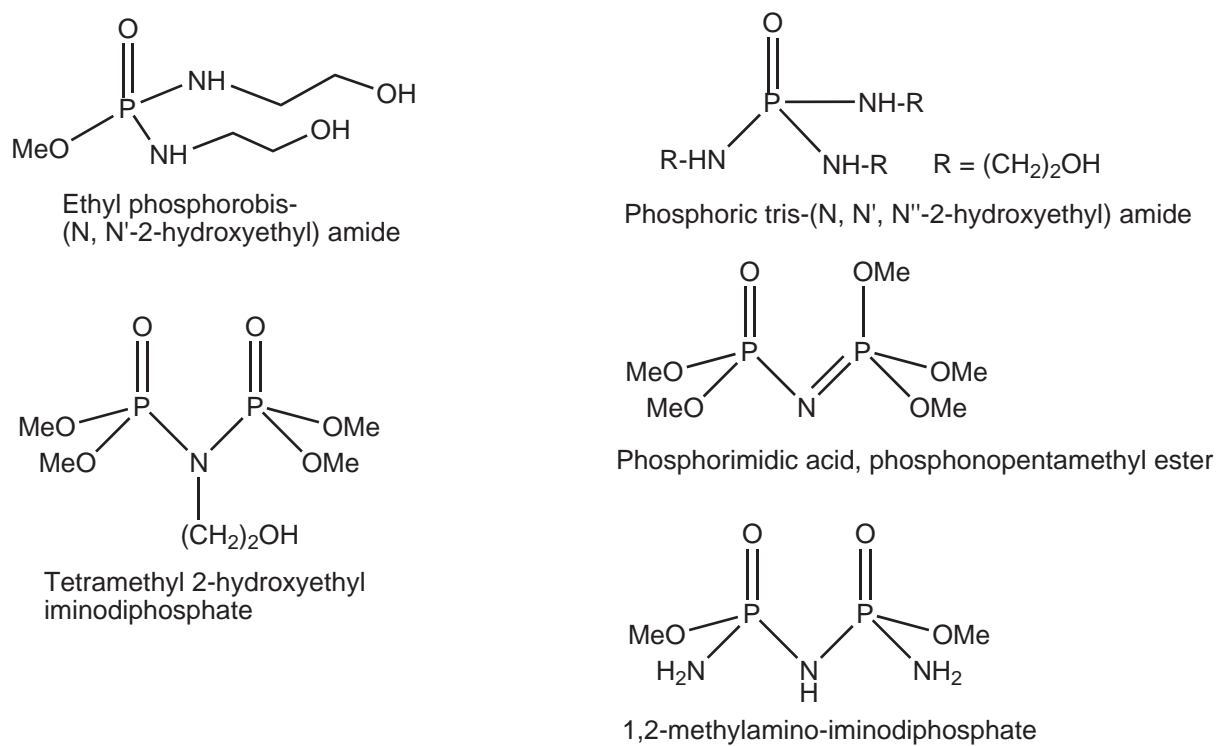


Figure 9.2 Phosphoramidates, phosphorimides and iminophosphates to complement the studies

- The detailed analysis of the decomposition of **MPDA** and **PTA**. The FTIR analysis of species that might evolve during heating of **MPDA** and **PTA**, FTIR-ATR analysis of polymers these compounds form, microscopic investigation of chars could provide further valuable information to support the findings of the present Thesis.

- The complexity of the cellulose molecule made it extremely difficult to study its decomposition in the presence of phosphoramidates. Several alternative compounds as a substitute for cellulose for a decomposition study are suggested in Fig. 9.1.

- Hyphenated techniques like Pyrolysis-GC-MS might be involved for the further studies of the decomposition of phosphoramidates.

- Several interesting structures can be designed to further complement the studies (Fig. 9.2)

# Chapter 10

# Experimental

## 10.1  Materials

Cotton fabrics ($180\,\text{g/m}^2$, plain weave, bleached, without optical brightener, yarn count 26 per $\text{cm}^2$ in the wrap and 23 yarn per $\text{cm}^2$ in the weft with the density of 35 tex) were kindly supplied by Empa Testmaterialien AG (St. Gallen, Switzerland). Avicel PH-101 were obtained from Sigma-Aldrich (Switzerland). Oxygen and nitrogen gases used for LOI, MCC, TGA and TGA coupled techniques were dry ultra-high purity grades obtained from Carbagaz (Switzerland).

## 10.2  Chemicals

Diethyl hydrogen phosphate **DEHP**, diethyl ethylphosphonate **DEEP**, triethyl phosphate **TEP** and dimethyl phosphoramidate **DEP** were purchased from Fluka (Switzerland) and were used as received without further purification. Phenyl phosphorodiamide **PPDA** was purchased from Alfa Aesar (USA) and was used without further purification.

## 10.3   Syntheses

**Dimethyl phosphoramidate DMP**

MF: $C_2H_{10}O_3PN$

MW: 127.079 g/mol

w/w %: P 24.37 %, N 11.02 %
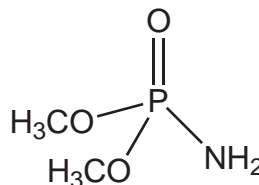
Dried ammonia was bubbled through a solution of dimethyl hydrogen phosphite (22.01 g, 18.34 mL, 0.20 mol) and carbon tetrachloride (30.76 g, 19.35 mL, 0.20 mol) in dried DCM. The reaction mixture was cooled down to −5°C using ice-salt bath. Ammonia was purged through the solution during 2 h, and afterwards ammonium chloride was filtered off and washed with DCM to remove the rests of dimethyl phosphoramidate. DCM was removed from the filtrate and the resulting dimethyl phosphoramidate was collected without further purification.

Yield 98.7 %. Colourless oil, bp = 214°C (760 Torr)

$^1$H NMR (250.13 MHz, CDCl$_3$): $\delta$ = 3.70 (d, $^3$J$_{PH}$ = 11.2 Hz, 6H, C$H_3$O), $\delta$ = 3.35 (s, 2H, NH$_2$)

$^{13}$C NMR (62.9 MHz, CDCl$_3$): $\delta$ = 53.1 (d, $^2$J$_{PC}$ = 5.5 Hz, 2C, $C$H$_3$O)

$^{31}$P NMR (101.3 MHz, CDCl$_3$): $\delta$ = 12.0 (s)

IR (cm$^{-1}$): 3241 (N–H), 3122 (NH$_2$), 2954 (as, CH$_3$), 2852 (s, CH$_3$), 1573 (NH$_2$, scissoring), 1462 (as, $\delta$, CH$_3$), 1223 (P=O), 1018 (as, P–O–C), 817 (as, P–O)

Anal. calc. for $C_2H_8O_3PN$: C, 19.21 %; H, 6.45 %; O, 38.38 %; P, 24.77 %; N, 11.20 %

Found: C, 19.10 %; H, 6.73 %; O, 38.70 %; P, 24.53 %; N, 10.87 %

HPLC/MS (ESI): 1 peak, [M$^+$], $m/z$ = 126.0

## Di-n-butyl phosphoramidate DBP

MF: $C_8H_{20}O_3PN$

MW: 209.223 g/mol

w/w %: P 14.80 %, N 6.69 %
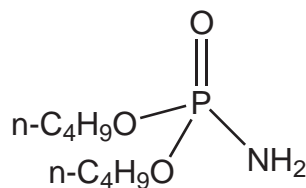


Synthesis of **DBP** was performed analogously to **DMP**. For the reaction, di-n-butyl hydrogen phosphite (19.42 g, 19.52 mL, 0.1 mol) and carbon tetrachloride (15.38 g, 9.68 mL, 0.10 mol) in dried DCM were taken. The reaction mixture was cooled down to $-5°C$ using ice-salt bath. Ammonia was purged through the system during 2 h, but the reaction was not intensive without a base. TEA (10.12 g, 14.00 mL, 0.10 mol) was added to the reaction mixture, and the flask was additionally heated up to 30°C. After approximately 3 h ammonium chloride and triethylamine hydrochloride were filtered off and washed with DCM to remove the rests of di-n-butyl phosphoramidate. DCM was removed from the filtrate and the resulting dimethyl phosphoramidate was collected without further purification.

Yield 87.4%, yellowish oil, bp = 270°C, (760 Torr)

$^1$H NMR (300.0 MHz, CDCl$_3$): $\delta$ = 0.95 (t, $^3$J$_{HH}$ = 7.2 Hz, 6H, C$H_3$–CH$_2$), 1.43 (sex, $^3$J$_{HH}$ = 7.0 Hz, 4H, CH$_3$–C$H_2$), 1.69 (quin, $^3$J$_{HH}$ = 7.6 Hz, 4H, CH$_3$–CH$_2$–C$H_2$), $\delta$ = 2.89 (s, 2H, NH$_2$), 4.07 (q, $^3$J$_{HH}$ = 6.6 Hz, 4H, C$H_2$–O)

$^{13}$C NMR (50.3 MHz, CDCl$_3$): $\delta$ = 13.6 (s, 2C, C$H_3$–CH$_2$), 18.8 (s, 2C, CH$_3$–$C$H$_2$), 32.5 (d, $^2$J$_{PC}$ = 7.0 Hz, 2C, O–CH$_2$–$C$H$_2$), 66.4 (d, $^2$J$_{PC}$ = 5.6 Hz, 2C, O–$C$H$_2$)

$^{31}$P NMR (121.5 MHz, CDCl$_3$): $\delta$ = 9.5 (s)

IR (cm$^{-1}$): 3251 (N–H), 3131 ( NH$_2$), 2958 (as, CH$_3$), 2848 (s, CH$_3$), 1574 (NH$_2$, scissoring), 1466 (as, $\delta$, CH$_3$), 1239 (P=O), 1028 (as, P–O–C)

Anal. calc. for $C_8H_{20}O_3PN$: C, 45.93 %; H, 9.63 %; O, 22.94 %; P, 14.80 %; N, 6.69 %

Found: C, 45.64 %; H, 9.58 %; O, 22.85 %; P, 14.87 %; N, 6.57 %

HPLC/MS (ESI): 1 peak, [M$^+$], $m/z$ = 209.0

**Di-isopropyl phosphoramidate DiPP**

MF: $C_6H_{16}O_3PN$

MW: 181.170 g/mol

w/w%: P 17.10 %), N 7.73 %
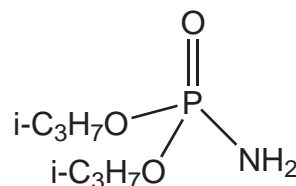


Synthesis of **DiPP** was performed analogously to **DMP** and **DBP**. For the reaction, di-iso-propyl hydrogen phosphite (16.61 g, 16.67 mL, 0.1 mol), carbon tetrachloride (15.38 g, 9.68 mL, 0.1 mol) and TEA (10.12 g, 14.0 mL, 0.1 mol) were taken.

Yield 92.7 %, slightly yellow crystals, mp = 67°C, bp = 234°C (760 Torr)

$^1$H NMR (300.0 MHz, CDCl$_3$): $\delta$ = 1.36 (d, $^3J_{HH}$ = 6.0 Hz, 12H, C$H_3$–CH), $\delta$ = 2.69 (s, 2H, NH$_2$), 4.66 (sex, $^3J_{HH}$ = 7.2 Hz, 2H, CH$_3$–C$H$)

$^{13}$C NMR (75.5 MHz, CDCl$_3$): $\delta$ = 23.8 (ddd, $^2J_{PC}$ = 1.6 Hz, $^3J_{PC}$ = 14.6 Hz, 4C, $C$H$_3$–CH), 71.0 (d, $^2J_{PC}$ = 5.5 Hz, 2C, CH$_3$–$C$H)

$^{31}$P NMR (121.5 MHz, CDCl$_3$): $\delta$ = 7.6 (s)

IR (cm$^{-1}$): 3341 (N–H), 3255 (NH$_2$), 2974 (as, CH$_3$), 2848 (s, CH3), 1571 (NH$_2$, scissoring), 1468 (as, $\delta$ CH$_3$), 1217 (P=O), 1019 (as, P–O–C)

Anal. calc. for $C_6H_{16}O_3PN$: C, 39.78 %; H, 8.90 %; O, 26.49 %; P, 17.10 %; N, 7.73 %

Found: C, 40.31 %; H, 8.99 %; O, 27.42 %; P, 15.79 %; N, 7.46 %

HPLC/MS (ESI): 1 peak, [M$^+$], $m/z$ = 181.7

## Dimethyl-(methyl) phosphoramidate DMMP

MF: $C_3H_{10}O_3PN$

MW: 139.090 g/mol

w/w%: P 22.27 %, N 10.07 %
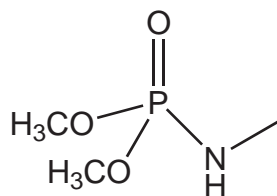
Synthesis of **DMMP** was performed as following: to the methylamine, taken as 2M solution in THF (6 g of methylamine, 100 mL of solution) and TEA (14.21 g, 19.53 mL, 0.2 mol) in tetrahydrofurane, dimethyl hydrogen phosphite (22.01 g, 18.34 mL, 0.2 mol) together with carbon tetrachloride (30.76 g, 19.35 mL, 0.2 mol) was added slowly dropwise. The reaction mixture was cooled to −5°C using ice-salt bath. At the end of the reaction, solution was filtered to remove triethylamine hydrochloride, and the rest components together with solvent were removed under vacuum. Dimethyl methylphosphoramidate was washed with diethyl ether to purify the product from the rests of the triethylamine hydrochloride.

Yield 88.1 %, yellowish oil, hygroscopic, bp = 204°C (760 Torr)

$^1$H NMR (250.13 MHz, CDCl$_3$): $\delta$ = 2.59 (dd, $^3J_{PH}$ = 11.7 Hz, $^3J_{HH}$ = 5.2 Hz, 3H, NH-C$H_3$), 3.71 (d, $^3J_{PH}$ = 11.0 Hz, 6H, C$H_3$O)

$^{13}$C NMR (75.5 MHz, CDCl$_3$): $\delta$ = 27.3 (s, 1C, NH-$C$H$_3$), 52.8 (d, $^2J_{PC}$ = 5.3 Hz, 2C, $C$H$_3$O)

$^{31}$P NMR (101.3 MHz, CDCl$_3$): $\delta$ = 12.9 (s)

IR (cm$^{-1}$): 3243 (N–H), 2953 (as, CH$_3$), 2851 (s, CH$_3$), 1432 (as, $\delta$ CH$_3$), 1229 (P=O), 1016 (as, P–O–C), 822 (as, P–O)

Anal. calc. for $C_3H_{10}O_3PN$: C, 25.91 %; H, 7.25 %; O, 34.51 %; P, 22.27 %; N, 10.07 %

Found: C, 26.71 %; H, 7.54 %; O, 35.41 %; P, 21.23 %; N, 9.50 %

HPLC/MS (ESI): 1 peak, [M$^+$], $m/z$ = 139.9

**Dimethyl-(ethyl) phosphoramidate DMEP**

MF: $C_4H_{12}O_3PN$

MW: 153.117 g/mol

w/w %: P 20.23 %, N 9.15 %
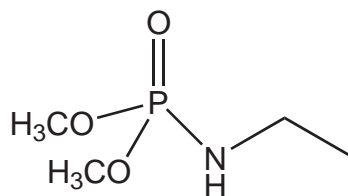


Synthesis of **DMEP** was performed analogously to **DMMP**: solution of ethylamine (6 g of ethylamine, 100 mL of solution) in THF was taken to react with dimethyl hydrogen phosphite.

Yield 87.7 %, hygroscopic, yellowish oil, bp = 217°C (760 Torr)

$^1$H NMR (250.13 MHz, CDCl$_3$): $\delta$ = 1.09 (t, $^3$J$_{HH}$ = 7.2 Hz, 3H, C$H_3$), 2.87 (m, 2H, NH–C$H_2$), $\delta$ = 3.12 (s, 1H, NH), 3.64 (d, $^3$J$_{PH}$ = 11.0 Hz, 6H, C$H_3$–O)

$^{13}$C NMR (75.5 MHz, CDCl$_3$): $\delta$ = 17.2 (d, $^3$J$_{PC}$ = 6.0 Hz, 1C, $C$H$_2$–CH$_3$), 36.0 (s, 1C, NH–$C$H$_2$), 52.6 (d, $^2$J$_{PC}$ = 5.4 Hz, 2C, CH$_3$O)

$^{31}$P NMR (101.3 MHz, CDCl$_3$): $\delta$ = 12.0 (s)

IR (cm$^{-1}$): 3230 (N–H), 2952 (as, CH$_3$), 2844 (s, CH$_3$), 1435 (as, $\delta$ CH$_3$), 1229 (P=O), 1019 and 968 (as, P–O–C), 822 (as, P–O)

Anal. calc. for $C_4H_{12}O_3PN$: C, 31.38 %; H, 7.90 %; O, 31.35 %; P, 20.23 %; N, 9.15 %

Found: C, 31.05 %; H, 7.95 %; O, 32.79 %; P, 19.43 %; N, 8.87 %

HPLC/MS (ESI): 1 peak, [M$^+$], $m/z$ = 153.8

**Dimethyl-(propyl) phosphoramidate DMPP**

MF: $C_5H_{14}O_3PN$
MW: $167.143\,g/mol$
w/w %: P $18.53\,\%$, N $8.38\,\%$
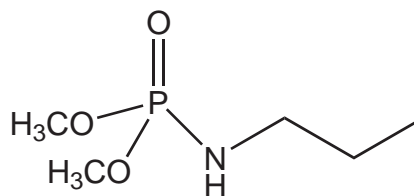
Synthesis of **DMPP** was performed analogously to **DMMP** and **DMEP**: to the solution of propylamine ($11.82\,g$, $16.44\,mL$, $0.2\,mol$) and TEA ($14.21\,g$, $19.53\,mL$, $0.2\,mol$) in THF, dimethyl hydrogen phosphite ($22.01\,g$, $18.34\,mL$, $0.2\,mol$) together with carbon tetrachloride ($30.76\,g$, $19.35\,mL$, $0.2\,mol$) were added slowly dropwise. The rest of the work up was the same as for **5**.

Yield $89.8\,\%$, yellowish oil, bp $= 216°C$ ($760$ Torr)
$^1$H NMR ($250.13$ MHz, CDCl$_3$): $\delta = 0.83$ (t, 3H, $^3J_{HH} = 7.5$ Hz, C$H_3$–CH$_2$), $1.44$ (sex, $^3J_{HH} = 7.5$ Hz, 2H, C$H_2$–CH$_3$), $2.78$ (m, 2H, C$H_2$–NH), $3.75$ (d, $^3J_{PH} = 11.0$ Hz, 6H, C$H_3$O)
$^{13}$C NMR ($50.3$ MHz, CDCl$_3$): $\delta = 11.3$ (s, 1C, CH$_2$–$C$H$_3$), $24.8$ (d, $^3J_{PC} = 5.9$ Hz, 1C, $C$H$_2$–CH$_3$), $43.0$ (s, 1C, NH–$C$H$_2$), $52.7$ (d, $^2J_{PC} = 5.5$ Hz, 2C, $C$H$_3$O)
$^{31}$P NMR ($101.3$ MHz, CDCl$_3$): $\delta = 12.0$ (s)
IR (cm$^{-1}$): $3219$ (N–H), $2952$ (as, CH$_3$), $2849$ (s, CH$_3$), $1456$ (as, $\delta$ CH$_3$), $1232$ (P=O), $1030$ (as, P–O–C), $929$ (C–C), $826$ (as, P–O)
Anal. calc. for $C_5H_{14}O_3PN$: C, $35.93\,\%$; H, $8.44\,\%$; O, $28.72\,\%$; P, $18.53\,\%$; N, $8.38\,\%$
Found: C, $35.40\,\%$; H, $8.44\,\%$; O, $29.32\,\%$; P, $18.75\,\%$; N, $8.17\,\%$
HPLC/MS (ESI): 1 peak, [M$^+$], $m/z = 167.9$

**Dimethyl-(dimethyl) phosphoramidate DMDMP**

MF: $C_4H_{12}O_3PN$
MW: 153.17 g/mol
w/w %: P 20.23 %, N 9.15 %
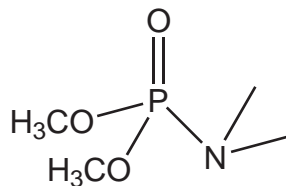
Synthesis of **DMDMP** was performed as following: to the dimethylamine, taken as 2M solution in THF (6 g of dimethylamine, 100 mL of solution) and TEA (14.21 g, 19.53 mL, 0.2 mol) in tetrahydrofurane, dimethyl hydrogen phosphite (22.01 g, 18.34 mL, 0.2 mol) together with carbon tetrachloride (30.76 g, 19.35 mL, 0.2 mol) was added slowly dropwise. The reaction mixture was cooled to $-5°C$ using ice-salt bath. At the end of the reaction, solution was filtered to remove triethylamine hydrochloride, and the rest components together with solvent were removed under vacuum. Dimethyl (dimethyl) phosphoramidate was washed with diethyl ether to purify the product from the rests of the triethylamine hydrochloride. However, the product still contained some impurities. Further it was purified on the chromatography column.

Yield 87.6 %, yellowish oil, bp = 182°C, (760 Torr)
$^1$H NMR (250.13 MHz, CDCl$_3$): $\delta = 2.64$ (d, $^3J_{PH} = 10.0$ Hz, 6H, NH(C$H_3$)$_2$), 3.63 (d, $^3J_{PH} = 11.0$ Hz, 6H, C$H_3$–O)
$^{13}$C NMR (75.5 MHz, CDCl$_3$): $\delta = 36.4$ (d, $^2J_{PC} = 3.8$ Hz, 2C, NH($CH_3$)$_2$), 52.8 (d, $^3J_{PC} = 5.8$ Hz, 2C, $C$H$_3$O)
$^{31}$P NMR (101.3 MHz, CDCl$_3$): $\delta = 13.6$ (s)
IR (cm$^{-1}$): 2951 (as, CH$_3$), 2851 (s, CH$_3$), 1457 (as, $\delta$ CH$_3$), 1308 (as, C–N–C), 1243 (P=O), 1020 and 993 (as, P–O–C)
Anal. calc. for $C_4H_{12}NO_3P$: C, 31.38 %; H, 7.90 %; O, 31.35 %; P, 20.23 %; N, 9.15 %
Found: C, 31.30 %; H, 7.68 %; O, 31.24 %; P, 20.18 %; N, 9.08 %
HPLC/MS (ESI): 1 peak, [M$^+$], $m/z = 153.9$

## Dimethyl-(2-hydroxyethyl) phosphoramidate DMHEP

MF: $C_4H_{12}O_4PN$
MW: 169.116 g/mol
w/w %: P 18.32 %, N 8.28 %
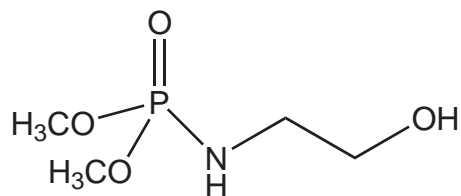


To a solution of ethanolamine (12.21 g, 12.10 mL, 0.2 mol) and triethylamine (13.50 g, 18.55 mL, 0.19 mol) in THF, dimethyl hydrogen phosphite (22.01 g, 18.34 mL, 0.2 mol) together with carbon tetrachloride (30.76 g, 19.35 mL, 0.2 mol) were added slowly dropwise. The reaction mixture was cooled to $-5°C$ using ice-salt bath. After reaction was finished, triethylamine hydrochloride was filtered off, and the rests of reagents were removed from the filtrate under vacuum. The product was used for further treatments without additional purification. 5 % less of triethylamine was used in this reaction to avoid deprotonation of the hydroxyl group of the final product.

Yield 95 %, colourless oil, bp = 221°C (760 Torr)
$^1$H NMR (300.1 MHz, CDCl$_3$): $\delta$ = 3.02 (m, 2H, NH–C$H_2$), 3.69 (m, 2H, C$H_2$OH), 3.68 (m, 6H, C$H_3$O)
$^{13}$C NMR (75.5 MHz, CDCl$_3$): $\delta$ = 38.3 (s, 1C, NH–$C$H$_2$), 53.0 (d, $^2J_{PC}$ = 5.2 Hz, 2C, $C$H$_3$O), 59.5 (s, 1C, $C$H$_2$OH)
$^{31}$P NMR (121.5 MHz, CDCl$_3$): $\delta$ = 12.5
IR (cm$^{-1}$): 3233 (N–H), 2952 (as, CH$_3$), 2847 (s, CH$_3$), 1445 (as, $\delta$ CH$_3$), 1221 (P=O), 1016 (as, P–O–C), 825 (as, P–O)
Anal. calc. for $C_4H_{12}O_4PN$: C, 28.41 %; H, 7.15 %; O, 37.84 %; P, 18.32 %; N, 8.28 %
Found: C, 28,19 %; H, 7.28 %; O, 38.05 %; P, 18.07 %; N, 8.12 %
HPLC/MS (ESI): 1 peak, [M$^+$], $m/z$ = 169.9

## Dimethyl-(2-hydroxypropyl) phosphoramidate DMHPP

MF: $C_5H_{14}O_4PN$

MW: $183.143$ g/mol

w/w %: P $16.91$ %, N $7.65$ %
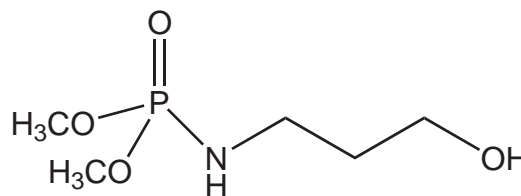
Synthesis of **DMHPP** was performed analogously to **DMHEP**. 3-aminopropanol-1 ($15.02$ g, $15.22$ mL, $0.2$ mol), triethylamine ($13.50$ g, $18.55$ mL, $0.19$ mol), dimethyl hydrogen phosphite ($22.01$ g, $18.34$ mL, $0.2$ mol) and carbon tetrachloride ($30.76$ g, $19.35$ mL, $0.2$ mol) were taken for the reaction. The rest work up was the same as for **DMHEP**.

Yield $89.6$ %, colorless oil, bp = $220$°C ($760$ Torr)

$^1$H NMR ($250.1$ MHz, $CDCl_3$): $\delta = 1.66$ (quin, $^3J_{HH} = 6.0$ Hz, 2H, $CH_2$–$CH_2$–OH), $3.02$ (m, 2H, NH–$CH_2$), $3.52$ (t, $^3J_{HH} = 6.2$ Hz, 2H, $CH_2$–$CH_2$–OH), $3.72$ (d, $^3J_{PH} = 11.2$ Hz, 6H, $CH_3$–O)

$^{13}$C NMR ($100.6$ MHz, $d_6$–DMSO): $\delta = 34.1$ (d, $^2J_{PC} = 6.0$ Hz, 2C, $CH_2$–$CH_2$–OH), $37.9$ (s, NH–$CH_2$), $52.2$ (d, $^2J_{PC} = 5.0$ Hz, 2C, $CH_3$–O), $58.3$ (s, 2C, $CH_2$–$CH_2$–OH)

$^{31}$P NMR ($161.9$ MHz, $d_6$–DMSO): $\delta = 13.2$ (s)

IR (cm$^{-1}$): 3243 (N–H), 2951 (as, $CH_3$), 2847 (s, $CH_3$), 1445 (as, $\delta$ $CH_3$), 1224 (P=O), 1017 (as, P–O–C), 824 (as, P–O)

Anal. calc. for $C_5H_{14}O_4PN$: C, $32.79$ %; H, $7.71$ %; O, $34.94$ %; P, $16.91$ %; N, $7.65$ %

Found: C, $32.61$ %; H, $7.65$ %; O, $36.97$ %; P, $16.84$ %; N, $7.72$ %

HPLC/MS (ESI): 1 peak, [M$^+$], $m/z = 183.8$

**Dimethyl bis(2-hydroxyethyl) phosphoramidate DMBHP**

MF: $C_6H_{16}O_5PN$
MW: 213.169 g/mol
w/w %: P 14.53 %, N 6.57 %
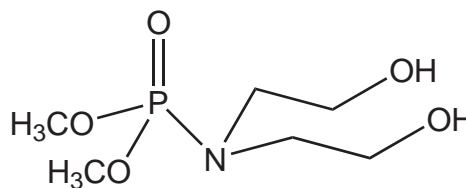


Synthesis of **DMBHP** was performed analogously to **DMHEP** and **DMHPP**. Diethanolamine (21.02 g, 19.30 mL, 0.2 mol), triethylamine (13.50 g, 18.55 mL, 0.19 mol), dimethyl hydrogen phosphite (22.01 g, 18.34 mL, 0.2 mol) and carbon tetrachloride (30.76 g, 19.35 mL, 0.2 mol) were taken for the reaction. The rest work up was the same as for **DMHEP**.

Yield 95.6 %, yellowish oil, bp = 218°C (760 Torr)
$^1$H NMR (80.0 MHz, CDCl$_3$): $\delta$ = 3.74 (d, $^3J_{PH}$ = 11.0 Hz, 6H, C$H_3$O), 3.2 (m, 8H, C$H_2$–C$H_2$–OH)
$^{13}$C NMR (50.3 MHz, CDCl$_3$): $\delta$ = 61.3 (s, 2C, $C$H$_2$OH), 53.3 (d, $^2J_{PC}$ = 5.5 Hz, 2C, $C$H$_3$O), 50.4 (s, 2C, N–$C$H$_2$)
$^{31}$P NMR (80.0 MHz, CDCl$_3$): $\delta$ = 13.7 (s)
IR (cm$^{-1}$): 3230 (O–H), 2952 (as, CH$_3$), 2839 (s, CH$_3$), 1462 (as, $\delta$ CH$_3$), 1234 (P=O), 1195 (C–N), 1018 (as, P–O–C), 830 (as, P–O)
Anal. calc. for $C_6H_{16}O_5PN$: C, 33.81 %; H, 7.56 %; O, 37.53 %; P, 14.53 %; N, 6.57 %
Found: C, 33.28 %; H, 7.47 %; O, 38.05 %; P, 14.63 %; N, 6.47 %
HPLC/MS (ESI): 1 peak, [M$^+$], $m/z$ = 213.7

## Dimethyl-(2-methoxyethyl) phosphoramidate DMMEP

MF: $C_5H_{14}O_4PN$

MW: 183.143 g/mol

w/w %: P 16.91 %, N 7.65 %
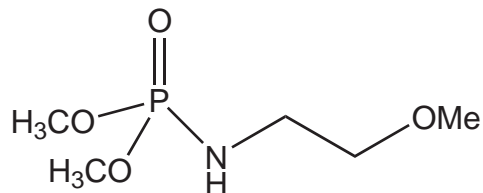
Synthesis of **DMMEP** was performed analogously to **DMHEP** and **DMHPP**. 2-methoxy-ethylamine (15.02 g, 19.30 mL, 0.2 mol), triethylamine (13.50 g, 18.55 mL, 0.19 mol), dimethyl hydrogen phosphite (22.01 g, 18.34 mL, 0.2 mol) and carbon tetrachloride (30.76 g, 19.35 mL, 0.2 mol) were taken for the reaction. The rest work up was the same as for **DMHEP**.

Yield 82.2 %, yellowish oil, bp = 215°C (760 Torr)

$^1$H NMR (250.13 MHz, CDCl$_3$): $\delta$ = 3.02 (m, 2H, C$H_2$–CH$_2$), 3.31 (s, 3H, C$H_3$), 3.38 (d, $^3$J$_{HH}$ = 5.0 Hz, 2H, C$H_2$O), 3.70 (d, $^3$J$_{PH}$ = 11.1 Hz, 6H, C$H_3$O)

$^{13}$C NMR (50.3 MHz, CDCl$_3$): $\delta$ = 40.6 (s, 1C, NH–$C$H$_2$), 52.6 (d, $^2$J$_{PC}$ = 5.5 Hz, 2C, $C$H$_3$O), 58.3 (s, 1C, O–$C$H$_3$), 72.5 (d, $^2$J$_{PC}$ = 5.5 Hz, 1C, $C$H$_2$O)

$^{31}$P NMR (101.3 MHz, CDCl$_3$): $\delta$ = 11.8 (s)

IR (cm$^{-1}$): 3229 (N–H), 2952 (as, CH$_3$), 2846 (s, CH$_3$), 1449 (as, $\delta$ CH$_3$), 1232 (P=O), 1018 and 970 (as, P–O–C), 821 (as, P–O)

Anal. calc. for $C_5H_{14}O_4PN$: C, 32.79 %; H, 7.71 %; O, 34.94 %; P, 16.91 %; N, 7.65 %

Found: C, 32.15 %; H, 7.64 %; O, 36.07 %; P, 16.49 %; N, 7.25 %

HPLC/MS (ESI): 1 peak, [M$^+$], $m/z$ = 183.8

**Dimethyl-(2-methoxypropyl) phosphoramidate DMMPP**

MF: $C_6H_{16}O_4PN$

MW: 197.169 g/mol

w/w %: P 15.71 %, N 7.10 %
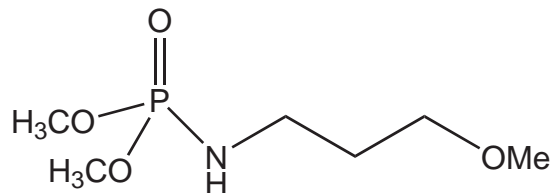


Synthesis of **DMMPP** was performed analogously to **DMMEP**. Methoxy-3-aminopropanol (15.02 g, 19.30 mL, 0.2 mol), triethylamine (13.50 g, 18.55 mL, 0.19 mol), dimethyl hydrogen phosphite (22.01 g, 18.34 mL, 0.2 mol) and carbon tetrachloride (30.76 g, 19.35 mL, 0.2 mol) were taken for the reaction. The rest work up was the same as for **DMHEP**.

Yield 95.6 %, yellowish oil, bp = 212°C (760 Torr)

$^1$H NMR (250.13 MHz, CDCl$_3$): $\delta$ = 1.69 (quin, $^3J_{HH}$ = 5.8 Hz, 2H, CH$_2$–C$H_2$–CH$_2$), 2.94 (m, 2H, NH–C$H_2$), 3.26 (s, 3H, O–C$H_3$), 3.40 (m, 2H, CH$_2$–C$H_2$–O), 3.66 (dd, $^3J_{PH}$ = 11.0 Hz, 6H, C$H_3$O)

$^{13}$C NMR (62.9 MHz, CDCl$_3$): $\delta$ = 31.2 (d, $^3J_{PC}$ = 5.8 Hz, 1C, CH$_2$–$C$H$_2$–CH$_2$), 39.3 (s, 1H, NH–$C$H$_2$), 52.8 (d, $^2J_{PC}$ = 5.3 Hz, 2C, $C$H$_3$–O), 58.6 (s, 1C, O–$C$H$_3$), 70.7 (s, 1C, $C$H$_2$–O–CH$_3$)

$^{31}$P NMR (101.3 MHz, CDCl$_3$): $\delta$ = 11.9 (s)

IR (cm$^{-1}$): 3220 (N–H), 2949 (as, CH$_3$), 2848 (s, CH$_3$), 1454 (as, $\delta$ CH$_3$), 1234 (P=O), 1021 and 995 (as, P–O–C), 930 (C–C), 823 (as, P–O)

Anal. calc. for $C_6H_{16}NO_4P$: C, 36.55 %; H, 8.18 %; O, 32.46 %; P, 15.71 %; N, 7.10 %

Found: C, 36.14 %; H, 8.20 %; O, 32.93 %; P, 15.18 %; N, 7.13 %

HPLC/MS (ESI): 1 peak, [M$^+$], $m/z$ = 197.8

**Methylphosphorodiamide MPDA**

MF: $CH_7O_2PN_2$
MW: 110.05 g/mol
w/w %: P 28.14 %, N 25.45 %
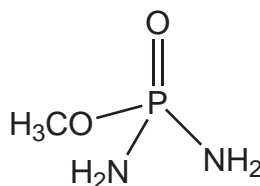
Gaseous ammonia was bubbled through dry chloroform at the temperature of $-10°C$. Phosphorus oxychloride was distilled before to remove impurities. The solution of methyl phosphoric dichloride (7.45 g, 0.05 mol) in 40 mL of chloroform was added dropwise to dissolved ammonia during 1.5 hours and intensively stirred at $-10°C$. After the full addition of methyl phosphoric dichloride, the reaction mixture was stirred additionally for 2 hours. Chloroform was removed from the system, and the rest dried in vacuum. Ca. 50 mL of chloroform was added to the product and reacted with diethylamine (21.95 g, 0.3 mol, 31.0 mL), and the mixture was refluxed during 4 hours. Diethylammonium chloride was dissolved in chloroform, and product was filtered off and dried in vacuum.

Yield 92.6 %, mp = 128°C, (760 Torr)
$^1$H NMR (250.13 MHz, $CDCl_3$): $\delta = 3.75$ (d, $^3J_{PH} = 11.2$ Hz, 3H, C$H_3$O)
$^{13}$C NMR (75.5 MHz, $CDCl_3$): $\delta = 53.0$ (s, 1C, $C$H$_3$O)
$^{31}$P NMR (101.3 MHz, $CDCl_3$): $\delta = 17.4$
IR ($cm^{-1}$): 3220 (N–H), 2949 (as, $CH_3$), 2848 (s, $CH_3$), 1454 (as, $\delta$ $CH_3$), 1234 (P=O), 1021 and 995 (as, P–O–C), 930 (C–C), 823 (as, P–O)
Anal. calcd. for $CH_7O_2PN_2$: C, 10.91 %; H, 6.41 %; O, 29.07 %; P, 28.14 %; N, 25.45 %
Found: C, 10.73 %; H, 6.53 %; O, 30.12 %; P, 28.14 %; N, 26.25 %
HPLC/MS (ESI): 1 peak, $[M^+]$, $m/z =110.7$

**Phosphoric triamide PTA**

MF: $PH_6ON_3$
MW: 95.04 g/mol
w/w %: P 32.59 %, N 44.21 %
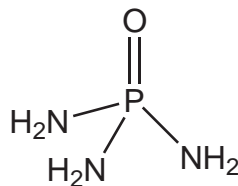
Gaseous ammonia was bubbled through dry chloroform at the temperature of $-10°$C. Phosphorus oxychloride was distilled before to remove impurities. The solution of phosphoroxychloride (7.67 g, 0.05 mol, 4.65 mL) in 40 mL of chloroform was added dropwise to dissolved ammonia during 1.5 hours and intensively stirred at $-10°$C. After the full addition of phosphorus oxychloride, the reaction mixture was stirred additionally for 2 hours. Chloroform was removed from the system, and the rest dried in vacuum. Ca. 50 mL of chloroform was added to the product and reacted with diethylamine (21.95 g, 0.3 mol, 31.0 mL), and the mixture was refluxed during 4 hours. Diethylammonium chloride was dissolved in chloroform, and product was filtered off and dried in vacuum.

Yield 92.3 %, mp = °C, (760 Torr)
$^{31}$P NMR (101.3 MHz, CDCl$_3$): $\delta = 18.8$
IR (cm$^{-1}$): 3220 (N–H), 1234 (P=O)
Anal. calc. for $PH_6ON_3$: H, 6.36 %; O, 16.83 %; P, 32.59 %; N, 44.21 %
Found: H, 6.32 %; O, 16.91 %; P, 31.93 %; N, 44.86 %
HPLC/MS (ESI): 1 peak, [M$^+$], $m/z$ =95.7

## 10.4 Methods of flame retardancy investigation

### Limiting Oxygen Index Test

The LOI measurements of the treated cotton fabrics were performed according to the ASTM D 2863-95 using Oxygen Index Test (Fire Testing Technology). The dimensions of each sample were 50 x 70 mm. The measurement was performed 3 to 4 times and the average LOI value was calculated.

### Microscale Combustion Calorimetry

For the measurements of the heat release rates a Microscale Combustion Calorimeter was used (Fire Testing Technology, England). Using this instrument, the maximum heat release $Q_{t1}$ and the temperature at the maximum heat release $T$ were recorded. Such parameters as heat of combustion $h_c^0$, total heat of combustion $h_{c,t}^0$ and heat release capacity $\eta c$ were calculated according to the formulae (see Section *Microscale Combustion Calorimetry* in the Introduction Chapter). The heating rate was chosen to be $1°\mathrm{Cs}^{-1}$, the maximum pyrolysis temperature was 750°C and the combustion temperature 900°C. The flow was a mixture of $O_2/N_2$ 20/80 cm$^3$ min$^{-1}$ and the sample weight was $5 \pm 0.5$ mg.

### Thermogravimetric Analysis

The dependence of the mass-loss on the temperature was recorded using TGA-SDTA 851 (Mettler Toledo) and Netzsch TG F209 Iris. The heating rate was set to 10°C min$^{-1}$. The measurement was performed in the range of 40 to 800°C in the continuous flow of nitrogen or air at a rate of 100 ml min$^{-1}$. Cellulose samples were cut into powdery pieces with scissors. The sample mass was $10 \pm 0.5$ mg.

## 10.5    Characterization methods

### Elemental Analysis

The content of carbon, hydrogen and nitrogen was determined using a LECO CHN analyzer. Phosphorus was determined by Inductively-Coupled Plasma – Optical Emission Spectrometry (ICP–OES). The distribution of phosphoramidates in the fabric was homogeneous.

### Scanning Electron Microscopy (SEM)

Scanning Electron Microscopy is an important analytical tool employed in the study of charred surfaces. Using this technique attempts have been made to characterize the nature of chars and to correlate these observations with the efficiencies of the chemicals used as flame retardants for cellulose.

The surface morphology of the fabrics (untreated and treated) and chars was investigated by SEM using Hitachi S-4800 Microscope. Char samples have been used without further modification because they maintained their original fabric structure and size. Pieces of about 1 cm$^2$ were cut with razor blades and mounted on metal stubs with double faced adhesive carbon tape. The electron beam was set up to 5.0 kV unless specified otherwise. Prior to microscopic investigations samples were coated with a thin film of gold using an ion sputtering device (SEM Coating Unit E5100, Polaron Equipment Limited, 2 min exposure time).

### Energy Dispersive X-Ray Analysis (EDX)

EDX investigations (Inca X-sight, Oxford Instruments) were applied in combination with a scanning electron microscope (Hitachi S-4800). For each sample, the EDX analysis was performed at three different areas on the completely charred sample, and an average value was obtained from the resulting elemental compositions. The EDX spectra were taken at a magnification of x5000, thereby scanning an area of approximately 5mm x 5mm, depth

$1 - 3$ $\mu$m (the diameter of a single fiber of the charred sample is roughly 10 $\mu$m). Other parameters in the EDX investigation were an acceleration voltage of the electron beam of 5 kV, an emission current of 15 mA and a working distance of 15 mm.

## Nuclear Magnetic Resonance (NMR)

NMR Spectra were recorded on Bruker Avance 500, 400, 300, 250 and 200 spectrometers. The chemical shifts were measured according to IUPAC and expressed in ppm relative to TMS and $H_3PO_4$ for $^1$H, $^{13}$C and $^{31}$P, respectively. Coupling constants $J$ are given in Hertz [Hz] as absolute values, unless specifically stated. Where a first order analysis is appropriate, the multiplicity of signals is indicated as s, d, t, q or m for singlets, doublets, triplets, quartets, or multiplets, respectively. Otherwiese the spin systems are specified explicitly.

## Gas Chromatography - Mass Spectrometry (GC-MS)

Gas Chromatography was performed using Hewlett Packard chromatograph HP 5890 equipped with a mass spectrometer HP 5970 detector. Analysis of the mixture pyrolysates was accomplished using DB-5 (J&W) column, filling material, 25 m long, with 0.2 mm diameter. The temperature-programmed chromatograms were performed under the following conditions: injector temperature 280°C; column program: initial 50°C, 1 min, heating rate 10°Cmin$^{-1}$, final temperature 320°C, 5 min; helium carrier flow: 10ml min$^{-1}$.

## Liquid Chromatography - Mass Spectrometry (LC-MS)

Our system for routine LC-MS was comprised of an Agilent 1100 HyStar LC system (Agilent, Wilmington, Germany) and Esquire HCT mass spectrometer (Bruker Daltonics, Bremen, Germany). Mobile phase A was 0.5 % formic acid in water. Mobile phase B was 0.1 % formic acid in acetonitrile. Flow rate was 0.1 mL/min for 20 min. Chromatographic column used was Gemini 5u C18 110A, 250 x 2.00 mm, with the particle size of 5$\mu$m.

## Attenuated Total Reflectance Fourier Transform - Infrared Spectroscopy (ATR-FTIR)

The BioRad, FTS-175 ATR-FTIR Spectrometer was used to characterize synthesized products. The software used to evaluate the data was Digilab Resolution Pro 4.0. 128 scans at a resolution of $4\,cm^{-1}$ were recorded between 4000 and $700\,cm^{-1}$.

## Thermogravimetric analysis coupled with Fourier Transform - Infrared Spectroscopy (TGA-FTIR)

The TGA-FTIR system used in our studies was a Netzsch STA-449C instrument coupled with Bruker Tensor-27. For the determination of the composition of the gas phase, the following procedure was applied. $10\,mg$ of sample was heated from 50 to 600°C at a rate of 10°C/min under the helium flow. The flow rate of helium was fixed to $70\,mL\,min^{-1}$. The line that transfers the evolved gases from the TGA to IR cell was maintained at 220°C. IR spectra were recorded in the spectral range from 4000 to $600\,cm^{-1}$ with a resolution of $4\,cm^{-1}$. The FTIR and TGA data obtained during the measurements was analyzed using the Netzsch Proteus - Thermal Analysis Software.

# References

[1] A. R. Horrocks and D. Price. *Fire retardant materials.* Woodhead Publishing Limited, 2001.

[2] H. Hochkirch, D. Paul, and G. Heiseler. Vorrichtung zur Herstellung von N-Unsubstituierten Phosphorsäure-Esteramiden, 1979.

[3] W.H. Perkin. *J. Ind. Eng. Chem.*, 5(57), 1913.

[4] J. W. Lyons. *The Chemistry and Use of Fire Retardants.* Wiley Interscience, New York, 1970.

[5] S.M. Lomakin and G.E. Zaikov. *Modern Polymer Flame Retardancy.* VSP, Utrecht. Boston., 2003.

[6] K. Akita and M. Kase. Determination of kinetic parameters for pyrolysis of cellulose and cellulose treated with ammonium phosphate by differential thermal analysis and thermal gravimetric analysis. *Journal of Polymer Science*, 5:833, 1967.

[7] B. Kaur, I. S. Gur, and H. L. Bhatnagar. Thermal degradation studies of cellulose phosphates and cellulose thiophosphates. *Angewandte Makromolekulare Chemie*, 147:157–183, 1987.

[8] K. Katsuura and N. Inagaki. Thermal degradation of phosphorus-containing polymers. VIII. Relation between the thermal reaction of flame-retardant cellulose and its flammability. *Textile Research Journal*, 45:103, 1975.

[9] I.G. Bhatt, A.W. Shringarpure, V. Sundaram, S.N. Bailur, and G.R. Phalgumani. Durable flame retardant (FR) finish to cellulosic fabrics by phosphorylation. *Colourage*, 21:3, 1985.

[10] C. F. Cullis, M. M. Hirschler, and R. G. Madden. Studies of the effects of phosphorus and its compounds on the combustion of cellulose. *European Polymer Journal*, 28(5):493–497, 1992.

[11] S.M. Mostashari and S.Z. Mostashari. The effect of selected phosphates on the flame retardancy of cotton and polyester fabrics. *International Journal of Polymeric Materials*, 57:338–342, 2008.

[12] E. D. Weil, S. V. Levchik, M. Ravey, and W. M. Zhu. A survey of recent progress in phosphorus-based flame retardants and some mode of action studies. *Phosphorus Sulfur and Silicon and the Related Elements*, 146:17–20, 1999.

[13] Anon. *Ciba-Geigy Rev.*, 4:49, 1969.

[14] J.E. Hendrix and J.L. Drake. Pyrolysis and combustion of cellulose. II. Thermal analysis of mixtures of methyl-D-glucopyranoside and levoglucosan with model phosphate flame retardants. *Journal of Applied Polymer Science*, 16:41–59, 1972.

[15] B. Kaur, I. S. Gur, and H. L. Bhatnagar. Studies on thermal degradation of cellulose and cellulose phosphoramides. *Journal of Applied Polymer Science*, 31:667–683, 1986.

[16] J.P. Stevens. Flammverzögernde Zellulose und Verfahren zu ihrer Herstellung, 1969.

[17] R.D. Sibrikova, T.D. Zakharova, and B.N. Melnikov. Composition for fireproofing and crease-resistant finishing of cellulose textile materials, 1978.

[18] V.M. Yurchenko, N. S. Zubkova, and M.A. Tyuganova. Synthesis and study of fireproofing properties of phosphorus-containing cellulose esters. *Koksnes Kimija*, 4:37–41, 1980.

[19] V.I. Khodyrev, L.V. Lavrenova, R.G. Zhbankov, and V.A. Kulakov. Composition for fireproofing linen fabrics, 1981.

[20] E.N. Pokrovskaya, T.P. Nikiforova, and Y.N. Nedoshivin. Fireproofing effect of some phosphorus-containing compounds. *Koksnes Chimiya*, 3:99–102, 1984.

[21] A.A. Kapura, B.N. Solomonov, and G.N. Pesternikov. Behavior of triamidophosphate on cellulosic textile materials. *Zhurnal Prikladnoi Khimii*, 64(6):1307–12, 1991.

[22] P. Aggarwal and D. Dollimore. Thermal studies on the combustion process of treated and untreated cellulose. *ASTM special technical publication*, pages 29–43, 1997.

[23] J.L. Drake, B.M. Kopacz, and F.S. Perkerson. *Agr. Res. Serv. Document*, 72(14), 1958.

[24] M. Lewin and F.H. Mark. Some aspects of synergism and catalysis in FR of polymeric materials - an overview. *Ninth Annual BCC Conference on Flame Retardancy*.

[25] H. B. Pandya and M. M. Bhagwat. Mechanistic aspects of phosphorus-nitrogen synergism in cotton flame retardancy. *Textile Research Journal*, 1981.

[26] A. I. Balabanovich, G. F. Levchik, S. V. Levchik, and J. Engelmann. Fire retardant synergism between cyclic diphosphonate ester and melamine in poly(butylene terephtalate). *Journal of Fire Sciences*, 20:71–83, 2002.

[27] R.W. Little. *Flameproofing of Textile Fabrics*. Reinhold, New York, 1947.

[28] D.M. Jones and T.M. Noone. Some approaches to the permanent flameproofing of cotton: Systems containing phosphorus. *Journal of Applied Chemistry*, 12(9):397–405, 1962.

[29] G.C. Tesoro, S.B. Sello, and J.J. Willard. Nitrogen-phosphorus synergism in flame retardant cellulose. *Textile Research Journal*, 39(2):180–190, 1969.

[30] C. F. Cullis. The role of pyrolysis in polymer combustion and flame retardance. *Journal of Analytical and Applied Pyrolysis*, 11:451–463, 1987.

[31] A. Granzow. Flame retardation by phosphorus compounds. *Accounts of Chemical Research*, 11(5):177–83, 1978.

[32] F. Shafizadeh. *Adv. Carbohydr. Chem.*, 23:419, 1968.

[33] F. Shafizadeh and Y.L. Fu. Pyrolysis of cellulose. *Carbohydrate Research*, 29:113–122, 1972.

[34] F. Shafizadeh, R.H. Furneaux, T.G. Cochran, J.P. Scholl, and Y. Sakai. Production of levoglucosan and glucose from pyrolysis of cellulosic materials. *Journal of Applied Polymer Science*, 23:3525–39, 1979.

[35] R. Ball, A. C. McIntosh, and J. Brindley. The role of char-forming processes in the thermal decomposition of cellulose. *Physical Chemistry Chemical Physics*, 1(21):5035–5043, 1999.

[36] R. Ball, A. C. McIntosh, and J. Brindley. Feedback processes in cellulose thermal decomposition: implications for fire-retarding strategies and treatments. *Combustion Theory and Modelling*, 8(2):281–291, 2004.

[37] A. G. W. Bradbury, Y. Sakai, and F. Shafizadeh. Kinetic model for pyrolysis of cellulose. *Journal of Applied Polymer Science*, 23(11):3271–3280, 1979.

[38] A. Broido, A. Javierso, A. C. Ouano, and E. M. Barrall. Molecular weight decrease in early pyrolysis of crystalline and amorphous cellulose. *Journal of Applied Polymer Science*, 17(12):3627–3635, 1973.

[39] M. E. Calahorra, M. Cortazar, J. I. Eguiazabal, and G. M. Guzman. Thermogravimetric analysis of cellulose - effect of the molecular weight on thermal decompositions. *Journal of Applied Polymer Science*, 37(12):3305–3314, 1989.

[40] R. Capart, L. Khezami, and A. K. Burnham. Assessment of various kinetic models for the pyrolysis of a microgranular cellulose. *Thermochimica Acta*, 417(1):79–89, 2004.

[41] W. E. Franklin. Initial pyrolysis reactions in unmodified and flame retardant cotton. *Journal of Macromolecular Science-Chemistry*, A19(4):619–641, 1983.

[42] M. M. Tang and R. Bacon. Carbonization of celulose fibers. I. Low temperature pyrolysis. *Carbon*, 2:211–220, 1964.

[43] D. F. Arseneau. Competitive reactions in thermal decomposition of cellulose. *Canadian Journal of Chemistry*, 49(4):632, 1971.

[44] B. K. Kandola, A. R. Horrocks, D. Price, and G. V. Coleman. Flame retardant treatments of cellulose and their influence on the mechanism of cellulose pyrolysis. *J. M. S. - Rev. Macromol. Chem. Phys.*, C36(4):712–794, 1996.

[45] R. M. Rowell and S. L. LeVan-Green. *Handbook of Wood Chemistry and Wood Composites*. 2005.

[46] J. W. Lyons. Mechanisms of fire retardation with phosphorus compounds: Some speculation. *Journal of Fire and Flammability*, 1:302–311, 1970.

[47] G.A. Byrne, D. Gardiner, and F.H. Holmes. Pyrolysis of cellulose and the action of flame-retardants. II. Further analysis and identification of products. *Journal of Applied Chemistry*, 16(81), 1966.

[48] John W. Lyons. *The Chemistry and Uses of Fire Retardants*. Wiley Interscience, New York, 1970.

[49] B. K. Kandola, A. R. Horrocks, D. Price, and G. V. Coleman. Flame retardant treatments of cellulose and their influence on the mechanism of cellulose pyrolysis. *J.M.S.-Rev.Macromol.Chem.Phys.*, C36(4):721–794, 1996.

[50] R. E. Lyon and R.N. Walters. A microscale combustion calorimeter. Technical report, Federal Aviation Administration, 2002.

[51] R.E. Lyon. Heat release rate calorimeter for milligram samples, 2002.

[52] R. E. Lyon and R.N. Walters. A pyrolysis combustion flow calorimeter: Study of polymer heat release rate. In *Ninth Annual BCC Conference on Flame Retardancy*.

[53] R. E. Lyon and R.N. Walters. Pyrolysis combustion flow calorimetry. *J. Anal. Appl. Pyrolysis*, 71:27–46, 2004.

[54] C. Q. Yang, Q. He, R. E. Lyon, and Y. Hu. Investigation of the flammability of different textile fabrics using micro-scale combustion calorimetry. *Polymer Degradation and Stability*, 95:108–115, 2010.

[55] R.E. Lyon, R.N. Walters, and S.I. Stoliarov. Thermal analysis of flammability. *Journal of Thermal Analysis and Calorimetry*, 89:441–448, 2007.

[56] M. Webb, P.M. Last, and C. Breen. Synergistic chemical analysis - the coupling of TG with FTIR, MS and GC-MS 1. The determination of the gases released during the thermal oxidation of a printed curcuit board. *Thermochimica Acta*, 326(151-8), 1999.

[57] A. Pappa, S.A. Kyriakou, K. Mikedi, N. Tzamtzis, and M. Statheropoulos. Design considerations and an example of application of an in-house made TGA-MS interface. *Journal of Thermal Analysis and Calorimetry*, 78:415–426, 2004.

[58] A. Pappa, K. Mikedi, N. Tzamtzis, and M. Statheropoulos. TG-MS analysis for studying the effects of fire retardants on the pyrolysis of pine-needles and their components. *Journal of Thermal Analysis and Calorimetry*, 84(3):655–61, 2006.

[59] F. Eigenmann, M. Maciejewski, and A. Baiker. Quantitative calibration of spectroscopic signals in combined TG-FTIR system. *Thermochimica Acta*, 440:81–92, 2006.

[60] Y. Soudais, L. Moga, J. Blazek, and F. Lemort. Coupled DTA-TGA-FT-IR investigation of pyrolytic decomposition of EVA, PVC and cellulose. *Journal of Applied Pyrolysis*, 78:46–57, 2007.

[61] S. Materazzi. Thermogravimetry - Infrared Spectroscopy (TG-FTIR) coupled analysis. *Applied Spectroscopy Reviews*, 32(4):385–404, 1997.

[62] S. Materazzi. Mass spectrometry coupled to thermogravimetry (TG-MS) for evolved gas characterization: A review. *Applied Spectroscopy Reviews*, 33(3):189–218, 1998.

[63] W.C. Arney and W.C. Kuryla. Structure-property relationships in flame retardant systems. Relative effects of alkylphosphates, phosphonates and phosphites on cellulose flammability. *Journal of Fire and Flammability*, 3:183–191, 1972.

[64] M. J. Tsafack and J. Levalois-Grützmacher. Towards multifunctional surfaces using the plasma-induced graft-polymerization (PIGP) process: Flame and waterproof cotton textiles. *Surface and Coatings Technology*, 201:5789–5795, 2007.

[65] S. Gaan and G. Sun. Effect of phosphorus and nitrogen on flame retardant cellulose: A study of phosphorus compounds. *Journal of Analytical and Applied Pyrolysis*, 78(2):371–377, 2007.

[66] S. Gaan and G. Sun. Effect of phosphorus flame retardants on thermo-oxidative decomposition of cotton. *Polymer Degradation and Stability*, 92(6):968–974, 2007.

[67] U. Braun, A. I. Balabanovich, B. Schartel, U. Knoll, J. Artner, M. Ciesielski, M. Doring, R. Perez, J. K. W. Sandler, V. Altstadt, T. Hoffmann, and D. Pospiech. Influence of the oxidation state of phosphorus on the decomposition and fire behaviour of flame-retarded epoxy resin composites. *Polymer*, 47(26):8495–8508, 2006.

[68] J.J. Willard and R.E. Wondra. Quantitative evaluation of flame-retardant cotton finishes by the limiting-oxygen index (LOI) technique. *Textile Research Journal*, 40(3):203–210, 1970.

[69] W.A. Reeves, R.M. Perkins, B. Piccolo, and J.L. Drake. Some chemical and physical factors influencing flame retardancy. *Textile Research Journal*, 40:223–231, 1970.

[70] E. D. Weil and G. F. Levchik. *Flame Retardants for Plastics and Textiles: Practical Applications.* Munich, 2009.

[71] B.W. Lew. Polyol poly(hydrogen alkyl phosphite) monomers, 1967.

[72] R. T. Major and R. J. Hedrick. Reactions of diethyl n-alkoxyphosphoramidate anions with carbon dioxide and carbon disulfide. *Journal of Organic Chemistry*, 30(4):1268, 1965.

[73] E.J. Gonzales and S.L. Vail. Dimethyl and diethyl phosphoramidates as flame retardants for cotton. *Journal of Fire Retardant Chemistry*, 1:142–151, 1974.

[74] E. J. Gonzales, Jr. Pepperman, A.B., and S.L. Vail. A durable flame retardant for cotton cellulose based on diethyl phosphoramidate DEPA and THPOH. *Journal of Fire Retardant Chemistry*, 2:171–182, 1975.

[75] P.M. Burke. Dialkyl n-substituted phosphoramidate containing flame retardants, 1973.

[76] F.-Y. Hshieh and H. Beeson. Flammability testing of pure and flame retardant-treated cotton fabrics. *Fire and Materials*, 19:233–239, 1995.

[77] M. J. Tsafack and J. Levalois-Grützmacher. Flame retardancy of cotton textiles by plasma-induced graft-polymerization (PIGP). *Surface Coatings Technology*, 201(6):2599–2610, 2006.

[78] C.M. Tian, Z.H. Shi, H.Y. Zhang, J.Z. Xu, J.R. Shi, and Guo H.Z. Thermal degradation of cotton cellulose. *Journal of Thermal Analysis and Calorimetry*, 55:93–98, 1999.

[79] D. Katovic, S. Flinec Grgac, S. Bischof-Vikusic, and A. Katovic. Formaldehyde free binding system for flame retardant finishing of cotton fabrics. *Fibres Textiles in Eastern Europe*, 20(1):90, 2012.

[80] P.F. Schmidt. *Praxis der Rasterelektronenmikroskopie und Mikrobereichsanalyse*. Expert Verlag, Germany, 1994.

[81] E.N. Pokrovskaya. Action mechanism of phosphorus-containing compounds as flame retardants for cellulose and wood products. *Koksnes Chimiya*, (4):91–94, 1991.

[82] R.R. Mod, J.A. Harris, JC Jr. Arthur, F.C. Magne, G. Sumrell, and A.F. Novak. Free radical addition of dialkyl phosphites to n,n-disubstituted amides of unsaturated fatty acids and screening of the products for antimicrobial activity. *Journal of the Americal Oil Chemists' Society*, 49(11):634–635, 1972.

[83] C. Walling and R. Rabinowitz. The reaction of trialkyl phosphites with thiyl and alkoxy radicals. *J. Am. Chem. Soc.*, 81(5):1243–1249, 1959.

[84] K.V. Nikonorov, E.A. Guryler, and A.V. Chernova. Condensation of chloral with amidophosphates and some properties of the resulting compounds. *fide Chemical Abstracts*, 69, 1968.

[85] R. Khazanchi and N. K. Roy. Synthesis and phytotoxic properties of o,o-dimethyl phosphoramidates and o-methyl phosphoric diamides. *Indian Journal of Agricultural Sciences*, 56(10):726–731, 1986.

[86] C. Grison, P. Coutrot, C. Comoy, L. Balas, S. Joliez, G. Lavecchia, P. Oliger, B. Penverne, V. Serre, and G Herve. Design, synthesis and activity of bisubstrate, transition-state analogues and competitive inhibitors of aspartate transcarbamylase. *European Journal of Medicinal Chemistry*, 39:333–344, 2004.

[87] J. Steinbach, E. Herrmann, and L. Riesel. Zur Umsetzung des Zweikomponentensystems Triaikylphosphit/Tetrachlorkohlenstoff mit wasserstoffhaltigen Nucleophilen 2. Die Reaktion mit Ammoniak und Aminen. *Z. anorg. allg. Chem.*, 523:180–186, 1985.

[88] S. Albrecht and E. Herrmann. Eine neue Möglichkeit zur Darstellung von N-Alkyl-phosphorsäurediesteramiden. *Z. Chem.*, 25(12):429, 1985.

[89] F.R. Atherton, H.T. Openshaw, and A.R. Todd. Phosphorylation. II. Reaction of dialkyl phosphites with polyhalogen compounds in presence of bases. New method for the phosphorylation of amines. *Journal of the Chemical Society*, pages 660–663, 1945.

[90] E.M. Georgiev, J. Kaneti, K. Troev, and D.M. Roundhill. An ab initio study of the mechanism of the Atherton-Todd reaction between dimethyl phosphonate and chloro- and fluoro-substituted methanes. *Journal of the American Chemical Society*, 115:10964–73, 1993.

[91] K. Troev, E.M.G. Kirilov, and D.M. Roundhill. A study of the Atherton-Todd reaction mechanism. *The Chemical Society of Japan*, 63:1284–5, 1990.

[92] A. Kong and R. Engel. A mechanistic investigation of the Todd-Atherton reaction. *The Chemical Society of Japan*, 58:3671–3672, 1985.

[93] F.R. Atherton and A.R. Todd. Studies on phosphorylation. Part III. Further observations on the reaction of phosphites with polyhalogen compounds in presence of bases and its application to the phosphorylation of alcohols. *J. Chem. Soc.*, pages 674–678, 1947.

[94] L. Riesel, E. Herrmann, and J. Steinbach. On the reaction of phosphorus acid esters with nucleophiles in the presence of carbon tetrachloride. *Phosphorus and Sulfur*, 18:253–256, 1983.

[95] T. Kasparek, V. Stasova, and J. Mollin. Transesterification of aryl diamidophosphates. *Acta Universitatis Palackinae Olomucensis*, 102, 1991.

[96] R. Klement and O. Koch. Phosphoroxy triamid und Phosphorthio-triamid. 3:333–340, 1954.

[97] N.J. Glade, Ingenuin Hechenbleickner, and D.W. Kaiser. Textile fire retardant treatment, 1958.

[98] P.S. Blatz and W. Del. Flame resistant hydrocarbon polymers, 1969.

[99] A.K. Kulshreshtha, H. B. Pandya, and M. M. Bhagwat. Application of external reflection spectroscopy to a study of chars formed during fabric combustion. *Indian Journal of Textile Research*, 7:45–48, 1982.

[100] H. B. Pandya, R. S. Chauhan, M. M. Bhagwat, and N. E. Dweltz. Microscopic studies of the char of phosphoramide treated cotton fabrics. *Journal of Fire Retardant Chemistry*, 7(1):27–35, 1980.

[101] M. K. Tomioka and S. H. Zeronian. Morphological studies on fabrics treated with flame retardant finishes. *Textile Research Journal*, 44(1):1–4, 1974.

[102] G.D. Titskii, L.M. Litvinenko, and O.P. Stepko. Catalytic activity of organophosphorus acid amides in the reaction of benzoyl chloride with m-chloroaniline in benzene. *Zhurnal Obshchei Khimii*, 44(8):1688–94, 1974.

[103] V.A. Tomilets, V.I. Dontsov, L.K. Nikanorova, N.P. Grechkin, and G.S. Gubanova. Antiallergic properties of certain alkylating organophosphorus compounds. *Khimiko-Pharmatsevtichesky Zhurnal*, 15(9):34–39, 1982.

[104] B. Dawidowitz and T.A. Madro. Phosphoric amides. 7. Mass spectrometry of phosphoric amido esters: Fragmentation patterns and migratory aptitudes. *Organic Mass Spectrometry*, 19(3), 1984.

[105] B. Dawidowitz and T. A. Modro. Phosphoric amides. Part 8. The effect of the ethylenimine substituent on the solvolytic reactivity of phosphate and phosphoramidate bonds. *J. Chem. Soc. Perkin Trans. II*, 1985.

[106] O.V. Osipova, V.A. Kolesova, P.V. Kazakov, L.I. Virin, and I.Yu. Popova. Phosphorus-containing allophanates. Mass spectra and structure. *Zhurnal Obshchei Khimii*, 59(7):1523–9, 1989.

[107] V.A. Kolesova, O.V. Osipova, N.E. Karabut, and Yu.A. Strepikheev. Phosphorus-containing derivatives of allophanic acid. *Trudy Instituta - Moskovskii Khimiko-Technologicheskii Institut imeni D.I. Mendeleeva*, 149:81–7, 1987.

[108] M. van Nooy, L. Willms, H. Mildenberger, K. Bauer, and H. Bieringer, 1989.

[109] M.A. Goodman, S.M. Schmann, R. Atkinson, and A.M. Winer. Atmospheric reactions of a series of dimethyl phosphoramidates and dimethyl phosphorothioamidates. *Environmental Science and Technology*, 22(5):578–83, 1988.

[110] P.A. D'Agostino and L.R. Provost. Mass spectrometric identification of products formed during degradation of ethyl dimethylphosphoramidocyanitide (tabun). *Journal of Chromatography*, 598(89-95), 1992.

[111] M. Palit, D. Pardasani, A.K. Gupta, P. Shakya, and D.K. Dubey. Microsynthesis and electron ionisation mass spectrometric analysis of chemical weapons convention (CWC)-related o,o-dialkyl-n,n-dialkylphosphoramidates. *Analytical and Bioanalytical Chemistry*, 381(2):477–86, 2005.

[112] A.K. Gupta, D. Pardasani, H.K. Gupta, and D.K. Dubey. N,N'-dichlorobis(2,4,6-trichlorophenyl)urea (CC-2): an efficient reagent for the synthesis of chemical weapons convention-related dialkyl N,N-dialkylphosphoramidates from dialkyl phosphites. *Australian Journal of Chemistry*, 60(11):879–82, 2007.

[113] S.M. Verchunov, S.S. Rimov, and N.I. Koltsov. Polyurethane elastomers based on dimethylphosphite, mono and diethanolamines. *Kauchuk i Resina*, 1, 2006.

[114] M. J. Tsafack, F. Hochart, and J. Levalois-Grützmacher. Polymerization and surface modification by low pressure plasma technique. *European Physical Journal Applied Physics*, 26:215–219, 2004.

[115] P. Rupper, S. Gaan, V. Salimova, and M. Heuberger. Characterization of chars obtained from cellulose treated with phosphoramidate flame retardants. *Journal of Analytical and Applied Pyrolysis*, 87:93–98, 2010.

[116] S. Gaan, P. Rupper, V. Salimova, M. Heuberger, S. Rabe, and F. Vogel. Thermal decomposition and burning behavior of cellulose treated with ethyl ester phosphoramidates: Effect of alkyl substituent on nitrogen atom. *Polymer Degradation and Stability*, 94, 2009.

[117] E.N. Rasadkina, D.A. Predvoditelev, and E.E. Nifantiev. Amidophosphate glycolic phospholipides. *Bioorganic Chemistry*, 18(2):302–304, 1992.

[118] P. Petrov. Preparation of n,n-dialkoxy bis(2-hydroxyethyl)phosphoramide, 1992.

[119] R. Greenhalgh and M. A. Weinberger. The selective phosphylation of ethanolamine. *Canadian Journal of Chemistry*, 45:495–500, 1967.

[120] E.K. Ryu and L.A.Cates. Phosphorus-nitrogen compounds. 13. Methoxyethyl and propylamine derivatives. *Journal of Medicinal Chemistry*, 14(10):1022, 1971.

[121] S. Gaan, V. Salimova, M. Heuberger, P. Rupper, and L. M. Schoenholzer. Phosphoramidate flame retardants: mechanism and application. In *Annual Conference on Recent Advances in Flame Retardancy of Polymeric Materials*.

[122] S.A. Vilkova, V.G. Krupkin, and A.D. Margolin. Critical conditions for combustion of materials from fiber-forming polymers. *Fizika Goreniya i Vzriva*, 22(3):67–73, 1986.

[123] N.J. Glade. Flame-resistant, water-repellent textile finishes, 1961.

[124] N.J. Glade, I. Hechenbleikner, and D.W. Kaiser. Fire-retardant textile treatment, 1958.

[125] C.W. Heitsch, P.R. Schenkenberg, and I.A. Boenig. Fire retardant textiles - cotton treated with amidophosphazene. *Organic Coatings and Plastics Chemistry*, 41:97–102, 1979.

[126] M.D. Swerdloff, M. Van Der Puy, J.F. Kolc, M.M. Rogic, L.G. Anello, and L.L. Hendrickson. Urease inhibited ures based fertilizer compositions containing phosphorus compounds, 1984.

[127] A.V. Sokolov, L.V. Sidorina, A.S. Lenskii, A.I. Pichak, and A.S. Allilueva. New forms of nitrogen-phosphorus fertilizers. *Probl. Khim. Tekhnol.*, pages 279–284, 1977.

[128] S.B. Sello and G.N.J. Cedar. Verfahren zum Flammfestmachen von zellulosehaltigen Stoffen, 1971.

[129] L.H. Chance, J.L. Drake, and W.A. Reeves. Process for flameproofing cellulosic material, 1968.

[130] S. Tadao Sasakura, I. Yasuyuki Anasako, and O. Yoshiyuki Hayashi. Finishing agent for cellulosic materials and method for treating cellulosic mateerials with aqueous solution of aged phosphoric acid amide for aged amidophosphazene, 1992.

[131] E.N. Pokrovskaya, T.P. Nikiforova, E.L. Gefter, and A.I. Semenova. Flame retardancy of wood modified with some phosphoric acid derivatives. *Koksnes Chimiya*, (5):92–94, 1988.

[132] L. Govaerts, S. Talibuddin, and De Wit. G. Flame retardant polyester composition, method for the preparation thereof, and articles derived therefrom, 2003.

[133] K. Kosaka, X. Li, and Y. Xiao. Flame retardant thermoplastic composition and articles comprising the same, 2008.

[134] G.W. McCarty, J.M. Bremner, and J.S. Lee. Inhibition of plant and microbial ureases by phosphoramides. *Plant and Soil*, 127:269–283, 1990.

[135] D.A. Martens and J.M. Bremner. Effectiveness of phosphoramides for retardation of urea hydrolysis in soils. *Soil Sci. Soc. Am. J.*, 48:302–305, 1984.

[136] P. Gigler. Liquid composition containing phosphoric or thiophosphoric triamide derivative and use thereof, 2010.

[137] C.E. Morris and L.H. Chance. A comparison of some phosphorus amides as flame retardants for cotton. *Textile Research Journal*, 43:336, 1973.

[138] L.A. Cates. Phosphorus-nitrogen compounds. XI. Phosphamidase studies. I. Unsubstituted amides. *Journal of Medicinal Chemistry*, 13(2):301–2, 1970.

[139] G.L. Bolton, J.K. Padia, and B.K. Trivedi. Phosphorus-containing compounds as antihypercholesteroemic and antiatherosclerotic agents, 1993.

[140] J.D. Moore, D. Niu, G. Xu, D. Liu, Y.S. Or, and Z. Waug. Preparation of phosphorus-containing peptides as hepatitis C serine protease inhibitors, 2008 2008.

[141] M. Font, M.-J. Dominguez, C. Sanmartin, J.A. Palop, S. San-Francisco, and O. Urrita. Structural characteristics of phosphoramide derivatives as urease inhibitors. requirements for activity. *Agricultural and Food Chemistry*, 56:8451–8460, 2008.

[142] H. B. Pandya and M. M. Bhagwat. Studies on the efficacy of phosphorus-nitrogen flame retardants on cotton. *Journal of Fire Retardant Chemistry*, 5:86–92, 1978.

[143] C. Shimasaki, Y. Mutou, E. Tsukurimichi, and T. Yoshimura. Thermal decomposition and mass spectra of phosphoramidates esters. *The Chemical Society of Japan*, 63:370–377, 1990.

[144] M.J. Nielsen, J.V. Pustinger, and J. Strobel. Phosphorus-31 nuclear magnetic resonance chemical shifts of phosphorus compounds. *Journal of Chemical and Engineering Data*, 9(2):167–170, 1964.

[145] Martin Grayson and Edwards J. Griffith. *Topics in Phosphorus Chemistry. Vol. V Phosphorus-31 Nuclear Magnetic Resonance.* 1967.

[146] K. D. Pressl and A. Schmidt. Preparation and IR spectra of dimethylamino methoxyphosphonium hexachloroantimonates(V). *Zeitschrift für Anorganische und Allgemeine Chemie*, 434(1):175–182, 1977.

[147] Arnold C. Satterthwait and F.H. Westheimer. Monomeric methyl metaphosphate: reactions with carbonyl groups. *Journal of the American Chemical Society*, 102(13):4464–72, 1980.

[148] N.N. Preobrazhenskaya. Reactions of phosphoramidic acids. *Russian Chemical Reviews*, 41(1):54–65, 1972.

[149] J. T. Langley, M. J. Drews, and R. H. Barker. Pyrolysis and combustion of cellulose. 7. Thermal analysis of the phosphorylation of cellulose and model carbohydrates during pyrolysis in the presence of aromatic phosphates and phosphoramides. *Journal of Applied Polymer Science*, 25(2):243–262, 1980.

[150] J. R. Van Wazer, C. F. Callis, J. N. Shoolery, and R. C. Jones. Principles of phosphorus chemistry. II. Nuclear Magnetic Resonance measurements. *Journal of the American Chemical Society*, 78(5715-26), 1956.

[151] E.F. Mooney. Annual reports on NMR-spectroscopy. Technical report, Academic Press, 1973.

[152] A. J. R. Costello, T. Glonek, and J. R. Van Wazer. Phosphorus-31 chemical shift variations with countercation and ionic strength for the various ethyl phosphates. *Inorganic Chemistry*, 15:972–974, 1976.

[153] M.J. Nielsen and J.V. Pustinger. Phosphorus-31 nuclear magnetic resonance (N.M.R.) studies of phosphorus-nitrogen compounds. *Journal of Physical Chemistry*, 68(1):152–8, 1964.

[154] H. Richter, E. Fluck, H. Riffel, and H. Hess. Tetraphenyl imidodiphosphate, salts, and complexes. *Zeitschrift für Anorganische und Allgemeine Chemie*, 496:109–116, 1983.

[155] F. A. Cotton and R. A. Schunn. Metal salts and complexes of dialkoxyphosphonylacetyl-methanide ions. *Journal of the American Chemical Society*, 85(16):2394–23402, 1963.

[156] F. Ramirez and J. F. Marecek. Reactions of phosphodiester anions with phosgene. *Journal of Organic Chemistry*, 48(6):847–850, 1983.

[157] M. M. Crutschfield, C. F. Callis, R. R. Irani, and G. C. Roth. Phosphorus nuclear magnetic resonance (N.M.R.) studies of ortho and condensed phosphates. *Inorganic Chemistry (Washington, DC, United States)*, 1(813-7), 1962.

[158] G. A. Olah and C. W. McFarland. Organophosphorus compounds. XII. Proton and phosphorus-31 NMR spectroscopic studies of the protonation and cleavage of trialkyl(aryl)phosphates and phosphites, dialkyl phosphonates, and phosphorus oxy acids in fluorosulfuric acid, and fluorosulfuric acid-antimony pentafluoride. *Journal of Organic Chemistry*, 36(10):1374–8, 1971.

[159] S. Huenig, H. Balli, and H. Quast. Pentaazapentamethine cyanines. *Angewandte Chemie*, 74:28–9, 1962.

[160] D. P. Ames, S. Ohashi, C. F. Callis, and J. R. Van Wazer. Principles of phosphorus chemistry. IV. The system of fluorophosphoric acids. *Journal of the American Chemical Society*, 81:6350–7, 1959.

[161] F. Ekkehard. Nuclear magnetic resonance of phosphorus compounds. IX. 31P nuclear resonance data of chain and cyclic phosphorus compounds. *Zeitschrift für Naturforschung*, 20b(6):505–8, 1965.

[162] M.J. Nielsen and J.V. Pustinger. Phosphorus-31 Nuclear Magnetic Resonance studies of phosphorus-nitrogen compounds. *The Journal of Physical Chemistry*, page 152, 1963.

[163] K. Klement and H. Baer. Das Verhalten von Amidophosphaten beim Erhitzen. *Zeitschrift für anorganische und allgemeine Chemie*, 300:221–224, 1959.

# List of Figures

# List of Tables

# Curriculum Vitae

## Viktoriya Salimova

| | |
|---|---|
| Nationality | Kasachstan |
| Date of Birth | 5 Aug 1984 |

## Education

| | |
|---|---|
| **2007 - 2011** | Doctoral Studies at Empa, Department of *Advanced* Fibers in St. Gallen, Switzerland |
| **2001 - 2006** | Diploma at the North Kazakhstan State University, Petropavlovsk, Kazakhstan |
| **1998 - 2001** | Gymnasium, Petropavlovsk, Kazakhstan |
| **1991 - 1998** | Secondary School, Petropavlovsk, Kazakhstan |

# Publications

## Patent

- Phosphoramidate flame retardants.
  Gaan S., <u>Salimova V.</u>, Ottinger S., Heuberger M., Ritter A.
  PCT Int. Appl. (2009). WO 2009153034; A1 20091223

## Paper Publication

- Thermal degradation of cellulose acetate in presence of bis-phosphoramidates.
  Gaan S., Mauclaire L., Rupper P., <u>Salimova V.</u>, Tran T.-T., Heuberger M.
  *Journal of Analytical and Applied Pyrolysis*, 2011, **90** (1), 33-41

- Characterization of chars obtained from cellulose treated with phosphoramidate flame retardants.
  Rupper P., Gaan S., <u>Salimova V.</u>, Heuberger M.
  *Journal of Analytical and Applied Pyrolysis*, 2010, **87** (1), 93-98

- Thermal decomposition and burning behavior of cellulose treated with ethyl ester phosphoramidates: Effect of alkyl substituent on nitrogen atom.
  Gaan S, Rupper P., <u>Salimova V.</u>, Heuberger M., Rabe S., Vogel F.
  *Polymer Degradation and Stability*, 2009, **94** (7), 1125-1134

## Conference Proceedings

- Phosphoramidate flame retardants: mechanism and application.
  Gaan S., <u>Salimova V.</u>, Heuberger M., Rupper P., Schoenholzer L.
  Proceedings of the Annual Conference on Recent Advances in Flame Retardancy of
  Polymeric Materials, 2009, 68-77

- Thermal decomposition and flammability of cellulose acetate in the presence of bis-
  phosphoramidates.
  Gaan S., Heuberger M., Rupper P., Mauclaire L., <u>Salimova V.</u>
  *Abstracts of Papers, 239th ACS National Meeting, San Francisco, CA, United States*,
  2010, CELL-323

- Effect of chemical environment of organophosphorus compounds on thermal decom-
  position of cellulose.
  <u>Salimova V.</u>, Nazarov D., Gaan S.
  *Abstracts of Papers, 235th ACS National Meeting, New Orleans, LA, United States*,
  2008, PMSE-155

- Effect of phosphorus compounds on burning behavior of cellulose.
  Gaan S., <u>Salimova V.</u>, Nazarov D.
  *Abstracts of Papers, 235th ACS National Meeting, New Orleans, LA, United States*,
  2008, CELL-098

## Oral Presentation

- Influence of the structure of phosphoramidates on flame retardant properties of cel-
  lulose.
  <u>Salimova V.</u>, Gaan S., Grützmacher J.
  American Chemical Society 240-th National Meeting, August 2010, Boston, MA,
  United States

- Influence of functional groups in phosphoramidate compounds on flame retardant
  properties of cellulose.

Salimova V., Gaan S., Grützmacher J.

Empa PhD Student Symposium 2009, November 2009, Dübendorf, Switzerland

- Studies on the influence of functional groups in phosphoramidate on thermal decomposition and flame retardant properties of cellulose.
  Salimova V., Gaan S., Grützmacher J.
  Flame retardant Polymer Meeting 2009, August 2009, Poznan, Poland

## Poster Presentation

- Influence of the structure of phosphoramidates on flame retardant properties of cellulose.
  Salimova V., Gaan S., Grützmacher J.
  Swiss Chemical Society Meeting, September 2010, Zürich, Switzerland

- Effect of phosphorus compounds on the burning behavior of cellulose.
  Salimova V., Gaan S., Grützmacher J., Heuberger M.
  American Chemical Society 235-th National Meeting, 2008, New Orleans, LA, United States

- Development and application of novel phosphorus-containing flame retardants for polymeric materials.
  Salimova V., Gaan S., Grützmacher J., Heuberger M.
  Empa PhD Student Symposium, 2007, Dübendorf, Switzerland